Conclusions: Although MGMT may have limited prognostic value, BRAF, CIMP, KRAS and MSI status may interact with each other to modify clinical outcome. These features will likely play a significant role in a future molecular classification of colorectal cancer.

731 CDX2 Expression as a Potential Surrogate Marker for CpG Island Methylator Phenotype in Colorectal Cancers.

I Zlobec, M Bihl, A Foerster, A Rufle, A Lugli. University Hospital Basel, Switzerland.

Background: CpG Island Methylator Phenotype (CIMP) is currently being investigated for its role in colorectal cancer pathogenesis and impact on clinical outcome. However, the assessment of CIMP in routine diagnostic pathology is complicated by the technical challenge and costs associated with its assessment. The aim of this study was to identify a protein marker capable of predicting CIMP status from a panel of 50 potential candidates.

Design: 404 patients were included in this study. MSI-H was defined as instability in ≥2 Bethesda-panel markers. CIMP-high was defined as methylation in ≥4/5 loci including CACNA1G, CDKN2A, CRABP1, MLH1, and Neurog1. Using tissue microarrays, 50 tumor and immune cell markers were investigated by immunohistochemistry.

Results: Only 7/50 markers were associated with CIMP-high including increased numbers of granzyme B+ (p=0.002; AUC:0.65), and CD8+ (p<0.001; AUC:0.66) cells, increased tumor cell expression of nuclear MST1 (p=0.012; AUC:0.67), and loss of cytoplasmic RKIP (p=0.007; AUC: 0.64), membranous/cytoplasmic EphB2 (p=0.007; AUC:0.7), and cytoplasmic CK20 (p=0.002; AUC:0.67). However, loss of cytoplasmic CDX2 was the strongest predictor of CIMP-high (p<0.001; AUC: 0.81). Of the 206 tumors with diffuse CDX2 staining, 202 (98%) were CIMP-negative/low. Similarly, of the 23 CIMP-high cases, 19 (82.6%) showed a loss of CDX2 expression.

Conclusions: CIMP-high colorectal cancers show a considerable loss of CDX2 expression. Since loss of CDX2 has previously been associated with BRAF mutation and MSI-H, two features closely related to CIMP, these preliminary results suggest that CDX2 may be useful as a possible surrogate marker for the determination of CIMP status.

Genitourinary

732 Molecular Genetic Abnormalities in Regulators of Cell Cycle and Apoptosis in High Grade Urothelial Carcinoma of Bladder.

HA Al-Ahmadie, GV Iyer, O Lin, A Gopalan, SW Fine, Y Chen, SK Tickoo, VE Reuter, BH Bochner, DF Bajorin, MI Milowsky, DB Solit. Memorial Sloan-Kettering Cancer Center, New York, NY.

Background: Cell cycle dysregulation and inhibition of apoptosis both drive tumorigenesis in multiple malignancies, including urothelial carcinoma (UC). Copy number alteration (CNA) is a well-known mechanism for dysregulation of these cardinal functions. Deletion of *CDKN2A* and *TP53* and amplification of *MDM2* has been observed in UC, but the exact frequency and functional consequence of such alterations is less known. We sought to define the frequency of amplification, deletion and mutations of genes that regulate cell cycle or apoptosis in a panel of 96 cases of high-grade UC (HGUC) of bladder.

Design: DNA was isolated from 96 frozen samples of HGUC (including 10 cases of small cell carcinoma of bladder) and analyzed for CNA through comparative genomic hybridization (CGH) using a 1 million oligonucleotide probe array from Agilent. The targeted genes included *TP53*, *MDM2*, *CCND1*, *CCNE1*, *CDKN2A/B*, *E2F3* and *Rb1*. Traditional Sanger sequencing to screen for mutations within select genes (*TP53*, *Rb1*, and *CDKN2A*) was also performed.

Results: Table 1 depicts the frequency of CNA and mutations found within the studied genes.

Table 1. Copy number alterations and mutations in genes of cell cycle regulation or apoptosis

Gene	Abnormality (n)
CCND1	Amp (11)
CCNE1	Amp (4)
CDKN2A/B	Del (13), Amp (1), Mut (2)
E2F3	Amp (13)
RB1	Del (5), Mut (1)
TP53	Mut (12), Del (9)
MDM2	Amp (4)

Amp: amplification; Del: deletion; Mut: mutation

Overall, 54 of the 96 cases (56%) showed some CNA (45) or mutation (13). Deletion of *CDKN2A/B* and amplification of *E2F3* were the most common CNA events identified within cell cycle regulatory genes, occurring in 13 samples each (14%), followed by amplification of *CCND1* in 11 samples (11%). There was no co-amplification of *CCND1* and *CCNE1* in any of the samples. *Rb1* deletions were observed in 5 samples. CNA in *E2F3* and *Rb1* were mutually exclusive in 14 of the 16 samples (88%) and were both present in 2 samples only. Mutations in *TP53* were noted in 13 samples and deletions in 9 samples. Amplification of *MDM2* was noted in 4 samples, none of which overlapped with *TP53* deletions or mutations. Overexpression of *E2F3* was significantly more common in small cell carcinoma (5/11) compared to conventional UC (8/85), $p = 0.006$.

Conclusions: Regulators of cell cycle and apoptosis are amplified, deleted or mutated in more than half of cases (56%) of high grade urothelial carcinoma. The overwhelming majority of these abnormalities are nonoverlapping. Amplification of *E2F3* seems to be overrepresented in small cell carcinoma of the bladder.

733 Increased Phosphorylated 4EBP1 Expression in Minute Prostatic Adnocarcinoma.

R Albadine, A Chaux, J Hicks, AM De Marzo, GJ Netto. Johns Hopkins Medical Institution, Baltimore.

Background: Phosphorylation of 4EBP1 results in the release of eukaryotic initiation factor 4E and increased cap-dependent translation of a set of proteins involved in G_1-S-phase. Reduced phosphorylated 4EBP1 expression was significantly associated with dramatically shortened survival in prostatic cancer. We aimed to evaluate phosphorylated 4EBP1 expression in minimal (insignificant) prostate adenocarcinoma (MinPCa), defined as tumors with insufficient virulence to threaten survival.

Design: Tissue microarrays were constructed from 33 consecutive radical prostatectomy spemcimens containing MinPCa. Each tumor and paired benign tissue was represented by up to triplicate,1mm, spots. Standard immunohistochemistry analysis for phosphorylated 4EBP1 was performed. Staining pattern was evaluated as nuclear vs. cytoplasmic, Percentage of positive cells (extent) and intensity (0 to 3+) of staining was assigned in each spot. A final H-score (product of intensity x extent) was calculated per spot and averaged among spots representing a single sample.

Results: Cytoplasmic and nuclear p4EBP1 expression (H scores) were significantly higher in MinPCa cancer tissues compared to benign tissues (p=0.0001 and p=0.0003 respectively). Only a minorty of MinPCa tumors (4/34; 11%) revealed cytoplasmic p4EBP1 levels lower than the mean level of their paired benign glands (Hscore <25).

p4EBP1 Hscore in benign prostatic tissue vs. adenocarcinoma

	No cases	Cytoplasmic p4EBP1 Hscore mean (range)	nuclear p4EBP1 Hscore mean	p value
Benign prostatic tissue	34	25 (0-100)	96 (10-230)	0.0001
Adenocarcinoma	34	136 (0-300)	162 (0-300)	0.0003

Conclusions: We found significantly increased cytoplamic and nuclear expression of phosphorylated 4EBP1 in our cohort of MinPCa compared to paired non neoplastic prostate tissue. Our finding of decreased phosphorylated 4EBP1 levels only in a minority of tumors in this cohort of clinically insignificant minimal prostate carcinoma is in line with the previously suggested aggressive prognostic implication for marked reduction in phosphorylated 4EBP1 expression.

734 PTEN and Phosphorylated S6 Expression in Clinically insignificant Prostate Adenocarcinoma: Correlation with *ERG* Fusion Status.

R Albadine, A Chaux, J Hicks, A De Marzo, GJ Netto. Johns Hopkins Medical Institution, Baltimore.

Background: Loss of PTEN leads to activation of mTOR pathway and has been linked to poor survival in patients with prostatic cancer (PCa). Phosphorylated S6 (pS6) expression is a potential predictive marker of response in mTOR targeted therapy. Minimal or insignificant prostatic adenocarcinoma (MinPCa) is defined as PCa with Gleason Score 6 and tumor volume < 0.5 CC. Studies assessing mTOR pathway status in MinPCa are lacking. The current study evaluates PTEN and pS6 expression in MinPCa in correlation with previously assessed *ERG* fusion status.

Design: Tissue microarrays (TMA) were constructed from 45 consecutive prostatectomies performed in our hospital (2002-2003) and diagnosed as MinPCa. Each tumor and paired benign tissue was represented by up to triplicate 1mm spots. Standard immunohistochemistry analysis for mTOR pathway members PTEN, pS6 was performed. H-score was generated for each marker as a product of intensity (0 to 3+) x percent of positive cells. FISH analysis was previously performed using break-apart probes for 5' and 3' regions of *ERG*.

Results: PTEN expression was retained in 28/29 (97%) evaluable MinPCa while pS6 positivity was present in 9/29 (31%). We found a significant correlation between pS6 expression and *TMPRSS2-ERG* fusion status (p<0.05) with 77% of pS6 positive tumors showing *ERG* fusion. Surprisingly, of 9 tumors demonstrating pS6 expression, 8 (89%) did not show associated loss of PTEN tumor suppressor gene suggesting an alternative mechanism controlling pS6 activation in MinPCa.

PTEN and pS6 expression vs. ERG rearrangement in minute protatic carcinoma

	No. cases	No ERG Rearangement	ERG Rearangement	p value
PTEN loss	1	0 (0%)	1 (100%)	p=1
No PTEN loss	28	14 (50%)	14 (50%)	
pS6 negative	20	13 (65%)	7 (35%)	p=0.014
pS6 positive	9	2 (22%)	7 (77%)	

Conclusions: In our cohort of MinPCa, loss of PTEN was only a rare event (1/29 tumors). Loss of PTEN was not associated with *ERG* fusion. The latter is in contrast to prior studies suggesting a collaborative role of PTEN loss and *ERG* fusion in early prostate cancer development. *ERG* rearrangement was associated with pS6 expression independent of PTEN loss. This finding suggests an alternative signaling mechanism controlling pS6 activation in MinPCa and call for further analysis.

735 Initial High Grade Prostatic Intraepithelial Neoplasia (HGPIN) with Carcinoma on Subsequent Prostate Needle Biopsy: Findings at Radical Prostatectomy.

T Alhussain, J Epstein. The Johns Hopkins Hospital, Baltimore, MD.

Background: There are only a few small studies on men with an initial biopsy showing HGPIN who later have cancer on repeat biopsy and then undergone radical prostatectomy. It is unknown whether this scenario impacts the prognosis of the subsequent radical prostatectomy.

Design: We compared radical prostatectomy findings in 45 men with an initial diagnosis of HGPIN who subsequently were diagnosed with cancer to 18,450 men diagnosed with cancer who lacked a prior diagnosis of HGPIN. All cases were retrieved from our institution between 1993 and 2008.

Results: The mean patient age was 60.2 years and the mean serum PSA value was 9.0 ng/mL. for the 45 men with an initial HGPIN diagnosis. 21/45 (46.7%) men were

found to have cancer within 6 months and 29/45 (64.4%) within 1 year following the diagnosis of HGPIN. Cancer involved a single core in 32/45 (71.1%) and the maximum tumor volume was 5% in 59.1% of the 45 cases. Men with initial HGPIN had 84.4% organ confined cancer while cases without HGPIN had 65.4% organ confined cancer (p=0.007) at radical prostatectomy. Favorable pathologic stage was maintained even when we restricted the analysis to men with only Gleason score 6 cancer on biopsy. In men with Gleason score 6 cancer on biopsy, men with an initial diagnosis of HGPIN had 88.9% organ confined vs. 73.2% for men with no prior biopsy diagnosis of HGPIN, (p=0.03). For all men, there was no significant difference in Gleason score at radical prostatectomy between the two groups. Gleason score was ≤ 6 in 79.6% and 73.6% for men with and without a prior HGPIN diagnosis on biopsy, respectively.
Conclusions: Prostatic adenocarcinomas discovered after an initial HGPIN diagnosis on biopsy are more likely to be organ confined, yet of similar grade compared to cases diagnosed as cancer on the first biopsy. These findings likely reflect cancers associated with HGPIN, where the cancers were missed on the initial biopsy as a result of smaller size.

736 Significance of Prostatic Adenocarcinoma Perineural Invasion on Biopsy in Patients Who Are Otherwise Candidates for Active Surveillance.

T Alhussain, JI Epstein. The Johns Hopkins Hospital, Baltimore, MD.
Background: The finding of perineural invasion on biopsy is associated with an increased of extra-prostatic extension at radical prostatectomy (RP). However, the significance of perineural invasion on biopsy in patients who otherwise meet biopsy criteria for active surveillance has not been studied.
Design: We utilized the most common biopsy criteria for active surveillance: 1) Gleason score ≤6; 2) ≤3 positive cores; and 3) ≤50% involvement any positive core. In addition, all cases had at least 12 biopsy cores (12-30), as this is also one of the criteria for our active surveillance program. We retrieved 313 cases which met the biopsy criteria for active surveillance, although men elected to undergo immediate RP at our institution between 1992 and 2008. These included 51 cases with perineural invasion and 262 cases without perineural invasion.
Results: Mean patient age was 58.2 years. There was no significant difference in patient age and mean serum PSA values in cases with perineural invasion and without perineural invasion, respectively). The maximum percentage of cancer per core per case was 40% (range 2-40% and mean 15.6%). Cases with perineural invasion on biopsy had a higher maximum percentage of cancer on biopsy (18.6%) vs. those w/o perineural invasion (15.0%), p=0.02. Cases with perineural invasion also had slightly more cases with 2 positive cores, compared to cases without perineural invasion (56.9% and 39.7% respectively, p=0.02). Despite a greater extent of cancer on biopsy, cases with and without perineural invasion on biopsy showed no significant difference in surgical margin involvement [3/50 (6%) vs. 19/262 (7.3%), respectively] or having organ confined disease [43/51 (84.3%) vs. 240/262 (91.6%), respectively]. In one case with perineural invasion the surgical margin was equivocal.

Pathologic findings at RP

	Organ Confined	Margin (+)	RP GS > 6
PNI	43/51 (84.3%)	3/50 (6%)	13/51 (25.5%)
No PNI	240/262 (91.6%)	19/262 (7.3%)	54/259 (20.8%)

PNI, perineural invasion; RP, radical prostatectomy; GS, Gleason score.

Conclusions: Although perineural invasion generally increases the risk of extraprostatic extension, cases that meet biopsy criteria for active surveillance yet have perineural invasion showed no significant difference from those without perineural invasion in terms of adverse findings at RP. Patients with perineural invasion who meet criteria for active surveillance should not be excluded from this treatment option.

737 Increased Expression of Intratumoral C-Reactive Protein Predicts Mortality in Patients with Localized Clear Cell Renal Cell Carcinoma.

S Ali, VA Master, A Abbasi, O Kucuk, AN Young, K Ogan, JG Pattaras, PT Nieh, FF Marshall, AO Osunkoya. Emory University School of Medicine, Atlanta, GA.
Background: C-reactive protein (CRP) is an acute phase reactant typically produced in the liver following stimulation by interleukin-6. Serum CRP has recently been shown in some studies, to be a potential predictor of outcome in patients with localized and metastatic renal cell carcinoma (RCC). However, the prognostic significance of intratumoral CRP expression with emphasis on clinical outcome in patients with RCC remains unknown.
Design: 102 patients with fully resected, clinically localized (pT1-T3N0M0) clear cell RCC were followed postoperatively. Intratumoral CRP expression was assessed in radical nephrectomy specimens using immunohistochemical analysis. Patients were categorized by intratumoral CRP expression as follows: negative, 0; weak, 1+, moderate, 2+; strong, 3+. Univariate, Kaplan-Meier, and multivariate Cox regression analyses examined overall survival (OS) across patient and disease characteristics. Variables examined in multivariate Cox regression analysis included: pT-Stage and Fuhrman nuclear grade; tumor size; UCLA Integrated Staging System (UISS); Mayo Clinic stage, size, grade, and necrosis (SSIGN) score; Kattan normogram; preoperative serum CRP, and intratumoral CRP expression.
Results: Follow-up ranged from 19 to 42 months, with a mean (SD) of 29.8 (6.0) months. During this follow-up, 19/102 patients (19%) died of disease. Of all tumors, 30%, 43%, and 27% were graded as 0, 1-2+, and 3+ for intratumoral CRP expression, respectively. Of these patients, 7%, 14%, and 41% died of disease, respectively. Mean (SD) survival for these groups was 24.5 (3.5), 16.7 (2.7), and 7.5 (1.2) months, respectively (p=0.001). After controlling for variables significant in univariate analysis, patients with staining intensity of 1+ to 2+ and 3+ experienced a 3.5-fold (HR: 3.492, 95% CI: 0.413-29.505, p=0.251) and 22-fold (HR: 22.661, 95% CI: 2.171-246.558, p=0.009) increased risk of mortality, respectively, compared to patients with intratumoral CRP expression of 0.
Conclusions: To our knowledge, this is the first study to correlate intratumoral CRP expression with clinical outcome data. Increased expression of intratumoral CRP represents a significant prognostic measure of mortality in patients with localized clear cell RCC.

738 CRP Expression in Prostatic Adenocarcinoma.

S Ali, E Chastain, Q Yin-Goen, AN Young, AO Osunkoya. Emory University School of Medicine, Atlanta.
Background: Prostatic adenocarcinoma is the most common non-cutaneous malignancy in men here in the United States, and is one of the leading causes of cancer related deaths in men. C-reactive protein (CRP) is an acute phase reactant that is stimulated by interleukin-6. It has recently been demonstrated that elevated plasma CRP levels appears to be one of the strong predictors of biochemical failure and poor outcome in patients undergoing androgen deprivation therapy for prostatic adenocarcinoma. However, the correlation between intratumoral CRP expression and Gleason score of prostatic adenocarcinoma has not been studied.
Design: A search of the surgical pathology files at our academic institution was performed for radical prostatectomy, transurethral resection of prostate, and prostate needle core biopsy specimens signed out as prostatic adenocarcinoma. A representative unstained section of the tumor in each of the selected cases was obtained. TMA was not utilized to avoid the possibility of variability of marker expression between tissue cores. Immunohistochemical stains for CRP were performed. Staining intensity was graded as follows: negative, 0; weak, 1+; moderate, 2+; and strong, 3+. The staining intensity was then correlated with the Gleason score for each selected case.
Results: A total of 100 cases were selected. Cases were stratified based on Gleason score. 25 cases each of prostatic adenocarcinoma, Gleason scores 3+3=6, 3+4=7, 4+4=8 and 4+5=9 were analyzed. Mean patient age was 64 years (range 36-92 years). There was increased intratumoral expression of CRP in cases of prostatic adenocarcinoma, Gleason score 3+4=7 compared to cases of prostatic adenocarcinoma, Gleason score 3+3=6. However, there was more statistically significant increase in the intratumoral expression of CRP in cases of prostatic adenocarcinoma, Gleason score 4+5=9 (p=0.001), compared to all the other Gleason scores in this cohort, including cases of prostatic adenocarcinoma, Gleason score 4+4=8.
Conclusions: To our knowledge, this is the first study to date on the analysis of intratumoral expression of CRP in prostatic adenocarcinoma. There is a statistically significant increase in intratumoral CRP expression in cases of prostatic adenocarcinoma, Gleason score 4+5=9 compared to cases with lower Gleason scores. It is highly conceivable that increased intratumoral expression of CRP occurs as prostate cancer dedifferentiates. Intratumoral CRP may also play a critical role in the pathobiology of androgen-independent prostatic adenocarcinoma, thus leading to biochemical failure in patients who are undergoing androgen deprivation therapy for prostatic adenocarcinoma.

739 Regional Variation in Epigenetic Patterns in Prostate Cancer.

FZ Aly, JC Hanson, W Yang, MS Kreitman, MJ Merino, MW Linehan, PA Pinto, LG Adams, HS Stevenson, DC Edelman, MR Emmert-Buck, J Rodriguez-Canales. National Cancer Institute, Bethesda, MD.
Background: GSTP1 gene promoter methylation is present in >90% of prostate cancers. Using laser microdissection (LCM) mapping of a prostatectomy specimen with cancer, we found that cancer epithelium was methylated throughout the gland, whereas the cancer associated stroma (CAS) was methylated only at the apical pole. At present, it is not known if this epigenetic pattern is a common feature of prostate cancer, whether it correlates with reactive stroma, or if methylation patterns are unique to individual tumor clones. The goals of the present study were to expand the LCM-based epigenetic mapping strategy to additional cases.
Design: Four radical prostatectomy specimens containing cancers that extended from apex to base were analyzed. LCM mapping included normal and cancer epithelium, and normal stroma and CAS. Pyrosequencing of the *GSTP1* gene promoter was used to quantify the percentage of methylation in each sample. Whole-genomic amplification (WGA) and comparative genomic hybridization (CGH) were used for clonal analysis of cancer cells from the apex and base of the tumors. Masson stain was used to analyze the grade of reactivity of the CAS.
Results: Cancer epithelium showed variable but generally high GSTP1 methylation, ranging from 21 to 98%. A second case showed methylation (20%) of the CAS in the apical pole, similarly to our previously reported case. CGH data showed that tumors at the apex and base of the gland share the same clonal origin. Masson staining showed no differences in stromal reactivity at the apex or base of the tumors.
Conclusions: These results suggest that prostate cancers extending from apex to base within a gland can have the same clonal origin yet show regional variations in their methylation patterns. These findings are important for both the application of DNA methylation assays to prostate biopsies and to the understanding of basic prostate cancer biology.

740 Assessment of the Aggressivenss of Ductal Adenocarcinoma (Adenoca) of the Prostate: A Radical Prostatectomy (RP) Study of 93 Cases.

A Amin, JI Epstein. The Johns Hopkins Hospital, Baltimore, MD.
Background: It is unknown whether ductal adenoca. are more aggressive when matched for Gleason score (assigning the ductal component as Gleason pattern 4). Also, little is also known whether a certain percent of ductal component is needed to account for the more aggressive behavior.

Design: Out of 18,552 RPs performed from 1995 to 2008, 93 cases with a ductal adenoca. component were identified. Cases were classified based on their ductal/acinar ratio (1: <10%; 2: ≥10% and <50%; 3: ≥50%). There was no difference in the distribution of Gleason score 3+4=7 vs. 4+3=7 between ductal and non-ductal tumors, such that cases were combined as Gleason score 7.

Results: There was no age, race and serum PSA difference between patients with and without ductal adenoca. Cases with ductal adenoca. were less likely be organ confined (36.6% vs. 65.6%) and more likely to have seminal vesicle invasion (SVI) (19.3% vs. 5.3%), p<0.0001. There was no difference in lymph node (LN) metastases or positive margins between cases with and without ductal features. An increasing percentage of ductal component correlated with an increased risk of extra-prostatic extension (EPE) (p=0.04) and SVI (p<0.0001). To account for overall different Gleason scores between ductal and non-ductal cases as well as the affect of differing percentages of ductal features, the following analysis was done. For Gleason score 7 cases and ≥10% ductal features, cases with ductal features were more likely to have non-focal EPE (64.0%) vs. cases without ductal features (34.7%), p=0.002. In this group, there was no statistically significant difference in SVI or LN involvement between Gleason score 7 ductal and non-ductal tumors, possible due to the small number of positive events. For Gleason score 7 cases with <10% ductal features, there was no difference in pathological stage vs. non-ductal cases. There was no difference in pathological stage between ductal and non-ductal cases for Gleason score 8-10 cases, regardless of the percent ductal component or the Gleason score.

Conclusions: The current study demonstrates that ductal adenoca. admixed with Gleason pattern 3 is more aggressive than Gleason score 7 acinar cancer, as long as the ductal component is ≥10%. In cases with a very minor ductal component, these differences are lost. Also Gleason score 8-10 tumors with ductal features are not more aggressive that acinar Gleason score 8-10 cancers, where the high grade, regardless of ductal features, determines the aggressiveness.

741 Long-Term Clinical Outcome in Urothelial Papillomas of the Urinary Bladder.

A Amin, SF Faraj, A Chaux, T Al-hussain, R Cox, M Nagar, GJ Netto. The Johns Hopkins Hospital, Baltimore.

Background: Urothelial Papilloma (UP) is a benign neoplasm of the genitourinary tract. A need for long-term follow up in UP patients is questioned due to its benign biologic behaviour. This is the largest series to date evaluating clinical outcome of UP.

Design: We retrospectively retrieved all cases with a diagnosis of UP from our surgical pathology archives for the period between 1998-2009. All cases with a history of a higher grade urothelial lesion prior to the diagnosis of UP were excluded. Fifty three 'primary" UP cases were thus found forming the current study cohort. Electronic medical records were retrospectively reviewed in all cases. On follow up, recurrence was defined as the development of any subsequent neoplastic lesion of the bladder while progression was defined as the development of any subsequent neoplastic lesion of higher histologic grade or stage.

Results: Follow up was available in 40 cases while the remaining patients were lost to follow up. Mean patient age was 67.4 yrs (median 67.5, range 24–90). The follow-up length ranged from 1–60 mo (mean 16.6, median 12). Recurrence was identified in 19 cases (35%) after a mean duration of 12.7 mo (median 9, range 1–39) from initial UP diagnosis. Seventeen of nineteen (32%) recurrences were associated with progression to a higher grade non invasive urothelial lesion while the remainder 2 recurrent lesions were UP. None of the patients developed invasive urothelial carcinoma. Most frequent progression was to low grade urothelial carcinoma in 7 cases (13%) followed by high grade urothelial carcinoma (4 cases, 7%), urothelial dysplasia and PUNLMP (3 cases each, 5%). None of the 53 patients died of urothelial carcinoma while seven patients died from unrelated causes.

Conclusions: Although none of our patients developed invasive urothelial carcinoma or died of urothelial carcinoma, we found a relatively high rate of recurrence and progression in our UP cohort compared to previous studies.

742 Epithelial p16 Expression Is Associated with Chromophobe Renal Cell Carcinomas but Not Oncocytic Renal Lesions.

V Ananthanarayanan, M Tretiakova, J Taxy, T Antic. University of Chicago, IL.

Background: p16 protein expression by immunohistochemistry (IHC) is commonly used as a surrogate marker for human papilloma virus (HPV) infection in the cervix. Given the histologic similarity between viropathic koilocytes and nuclear changes of chromophobe renal carcinomas (CHRCC), we sought to analyze p16 expression in CHRCC, to evaluate its role in carcinogenesis. Additionally, we assessed the diagnostic utility of this marker to distinguish CHRCC from renal oncocytoma/oncocytosis (ONC), a close differential diagnoses.

Design: Tissue microarrays (TMAs) were constructed using 1 mm triplicate cores from 43 CHRCC and 24 ONC cases. Normal kidney tissues were included as controls. TMAs were immunostained for p16 using a mouse monoclonal antibody (Biocare, 1:400 dilution). Spots were evaluated in a blinded fashion to estimate the percentage of staining in the vascular, epithelial nuclear (EN) and epithelial cytoplasmic/membranous compartments (ECM).

Results: Normal kidney was devoid of p16 staining within any of the compartments. CHRCC was significantly associated with any epithelial nuclear p16 expression (8/43 cases) vs. ONC (0/24 cases) ***[Fisher exact p=0.043]***. A greater proportion of CHRCC (12/43 cases) showed epithelial cytoplasmic staining when compared to ONC (2/24 cases) *[Fisher exact p=0.069].* Variable endothelial staining was noted in a subset of both CHRCC and ONC. As shown in Table. 1, no difference was observed in percent staining for vascular and ECM compartments between the two groups.

Table 1. Percent staining in ONC and CHRCC across various histologic compartments

Histologic Compartment	ONC	CHRCC	p-value
	Average % Staining (n)	Average % Staining (n)	
Vascular	24.43 (09)	25.37 (11)	0.92
Tumor ECM	6.25 (02)	25.05 (12)	0.36
Tumor EN	No staining	28.70	

Furthermore, there was no correlation between the p16 staining and pT stage in CHRCC.

Conclusions: Epithelial p16 expression is more frequent in CHRCC than ONC. However, no association was observed between pT stage and p16 staining. Vascular p16 staining, albeit a novel finding, was not statistically different between CHRCC and ONC. Epithelial p16 expression in a significant subset of CHRCC suggests a possible role of HPV that merits further investigation.

743 MLH1 and PMS2 Define Prognosis in Sporadic Urothelial Carcinoma of Renal Pelvis and Ureter.

L Andres, L Zaldumbide, A Gaafar, J Gonzalez, A Garcia Tello, JC Angulo, JI Lopez. Hospital de Cruces, University of the Basque Country, Barakaldo, Spain; Hospital de Mendaro, Spain; Hospital de Getafe, Spain.

Background: Most cases of hereditary non-polyposis colorectal cancer are associated to mismatch repair (MMR) gene mutations and microsatellite instability. Although a subset of urothelial carcinomas of the upper urinary tract has also been included in this syndrome, sporadic cases with this genetic anomaly also occur. Our aim is to evaluate the expression pattern of MMR gene products and their correlation with histological features and with prognosis in a retrospective series of urothelial carcinomas of renal pelvis and/or ureter homogeneously treated.

Design: Eighty sporadic urothelial carcinomas of the renal pelvis and/or ureter with long term follow-up were analysed for the protein expression of 4 MMR genes (*hMLH1, hMSH2, hMSH6, and hPMS2*). Classic histopathological parameters and angiogenesis (CD31) were re-evaluated and correlated with the immunohistochemical expression of these proteins (cut-off: <5% of stained nuclei).

Results: Males predominated in the series (66M/14F), with an average age of 67 years. Pure TCC histology was seen in 91.2% of the cases, with papillary phenotype in 85% and pushing border in the stromal invasion in 81.2%. Median follow-up was 37 months. MSH2 and MSH6 were expressed in 100% of the cases, MLH1 in 85%, and PMS2 in 72.5%. MLH1 and PMS2 expression was strongly associated (Cramer V, 0.60) and encompassed a shorter survival for both MLH1 (log-rank, p=0.0001) (Figure 1) and PMS2 (log rank, p=0.004) (Figure 2) MLH1 expression was associated to high tumour grade (p=0.009) and pT stage (p=0.05).

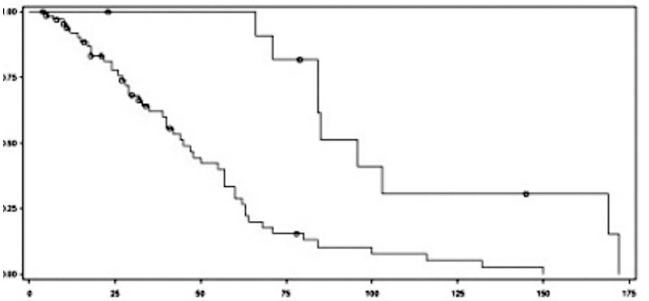

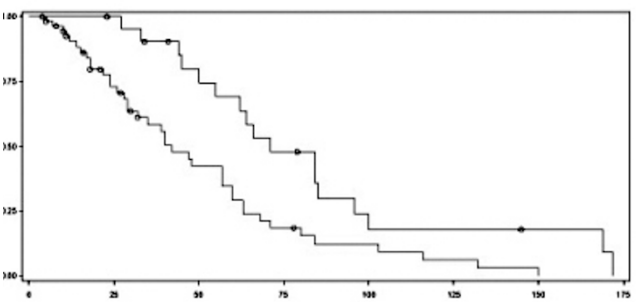

PMS2 was associated to infiltrative-type border of invasion in the stroma (p=0.008) and to increased neoangiogenesis (p=0.008).

Conclusions: The immunohistochemical expression of MLH1 and PMS2 may be considered as a new prognostic marker also in sporadic forms of upper urinary tract urothelial carcinoma.

744 Atypical Prostatic Ductal Lesions (APDL) Presenting as Small Prostatic Urethral Polyps: A Clinicopathologic Study of 7 Cases and Documentation of a Unique form of Prostatic Ductal Neoplasia Warranting Active Surveillance.

C Annaiah, BL Balzer, RS Parakh, LP Herrera, K Arora, DJ Luthringer, MB Amin. Cedars-Sinai Medical Center, Los Angeles, CA.

Background: Prostatic ductal carcinoma (PDCa) involves the prostate as: a) as papillary transition zone lesions with obstructive symptoms in transurethral (TURP) specimens, or b) as diffuse proliferations in the parenchyma with elevated PSA, abnormal rectal

exam in needle biopsies (NBx). It is an aggressive variant of prostatic cancer (PCa) when pure in histology and when it is occurs concurrently with acinar PCa, it is associated with high stage disease.
Design: We describe 7 cases of APDLs that presented with hematuria and as small urethral polyps. At the time of diagnosis, due to restriction to suburethral tissue, active surveillance with repeat TURP and multiple peripheral zone NBxs was recommended to document further extent of disease.
Results: Patients presented with hematuria, the mean age was 73 (64-83) yrs. The lesions occurred in the prostatic urethra & varied in size from 0.2 to 0.9 (mean 0.5) cm. All lesions had a large glandular tubuolopapillary pattern with intraductal growth. Four cases had a component of ductal histology without basal cells (invasive growth); three were exclusively intraductal. These findings were supported by reactivity pattern of basal cell markers (p63 & HMCK). The cells were predominantly elongated with prominent nucleoli & showed pseudostratification. All cases strongly expressed racemase & prostatic lineage markers (PSA, PSAP, PSMA). CDX2 & PAX2 were negative. On follow up [6 cases – 7-72 (mean 30.5) months] invasive PDCa or acinar PCa was diagnosed in peripheral zone NBxs (2 cases) & no evidence of neoplasia was detected in repeat TURP or NBxs (3 cases); 1 case had a 1 cm APDL in a repeat urethral biopsy with no further disease progression in 30 months.
Conclusions: 1) APDL may present as small urethral polyps raising the differential diagnosis of villous adenoma and nephrogenic adenoma. 2) There are only 2 papers in the literature of similar cases whereby, diagnostic criteria employed designate them as PDCa, a diagnosis which generally evokes radical treatment due to implied poor prognosis. 3) Our study describes a unique form of prostatic ductal neoplasia, distinct from cancers more typically detected in TURP or NBxs, in which there is prominent intraductal growth. 4) Follow up data showing lack of involvement of the prostate gland or significant disease progression (67%), suggesting that these patients may be candidates for active surveillance, a treatment modality conventionally not associated with PDCa.

745 Detailed Immunohistochemical (IHC) Evaluation of Novel Markers Associated with Urothelial Differentiation in a Comprehensive Spectrum of Variants of Urothelial Carcinoma (UCa): A Study of 80 Cases.

C Annaiah, GP Paner, C Gulmann, P Rao, JY Ro, DE Hansel, SS Shen, A Lopez-Beltran, K Arora, RS Parakh, LP Herrera, DJ Luthringer, J Zhai, YM Cho, MB Amin. Beaumont Hospital, Dublin, Ireland; University of Chicago, IL; Cedars-Sinai Medical Center, Los Angeles, CA; Cleveland Clinic, OH; The Methodist Hospital, Houston, TX; Faculty of Medicine, Cordoba, Spain; MD Anderson Cancer Center, Houston, TX.
Background: Variants of UCa have diagnostic, prognostic, and therapeutic implications. Many of these variants present at metastatic sites and while dealing with variant morphology in the bladder, it is often important to rule out a metastatic tumor from other sites before the tumor is deemed to be a primary. IHC may play an important role, although expression of markers associated with urothelial differentiation has not been comprehensively evaluated in variants to date.
Design: 80 cases (26 micropapillary (MP), 7 nested, 2 microcystic, 2 clear cell, 11 plasmacytoid, 6 lymphoepithelioma-like (LELC),12 small cell and 14 sarcomatoid were evaluated with three **u**rothelial-**l**ineage **a**ssociated (ULA) markers (GATA3, Uroplakin, S100P) and five markers **s**upportive of **u**rothelial **d**ifferentiation (SUD) (thrombomodulin, CK7, CK20, p63, HMCK-34BE12). Immunoprofile was deemed diagnostic of urothelial differentiation if 2 of the 3 ULA markers or 3 of the 5 SUD markers were positive. % positivity was graded as 1 to 3+.
Results: Staining in urothelial variants was as follows: MP (90% ULA & 85% SUD); nested (57% ULA & 100% SUD); plasmacytoid (100% ULA & 70% SUD), microcystic (100% ULA and 50% SUD); clear cell U Ca (100% ULA & 100% SUD). Undifferentiated variants had lower positivity: small cell (0% ULA & 0% SUD); sarcomatoid (8 % ULA & 50% SUD); & LELC (17 % ULA & 83% SUD). Gata 3 & S100P were most commonly expressed ULA markers (84% & 96% in better differentiated variants respectively, & 23% & 31% in undifferentiated variants). Most commonly expressed SUD markers, besides CK7 were, p63 & HMCK (61% & 96% in better differentiated variants respectively, & 50% & 48% in undifferentiated variants).
Conclusions: This study presents the first comprehensive data of novel urothelial lineage markers with comparison to markers traditionally used to support urothelial differentiation in variant of UCa. The findings have important implications in the work-up of unusual primary bladder carcinomas & carcinomas at metastatic sites.

746 Role of Immunohistochemistry (IHC) in the Differential Diagnosis of Invasive Urothelial Carcinoma (UCa) Versus High-Grade Tumors of the Renal Collecting System [Collecting Duct Carcinoma (CDC) and Renal Medullary Carcinoma (RMC)].

C Annaiah, GP Paner, AM Gown, C Gulmann, M Amin, AO Osunkoya, M Vankalakunti, LP Herrera, R Gupta, K Arora, MB Amin. Cedars-Sinai Medical Center, Los Angeles, CA; University of Chicago, IL; PhenoPath Laboratories, Seattle, WA; William Beaumont Hospital, Detroit, MI; Emory University Hospital, Atlanta, GA.
Background: A high-grade infiltrative carcinoma associated with desmoplasia and an inflammatory stromal response in the renal medullary region poses challenging differential diagnostic considerations between invasive UCa, CDC and RMC. The problem is compounded in limited sampling in needle core biopsies of the kidney and at metastatic sites when a primary mass in the kidney (histology not known) is detected.
Design: Twenty-six (26) tumors were analyzed by a focused IHC panel comprised of 8 markers including novel urothelial differentiation-associated markers (S-100p, GATA3), markers frequently positive in urothelial tumors [high molecular weight cytokeratin (HMCK) & p63], metanephric differentiation-associated markers (PAX-2, PAX-8), marker associated with CDC [Ulex Europaeus Agglutanin 1 (UEA-1)] and INI-1/hSNF5, loss of expression of which is reported to occur in RMC with rhabdoid morphology or tumors with aggressive behavior.
Results: UCa (n=11) showed S-100p, GATA3, p63, HMCK positivity and PAX-2, PAX-8 – negativity in 100% of the cases. UEA-1 was positive in 55% of cases and INI-1 expression was positive in all cases. High-grade tumors of the renal collecting system showed greater variability in immunoprofile. Positive markers included UEA-1 (50%), PAX-8 (33%), HMCK and p63 (17% each); 14% showed rare focal positivity for S-100p. Negative markers included GATA3 and PAX-2 (100%). INI-1 was positive in all 9 cases of CDC and negative in all 6 cases of RMC.
Conclusions: 1) The typical immunoprofile for invasive UCa of the kidney is S-100p (+), GATA3 (+) and PAX-8 (-). 2) CDC and RMC have variable immunoprofile which overlaps with UCa in many traditionally used markers: UEA-1, p63 & HMCK; PAX-8 positivity & negativity for GATA3 is supportive of their diagnosis. 3) INI-1 expression is useful in the distinction of RMC versus CDC; it is lost in the former indicating biallelic inactivation of the INI-1/hSNF5 tumor suppressor gene on chromosome 22q11.2. 4) These findings may become even more crucial as specific targeted therapies are developed for each of these tumor types.

747 Spectrum of Histomorphology in "Vanished Testicular Remnants": Are Germ Cells Present?

T Antic, E Hyjek, JB Taxy. The University of Chicago, IL.
Background: The clinical rationale for orchiectomy in orchiopexy-resistant cryptorchidism is the risk for testicular malignancy posed by the presence of germ cells (GC) within seminiferous tubules (ST). In about 5% of undescended testicles, the scrotum is clinically empty, the "vanished" gonad presumably representing an in utero "vascular accident". The "vanished testicular remnants" (VTR) are often removed without orchiopexy. This study evaluates the histomorphologic spectrum in VTR.
Design: Scrotal explorations in twenty nine patients (30 testicles) with VTR were recovered from the surgical pathology files (2004-2008). Seven fetal autopsy testicles, eight castrate and two undescended testicles were used for histological and immunohistochemical comparison. H&E slides and a panel of immunostains were evaluated: SOX-9, inhibin, WT1, OCT 3/4, PLAP and CD117.
Results: In the thirty VTRs, the ages ranged from 11 months to 13 years (mean 4.5 years). Routine histology showed no STs in 18 (60%) VTRs which were characterized by combination of fibrosis (18), calcifications (16) and hemosiderin deposits (9). The twelve testicles (40%) with STs had no GC, being entirely lined by Sertoli cells (SC), immunoreactive for SOX-9, inhibin and WT1 and negative for OCT 3/4, PLAP and CD117. No Leydig cells were present. An epididymis and vas deferens were present in 22 and 23 VRTs respectively. The control fetal testicles showed STs with both GC and SC. The GC were positive for OCT 3/4, PLAP and CD117 and negative for SOX9, inhibin and WT1. The control castrate testicles (age range from 47 to 82, mean 71 years) and one cryptorchid testis (age 26 years) showed atrophic STs with histologically recognizable GC and SC. The GC were negative for OCT 3/4, PLAP, CD117, SOX9, inhibin and WT1. One cryptorchid testis (age 15 years) was negative for GC.
Conclusions: The histomorphology of VTR ranges from fibrosis only to ST without GC. This contrasts with fetal testes which do exhibit GCs; and cryptorchid testes which have variable GC presence. The reason(s) for GC absence in VTR is not certain, however, these gonads would not seem to be potential neoplastic sources.

748 Role of Percutaneous Renal Biopsy in the Evaluation of Renal Masses – The Cleveland Clinic Experience.

M Aron, M Zhou. Cleveland Clinic, OH.
Background: Percutaneous renal biopsy is a safe and reliable diagnostic tool in the diagnosis of unresectable renal cell carcinoma, metastatic masses and lymphoma. With the increase in the detection of incidental small renal masses (SRM's) and the use of ablative therapies in a select patient population, needle biopsy is evolving as a reliable tool for histopathological evaluation, directing patient management. We assessed the role of percutaneous renal biopsies in the evaluation of renal masses at the Cleveland Clinic from Jan 2007 to Aug 2010
Design: Renal biopsies performed for the primary diagnosis of renal masses from Jan 2007- August 2010 were retrieved from the histopathology files. Data pertaining to the biopsy indication, size of the mass, patient demographics, and the biopsy and resection specimen results were recorded and analyzed
Results: Biopsies from 136 cases were studied. The age range of the patients was 35-91 years with 85 males and 51 females. The size of the masses ranged from 0.5 cm to 22 cm, and 65 (48%) were small renal masses (≤ 4 cm, SRM). 24 cases had multiple masses of which 14 were bilateral. Resection specimens were available in 28 cases. Immunohistochemicl stains (IHC) were performed in 57 cases.
Table1. shows the distribution of the cases and the biopsy results. A tumor diagnosis was possible in 95.6% of the cases while it was non diagnostic in 4.4%. The tumor was classifiable on morphology alone in 55.8% of the cases, but with addition of IHC a total of 78.7% cases could be classified. 16.9% of the cases however could not be further classified. The addition of IHC increased the classifiable tumors in the SRM's significantly more than in the large tumors(87.7% vs 70.4%, p=0.001).

Renal Masses Diagnosed and Classified on Renal Biopsies(Table1)

	Tumor size ≤4 cm	Tumor size >4 cm	Total
Number of cases	65	71	136
Non-diagnostic	4 (6.1%)	2 (2.8%)	6 (4.4%)
Tumor diagnosis	61 (94%)	69 (97.2%)	130 (95.6%)
Tumor, classifiable*	57 (87.7%)	50 (70.4%)	107 (78.7%)
Tumor, unclassifiable*	4 (6.1%)	19 (26.8%)	23 (16.9%)

* p=0.001 by chi square test

Conclusions: A tumor diagnosis on percutaneous needle biopsy is possible in 96% of renal masses. Reliable classification can be achieved on morphology and IHC in approximately 80% of the cases, and in close to 90% of SRM's. These findings underscores the role of percutaneous renal biopsies in the clinical management of renal masses including SRM's.

749 Potential Role of HER2/Neu as a Molecular Target in the Treatment of High Grade Urothelial Cancer. Determination of Gene Amplification by FISH, CISH and IHC.

PP Aung, BA Walter, C Garcia, G Bratslavsky, MJ Merino. National Cancer Institute, Bethesda, MD; University of Salamanca, Spain.

Background: Bladder cancer is the fourth most common malignancy in men with more than 16,000 patients dying of the disease. Currently, the treatment of patients with advanced urothelial tumors is surgery and standard chemotherapy. Promising new targeted therapies as anti-Her2 drugs are currently under study in a variety of cancers. This study investigates the potential role of HER2/neu gene as a possible molecular target in bladder cancer.

Design: Forty-seven cases of urothelial carcinoma were analyzed. HER2/neu gene and chromosome 17 alterations were studied by FISH and chromogenic in situ hybridization (CISH) and protein expression by IHC. Correlation was done with tumor stage, grade and clinical behavior. Her2/neu IHC was evaluated following the CAP/ASCO guidelines and gene amplification by guidelines from the FDA-approved Her2 CISH kit (Invitrogen, CA). Polysomy of chromosome 17 was defined as 3 or more individual signals within a nucleus.

Results: Thirty tumor samples were high grade and 14 cases were low grade TCC. One case of mucinous adenocarcinoma and 2 cases of epithelial atypia were also evaluated. Superficial or locally invasion (pTa/PT1) was reported in 28 cases and muscle invasion (pT2+) in 17 cases. Patient's mean age was 47 years. In high grade tumors, Her2/neu protein expression by IHC was observed in 13 cases score 3+, indeterminate in 4 (2+) and no staining or weak in 2 cases (0-1). All 3+ cases also had Her2/neu gene amplification by CISH and FISH. Most of 2+ and all 0-1+ cases did not show gene amplification. The mucinous adenocarcinoma case was negative for Her2/neu expression and gene amplification. Eight low grade TCC cases did not show Her2/neu protein expression. Only 1 case was 3+ and 5 cases were 2+. None of the cases showed Her2/neu gene amplification. Polysomy of chromosome 17 was found in 96% of high grade tumors associated with Her2/neu gene amplification (22/23). Most of the low grade tumors had disomy of chromosome 17 (10/12).

Conclusions: Our study shows that high-grade urothelial carcinomas have Her2/neu protein overexpression and gene amplification in association with polysomy of chromosome 17. Low-grade cases were disomic with low expression and no amplification of the Her2/neu gene. These findings support the role that Her2/neu may have in the clinical management and treatment of patients with high-grade urothelial carcinoma that over express Her2/neu gene.

750 Refining the Histologic Criteria of Perinephric and Renal Sinus Fat Invasion for Staging Clear Cell Renal Cell Carcinoma.

H Aydin, P Elson, B Rini, R Baehner, C Magi-galluzzi, M Zhou. Cleveland Clinic; Genomic Health, redwood.

Background: Staging is critical for treatment and prognosis of clear cell renal cell carcinoma (CCRCC). Tumor invading into perinephric tissue/renal sinus fat is considered non-organ confined (pT3a). However, the histologic criteria of perinephric and renal sinus invasion are poorly defined. The purpose of this study is to determine the histologic criteria for invasion of perinephric tissue and renal sinus fat that correlate with clinical outcomes.

Design: 580 cases of clinically localized CCRCC were evaluated. The tumor perinephric tissue/renal sinus interface was classified according to the level of extension: tumor separate from perinephric/sinus tissue with a rim of renal parenchyma (level I) or fibrous capsule (level II); tumor penetrates into but not through a fibrous capsule (level III); or tumor extends into fat with smooth pushing border with a capsule (level IV) or without capsule (level V); or tumor extends into fat with desmoplastic response (level VI) or with infiltrative pattern (level VII); or tumor present in lymphovascular space in perinephric/sinus tissue (level VIII). The levels of tumor extension, tumor size and macroscopic vascular invasion were correlated to the 5-year recurrence-free survival using multivariable analysis and compared to historical staging and survival data.

Results: Case number and percentage for each level were as follows: I- 109 (19%), II-293 (51%), III-108 (19%), IV-35 (6%), V-10 (2%) and VI-VIII-25 (4%). The corresponding 5-year recurrence-free survival rates were: I- 96 ±2%, II-89 ±2%, III-77 ±4%, IV-57 ±9%, V-67 ±16%, and VI-VIII-25 ±9%. Multivariate analysis adjusted for tumor size and gross vascular invasion, showed that the level of extension was a significant independent prognostic variable ($p<0.001$). Estimated 5-year recurrence-free survival was 91$\pm$1% for patients with level I-II extension, 72%$\pm$4% for levels III-V, and 25$\pm$9% for levels VI-VIII. The 5-year survival rate for extension levels III-V is similar to the 5-year survival for AJCC stage II RCC (organ-confined disease, 73.7%), while that for levels VI-VIII is worse than AJCC stage III (non-organ confined disease, 53.3%).

Conclusions: Levels of perinephric/sinus tissue extension constitute a continuous risk factor for post-nephrectomy recurrence. Level III-V extension into perinephric/sinus tissue should be regarded as organ-confined while levels VI-VIII (tumor in fat with either desmoplasia, infiltrative pattern or lymphovascular space invasion) should be regarded as non-organ confined disease.

751 Relationship between Sporadic Clear Cell-Papillary Renal Cell Carcinoma (CP-RCC) and Renal Angiomyoadenomatous Tumor (RAT) of the Kidney: Analysis by Virtual-Karyotyping, Fluorescent In Situ Analysis and Immunohistochemistry (IHC).

A Behdad, FA Monzon, O Hes, M Hirsch, M Michal, E Comperat, P Camparo, P Rao, M Picken, R Montironi, C Annaiah, LP Herrera, K Arora, DE Westfall, P Tamboli, MB Amin. Cedars-Sinai Medical Center, Los Angeles, CA; The Methodist Hospital, Houston, TX; Charles University, Plzen, Czech Republic; l'Hotel-Dieu, Place du Parvis, Paris, France; Hôpital Foch, Suresnes, France; Brigham and Women's Hospital, Boston, MA; MD Anderson Cancer Center, Houston, TX; Loyola University Hospital, Chicago, IL; Polytechnic University of the Marche Region, Ancona, Italy.

Background: CP-RCC is a recently described (2006) unique subtype of renal cell carcinoma arising in the background of end-stage renal disease. Rare cases occurring sporadically have only recently been reported. RAT, a unique tumor composed of admixture of an epithelial clear cell component, and prominent leiomyomatous stroma, has also only recently (2009) been described. Both tumors display overlapping morphologic features including a distinct capsule, tubulopapillary architecture with luminal or mid-basally aligned nuclei resembling secretory endometrial glands with variable amount of clear cells. Papillae are seen secondarily within tubules and cysts occasionally with branching architecture. In addition, RAT has a conspicuous but still variable smooth muscle-rich stroma.

Design: We performed a detailed IHC (n=23) and molecular (n=6) profiling to understand the relationship between the two tumor types. We performed virtual karyotyping with SNP microarrys in representative samples of each tumor type to assess for chromosomal copy number imbalances. In addition, we performed 3p LOH, FISH for chromosomes 7, 17 and Y, and VHL mutation analyses.

Results: Both RAT (n=3) and CP-RCC (n=20) demonstrated identical immunoprofile: all tumors in both categories were positive for CK7, HMCK, PAX-2, PAX-8 and CAIX and negative for racemase and RCC. Neither tumor type showed any recurrent chromosomal imbalances by virtual karyotyping (n=3 each), FISH (n=10 CP-RCC, n=2 RAT) or 3p LOH (n=10 CP-RCC, n=2 RAT). Most tumors showed a normal diploid chromosomal complement. Only 3 CP-RCC tumors showed mutations in the VHL gene.

Conclusions: Both CP-RCC and RAT have identical morphologic features when the smooth muscle stroma of the latter is discounted. Similarities at the IHC and molecular levels further strengthen their interrelationship. Our analyses indicate that CP-RCC and RAT might be in the spectrum of the same category of tumors.

752 Characterization of Complex Chromosomal Aberrations in Primary Prostate Cancer Genomes.

MF Berger, MS Lawrence, F Demichelis, G Getz, MA Rubin, LA Garraway, For the Broad Institute and Weill Cornell Medical College Prostate Genome Consortium. The Broad Institute, Cambridge; Weill Cornell Medical College, New York; Harvard Medical School, Boston; Dana-Farber Cancer Institute, Boston.

Background: Prostate cancer remains the second most common cause of male cancer deaths in the United States. Although androgen withdrawal and/or antagonism-based treatment of advanced disease yields transient efficacy, most patients with relapsed or metastatic prostate cancer eventually die of their disease. These aspects underscore the critical need to articulate both genetic underpinnings and novel therapeutic targets in prostate cancer. Here we present the complete sequence of seven "high-risk" primary prostate cancers and their matched normal counterparts.

Design: Seven prostate cancers were selected from "high-risk", clinically localized tumors that were at least 80% enriched for tumor cells. Cancer and germline genomes were sequenced at 30 fold coverage.

Results: The average point mutation rate in these tumors was 1.0 per Megabase. Each prostate tumor also harbored dozens of chromosomal rearrangements, and several tumors contained complex patterns of balanced chromosomal breakpoints that occurred within or adjacent to several predicted cancer genes (See Table for details).

TABLE 1. Landscape of Somatic Alterations in 7 Primary Human Prostate Cancers

	PR-0508	PR-0581*	PR-1701*	PR-1783	PR-2832*	PR-3027	PR-3043
Tumor Bases Sequenced	97.8×10^9	93.9×10^9	110×10^9	90.9×10^9	106×10^9	93.6×10^9	94.9×10^9
Normal Bases Sequenced	96.7×10^9	57.8×10^9	108×10^9	92.3×10^9	103×10^9	87.8×10^9	96.6×10^9
Tumor Haploid Coverage	31.8	30.5	35.8	29.5	34.4	30.4	30.8
Normal Haploid Coverage	31.4	18.8	34.9	30.0	33.4	28.5	31.4
Nonsilent Coding Mutations (high confidence)	14 (5)	19 (3)	22 (6)	28 (19)	13 (7)	40 (15)	14 (10)
Rearrangements	53	67	90	213	133	156	43

*harbors TMPRSS2-ERG gene fusion

Rearrangement breakpoints were significantly associated with open chromatin, androgen receptor and ERG DNA binding sites in the setting of the *TMPRSS2-ERG* gene fusion, but inversely correlated with these regions in tumors lacking ETS gene fusions. Three ETS-negative tumors contained rearrangements that disrupted CADM2, indicative of a novel prostate cancer tumor suppressor mechanism. Furthermore, four of seven prostate tumors harbored chromosomal rearrangements disrupting either PTEN (unbalanced events), a prostate tumor suppressor; or a PTEN interacting protein not previously implicated in prostate tumorigenesis.

Conclusions: Together, these findings implicate chromatin and transcriptional regulation in the genesis of prostate cancer genomic aberrations and suggest that complex rearrangements engage multiple tumorigenic mechanisms in this malignancy.

753 Molecular Diagnosis of Prostate Cancer from Biopsy Needles Surplus Material.

R Bermudo, TM Thomson, D Abia, A Mozos, E Garcia, A Alcaraz, PL Fernandez. Hospital Clinic-IDIBAPS, Barcelona, Spain; Hospital Clinic, Barcelona, Spain; Instituto de Biología Molecular,CSIC, Barcelona, Spain; Hospital de la Santa Creu i Sant Pau, Barcelona, Spain; Centro de Biología Molecular Severo Ochoa,CSIC, Madrid, Spain.

Background: Histopathological diagnosis of prostate cancer in needle biopsies is fraught with substantial diagnostic uncertainties due to frequent false negative or inconclusive results. New analytical tools that enhance diagnostic accuracy and do not interfere with current practice would be extremely useful.

Design: Linear discriminant analysis (LDA) was applied to a microarray-generated dataset from 84 prostate samples to yield gene signatures that accurately discriminate between non-tumoral and tumoral tissue. Additionally, surplus biological material washed off from routine prostate biopsy needles was used to quantitate transcripts by real-time RT-PCR, and LDA-generated discriminant scores were benchmarked against pathological diagnoses of the corresponding biopsy cores from 53 patients.

Results: LDA based on transcript levels of a carefully validated group of 11 genes in material washed off from needle biopsies yielded a 6-gene signature (overexpressed: ABCC4, AMACR, HPN and MYO6; underexpressed: CSTA and LAMB3) that correctly assigned the biopsies as benign or tumoural in 92.6% of the cases, with 88.8% sensitivity and 96.1% specificity.

Conclusions: Surplus material from routine needle biopsies can be used to quantify transcripts corresponding to minimal-size gene signatures for sensitive and accurate discrimination between non-tumoral and tumoral prostates. These approaches could be useful adjuncts to current diagnostic procedures, with potential uses in prognosis and prediction.

754 The Utility of Sampling the Testicular Cord Margin in Germ Cell Tumors.

D Berney, A King, S Williams, I Bisson. Barts and The London School of Medicine, Queen Mary, University of London, United Kingdom.

Background: Sampling of the cord margin of orchidectomy specimens is performed routinely and considered an essential block. It has been recommended previously that it is sampled before incising the main tumour. However the incidence and type of tumor involvement of the testicular cord margin has not been assessed in a large series.

Design: The files of Barts and The London Hospital and The British Testicular Tumour Panel were examined for orchidectomy cases for germ cell tumors. Any case either suspicious or diagnostic of cord margin involvement was reviewed. The macroscopy was also reviewed to see if the cord appeared normal. Cases were examined for the type of tumour present and type of invasion (vascular or stromal) was identified. The presence or absence of vascular invasion from other blocks was also recorded.

Results: 1479 orchidectomy reports for germ cell tumor were examined. Forty-eight where cord margin involvement was either suspected or reported as present were reviewed. Cord margin involvement was confirmed in 29 cases (2.0%), including 7 seminomas and 22 non-seminomas. Twenty cases (1.3%) showed purely vascular invasion with no stromal invasion (4 seminomas and 16 non-seminomas). In all of these cases, vascular invasion was also identified adjacent to the tumour and in other sections of the cord. Eight cases (0.5%) showed both vascular and stromal invasion (2 seminomas and 6 non-seminomas) with a clear association between the 'plugged' tumour within the vessels and adjacent invasion of the vessel walls and fibro-adipose tissue. In all of these cases, the cord was reported as being macroscopically abnormal. One case showed purely stromal invasion in an undescended testis with clear macroscopic involvement of the margin.

Conclusions: The presence of tumor at the testicular cord margin is rare. The clinical relevance of cord margin involvement by intra-vascular tumour may be marginal as vascular invasion reported in the main specimen will lead to adjuvant therapy. Stromal invasion was not seen in any case with a macroscopically normal cord margin. In view of the highly favourable prognosis of germ cell tumors, even after lymph node metastasis, it is extremely unlikely that tumor at the cord margin is an independent prognostic factor. We suggest that assessment of the cord margin is of little importance for the staging and treatment of germ cell tumors. Sampling the cord margin prior to incision of the tumor is unnecessary and that if the cord is normal there may be no need to examine this routinely sampled margin at all.

755 Evaluation of Renal Tumors by Image Guided Biopsies with an Emphasis on Oncocytic Neoplasms: A Retrospective Four Year Study from a Large Academic Institution.

R Bhalla, A Wu, LP Kunju. University of Michigan Medical Center, Ann Arbor.

Background: Image guided needle core biopsies of renal masses (IGRB) are becoming increasingly common. We evaluated the adequacy, accuracy and limitations of IGRB in the management of patients with renal tumors in a high volume academic institution.

Design: The database was searched for all IGRB performed between 2006 and 2009 at our institution.

Results: Three hundred and seventy one IGRB in adults (age range 22-92 yrs, mean 62 yrs, M:F 1.4) were identified. IGRBs were sufficient for diagnosis in 329 (88.6%) patients. Biopsies were categorized as: 180 (48%) clear cell RCC; 47 (13%) tubulo-papillary RCC; 56 (15%) oncocytic neoplasms (ON){40 (11%) oncocytomas, 5 (1%) chromophobe RCC, and 11 (3%) ONs which could not be definitively classified}; 7 (2%) urothelial carcinomas; 19 (5%) benign/inflammatory; 20 (6%) miscellaneous {4 metastases, 4 high grade RCC, 4 Ewing sarcoma, 4 RCC with clear/papillary features, 2 sarcomas, 1 high grade carcinoma, unclassifiable, and 1 lymphoma}. Immunohistochemistry was performed in 90 (24%) cases. In the the majority (89%) of the ONs immunohistochemistry was performed, including CK7 (50 cases), vimentin (14), PAX-2 (6), c-kit (5), and RCC Ag (1). Of the 11 ONs which could not be classified, the diagnoses most often rendered was oncocytoma vs chromophobe RCC (5/11) and oncocytoma vs.other RCC (6/11). Followup was available in 51/56 ONs. Twenty four (42%) ONs (20 oncocytomas, 1 chromophobe, 3 unclassifiable) were followed up radiologically, 18 (32%) {13 oncocytomas, 2 chromophobes, 3 unclassifiable} underwent radiofrequency ablation, and 9 (16%) {2 oncocytomas, 2 chromophobes, 5 unclassifiable} underwent excision. The biopsy diagnosis was confirmed on excision in 3 cases. In one case, the biopsy diagnosis of oncocytoma was changed to chromophobe RCC on excision. Of the 5 ON which could not be classified on biopsy, the diagnoses on excision were chromophobe RCC (2), tubulocystic RCC (1), papillary RCC (1) and oncocytoma (1).

Conclusions: Image guided renal mass biopsies are generally adequate, and a definitive diagnosis can be established in the majority of cases. ONs provide the biggest diagnostic challenges; however, with the aid of immunohistochemistry, the majority (80%) could be still be definitively classified as either oncocytoma or chromophobe RCC. On excision, the ONs which cannot be classified are usually diagnosed as a variety of RCC.

756 A Retrospective Study on Pathologic Features and Racial Disparities in Prostate Cancer.

SA Bigler, X Zhou. University of Mississippi Medical Center, Jackson.

Background: Race along with age and family history are the established risk factors for prostate cancer. African Americans (AA) have higher incidence and mortality rates than Caucasians (Cau) from prostatic adenocarcinoma. However, racial disparities are still controversial in many clinical and pathologic features of prostate cancer. Imbalanced racial proportion of studied subjects and degree in mixture of ethnic origins are two factors which could contribute to differences among studies. Our patient population is approximately an equal proportion of AA and Cau with few other ethnic groups represented.

Design: Pathology reports and clinical information from 3,315 prostatic surgical specimens were reviewed. Racial disparities were analyzed between AA and Cau for clinical and pathological features at the time of first biopsy, time of diagnosis of prostate cancer and time of radical prostatectomy.

Results: At the time of the first biopsy, AA had significantly higher detection rate of prostate cancer (50.3% vs. 38.3%, $p<0.0001$), higher serum level of PSA (11.6 vs. 7 ng/ml, $p<0.0001$) and higher Gleason scores (6.9 vs. 6.3, $p<0.0001$) as compared to Cau at a significant younger age (63.2 vs. 64.7 years old, $p=0.027$). The disparities of these features remained similar at the time of diagnosis of prostate cancer between the two races. At the time of prostatectomy, AA, as compared to Cau had higher positive surgical margin (33.5% vs. 19.7%, $p=0.0005$), larger tumor size (8 vs. 3.4 ml, $p=0.002$) and more bilaterally distributed prostate cancer (61.5% vs. 35.4%, $p<0.0001$) at a significantly younger age (58.7 vs. 61.5 years old, $p=0.0005$). AA also had higher detection rate of prostate cancer by repeat sampling with a shorter time interval to diagnosis of prostate cancer from previous biopsies with diagnoses of PIN or ASAP. In addition, prostate cancer precursors was significantly left-sided predominance (62% at left, 38% at right, $p=0.00543$); this tendency remained for prostate cancer with lower grade (Gleason score 2-3).

Conclusions: This retrospective study conducted in a conservative area with a balanced distribution of AA and Cau populations demonstrated racial disparities in detection rate of prostate cancer, serum PSA level, tumor grade, positive surgical margins, tumor volume, and percentage of bilateralism. The study also demonstrated a left-sided predominance of prostate cancer precursors and prostate cancer with lower grade.

757 Focal and Diffuse Positive Surgical Margins in Radical Prostatectomies (RP): How Should Be Quantitated?

A Billis, L Meirelles, LLL Freitas, AGE Duarte, CAM Silva, MAM Busson, LA Magna, LO Reis, U Ferreira. School of Medicine, University of Campinas (Unicamp), SP, Brazil; School of Medicine, University of Campinas, Unicamp, SP, Brazil.

Background: Extent of margin positivity in RP correlates with time to biochemical recurrence (TBCR) in most studies. However, during the ISUP consensus conference on handling and staging of RP specimens, no consensus could be reached as to what definition to use for focal and diffuse margin positivity. In this study we propose a simple method for surgical margin extent evaluation.

Design: The study was based on 300 whole-mount consecutive surgical specimens. Each transversal section of the prostate was subdivided into 2 anterolateral and 2 posterolateral quadrants. Using the cone method, 8 sections from the bladder neck and 8 sections from the apex were obtained. Margin positivity was stratified into 2 groups: present up to 2 quadrants and/or sections from the bladder neck or apex (group 1: focal) and in more than 2 quadrants or sections (group 2: diffuse). The groups were compared according to several clinicopathological variables: age, preoperative PSA, RP Gleason score, RP tumor extent using a semiquantitative point-count method, seminal vesicle invasion (SVI), and biochemical recurrence following surgery defined as PSA $\geq$ 0.2ng/mL. TBCR was analyzed with the Kaplan-Meier product-limit analysis using the log-rank test for comparison between the groups and prediction of TBCR using univariate and multivariate Cox proportional hazards model.

Results: Positive margins were present in 128/300 (42.7%) patients, 65/300 (21.7%) present in group 1 and 63/300 (21%) in group 2. Group 2 tumors were significantly more extensive ($p<0.01$). There was no significant difference related to age, preoperative PSA, RP Gleason score, and SVI. In 5 years of follow-up, 70% of patients with negative margins, 60% of patients with positive margins in group 1, and 37% of patients in group 2 were free of biochemical recurrence (log-rank, $p<0.01$). In univariate Cox regression analysis, group 1 was not predictive of TBCR ($p=1.65$); group 2 was predictive in univariate ($p<0.01$) as well as in multivariate ($p<0.01$) analyses.

Conclusions: In whole-mount surgical specimens, only positive margins in more than 2 quadrants and/or sections from the bladder neck or apex significantly predicted time for biochemical recurrence following radical prostatectomy in univariate and multivariate analyses. This is an easy and valuable method for reporting and quantitating focal and diffuse positive surgical margins.

758 CAIX Immunohistochemical Expression in Epithelial Tumors.

S Bishu, V Parimi, XJ Yang. Northwestern University, Chicago, IL.

Background: Carbonic Anhydrase IX (CA IX), a transmembrane protein regulated by the Von Hippel Lindau (VHL) gene, is involved in tumor genesis through regulation of cell adhesion, and pH via the HIF-1alpha activation cascade. CA IX is also a potential prognostic marker and chemotherapeutic target in renal cell carcinoma as high expression indicates a favorable prognosis and may predict response to interleukin-2 therapy. Although CAIX expression has been well documented in renal epithelial neoplasms, its expression in other epithelial tumors has not been well characterized.

Design: After IRB approval 183 in-house cases of viable (non-necrotic) epithelial malignancies were retrieved for construction of tissue microarrays, which were subsequently stained via immunohistochemistry using monoclonal antibody specific for CA IX. The cases include; renal cell carcinoma (RCC), clear cell type (ccRCC, n=37), chromophobe (chRCC, n=18), papillary (papRCC n=20), oncocytoma (n=16), and various carcinomas including urothelial (n=10), breast (ductal, n=8), colonic (n=10), endometrial (n=8), esophageal adenocarcinoma (n=9), hepatocellular (n=10), lung (NSCLC, n=10), pancreatic (n=9), prostatic (n=10), and ovarian epithelial (n=8). Transmembrane immunohistochemical expression on tumor cells was deemed a positive result. CAIX staining was further stratified for distribution (focal vs. diffuse), and intensity, on a scale from 1+ to 3+ (3+= strongest).

Results: CAIX expression was diffusely positive in all cases of ccRCC, with a majority showing strong staining (2+ or 3+) in 33/37 cases (89%). In contrast the large majority of other primary renal epithelial neoplasms were completely negative for CAIX (50/54 cases, 93%). The four positive cases were papillary RCC showing focal staining only (2 with 2+, and 2 with 1+). Of the other epithelial malignancies, only colonic adenocarcinoma showed a primarily positive pattern of staining (7/10, 70%,) with a majority of these being diffuse (5/7, 72%). Conversely, hepatocellular carcinoma (HCC) and prostatic adenocarcinoma showed absence of CA IX staining in all cases. All other epithelial malignancies showed variable staining patterns.

Conclusions: In the setting of evaluating primary renal epithelial neoplasms, CA IX is a very good marker for renal cell carcinoma, clear cell type. In the context of metastatic disease however, CA IX staining should be used with caution, as many tumors showed variable expression, with the exceptions being HCC and prostatic adenocarcinoma (which both showed none). This is particularly true with colonic adenocarcinoma, with the majority of cases showing positive and diffuse expression.

759 High-Grade Prostatic Intraepithelial Neoplasia (HGPIN): Preinvasive Lesion of Adenocarcinoma (CA) or Epiphenomenon? A Topographic Study of HGPIN and CA in Radical Prostatectomies (RP).

AAAV Brasil, A Billis, L Meirelles, LLL Freitas, PH Poletto, P Zubioli, WJ Favaro, VHA Cagnon, LO Reis, U Ferreira. School of Medicine, University of Campinas (Unicamp), SP, Brazil.

Background: The clinical importance of recognizing HGPIN is based on its strong association with prostatic CA. It is the most important risk factor for concomitance of prostate cancer on needle biopsy specimens. HGPIN coexists with cancer in >85% of cases. In spite of this high frequency of coexistence, transitions between HGPIN and stromal invasion very rarely are seen. This fact highlights the possibility of HGPIN to be an epiphenomenon. To address this issue we studied the topographic relation of HGPIN and CA in RP.

Design: We studied the frequency of quadrants showing only HGPIN, only CA, and HGPIN+CA in a total of 3186 quadrants from 100 whole-mount consecutive surgical specimens. Extent of HGPIN and CA was evaluated by a semiquantitative point-count method previously described. Points were considered coincident whenever HGPIN or CA were seen in a distance ≤5mm; non-coincident whenever in a distance >5mm. The means were compared using the Kruskal-Wallis and the Mann-Whitney tests. For the comparison of extent we used the Spearman correlation coefficient.

Results: HGPIN was present in 80/100(80%) radical prostatectomies. The mean (range) of quadrants showing only HGPIN, only CA, and HGPIN + CA was 0.74 (0-7), 8.53 (0-29), and 1.88 (0-13), respectively ($p<0.01$). The mean (range) of coincident points was 0.60 (0-4) and non-coincident 2.00 (0-15) ($p<0.01$). There was no significant correlation between extent of HGPIN and CA ($r=0.16$, $p=0.11$). The mean (range) of anterolateral quadrants showing HGPIN was 1.31 (0-8), and of posterolateral quadrants 1.80 (0-10) ($p=0.07$). Unequivocal transition between HGPIN and stromal invasion was seen in only 1/100 (1%) radical prostatectomies.

Conclusions: In specimens of radical prostatectomy most of the quadrants showed only CA and not HGPIN+CA. Extent of HGPIN did not correlate with extent of CA and the foci of HGPIN were significantly located in a distance >5mm from CA comparing to foci in a distance ≤5mm. No significant difference in frequency of HGPIN was found comparing anterolateral quadrants vs posterolateral quadrants. The lack of topographical association between HGPIN and CA and the very rare transition between HGPIN and stromal invasion, seem to favor the possibility that HGPIN may be an epiphenomenon.

760 Lymphovascular Invasion Is a Risk Factor for Understaging in pT1 Urothelial Carcinoma of the Bladder.

M Braun, G Gakis, T Todenhofer, F Fend, A Stenzl, S Perner. University Hospital Bonn, Germany; University Hospital Tuebingen, Germany.

Background: Urothelial carcinoma of the bladder (UCB) is often clinically understaged at primary diagnosis via transurethral resection of the bladder (TURB). Aim of this study was to evaluate the incidence, risk factors and clinical outcome of patients with urothelial carcinoma of the bladder staged pT1 at primary diagnosis via TURB.

Design: Of 275 patients with diagnosed UCB undergoing radical cystectomy (RC), 32 patients had histologically confirmed pT1 UCB at primary diagnosis via TURB. The presence of lymphatic and vascular invasion in TURB specimens and corresponding RC was assessed using conventional H&E staining, as well as immunohistochemical staining (IHC) against the lymphatic endothelium marker D2-40 and vascular endothelium marker CD31. Kaplan-Meier plots with the log-rank test were used to estimate recurrence-free and cancer-specific survival at a mean follow-up of 26.3 months (3-74).

Results: In RC specimens, pT1 stage was confirmed in 15/32 cases (47%). Of these, 17 cases (53%) were understaged in TURB specimens (pT2, pT3, and pT4 in 10, 3, and 4 cases, respectively). Lymphovascular invasion was detected in 8/17 understaged cases (47%) but in no case with confirmed pT1 UCB ($p=0.003$). In TURB specimens, none of the cases with confirmed pT1 UCB showed lymphovascular invasion, but 2/8 cases with understaged disease (25%)(sensitivity 12%, specificity 100%, PPV 100%, NPV 50%). Of note, on conventional H&E slides, lymphovascular invasion was not detectable in 2 TURB and 6 RC specimens, but detected in subsequent IHC. Actuarial recurrence-free and cancer-specific survival was significantly improved in patients with L0/V0 compared to patients with L1 and/or V1 ($p<0.05$).

Conclusions: Lymphovascular invasion is associated with decreased recurrence-free and cancer-specific survival. Understaging in pT1 urothelial carcinoma of the bladder is frequent (53%) and significantly more likely when lymphovascular invasion is present at primary or final diagnosis. Further, for patients with UCB, additional immunohistochemical assessment for lymphaticovascular invasion on a regular basis might be indicated. This could decrease understaging in UCB and result in an earlier radical treatment of the disease.

761 ALDH1A1 as a Marker of Stem Cells in Prostate Cancer: Correlation with Gleason Scores & Tumor Stage and Relevance for Patient Outcome.

R Bremer, D Tacha. Biocare Medical, LLC, Concord, CA.

Background: Mounting evidence supports the role of cancer stem cells (CSCs) in the recurrence and metastasis of several malignancies, including prostate cancer (CaP). Markers of CSCs potentially offer valuable diagnostic tools and predictors of disease progression. ALDH1A1, a member of the aldehyde dehydrogenase (ALDH) family of enzymes, has been shown to be a useful marker of CSCs. Expression of ALDH1A1 is associated with poor patient outcomes in several cancers, including breast, lung, and bladder. Additionally, in prostate cancer patients, ALDH1A1 expression has recently been shown to be associated with higher Gleason sums and advanced tumor stage. Most importantly, ALDH1A1 expression is a predictor of prostate cancer patient outcomes. Patients with high expression of ALDH1A1 have significantly reduced overall and cancer-specific survival rates compared to those with low expression of ALDH1A1 ($P=0.0093$ and $P=0.0017$, respectively).

Design: Tissue micro-arrays, with known Gleason sums and TNM staging, containing 169 samples of prostate adenocarcinoma were evaluated for expression of ALDH1A1 by immunohistochemistry, using a rabbit monoclonal antibody for ALDH1A1. Positive ALDH1A1 staining was determined for each sample and classified as either "Negative or Low" (<10% of cells staining) or "High" (>10%) expression.

Results: 37 of 169 (22%) CaP samples exhibited high expression of ALDH1A1. Samples with Gleason sums ≥8 had high expression of ALDH1A1 in 21 of 60 (35%) cases, whereas those with an intermediate Gleason sum of 7 showed high expression in 8 of 34 (19%) cases, and only 8 of 59 (12%) cases with Gleason sums ≤6 exhibited high expression of ALDH1A1.

	ALDH1A1 Expression			
Gleason Sum	Neg or Low	High	Total	% High Expression
≤6	59	8	67	12%
7	34	8	42	19%
≥8	39	21	60	35%
Total	132	37	169	22%

Additionally, high expression of ALDH1A1 was observed in 19 of 66 (29%) samples from patients with pathologic tumor stages ≥3, compared to 20 of 109 (18%) samples from patients where pT ≤2.

Conclusions: Evaluation of ALDH1A1 expression in CaP samples was readily performed using a rabbit monoclonal antibody and routine immunohistochemical procedures. Using an alternative antibody to ALDH1A1, previous reports of ALDH1A1 expression in CaP samples have been validated. Expression of ALDH1A clearly correlates with higher Gleason sums and more advanced pathologic stage. Considering its demonstrated effectiveness as a marker for cancer stem cells and as a predictor of patient outcome, ALDH1A1 expression may be a useful diagnostic and prognostic tool for the evaluation of prostate cancer cases.

762 Testicular Infarction with Associated Vasculitis: A Series of 19 Cases.

F Brimo, JI Epstein. McGill University Health Center, Montreal, QC, Canada; Johns Hopkins Hospital, Baltimore, MD.

Background: As a result of only very small series and case reports on testicular vasculitis, it is unknown how often they are a manifestation of isolated or systemic vasculitis.

Design: We herein report the clinical and pathological findings in a series of 19 cases (15 consultation and 4 in-house cases) of localized testicular infarction with associated vasculitis spanning 24 years.

Results: All cases were orchiectomy specimens and up to the time of abstract submission detailed clinical information was available in 14 cases. Mean age was 38 years. While the initial clinical presentation was testicular pain in 11 and testicular mass in three patients, the pre-operative impression was testicular cancer in 13 cases and in one case orchiectomy was performed for pain alleviation. In all cases, localized testicular infarction associated with vasculitis was present and in none was tumor identified. The majority of cases (n=14) showed polyarteritis nodosa (PAN)-like features with transmural necrotizing inflammation of medium to small arteries associated with fibrinoid necrosis and acute inflammatory reaction. In four cases, the vasculitis was granulomatous (two necrotizing and two non-necrotizing) and in one case it was lymphocytic. An infectious etiology was excluded clinically and by performing special stains. While seven patients did not show evidence of systemic vasculitis, two were confirmed with Wegener vasculitis, one with Churg-Strauss syndrome and one with subclinical systemic vasculitis. Two of those four patients had testicular PAN-like vasculitis and two had granulomatous vasculitis. Three patients had elevated serum inflammatory response proteins/abnormal urinalysis without definite evidence of systemic vasculitis.

Conclusions: Testicular vasculitis can cause localized infarction clinically mimicking cancer. While testicular vasculitis is an isolated finding in the majority of patients (10/14 or 71%), an associated systemic vasculitis is not a rare event (4/17 or 29%), especially if the vasculitis is granulomatous (50% in this series) and therefore all patients should be investigated for systemic disease clinically.

763 Activation of mTOR Pathway in Malignant Pheochromocytoma: A Potential Therapeutic Target.

F Brimo, A Chaux, L Schultz, JI Epstein, AM Demarzo, P Argani, GJ Netto. McGill University Health Center, Montreal, Canada; Johns Hopkins Hospital, Baltimore.

Background: mTOR pathway activation regulates protein translation and cell proliferation. Dysregulation of the mTOR pathway is present in several types of malignancies in which agents targeting mTOR are being evaluated. We herein assess the status of mTOR pathway components and their prognostic role in a series of benign and malignant pheochromocytomas.

Design: Immunohistochemical analysis was performed for PTEN, phos Akt, phos S6, p27, and c-myc using a tissue microarray constructed from 47 pheochromocytomas treated at our hospital (1996-2009). Duplicate tumor samples were used. For each marker the percentage of positive cells (extent) and the intensity of staining (0, 1, 2, 3) were recorded and an H-score (intensity x extent) was calculated. Markers exression was correlated with tumor biologic behavior (benign vs malignant) and tumor primary vs metastatic status.

Results: 39 primary (20 benign and 19 with indeterminate clinical course) and eight metastatic pheochromocytomas were included. 28 patients were males and 19 were females with a mean age of 47 years and a mean tumor size of 5.3 cm (range 0.9-12.5). While the expression of PTEN, phos S6, p27, and c-myc did not differ between benign and malignant (metastatic) tumors, phos AKT was significantly overexpressed in malignant pheochromocytomas (p=0.01). see table 1. Similar findings were obtained when comparing primary (n=39) and metastatic (n=8) tumors.

	No. Cases	Benign (%)	Malignant (%)	P value
Phos AKT				0.012
Negative	24	20 (100)	4 (57.1)	
Positive (H>210)	3	0 (0)	3 (42.9)	
PTEN				1
Negative	15	11 (57.9)	4 (57.1)	
Positive (H>10%)	11	8 (42.1)	3 (42.9)	
P27				0.628
Negative	18	13 (65)	5 (83.3)	
Positive (H>0)	8	7 (35)	1 (16.7)	
pS6				0.686
Negative	13	10 (50)	3 (37.5)	
Positive (H>0)	15	10 (50)	5 (62.5)	

Conclusions: We found significantly higher expression levels of PhosAkt in malignant pheochromocytomas in comparison to benign tumors indicating activation of the mTOR pathway in this subset of pheochromocytomas. The potential role of the mTOR pathway-targeted therapy in malignant pheochromocytomas should be further investigated and pursued.

764 7q31 (C-MET) Amplification Is a Constant Finding in Tubulo-Cystic Renal Cell Carcinoma.

M Brunelli, D Segala, S Gobbo, S Bersani, E Bragantini, M Gardiman, I Alvarado Cabrero, M Chilosi, G Martignoni. University of Verona, Italy; S. Chiara Hospital, Trento, Italy; Univeristy of Padua, Italy; Centro Medico, Mexico City, Mexico.

Background: Among new emerging described renal neoplasms, the tubulo-cystic renal cell carcinoma may be considered a unique morphologic entity with distinctive gross and microscopic features. However, before it is accepted as a distinct renal cell carcinoma subtype, further studies are needed to document a characteristic molecular pattern associated with this tumor. It has also been questioned its relationship to papillary renal cell carcinoma. We sought to evaluate the fluorescent molecular signature expanding the chromosomal in situ analysis.

Design: Nine tubulo-cystic renal cell carcinomas were recruited, 5 of which from a single patient. Clinico-pathological analyses were recorded. Immunophenotypical analysis using monoclonal antibody against cytokeratin 7 (CK7), S100A1, parvalbumin (PV), racemase, CD10 were performed. Centromeric probes for chromosomes 7, 12, 16, 17, 20 and Y and locus specific probes (LSI) for 7q31 (c-met), 7p12 (EGFR), 17p13.1 (p53), 17q11.2-12 (Her-2), *17q21*-q22 (Topoisomerase-IIa) were tested.

Results: Patients age ranged from 45 to 67, with a male preponderance (5:1). A patient presented a synchronous papillary renal cell carcinoma. Tumours had a diameter ranged from 0,8 to 3,5 cm and all staged pT1a. Furhman grade was G3 in all neoplasms. Cases stained for CD10 (10/10, 100%), S100A1 (10/10, 100%) and racemase (9/10, 90%); PV was weakly and focally positive in 3 tumors (3/10, 30%), whereas only one case immunoexpressed CK7 (1/10, 10%). LSI-7q31 (C-MET) was gained in all five cases, but only two showed gains of centromeric signals for chromosome 7, and LSI-7p12 (EGFR) resulted disomic. Regarding chromosome 17 two out of five cases showed gains of centromeric signals, whereas three cases showed gains of LSI-17p13.1 (p53), LSI-17q11.2-12 (Her-2) and LSI-*17q21*-q22 (topoisomerase-IIa). Only one case showed loss of Y and not alteration were identified for chromosomes 12, 16 and 20.

Conclusions: In conclusion: 1) tubulo-cystic renal cell carcinomas constantly show 7q31 (C-MET) amplification; 2) this is the single chromosome abnormality in common with those described in papillary renal cell carcinoma.

765 Expression of Seminal Plasma Proteins in Prostate Cancer: Prognostic Implications after Radical Prostatectomy.

AM Canacci, K Izumi, Y Zheng, J Gordetsky, JL Yao, H Miyamoto. University of Rochester, NY.

Background: Seminal plasma proteins, semenogelins I (SgI) and II (SgII), have been shown to play a critical role in semen clotting and subsequent liquefaction in the presence of zinc and prostate-specific antigen (PSA). However, little is known about the role of semenogelins in human malignancies, including prostate cancer.

Design: We investigated the expression of semenogelins in four human prostate cancer cell lines by reverse transcription-polymerase chain reaction and western blotting as well as in 70 radical prostatectomy specimens by immunohistochemistry. We then evaluated the associations between the expression of semenogelins and clinicopathologic features available for our patient cohort.

Results: mRNA and protein signals for SgI and SgII were detected in androgen sensitive LNCaP cells cultured in the presence of 100 µM zinc, but not in the other lines, including androgen receptor (AR)-positive CWR22Rv1 cells and AR-negative PC-3 and DU145 cells. Immunohistochemical studies on prostatectomy specimens then showed that SgI and SgII stain positively in 55 (79%) and 31 (44%) cancer tissues, respectively, which was significantly higher than in corresponding benign tissues [SgI-positive in 13 (19%) cases (p<0.0001) and SgII-positive in 15 (21%) cases (p=0.0066)]. Of the 55 SgI-positive tumors, 28 (51%) were also SgII-positive, whereas 28 (90%) of 31 SgII-positive tumors were SgI-positive. Among the histopathological parameters analyzed, there was an inverse association only between Gleason score (GS) and SgII expression (GS≤7 *vs.* GS≥8: p=0.0150; GS7 *vs.* GS≥8: p=0.0111; GS≤6 *vs.* GS≥8: p=0.0674). Kaplan-Meier and log-rank tests further revealed that patients with SgI-positive/SgII-negative tumor have the highest risk for biochemical (PSA) recurrence (p=0.0242), although the expression status of either SgI alone (p=0.5409) or SgII alone (p=0.2378) was not strongly correlated with recurrence.

Conclusions: Our results suggest the involvement of semenogelins in prostate cancer and their prognostic values in predicting cancer progression after radical prostatectomy. Further functional analysis of semenogelins in prostate cancer is necessary to determine their biological significance.

766 Hybrid Tumors: All You Need To Know and More.

P Cannata-Ortiz, B Walter Rodriguez, G Bratslavsky, WM Linehan, MJ Merino. National Cancer Institute, Bethesda, MD.

Background: Birt-Hogg-Dubé syndrome (BHD) is an autosomal dominant genodermatosis caused by mutations in the FLCN or BHD gene (17p11.2) that predisposes to the development of skin fibrofolliculomas, lung cysts and renal neoplasms. Most of the renal tumors in BHD share morphological features of both oncocytoma and chromophobe RCC and are called *hybrid* tumors. Knowledge about renal tumors in BHD syndrome is limited and questions remain about the morphology and clinical impact of these neoplasms.

Design: To better characterize these BHD renal neoplasms and to investigate if predominance of different cell elements has clinical significance, we studied 458 renal tumors from 68 BHD patients (39 males; 29 females). Clinico-pathological correlation, proliferative and prognostic markers were evaluated by IHC.

Results: Histology confirmed that hybrid tumors were the most frequent renal tumor (53.9%) followed by chromophobe RCC (39.5%) and clear cell RCC (3%). Multiple bilateral tumors were noted in 47% of the patients (average: 6.7 tumors per patient) at a mean age of 49.7 years. The mean size was 2.2 cm (range 0.5-9). Hybrid tumors are characterized by the presence of oncocytoma-like cells and chromophobe cells with granular eosinophilic cytoplasm and perinuclear *halos*. Cells with clear/pale cytoplasm and crisp borders are present. Typically, hybrid tumors show an admixture of all these types of cells. These tumors are not encapsulated and may have a central myxohyaline scar. Non-tumoral renal parenchyma showed oncocytosis in 56% of the cases. Nodules of classical chromophobe RCC can be found growing within some hybrid tumors and compress the hybrid component to the periphery. These nodules exhibit only one type of chromophobe cells and their homogeneity differentiates them from the hybrid tumor, where the admixture of different types of cells confers a more heterogeneous appearance. IHC showed that Mib1 proliferation index was under 10%, p53 stained

rare cells and CD10 and CD117 showed patchy staining in the hybrid component in contrast to the diffuse staining of chromophobe RCC. The percentage of different cells in the hybrid tumors had no clinical impact as no patient with hybrid tumors only has developed metastatic disease.

Conclusions: Our study demonstrates that hybrid tumors are the predominant renal neoplasias in BHD syndrome and that the percentage of different cell types in the hybrid tumor does not seem to have prognostic significance. Prognostic/proliferative markers suggest slow growth, with the prognosis of the patients likely dictated by the coexistence of other aggressive variants of renal cancer.

767 Pitfalls in Using High Molecular Weight Cytokeratin 34BE12 (CK903) and P63/Racemase Staining To Evaulate Cauterized Glands at the Margin in Radical Prostatectomy.

D Cao, P Humphrey. Washington University School of Medicine, St. Louis.

Background: Patients with a positive margin in radical prostatectomy (RP) have an increased risk of biochemical recurrence. Therefore it is critical to accurately assess the margin status in RP. However, sometimes the glands at the margin (ATM) in RP are cauterized making it difficult to determine their nature (benign versus malignant). The goal of this study to evaluate the utility of high molecular weight cytokeratin 34BE12 (CK903) and p63/racemase in distinguishing cauterized benign glands (CBGs) from cauterized malignant glands (CMGs) ATM in RP.

Design: Sixty RPs specimens with cauterized glands ATM were included: 32 with CBGs, 19 with CMGs, 9 with both CBGs and CMGs. One to two paraffin blocks containing CBGs and/or CMGs were used for staining with 34BE12 and p63/racemase. Both CBGs and MBGs ATM were evaluated for 34BE12 and p63/racemase staining, and their staining intensity was also compared to that in their non-cauterized counterparts [non-cauterized bengin glands (NCBGs), non-cauterized maignant glands (NCMGs)] in the immediate adajcent area.

Results: CBGs ATM showed negative 34BE12 and p63 staining in 3/41 and 5/41 cases, respectively. In additon, some but not all CBGs ATM showed loss of 34BE12 and p63 staining in 2/41 and 7/41 cases, respectively. The CBGs ATM showed weak racemase staining in 2/41 cases. When compared to adjacent NCBGs, CBGs ATM showed decreased staining intensity for 34BE12 and p63 in 25/38 (66%) and 31/36 (86%) cases, respectively. CMGs ATM showed negative 34BE12 and p63 staining in 28/28 cases. Positive racemase staining was seen in CMGs ATM in 22/28 cases (weak in 13, strong in 9). In cases with weak or no racemase staining in CMGs at the margin, the racemase staining intensity typically decreases from the adjacent NCMGs (strong intensity in 28/28) to CMGs not at the margin to CMGs ATM. 34BE12 and p63 demonstrated 93% (38/41) and 88% (36/41) sensitivity to distinguish CBGs from MBGs ATM, respectively (specificity 90% (28/31) and 85% (28/33), respectively). Racemase demonstrated 22/28 (79%) sensitivity and 22/24 (92%) specifivity for identifying CMGs ATM (strong racemase staining is 100% specific for CMGs ATM).

Conclusions: The immunoreactivity of 34BE12 and p63 was lost in CBGs ATM in a small percentage of cases. Negative racemase staining was seen in CMGs ATM in a higher percentage of cases. One should be cautious in using 34BE12 and p63/racemase staining to distinguish CBGs from CMGs at the margin. Immunohistochemical evaluation should be always used along with morphologic patterns.

768 Distinct Expression Profiles of p63 Isoforms during Bladder Cancer Progression.

M Castillo-Martin, O Karni-Schmidt, N Gladoun, J Domingo-Domenech, C Cordon-Cardo. Columbia University, New York, NY.

Background: The TP63 gene is expressed as at least six different isoforms due to alternative promoter usage. p63 expression has previously been correlated with bad prognosis in bladder cancer. Nevertheless, the lack of p63 isoform-specific antibodies has limited the understanding of their biological significance and clinical implications.

Design: We analyzed 10 normal bladders and 202 bladder cancers, distributed as follows: 147 "superficial" UC (31 pTa and 116 pT1) and 55 "invasive" UC, pT2+ (22 pT2, 23 pT3 and 10 pT4). Follow-up clinical data was available from 183 patients. Immunohistochemistry and Immunofluorescence were performed following standard protocols, using newly generated and commercially available antibodies.

Results: As expected, basal and intermediate cells of normal urothelium displayed nuclear expression of total p63, which corresponded to TAp63α. 96.8% of the pTa cases and 94.0% of the pT1 cases showed expression of total p63, whereas only 69.1% of the invasive pT2+ bladder cancers expressed total p63. On the contrary, ΔNp63 was undetectable in normal bladder urothelium, whereas it was expressed in 29% of the pTa, 17.2% of the pT1 and 41.8% of the pT2+ bladder tumors. Patients whose tumors displayed a total p63 positive phenotype had a better prognosis than those from whom their tumors had a p63 negative phenotype, with a longer disease specific survival ($p< 0.0001$). Since total p63 expression is correlated with tumor stage, we evaluated the clinical implications of p63 expression in "invasive" and "superficial" carcinomas separately. Total p63 and ΔNp63 expression showed significant prognostic connotations in "superficial" tumours, since patients with a negative phenotype showed a higher recurrence rate ($p<0.05$ and $p<0.01$, respectively). On the contrary, ΔNp63 was a marker of poor prognosis in invasive carcinoma, since patients whose tumors showed a ΔNp63 positive phenotype had a shorter survival ($p< 0.05$). Moreover, we observed a direct correlation between ΔNp63 and high molecular weight CKs (HMWCK) expression ($p<0.01$), and an inverse correlation with CK20 ($p<0.05$). Finally, and also importantly, we observed a correlation between expression of ΔNp63 and p53 mutation ($p<0.001$).

Conclusions: This study highlights the relevance of p63 isoforms in bladder carcinoma progression. We propose a new categorization of invasive bladder cancer into "basal-like" (ΔNp63 and HMWCK positive; CK20 negative) versus "luminal-like" (ΔNp63 and HMWCK negative; CK20 positive), being ΔNp63 expression associated with mutation of p53 and an aggressive clinical outcome.

769 Do Benign Glands at the Resection Margin Increase the Risk of Biochemical Failure Post Radical Prostatectomy?

SM Chan, FJ Garcia, MS Moussa, JL Chin, MY Gabril. London Health Sciences Center/ University of Western Ontario, ON, Canada; Division of Urology, London Health Sciences Center/ University of Western Ontario, London, ON, Canada.

Background: In radical prostatectomies for prostate cancer (PCa), the effect of benign glands at the resection margins on PSA levels is quesionable. In this study, we compare the risk of biochemical failure post radical prostatectomy in patients who have benign glands at the resection margins vs malignant glands vs no glands.

Design: 58 radical prostatectomies (without neoadjuvant therapy, extraprostatic extension, seminal vesicle invasion or lymph node metastasis) performed by a single surgeon at our institution (1993-2001) were included in this study. All slides from the cases were re-reviewed and pathological features (Gleason grade, PCa volume, margin status (malignant glands, benign glands, no glands at the margin)) were assessed. Clinical data (age, PSA, biochemical failure (3 consecutive rises in PSA with a minimum PSA level of ≥ 0.1 ng/mL), metastasis and survival) was also collected.

Results:

Table 1: Multivariate Statistical Analysis of the 3 Groups

	Malignant Glands (n=18)	Benign Glands (n=13)	No Glands (n=27)	P Value
Median Age, years	64	61	61	.093
Median Preopertive PSA	7.7	6.9	6.8	.767
Gleason Score (%)				.150
<7	33	8	37	
≥7	67	92	63	
Biochemical Failure (%)	28	8	15	.437
Average follow up time (months)	99	97	85	

*There were no cases of death or metastasis in any of the three groups.

Cox proportional hazards model was used to evaluate biochemical failure, using the no glands group as the reference, with the malignant glands group having a HR=1.72 (95% CI, 0.46 – 6.44) and the benign glands group having a HR=0.42 (95% CI, 0.05 – 3.78).

Conclusions: Our study showed that in cases without extraprostatic extension, seminal vesicle invasion or lymph node metastasis, the presence of benign glands at the resection margin does not increase the risk of biochemical failure when compared to cases that have no glands at the margin. The presence of malignant glands, however, does increase the risk of biochemical failure.

770 Utility of p63 and HMWCK in the Distinction between Urothelial Carcinoma with Prostatic Stromal Invasion and Urothelial Carcinoma with Colonization of Prostatic Ducts and Acini.

EC Chastain, IV Oliva, AO Osunkoya. Emory University School of Medicine, Atlanta.

Background: Urothelial carcinoma with prostatic stromal invasion (UCaPSI) is associated with poor clinical outcome, especially if the tumor arises from the urinary bladder (pT4a). However, patients with urothelial carcinoma with colonization of prostatic ducts and acini (UCaCPDA) without invasion (pTis) have a much better clinical outcome. Unfortunately, the distinction could be challenging in some cases on H&E, and is a relatively common reason for urologic pathology consultation. To our knowledge, no study has been published to date specifically addressing the utility of immunohistochemical stains in the distinction between UCaPSA and UCaCPDA. In this study, we sought to determine the utility of p63 and HMWCK in this setting.

Design: A search was made through the surgical pathology and consultation files at our institution for cases of UCaPSI. Only cases with foci of adjacent UCaCPDA were selected for analysis. Immunohistochemical stains for p63 and HMWCK were performed. In all cases, adjacent benign prostatic glands were used as internal controls for the presence of basal cells. Intensity of p63 and HMWCK expression in UCa, which may impact the interpretation of the immunohistochemical stains, was also analyzed.

Results: 41 cases of UCaPSI with adjacent UCaCPDA were identified. All cases showed strong expression of p63 and HMWCK in the basal cells. 27/41 cases (66%) of UCa showed no or weak expression of HMWCK in the tumor cells. 14/41 cases (34%) of UCa showed strong expression of HMWCK in the tumor cells. 30/41 cases (73%) of UCa showed strong expression of p63 in tumor cells. 11/41 cases (27%) of UCa showed no or weak expression of p63 in tumor cells. In the 27/41 cases (66%) which showed no or weak expression of HMWCK, the staining of basal cells in UCaCPDA distinguished it from UCaPSI. However, in the cases in which the tumor stains positively for HMWCK, the distinction was not readily evident. In the 11/43 cases (27%) of UCa which showed no to weak expression of p63 in tumor cells, the staining of basal cells in the UCaCPDA distinguished it from UCaPSI. In the cases in which the tumor stains positively for p63, larger malignant cells and smaller benign basal cells were easily distinguishable.

Conclusions: In difficult cases, p63 and HMWCK which are readily available markers can be utilized in the distinction between UCaPSI and UCaCPDA. These markers especially when used in combination may be utilized in radical cystoprostatectomy, transurethral resection of prostate, and needle core biopsy specimens.

771 Mucinous Tubular and Spindle Cell Carcinoma of the Kidney: A Clinicopathological, Immunohistochemical and Array Comparative Genomic Hybridization Study.

S Chaudhary, A Nayak, T Yang, I Chiosea, Q Pan, NJ Morgenstern, TY Chan, YA Yeh. North Shore University Hospital, Manhasset, NY; Long Island Jewish Medical Center, New Hyde Park, NY; Montefiore Medical Center, Bronx, NY.

Background: Mucinous tubular and spindle cell carcinoma (MTSCC), a rare variant of renal cell carcinoma, is characterized by its unique morphological, immunohistochemical and genetic findings. However, features which overlap with papillary renal cell carcinoma have been reported. We performed array comparative genomic hybridization (CGH) analysis on four cases of MTSCC.

Design: Four cases of MTSCC were retrieved from the pathology slide archives and array CGH was performed on all cases.

Results: Four cases included 2 men and 2 women with age range from 48 to 73 years. Two tumors occurred in the right and 2 in the left kidney. Partial nephrectomies were done and the tumor size varied from 2.1 to 4.0 cm. All the tumors had a pathologic stage of T1a. Macroscopically, MTSCCs displayed uniform light tan, yellow or gray tissues with minimal hemorrhage and necrosis. Microscopically, the neoplasms were composed of small elongated tubules embedded in a background of basophilic mucinous stroma. There were tumor cells arranged in curvilinear architecture separated by mucin. Closely parallel and collapsed tubular arrays with a spindle-cell appearance were present.

Case	CK7	CD10	AMACR	Vimentin	HMWK	CD117	CK19/CAM5.2
1	+	+	+	+	-	nd	nd/nd
2	+	-	+	+	nd	nd	nd/+
3	+	-	+	-	-	-	+/nd
4	+focal	-	+	+focal	-	-	+focal/nd

nd: not done

Case	Array CGH
1	-1,-6,-8,-13,-14,-15,-21,-22,12q del
2	+7,+17
3	-1,-4,-6,-8,-9,-13,-14,-15,-19,-21,-22, partial deletion 2q37,7p22,7p11-q11, 11p15,12q24,16p13,16q23
4	-1,-4,-6,-8,-9,-13,-14,-15,-18,-22, partial deletion 19p12

Conclusions: There is overlap in the immunohistochemical findings of MTSCC and papillary renal cell carcinoma. Loss of chromosomes 1, 4, 6, 8, 9, 13, 14, 15, 21, 22 is the most consistent recurrent chromosomal aberrations in MTSCC. One of our cases which showed morphologic features of MTSCC showed gains of chromosomes 7 and 17, supporting classification as papillary renal cell carcinoma and in contrast to previous reports of papillary renal cell carcinoma with low grade spindle cell foci, it does show mucinous stroma. Therefore, our study illustrates that MTSCC can show morphologic and immunohistochemical features in common with papillary renal cell carcinoma, and genetics studies of such tumors can be helpful for correct classification.

772 A Pathology-Based Mathematical Model Predicts Nodal Metastasis in Squamous Cell Carcinoma of the Penis.

A Chaux, G Guimaraes Cardozo, F Soares, I da Cunha, GJ Netto, AL Cubilla. Johns Hopkins University, Baltimore, MD; Hospital do Cancer A. C. Camargo, São Paulo, Brazil; Instituto de Patología e Investigación, Asunción, Paraguay.

Background: Inguinal nodal metastasis is the strongest predictive factor for survival in patients with penile squamous cell carcinomas (SCC). Accurate tools are needed for defining which patients will benefit with a groin dissection.

Design: Clinical and pathological data from 192 patients treated for penile SCC were evaluated. Among multiple factors, using binary logistic regression, it was found that clinical status of lymph nodes (CN), tumor histological subtype (HS), histological grade (HG), and perineural invasion (PNI) were significant predictors of nodal involvement. The following logistic regression model (LRE) was constructed using these covariates,

LRE = -4.542 + 1.829*CN + 1.777*HS + 2.536*HG + 1.389*PNI

Where each covariate assume a value of 1 if present and of 0 if absent. The probability P(M) of nodal metastasis in any given patient was calculated using the following equation

$P(M) = 1/(1 + e^{-LRE})$

Where e is the Euler's number (e ≈ 2.71828) and LRE is the value obtained using the first equation.

Results: Using a cut-off point of 40% for P(M) 78.9% of patients with negative and 79.7% with positive inguinal nodes were correctly classified. Overall accuracy was 79.2% (95% confidence interval 72.7–84.7%). Most false positive patients presented enlarged inguinal nodes while in most of false negative cases inguinal nodes were clinically impalpable.

Conclusions: This equation estimates the probability of inguinal nodal metastases in patients with penile SCC and it is based on the significance of pathological prognostic factors in resected specimens. The method accuracy is about 80% for all cases. The calculations, which can also be made using a handheld calculator, take only a few seconds in a standard personal computer. No specialized or paid software is needed.

773 Penile Squamous Cell Carcinomas: Preferential Association of Human Papillomavirus with High Histological Grade.

A Chaux, F Soares, I da Cunha Wernecke, GJ Netto, B Lloveras, N Munoz, S de Sanjose, FX Bosch, AL Cubilla. Johns Hopkins University, Baltimore, MD; Hospital do Cancer A. C. Camargo, São Paulo, Brazil; Instituto Catalán Oncológico, Barcelona, Spain; CIBER Epidemiologia y Salud Pública, Barcelona, Spain; Instituto de Patología e Investigación, Asunción, Paraguay.

Background: Approximately 40% of penile squamous cell carcinomas (SCC) are human papillomavirus (HPV) related and there is controversy regarding the prognostic impact of HPV in this subset of tumors.

Design: SCCs (202 cases) were tested for HPV using SPF-10 PCR. They were categorized in low and high-grade and according to warty and/or basaloid (WB) features. High-grade tumors had anaplastic cells, high nuclear/cytoplasmic ratio, pleomorphism, coarse chromatin, prominent nucleoli, irregular nuclear membrane, and high mitotic/apoptotic rate.

Results: HPV was found in 63 (31%) cases. High-grade features were present in 84 (42%) of all cases. Seventy tumors (35%) showed warty and/or basaloid features. Tables 1 and 2 shown association between HPV status and histological grade in all cases, and according to the presence of WB features, respectively.

Table 1

	No. cases	HPV+ (%)	HPV- (%)
Low-grade	118	19 (16)	99 (84)
High-grade	84	44 (52)	40 (48)

P<0.001

Table 2

Tumors with WB features	No. Cases	HPV+ (%)	HPV- (%)	P-value
Low-grade	20	7 (35)	13 (65)	P=0.016
High-grade	50	34 (68)	16 (32)	
Tumors without WB features	No. Cases	HPV+ (%)	HPV- (%)	P-value
Low-grade	98	12 (12)	86 (88)	P=0.031
High-grade	34	10 (29)	24 (71)	

Conclusions: HPV-related penile SCCs were of higher grade than HPV-unrelated tumors. Most HPV related WB carcinomas were of high grade. One third of high-grade non WB carcinomas were also associated with HPV. Knowing the impact of histological grade in the prognosis of patients with penile carcinomas the role of HPV as an adverse factor needs to be considered.

774 Distinctive Inmunohistochemical Profiles of Penile Intraepithelial Lesions – A Study of 74 Cases.

A Chaux, R Pfannl, IM Rodriguez, JE Barreto, EF Velazquez, GJ Netto, AL Cubilla. Johns Hopkins University, Baltimore, MD; Tufts Medical Center, Boston, MA; Instituto de Patología e Investigación, Asunción, Paraguay; Caris Life Sciences, Boston, MA.

Background: A new nomenclature of penile precancerous lesions have been proposed taking into consideration morphological and etiological factors. It is important to separate differentiated, HPV-unrelated penile intraepithelial neoplasia (PeIN) from nondifferentiated, HPV-related warty and basaloid PeIN.

Design: In order to determine the value of inmunohistochemical stains in the differential diagnosis and classification of PeIN 74 lesions classified as squamous hyperplasia (18 cases), differentiated (37 cases), basaloid (15 cases), and warty PeINs (4 cases) were pathologically evaluated using immunohistochemistry for p16INK4a, p53, and Ki67 expression. p16INK4a positivity required continuous, full thickness, nuclear and cytoplasmic stain in all epithelial cells. Intraepithelial lesions exhibiting p53 and Ki67 suprabasal or full thickenss nuclear staining were considered as positive.

Results: Results are depicted in Tables 1 and 2.

Table 1

	SH (%)	DPeIN (%)	BPeIN (%)	WPeIN (%)
p16INK4a+	0 (0)	2 (5)	14 (93)	4 (100)
p53 +	1 (6)	16 (43)	6 (43)	4 (100)
Ki67 +	8 (47)	28 (90)	15 (100)	4 (100)

Table 2: Profiles of immunoexpression

	p16INK4a	p53	Ki67
SH	Negative	Negative	Pos or Neg
DPeIN	Negative	Pos or Neg	Positive
W/BPeIN	Positive	Pos or Neg	Positive

Conclusions: p16INK4a distinguished SH and DPeIN from W/BPeIN while p53 can be used to separate SH from DPeIN and W/BPeIN. Ki67 is usually positive in DPeIN and W/BPeIN. The immunohistochemical profiles of penile precancerous lesions are distinctive and useful in the classification and differential diagnosis of PeIN.

775 Mesonephric Remnant Hyperplasia Involving the Prostate and Periprostatic Tissue: Findings at Radical Prostatectomy (RP).

Y-B Chen, S Fine, JI Epstein. Memorial Sloan-Kettering Cancer Center, New York; The Johns Hopkins Hospital, Baltimore.

Background: As an exceedingly rare benign mimicker of prostate cancer, the anatomic locations, histologic spectrum and immunohistochemical (IHC) profile of mesonephric remnant hyperplasia have not been well studied.

Design: We retrospectively studied 10 cases of mesonephric remnant hyperplasia involving the prostate and periprostatic tissue, including 8 cases at RP.

Results: Patients ranged in age from 48-70y (mean 60). 7 had concurrent prostatic adenocarcinoma and underwent RP; 1 underwent RP as a result of a misdiagnosis at an outside institution of mesonephric remnant hyperplasia as prostate cancer; and 2 had TURP for urinary obstruction. Lesions in the prostate and periprostatic tissue

were concentrated in 2 areas: 1 was the anterior fibromuscular stroma and adjacent anterolateral periprostatic tissue (6/8); and the other was posteriorly and posterolaterally towards the base within the prostate or in periprostatic tissue, and around the seminal vesicle (4/8). Histological patterns included: small-medium acini/tubules with a lobular distribution (9/10), cysts with secretions either in clusters or scattered (8/10), small or ill-formed glands with an infiltrative growth (7/10), glands with papillary infolding or micropapillary tufts (4/10), and 2 cases exceptionally displayed nodules of ill-formed small glands intermixed with spindle cells, mimicking sclerosing adenosis or Gleason pattern 5 prostate cancer. Most cases (7/10) had ≥3 growth patterns. By IHC, all cases were negative for PSA. Cytokeratin 34βE12 was diffusely positive in 4/9 cases, and only focally in the remaining 5 cases. The intensity of 34βE12 was weaker than basal cells of adjacent prostatic glands. p63 was largely negative with only focal positivity in 4/7 cases. Racemase was focally positive in 4/7cases. Small glands with an infiltrative pattern, which most closely mimicked prostate cancer on H&E, often also had an IHC pattern typical of prostate cancer; glands were negative (3/6) or only focally positive (3/6) for 34βE12, negative for p63 (6/6), and focally positive for racemase (4/6). All cases were diffusely positive for PAX8.

Conclusions: This study by having RP material was able to show the novel finding of some cases of mesonephric remnant hyperplasia presenting as a florid growth anteriorly in the prostate, closely mimicking prostate cancer. Also a new H&E pattern was described. While basal cell markers and racemase are unreliable IHC markers, PAX8 and PSA are helpful to distinguish them from prostate adenocarcinoma.

776 Primary Carcinoid Tumors of the Urinary Bladder and Prostatic Urethra: A Clinicopathologic Study of 7 Cases.

Y-B Chen, JI Epstein. The Johns Hopkins Hospital, Baltimore, MD.

Background: Only 8 histologically well-documented cases of pure primary carcinoid tumors of the bladder and 1 of the urethra have been reported in the literature. Although they have been considered as potentially malignant, some prior reports were associated with carcinoma that might have altered the outcome.

Design: We describe 7 additional primary pure carcinoid tumors arising in the bladder (5 cases) or prostatic urethra (2 cases).

Results: Patients (5 males, 2 females), mean age 52 (35-60), presented with hematuria (n=5/7), obstruction (n=2/7) or for concurrent genitourinary diseases (n=1/7). The 5 bladder cases were located within or near the trigone and bladder neck. 6 cases shared gross and microscopic findings. Cystoscopy revealed small smooth-surfaced or polypoid nodules. Microscopically, these 6 tumors were subepithelial and confined within lamina propria, associated with adjacent cystitis cystica et glandularis. Tumors were composed of uniform cuboidal or columnar cells with finely stippled chromatin and inconspicuous nucleoli with a prominent pseudoglandular pattern composed of acinar and cribriform structures. Cells had moderate to abundant cytoplasm and basally located Paneth cell-like eosinophilic granules. Although occasional atypical cells with prominent nucleoli could be seen, mitotic activity was absent or rare and cases lacked necrosis. The 7th case was estimated to be at least 3 to 4 cm. In contrast to the other 6 cases, the predominant histologic patterns of this tumor consisted of tightly packed anastomosing trabeculae and large nests with a pseudoglandular pattern, while deeper areas demonstrated cords, small nests or individual cells in dense fibrotic stroma. Eosinophilic cytoplasmic granules were not identified. Despite involvement of the muscularis propria, the lesion was cytologically bland, lacked necrosis, and had only 1 mitosis/10 HPF. Neuroendocrine differentiation was confirmed by immunohistochemistry in all 7 cases. 6 of 7 tumors were completely excised by biopsies. There was no evidence of disease recurrence or progression in all 6 patients who had complete excision, including 3 patients who had clinical follow-up for more than 4 years.

Conclusions: Primary pure bladder/urethral carcinoids have distinct pathologic characteristics, with their prominent pseudoglandular features leading to difficulty in their diagnosis. Bladder/urethral carcinoids have a very favorable clinical outcome, and should be distinguished from mixed carcinoid tumors or urothelial carcinomas with neuroendocrine differentiation that display focal carcinoid-like histologic features.

777 Cancer/Testis (CT) Antigens Show Differential Expression in Seminomas and Non-Seminomatous Germ Cell Tumors.

Y-T Chen, D Cao, R Chiu, LJ Old. Weill Cornell Medical College, New York; Washington University School of Medicine, St. Louis; Ludwig Institute for Cancer Research, New York.

Background: Cancer/testis (CT) antigens comprise a group of proteins that are normally only expressed in germ cells and yet are aberrantly activated in a wide variety of human cancers. In adult testis, many CT antigens show restricted expression in spermatogonia and primary spermatocytes. We recently showed that multiple CT antigens are expressed in fetal gonads, but only in germ cells that have lost the expression of OCT3/4, a pluripotent cell marker expressed in all seminoma and embryonal carcinoma, but not in other germ cell tumors.

Design: Expression of 7 CT antigens (MAGEA, NY-ESO-1, GAGE, CT7, CT10, CT45 and SAGE1) was evaluated immunohistochemically in 76 classical seminomas by tissue microarray and on whole sections on selected cases. Other germ cell tumors, including 24 embryonal carcinomas, 20 yolk sac tumors, 9 teratomas, 3 choriocarcinomas and 2 spematocytic seminomas, were evaluated using whole sections. Co-expression of OCT3/4 and CT antigens was evaluated by double staining of OCT3/4 and CT7 (or OCT3/4 and MAGEA).

Results: Classical seminomas expressed different CT antigens in highly variable frequencies, ranging from >80% (CT7, CT10, CT45 and GAGE), 63% (MAGEA), 18% (NY-ESO-1) to only 4% (SAGE1). Intratubular germ cell neoplasia (ITGCN), uniformly OCT3/4-positive, were almost always CT-negative, even in CT-positive classical seminomas. In comparison, both spermatocytic seminomas, including the intratubular growth component, showed diffuse strong expression of all 7 CT antigens. Non-seminomatous germ cell tumors expressed CT antigens much less frequently and often showed heterogeneous staining patterns in most cases. 21 of 24 embryonal carcinomas were either CT-negative (10 cases) or positive in <5% of the tumor cells (11 cases), and diffuse staining was observed in a single case. Similarly, teratomas were CT-negative (5/9) or minimally positive (4/9). Twelve of 20 yolk sac tumors and 2 of 3 choriocarcinomas expressed at least 1 CT antigen, but showed more focal staining than in seminomas.

Conclusions: Spermatocytic seminomas, originated from adult germ cells, retain their physiological expression of CT antigens. Classical seminomas, arising from prenatal gonocytes, show frequent CT antigen expression but not in ITGCN. Non-seminomatous germ cell tumors express CT antigens less frequently and often in small subsets of tumor cells. These differences likely reflect the different origin and differentiation states of the germ cell tumors.

778 Molecular Genetic Evidence Supporting the Neoplastic Nature of Fibrous Stroma in Testicular Teratoma.

L Cheng, S Zhang, SDW Beck, RS Foster, TM Ulbright. Indiana University, Indianapolis.

Background: Testicular teratoma consists of heterogeneous mixtures of diverse epithelial and stromal components. The biological nature and genetic characteristics of the fibrous stroma have not been adequately investigated.

Design: The fibrous stroma and other components from 21 testicular teratoma patients were investigated separately for chromosome 12 anomalies, including isochromosome 12p [i(12p)] and 12p overrepresentation using interphase fluorescence in situ hybridization analysis. All the cases contained only teratoma in the orchiectomy specimens.

Results: Overall, 90% (19/21) of the cases of fibrous stroma had chromosome 12p abnormalities. Isochromosome 12p was detected in 11 of 21 (52%) cases of fibrous stroma, and chromosome 12p overrepresentation was detected in 13 of 21 (62%) cases of fibrous stroma. Among the 11 cases of i(12p)-positive fibrous stroma, 5 (45%) also had 12p overrepresentation. Five of the 13 (38%) cases of fibrous stroma with 12p overrepresentation also had i(12p). Only 2 of 17 cases (12%) of fibrous stroma showed neither 12p overrepresentation nor the presence of i(12p). Isochromosome (12p) and 12p overrepresentation were identified in the gastrointestinal epithelium of 12/17 (71%) and 15/17 (88%) cases; in the respiratory epithelium of 3/8 (38%) and 6/8 (75%) cases; in the squamous epithelium of 5/7 (71%) and 5/7 (71%) cases; and in the cartilage of 4/5 (80%) and 0/5 (0%) cases, respectively. Concordant chromosomal 12p abnormalities were observed between the fibrous stroma and epithelial elements of testicular teratomas.

Conclusions: Our results show that the fibrous stroma of testicular teratomas frequently has genetic abnormalities similar to those of the teratomatous epithelial components. Concordant chromosome 12p alterations between the fibrous stroma and teratomatous epithelial elements provide further evidence that both epithelial and fibrous components of teratoma are derived from a common progenitor.

779 Metastatic Tumors to the Urinary Bladder.

J Chow, PD Unger, G-QQ Xiao. Mount Sinai School of Medicine, New York, NY.

Background: Secondary neoplasms involving the bladder are uncommon. True metastatic tumors to the bladder (MTB) are even rarer. Our experience with MTB along with the clinicopathologic findings is presented.

Design: We define bladder metastases as secondary tumors within the muscularis or lamina propria of the bladder, with the exclusion of direct extension of tumors from adjoining organs. A total of 15 cases of MTB were found from our archives between 1995 and 2010. Pathologic and clinical findings were recorded.

Results: 11/15 cases occurred in female patients. 9/11 individuals presented with hematuria or obstructive urinary symptoms. 9 cases were diagnosed by transurethral resection of bladder tumor, 2 cases were obtained by biopsy, and 4 cases were discovered on autopsy. 10/11 patients had MTB in the region of the trigone, posterior wall, or bladder neck. The vast majority presented with cystoscopic findings of a mass, nodule, or thickened bladder wall, with overlying normal appearing bladder mucosa. 11/14 had concomitant metastases elsewhere. 8/11 patients died within 2 years of being diagnosed with bladder metastases. Breast (3/15) and gastric (3/15) malignancies were the most common MTB. MTB from ileal carcinoid tumor, ileal gastrointestinal stromal tumor, pancreatic gastrinoma, and renal collecting duct carcinoma have not been previously reported in the literature. Results are summarized in the table.

Clinicopathologic Features of MTB

Age	Sex	Primary Tumor	Bladder Location	Other Metastasis	Bladder Metastasis to Death (months)
53	F	B Ca, Pleomorphic Lobular	T,N	+	0.5
46	F	B Ca, Lobular	T,P	-	1
76	F	B Ca, Ductal	N,Periurethra	U	U
77	M	G Ca, Poorly Differentiated	T,P	+	6
33	M	G Ca, Signet Ring	T	+	1
83	F	G Ca, Signet Ring	T	+	1.5
51	F	Ileal Carcinoid	U	+	A
72	M	Ileal Gastrointestinal Stromal	U	+	U
94	F	Endocervical Adenocarcinoma	Left Ureteral Orifice	-	A
70	F	Fallopian Tube Ca, Serous Papillary	U	+	12
65	F	Ovarian Ca, Squamous	U	+	U
70	M	Gallbladder Adenocarcinoma	T,P	+	18
46	F	Pancreatic Gastrinoma	T,Right Dome	+	A
80	F	Renal Collecting Duct Ca	N	-	9
88	F	Lung Adenocarcinoma	P	+	U

B=Breast, G=Gastric, Ca=Carcinoma, T=Trigone, N=Neck, P=Posterior Wall, U=Unknown, A=Alive, + Present, - Absent

Conclusions: MTB usually occur late in the course of disease, with the majority of patients presenting with urinary symptoms. MTB have a greater affinity for specific regions of the bladder. For proper therapy, MTB must be distinguished from primary bladder neoplasms. Clinical correlation and morphologic recognition supplemented with immunohistochemistry is essential for reaching a correct diagnosis.

780 Evidence for Clonal Fibroblast Proliferation and Autoimmune Process in Idiopathic Retroperitoneal Fibrosis.

JA Clevenger, M Wang, GT MacLennan, R Montironi, A Lopez-Beltran, L Cheng. Indiana University, Indianapolis; Case Western Reserve University, Cleveland, OH; Polytechnic University of the Marche Region, Ancona, Italy; Cordoba University, Spain.

Background: Idiopathic retroperitoneal fibrosis is a rare disease in which retroperitoneal structures are encased by fibrosis and chronic inflammation. Its etiology is unclear. This study seeks to better characterize the disease process through clonality studies and IgG4 analysis. First, we sought to determine if idiopathic retroperitoneal fibrosis is a clonal fibroblast proliferation by performing X-chromosome inactivation analyses. Second, IgG4-related sclerosing diseases have been well established at other body sites, so we sought to determine if idiopathic retroperitoneal fibrosis is an IgG4-driven process.

Design: Forty-five cases of idiopathic retroperitoneal fibrosis diagnosed between 1991 and 2010 were retrieved from the surgical pathology archives of the participating institutions. Cases with known causes of secondary fibrosis were excluded. Clonality studies were restricted to female patients and were performed on 18 specimens from 16 patients. Genomic DNA samples were prepared from formalin-fixed, paraffin-embedded tissue sections using laser-capture microdissection. X-chromosome inactivation analyses were performed on fibroblasts within the fibrous. IgG4 and ALK immunohistochemistry was performed on 30 specimens from 28 patients. IgG immunohistochemistry was performed only on the cases with positive IgG4 staining. The patients ranged in age from 19 to 71 years (mean 53 years) and included both males and females (M:F=1.46:1).

Results: For the clonality analysis, 17 specimens were informative and 1 specimen was non-informative. 8 cases (47%) showed non-random X-chromosome inactivation. Two separate specimens were received in one of the 8 cases showing non-random X-chromosome inactivation, and concordant X-chromosome inactivation patterns were observed. Of the 30 specimens for which IgG4 analysis was performed, 16 cases (53%) were positive for IgG4-positive plasma cells. All 30 specimens were negative for ALK. Of the cases positive for IgG4, IgG staining was also performed, and the IgG4:IgG ratio ranged from 0.30 to 1.00 (mean 0.83).

Conclusions: Our clonality analysis indicates that a significant proportion of cases of idiopathic retroperitoneal fibrosis are associated with a clonal expansion of fibroblasts. Our finding of IgG4-positive plasma cells in 53% of the cases provides evidence that a subset of idiopathic retroperitoneal fibrosis cases could be classified in the IgG4-related sclerosing disease spectrum.

781 Sarcomatoid Renal Cell Carcinoma Is an Example of Epithelial-Mesenchymal Transition.

JL Conant, Z Peng, MF Evans, S Naud, KC Cooper. University of Vermont College of Medicine, Burlington.

Background: Sarcomatoid renal cell carcinomas (SRCC) are composed of a sarcomatous component (SC) and a carcinomatous component (CC). Studies suggest that mesenchymal cells in SC have undergone a morphologic change from their epithelial origin through a process known as epithelial-mesenchymal transition (EMT). In EMT, cells lose their epithelial characteristics and gain a mesenchymal phenotype, leading to an increased ability to migrate and metastasize. The goal of this study was to evaluate cadherin switching, membranous vs. cytoplasmic/nuclear localization of β-catenin, and expression of Snail (Snai1, an E-cadherin transcriptional repressor) and SPARC (a mesenchymal marker) in SC and CC to determine if SRCC is an example of EMT.

Design: E-cadherin, N-cadherin, β-catenin, Snail, and SPARC expression was analyzed by immunohistochemistry on SC and CC of 21 formalin-fixed, paraffin-embedded SRCC specimens. Expression was scored as absent, mild, moderate, or strong according to intensity and extent (composite score 0-6).

Results: E-cadherin expression was decreased in SC compared to CC (Wilcoxon signed-rank test, p=0.0004) while N-cadherin expression was similar (p=0.46). Membranous β-catenin expression was decreased in SC (p<0.0001), but cytoplasmic expression was increased (p=0.0002). No nuclear expression of β-catenin was seen. Snail and SPARC were more likely to be expressed in SC (p=0.002 and <0.0001). When the scores were dichotomized into absent/mild and moderate/strong expression levels, the results using McNemar's test substantiated the results above (Table 1).

Table 1: Composite Score Expression in SC and CC

Marker	% SC¤	% CC¤	Mean Difference	McNemar's Test P-value
E-cadherin	5	48	-2.4*	0.004
N-cadherin	95	95	0.2	1.000
β-catenin (membranous)	24	95	-3.3*	<0.0001
β-catenin (cytoplasmic)	52	22	1.9*	0.03
Snail	100	81	1.0*	0.046
SPARC	100	48	1.9*	0.0009

¤percent with moderate/strong expression (composite score 4-6); *statistically significant

Conclusions: E- to N-cadherin switching, dissemination of β-catenin into the cytoplasm, and increased expression of Snail and SPARC in SC indicate that SRCC is an example of EMT. Increased expression of N-cadherin and Snail in CC suggest involvement in initiating EMT, before mesenchymal phenotypic expression. Once EMT is established, the loss of E-cadherin, release of β-catenin into the cytoplasm, and expression of SPARC correspond with SC seen in SRCC. Future studies will compare these markers in CC to non-sarcomatoid renal cell carcinomas.

782 Large Nested Pattern of Urothelial Carcinoma (UC): 17 Cases of a Novel Variant.

RM Cox, JI Epstein. The Johns Hopkins Hospital, Baltimore, MD.

Background: We describe a unique pattern of UC invasion consisting of large, irregular to regular nests with bland cytology.

Design: We prospectively retrieved 17 cases of large nested UC from one of the author's consult files (2004-2010).

Results: Mean patient age was 60.8 years (31-81), 82% male. 15/17 cases were TURBT, 1 a nephroureterectomy, and 1 a radical cystectomy (RC). 14/17 had low grade papillary UC as the surface component, 1 case high grade papillary UC, 1 low grade papillary UC with focal (<5%) high grade component, and 1 no surface component. 15/17 invaded into muscularis propria (MP), 1 into lamina propria (LP) with no MP present, and 1 into smooth muscle indeterminate between muscularis mucosae and MP. In all cases, the invasive component was composed of medium-large nests with irregular to regular shaped borders. 1 showed a verruciform, pushing border into the MP with the nests having central cyst formation. Nuclei lacked hyperchromasia with only mild-moderate nuclear atypia. Occasional slightly enlarged, hyperchromatic nuclei with small-indistinct nucleoli were noted. In 4 cases there was focal and 1 case more extensive necrosis. The mean mitotic count per 10 HPFs was 5.5 (range 0-39). A mild-moderate fibrous and/or inflammatory stromal reaction was present surrounding the nests in 13/17 cases with in 1 case a marked reaction; the remaining 3 cases had no stromal reaction. In 12/17 cases, the large, bland nests were the only invasive component present. Focal (<5%) areas of conventional invasive UC were identified in 4/17 cases; 1 case had an invasive component comprised of 70% large nests and 30% conventional UC. 1/17 cases had angiolymphatic invasion. 4 cases had subsequent RC available for review. 2/4 RC's had no residual carcinoma, 1 had large nested UC in MP, and 1 had mixed large nested UC and focal conventional UC invading through the MP into perivesicle tissue. Clinical follow-up was available for 15/17 patients [mean f.u. 35.8 months (5-52 mos)]. 3/15 developed metastatic disease (2 lung, 1 unknown) with 2 of these dead of disease; another patient was dead of disease with no known details. Of the 3 patients that died of disease, 2 had no and 1 had focal (<5%) conventional invasive UC on TURBT.

Conclusions: These cases which posed great diagnostic difficulty both for contributing pathologists as well as for the consultant represent the first description of a large nested pattern of UC that is distinguished from an inverted growth pattern of non-invasive UC by either MP invasion, irregularly infiltrating nests, or a stromal reaction. These tumors despite bland cytology have metastatic potential.

783 mTOR Pathway Activation in pT1 Urothelial Cell Carcinomas of the Bladder: A Potential Target of Therapy.

R Cox, A Chaux, J Solus, L Schultz, A Demarzo, E Comperat, GJ Netto. Johns Hopkins University, Baltimore, MD; Hopital Pitié, Paris, France.

Background: The mammalian target of rapamycin (mTOR) pathway has been implicated in a variety of urological malignancies, including urothelial carcinoma of the bladder. Currently, several ongoing clinical trials are evaluating the usefulness of pharmacological agents targeting this pathway. However, there is scant information on mTOR pathway activation in bladder carcinomas with invasion limited to lamina propria. Herein we assess the expression of mTOR pathway protein members and their prognostic role in predicting recurrence and progression in pT1 urothelial carcinomas of the bladder.

Design: Tissue microarrays (TMA) were constructed from 195 consecutive cases of pT1 papillary urothelial carcinomas of the bladder. Each tumor was represented by up to three 1-mm spots. Standard immunohistochemistry analysis for mTOR pathway members (PTEN, phos AKT, mTOR, phos S6, and phos 4EBP1) was performed. H-score was generated for each marker as a product of intensity (0 to 3+) by percent of positive cells. PTEN H-score <10 was considered as PTEN loss; any H-score >0 was considered positive for the remaining four mTOR pathway-related proteins.

Results: Loss of PTEN was found in 18.5% of tumors; phos AKT, mTOR, phos S6, and phos 4EBP1 were expressed in the majority of cases (expression rates of 83.1%, 75.4%, 80.5%, and 74.4%, respectively).

Table 1: Expression rates of mTOR pathway members in pT1 urothelial carcinoma (%)

	phos AKT+	mTOR+	phos S6+	phos 4EBP1+
PTEN loss	58.3	55.6	75.0	52.8
No PTEN loss	88.7	79.9	81.8	79.2
P-value	<0.0001	0.005	0.357	0.002

PTEN loss and immunoexpression levels of the four studied mTOR pathway proteins failed to predict recurrence or progression in the current cohort (P>0.05).

Conclusions: We found high expression rates of mTOR pathway members in pT1 stage urothelial carcinomas of bladder indicating activation of the mTOR pathway in the superficially invasive phase of disease. The current findings support a potential role for mTOR-targeted pharmacological therapies in superficially invasive bladder cancer. Our data suggests that PTEN loss may be responsible for only a minor fraction of such activation. Alternate molecular mechanisms may be implicated in our observed mTOR pathway activation.

784 Phimosis, Lichen Sclerosus, Smoking, Poverty, Sexually Related Epidemiological Factors and Late Diagnosis Are Prevalent among Patients with Penile Cancer in Paraguay.

AL Cubilla, A Chaux, IM Rodriguez, JE Barreto, GJ Netto, FX Bosch, S de Sanjose, N Munoz, A Hildesheim. Instituto de Patología e Investigación, Asuncion, Paraguay; Johns Hopkins University, Baltimore, MD; Instituto Catalán Oncológico, Barcelona, Spain; CIBER Epidemiologia y Salud Pública, Barcelona, Spain; National Cancer Institute, Bethesda, MD.

Background: The incidence of penile carcinoma in Paraguay is among the highest worldwide (4x100.000). Penile cancer has been related to environmental factors,

including human papillomavirus (HPV) infections. This study was designed to generate epidemiological data to guide future studies and a cancer control program.
Design: A questionnaire (prospectively administered to 103 patients referred to a Penile Cancer Center between 1993-2007) obtained information on age, residence, education, income, smoking, hygiene and sexual habits, and history of sexually transmitted diseases. Medical record abstraction collected information about tumor site and foreskin features. All cases were pathologically proven invasive penile carcinomas.
Results: Median age was 62 years. Tumors were large, involving multiple compartments in 56% of cases. Tumors exclusive of glans, foreskin or skin of the shaft were less frequent (32%, 11%, and 1%). Phimosis was detected in 57% of cases and the major cause was lichen sclerosus, present in 74% of such patients. Patients lived in either semi rural or rural regions (83%) and were typically moderate to heavy smokers (76%). A history of STD was present in 74% of the cases; 58% of the patients had more than 10 life-time female sexual partners. Minimal education and poverty were characteristic (91% and 75%). Histologically, 102 cases were squamous cell carcinomas (SCC) and 1 case was a clear cell carcinoma; 67% of carcinomas showed an associated lichen sclerosus. Evidence of HPV infection (evaluated by SPF-10 PCR in formalin-fixed, paraffin-embedded tissues in 86% of all cases) was found in 36% of tumors. Twenty-four percent of all patients received inguinal dissection and nodal metastasis was present in 72% of such cases.
Conclusions: Penile cancer patients in Paraguay are poorly educated smokers of low socio-economic conditions, living in semi-rural or rural areas of the country. They frequently report history of sexually transmitted diseases and a high number of female partners. Phimosis and lichen sclerosus are prevalent. Their tumors are typically large and locally advanced, with a high regional metastatic rate. These data may guide planning of a penile cancer public health control program in Paraguay.

785 Sexual History and Distinctive Pathological Features in HPV-Related Penile Carcinomas.

AL Cubilla, A Chaux, IM Rodriguez, JE Barreto, GJ Netto, FX Bosch, S de Sanjose, N Munoz, A Hildesheim. Instituto de Patología e Investigación, Asunción, Paraguay; Johns Hopkins University, Baltimore, MD; Instituto Catalán Oncológico, Barcelona, Spain; CIBER Epidemiologia y Salud Pública, Barcelona, Spain; National Cancer Institute, Bethesda, MD.
Background: Two distinct forms of penile squamous cell carcinomas (SCC) have been reported, one that is related to human papillomavirus (HPV) and another that is not. This study was designed to compare epidemiological and pathological characteristics for these two forms of penile SCC.
Design: A questionnaire was administered to 89 prospectively ascertained patients with invasive penile carcinomas at a Penile Cancer Reference Center in Paraguay. Data collected included: patients age, tumor site, residence (urban or rural), socioeconomic status, educational level, smoking, sexual and hygiene habits, and sexually transmitted disease history. Clinico-pathological data abstracted from records included: histological subtype, histological grade, p16INK4a staining status by IHC, presence of adjacent intraepithelial neoplasia (PeIN), presence of lichen sclerosus (LS), and nodal status. HPV was detected in paraffin embedded tumor tissue by PCR (SPF-10 with LIPA-25 genotypification). Categorical variables were compared using the Fisher's exact test. Student's t-test was used to compare continuous data. Odds ratios (OR) and 95% confidence intervals (95% CI) were calculated using logistic regression. A 2-tailed $P<0.05$ was required for statistical significance.
Results: HPV was present in 36% of cases. No significant risk factor differences were noted between HPV+ and HPV– patients, with one exception: HPV+ patients reported a higher number of female partners than HPV- patients (OR = 3.8 [95% CI = 3.1–4.6] for 10+ partners vs. <6 partners; p-trend = 0.03). Tumors with warty/ basaloid (WB) morphology, of high grade, and positive for p16INK4a were more likely to be HPV-related (all P-values ≤0.005). Differentiated PeIN and lichen sclerosus were more frequent in HPV– cases while WB PeIN was more frequently found in HPV+ tumors (p-values ≤0.001). Rates of inguinal metastasis were similar in both groups.
Conclusions: HPV positive tumors revealed distinctive pathological features: high grade, WB morphology, p16INK4a positivity and paucity of LS. Epidemiologically, a history of more female sexual partners was observed among HPV+ compared to HPV– patients.

786 Determining Carcinoma Extent Based on Percentage in Radical Prostatectomy (RP) Specimens by Non-Genitourinary Pathologists (N-GUPs) and Pathology Trainees (PTs).

V Dailey, O Hameed, Prostate Carcinoma Extent Group. University of Alabama at Birmingham.
Background: It is recommended that some measurement of tumor extent be provided when reporting carcinoma in RP specimens. We previously demonstrated that there was excellent agreement between visual tumor extent measurements among GUPs and image analysis. The aim of this study was to see if this can be replicated in N-GUPs and PTs.
Design: Replicate slides (n=108) of 10 partially-embedded RP specimens (9-15 slides/ case) were circulated to 7 N-GUPs and 9 PTs. PTs were first asked to estimate percentage of carcinoma in 5 specimens without any additional instructions. Following distribution of written instructions, all participants were asked to estimate the percentage of prostatic tissue involved by carcinoma in each section and to use the average to derive the total percentage of prostate involved by tumor. These percentages were broken down into 4 categories (< 5%, 6% to 20%, 21% to 50%, and > 50%) that have been found to correlate well with outcome (Urol. 2008;180:571) and compared with those obtained by image analysis to obtain agreement statistics. These were then compared with the agreement statistics among GUPs.
Results: Although there were no significant differences in the agreement rates (ARs) and kappa values between N-GUPs and PTs, they were significantly different from those among GUPs (Table). Both N-GUPs and PTs were more likely to underestimate the extent of carcinoma compared to GUPs. There was no correlation between years of experience (6-37 years; mean 22 years) and agreement statistics among N-GUPs. Although written instructions led to higher mean ARs (64% vs. 71%) and kappa values [0.57 vs. 0.60 (unweighted) and 0.67 vs. 0.72 (weighted)] among PTs, the differences were not statistically significant.
Conclusions: N-GUPs and PTs tend to underestimate the extent of prostatic carcinoma based on visual estimation. This could be potentially improved by additional training of pathology residents and fellows.

Parameter	N-GUP	PT	GUP	P value N-GUP vs. GUP	P value PT vs. GUP
Agreement rate					
Range	40 – 80	50 – 90	80 – 100	0.0004	0.0025
Mean ± SEM	71.4 ± .5.53	74.4 ± 5.56	92.1 ± 2.14		
Unweighted kappa					
Range	0.13 - 0.72	0.21 - 0.84	0.70 – 1.0	0.0002	0.0021
Mean ± SEM	0.56 ± 0.08	0.62 ± 0.08	0.88 ± 0.03		
Weighted kappa					
Range	0.36 – 0.80	0.36 - 0.87	0.84 – 1.0	0.0001	0.0023
Mean ± SEM	0.65 ± 0.06	0.71 ± 0.06	0.91 ± 0.02		

787 Focal Prostate Atrophic Lesions and Risk of Lethal Prostate Cancer.

S Davidsson, M Fiorentino, O Andren, F Fang, LA Mucci, E Varenhorst, K Fall, JR Stark. Orebro University Hospital, Orebro, Sweden; Bologna University, Italy; Brigham & Women´s Hospital, Boston, MA; Harvard School of Public Health, Boston, MA; Linkoping University Hospital, Linkoping, Sweden; Karolinska Institute, Stockholm, Sweden.
Background: Repeated tissue damage and regeneration in a highly reactive microenviroment may contribute to cancer development and progression, including prostate cancer. Chronic inflammation in the prostate is often associated with focal glandular atrophy, especially post-atrophic hyperplasia (PAH) and simple atrophy (SA). It has been hypothesized that these lesions in the presence of inflammation may represent a precursor of prostate cancer (PCa).
Design: We investigated PIA and cancer mortality in a cohort of Swedish men diagnosed through TURP between 1977-99 with early PCa stage T1a-b tumors. We utilized an "extreme" case-control design by selecting as cases men who died of PCa within 10 years after diagnosis (n=228) and as controls men who survived more than 10 years after PCa diagnosis without any metastases (n=387). Slides were assessed for Gleason grade, presence and type of inflammation. Focal prostate atrophy was characterized according to a new atrophic classification. We used multivariable logistic regression to calculate odds ratios (OR) and 95% Confidence Intervals (CI).
Results: We identified chronic inflammation in 74% of the specimens. SA (59.4%) and PAH (20.3%) were the two most common atrophy lesions present. We found that HGPIN was more frequently observed in tumors with evidence of PAH (22% PAH positive vs.11% PAH negative; $p<0.001$). We found no overall association between either SA or PAH and lethal PCa. However, the association between PAH and lethal PCa was modified by degree of chronic inflammation (p-interaction =0.02). In patients with moderate or severe chronic inflammation the presence of PAH was associated with a 2-fold increased risk of PCa death compared to those without evidence of PAH (OR: 2.05; 95% CI: 0.81-5.21).
Conclusions: This study provides evidence that PAH lesions may have prognostic significance for PCa in the presence of inflammation. Chronic inflammation was a common feature in men with PCa and present in almost all specimens with evidence of PAH. HGPIN was more frequently observed in tumors with PAH present. A higher frequency of PAH lesions in an environment of chronic inflammation may result in more cells sensitive to DNA alterations, enhancing the potential for epithelial transformations that may lead to lethal PCa.

788 Renal Cell Carcinoma with Novel *VCL-ALK* Fusion: New Representative of ALK-Associated Tumor Spectrum.

L Debelenko, S Raimondi, N Daw, B Shivakumar, M Nelson, D Huang, J Bridge. St. Jude Children's Hospital, Memphis, TN; Nebraska Medical Center, Omaha.
Background: Renal cell carcinoma (RCC) represents a model for contemporary classification of solid tumors; however, unclassifiable cases exist and are not rare in children and young adults. The anaplastic lymphoma kinase (*ALK*) gene has recently been implicated in subsets of pulmonary, esophageal, breast, and colon cancer strengthening the importance of molecular classification of carcinomas across different organ sites, especially considering the evolving therapies with ALK inhibitors.
Design: We studied 6 pediatric RCCs from the files of our institutions; conventional cytogenetic analyses were performed in 2 cases and all 6 cases were subjected to fluorescent in situ hybridization (FISH) with the Vysis LSI ALK break apart rearrangement probe (Abbott Molecular) and immunohistochmistriy (IHC) with the ALK/p80 monoclonal antibody (ThermoFisher Scientific). Rapid amplification of cDNA ends (RACE) was performed in 1 ALK-positive case using the 5'RACE system from Invitrogen. Western blot analysis was performed using standard protocols and ALK/p80 and hVIN-1 (Sigma-Aldrich) antibodies. Appropriate controls were run for each experiment.

Results: Two pediatric RCCs exhibited structural karyotypic abnormalities involving the *ALK* locus on chromosomal band 2p23. FISH studies were positive for an *ALK* rearrangement in one case with unusual histology and subsequent 5'RACE analysis of this tumor revealed that the 3' portion of the *ALK* transcript encoding for the kinase domain was fused in frame to the 5' portion of vinculin (*VCL*). The new fusion gene is predicted to have an open reading frame of 4122 bp encoding for a 1374-aa oncoprotein; its expression in the tumor was shown by immunoblotting and IHC with anti-VCL and anti-ALK antibodies; IHC demonstrated cytoplasmic and subplasmalemmal localization of the oncoprotein determined by its N-terminal VCL portion. FISH with a custom-designed VCL-ALK dual-fusion probe set confirmed the presence of the fusion in neoplastic cells. The 5 remaining RCCs did not show *ALK* rearrangement by FISH or ALK expression by IHC.
Conclusions: The data identify the kidney as a new organ site for ALK-associated carcinomas and *VCL* as a novel *ALK* fusion partner. The results should prompt further studies to advance the molecular classification of RCCs and help to select patients who would benefit from appropriate targeted therapies.

789 Periprostatic Lymph Node Metastasis in Prostate Cancer and Its Clinical Significance.

F-M Deng, SE Mendrinos, K Das, J Melamed. New York University Medical Center, NY.
Background: Lymph node (LN) stage in prostate cancer (PCa) is traditionaly based on evaluation of pelvic lymph nodes. The potential of the periprostatic lymph node incidentaly discovered in the radical prostatectomy specimen as a staging indicator has not been fully explored, particularly with use of methods for enhanced detection of micrometastasis.
Design: Radical prostatectomy cases accrued between 1997 and 2007 at our institution were retrieved based on the notation of periprostatic LN(s) in the pathology report. H& E slides were reviewed to characterize the LNs (number, size and location) and the histopathologic features of the metastasis in respect to the primary tumor. LNs were studied for micrometastasis using cytokeratin (AE1/AE3) immunostaining. The status of the periprostatic LN was correlated with tumor size, pre-operative serum PSA, histological grade, stage, surgical margin status and PSA recurrence.
Results: Twenty-one (0.8%) of 2663 radical prostatectomy specimens had periprostatic LN(s) with one case containing two periprostatic LNs (total number of LNs = 22). Lymph node size ranged from 0.8 to 4.7 mm (mean 1.9 mm). Most of the periprostatic LNs were located close to the posterior base. Seven (32%) of 22 LNs (6 cases) were involved by metastatic PCa including 5 detected on routine H & E slides and additional 2 detected only by immunohistochemistry. Cases with periprostatic LNs had a significantly higher metastatic rate (29%; 6 of 21) as compared to those with pelvic LNs sampled at radical prostectatomy in our institution (1.9%). The metastatic foci ranged from <0.1 mm to 4.2 mm. The concurrently submitted pelvic LNs in all 6 cases were negative for metastasis. The tumor characteristics of cases with metastatic periprostatic LNs (n=6) when compared to cases with negative periprostatic LNs (n=15) included higher tumor volume, Gleason score and pT stage. Cases with metastatic periprostatic LN showed a greater propensity for PSA recurrence [80%; 4 of 5] as compared to cases with negative periprostatic LN [27%; 4 of 15].
Conclusions: Periprostatic LNs are small lymph nodes infrequently identified in radical prostatectomy specimens, where they are usually located in the region of the posterior base. They are more commonly involved by metastatic PCa than pelvic LNs sampled at time of radical prostatectomy and predict for PSA recurrence. Despite their infrequent identification, periprostatic LNs if detected in the radical prostatectomy specimen should be evaluated with greater scrutiny (step sections and/ or immunohistochemical studies) to fulfil their prognostic potential.

790 Urachal Carcinoma: A Clinicopathologic Study of 46 Cases.

J Dhillon, B Czerniak, CC Guo. University of Texas M.D. Anderson Cancer Center, Houston.
Background: Urachal carcinoma is a rare tumor that arises in the remnant of the embryonic allantoic stalk. Limited studies have been conducted of this tumor because of its rarity. Therefore, we determined its pathologic and clinical features in a large retrospective series.
Design: We retrospectively searched our surgical pathology files from 1990 to 2010 and identified 46 cases of urachal carcinoma. The specimens included partial cystectomy (n=33), radical cystectomy (n=6), and transurethral resection (n=7). The slides were reviewed for pathologic analysis. Clinical information was collected from patients' medical records.
Results: The mean patient age was 53.4 years. Sixteen were women, and 30 were men. The common presenting symptoms included hematuria, mucinuria, and abdominal pain. On gross examination, the tumors usually appeared as sessile nodular masses, with a mean size of 3.7 cm (range, 1.0–10.5 cm). All tumors was located in the dome (n = 45) except one in the anterior wall. All tumors consisted of adenocarcinoma, including mucinous (n = 36), enteric (n = 5), mixed mucinous and enteric (n = 2), and not-otherwise-specified (n = 3) types. Signet-ring cells were present in 23 cases, but urothelial carcinoma in situ was not identified in any cases. Patients had undergone partial (n = 33) or radical (n = 6) cystectomies. Seven patients had presented with metastasis and had undergone chemotherapy, with no further surgery. We evaluated cystectomy specimens and found that the tumors had invaded the muscularis propria (pT2) (n=8), perivesical tissue (pT3) (n=28), or the abdominal wall (pT4) (n=3). Clinical follow-up data were available for all patients, with a mean follow-up period of 40.9 months (range, 1-230 months). Twenty patients died of disease a mean of 30.6 months (range, 6-71 months) after diagnosis, and 26 were alive at a mean of 48.8 months (range, 1-230 months). Of the 8 patients with pT2 tumors, 6 were alive and 2 had died of disease. Of the 31 with pT3 or pT4 tumors, 16 were alive and 15 had died of disease.
Conclusions: The urachal carcinomas in our series are composed exclusively of adenocarcinoma, with the mucinous subtype being the most common. Urachal carcinoma often presents at an advanced stage and is associated with a poor clinical outcome. Although several staging systems are available, the TNM staging system for bladder cancer can be used for urachal carcinomas and provides valuable information to help predict patient outcome.

791 Cancer Stem Cell Marker Expression in Muscle-Invasive Urothelial Carcinoma.

E Diaz, CB Ching, P Elson, DE Hansel. Cleveland Clinic, OH.
Background: Over the last decade, multiple cancer stem cell (CSC) markers have been identified, although few studies have evaluated the expression of these markers within urothelial carcinoma (UCC) or normal urothelium. In addition, few studies have correlated CSC marker expression with clinical outcome. Our objective was to assess known CSC marker expression in muscle-invasive UCC and benign urothelium and to determine effects on clinical outcome.
Design: A total of 118 UCC specimens and 21 benign urothelial specimens were processed into tissue microarrays and stained with commercial antibodies for CSC markers: CD15, CD24, CD44, CD44v6, CD47, CD67LR, CD117, OCT3/4. Tumors were considered positive if >5% of the cells demonstrated immunoreactivity and were then further substratified into focal or diffuse expression. The clinical course of patients with UCC was abstracted and clinical outcomes were correlated with CSC marker expression using statistical analysis.
Results: UCC specimens most commonly expressed diffuse immunoreactivity for CD24 (63%), CD44 (63%) and CD44v6 (69%), with co-expression of CD44 and CD44v6 in 50% of patients. CD67LR was diffusely expressed in 18% of cases, which corresponds to previously published data. Nuclear staining for OCT3/4 was present in only 5 cases (4%). No UCC specimen demonstrated immunoreactivity for the CSC markers CD47 or CD133. Evaluation of normal urothelium, in contrast, revealed only focal staining for CD24, CD44 and CD44v6 relative to carcinoma specimens ($p<0.01$) in 50%, 60% and 60% of normal cases, respectively. As in carcinoma specimens, CD44 and CD44v6 were co-expressed in 50% of cases. CD67LR was only expressed in 5% of normal specimens evaluated, but when present was diffusely expressed throughout the normal urothelium. Overall 35% of patients recurred (median recurrence-free survival 30.1 months) and 64% of patients died of disease (median survival 22.2 months). Analysis of recurrence-free and overall survival, when tiered for lymph node metastases, suggests that expression of CD67LR indicates an unfavorable prognosis in patients with lymph node metastases. Furthermore, specific combinations of CSC markers appear to impact outcomes.
Conclusions: CSC markers CD24, CD44, and CD44v6 appear to be expressed in higher percentages of UCC cells versus normal urothelium, suggesting a potential enrichment of CSCs in muscle-invasive UCC. Outcomes appear to be impacted by CD67LR in patients with lymph node metastases, as well as specific CSC marker combinations in patients with muscle-invasive UCC.

792 Primary Urothelial Dysplasia: Histopathologic Findings and Outcomes in a Consecutive Patient Series.

E Diaz, DE Hansel. Cleveland Clinic, OH.
Background: Primary urothelial dysplasia is a uncommon with a 14-19% chance of progressing to high grade urothelial carcinoma (HGUC) within 4-5 years of diagnosis. There are very few clinical series for primary urothelial dysplasia, and no series since the 2004 WHO classification recommended grouping of severe dysplasia with carcinoma in situ. The objective of this study is to review cases of primary urothelial dysplasia and provide an updated cohort for primary urothelial dysplasia.
Design: The pathologic database for our institution was queried for specimens with a final diagnosis of dysplasia of the bladder from 1995 to 2010. Primary urothelial dysplasia was defined as a de novo diagnosis of dysplasia without precedent urothelial pathology. Specimens were reviewed to determine histopathologic features. Patient follow-up was obtained by a retrospective review of clinical records.
Results: Thirty-three patients with urothelial dysplasia were identified, with specimens that included biopsy (84%), TUR (11%) and excision for non-neoplastic causes (5%). Gross hematuria (42%) and microhematuria (12%) were the most frequent presenting symptoms. Precedent cytology was negative (44%), atypical (24%), positive (3%), or unavailable (29%). Cystoscopic findings included erythema (40%), raised lesions (30%), negative findings (18%), or unavailable (9%). Only two of the 33 cases (6%) progressed to invasive carcinoma. One case progressed after 2.5 years, and the second case after 3 years. The former case demonstrated squamous features with atypia and would be re-classified as moderate squamous dysplasia; this case progressed to invasive squamous cell carcinoma with continued negative cytology. The latter case demonstrated moderate atypia and progressed to HGUC, with associated cytology progressing from negative to atypical. Upon re-review, the most common features that contributed to urothelial dysplasia diagnosis included increased mitotic activity in the basal and mid aspects of the urothelium (16%), urothelial hyperplasia including papillary hyperplasia (16%), reactive nuclear enlargement (16%), early squamous metaplasia (21%), and mechanical or staining artifact (21%). Nuclear atypia was generally minimal, with occasional moderate atypia of umbrella cells (10%) and binucleation with negative viral stains (5%). Inflammation was generally minimal.
Conclusions: Primary urothelial dysplasia diagnoses are uncommon. In our cohort, only 6% of urothelial dysplasia progressed to invasive carcinoma over 3 years, with the most common contributors to diagnosis including tissue and processing artifact and early squamous metaplasia.

793 Expression of Carbonic Anhydrase IX in Genitourinary and Adrenal Tumors.

DP Donato, MT Johnson, XJ Yang, DL Zynger. The Ohio State University Medical Center, Columbus; Northwestern University, Chicago, IL.

Background: Carbonic anhydrase IX (CAIX) expression is inducible by hypoxia through HIF 1-alpha, and is involved in cell adhesion, cell proliferation, tumor progression and mitigation of intracellular pH. High expression has been described in malignancies of the genitourinary tract including renal cell carcinoma (RCC), clear cell type. We investigated the expression of CAIX in needle biopsies and resections of the genitourinary tract, including organs with limited prior studies such as prostate, testis and adrenal gland.

Design: Sections from 436 tumors (renal cortex, n=130; bladder/renal pelvis/ureter, n=124; prostate, n=67; testis, n=52; adrenal, n=63) including 34 needle biopsies and 31 types of neoplasms were incubated with CAIX. Immunoreactivity was semi-quantitatively evaluated (0, <5% of cells stained; 1+, 5-10%; 2+, 11-50%; or 3+, >50%) and intensity was graded (0 to 3).

Results: Of the 14 types of renal cortical tumors tested, expression was predominately restricted to clear cell RCC (59/60), papillary RCC (8/10) and clear cell papillary RCC (1/1). Core biopsies of RCC clear cell were positive (25/25) and cores with angiomyolipoma, translocation RCC and oncocytoma were negative (0/5). Approximately half of the cases of urothelial carcinoma were positive (39/81) with expression in squamous, small cell, sarcomatoid and adenomatous differentiation but not signet ring or plasmacytoid variants. Pure urothelial tract adenocarcinoma (2/2), squamous cell carcinoma (6/8) and clear cell adenocarcinoma (3/3) were frequently positive. Only rare cases of prostatic adenocarcinoma expressed CAIX (3/66). Testicular germ cell and sex cord stomal tumors showed variable reactivity (seminoma, 0/10; yolk sac tumor, 0/10; embryonal carcinoma, 2/7; choriocarcinoma, 2/4; teratoma, 2/7; Leydig cell tumor, 0/2; Sertoli cell tumor, 2/3). CAIX was demonstrated in adrenal cortical carcinoma (6/11) and pheochromocytoma (2/11). Adrenal cortical adenoma (3/11) and non-neoplastic adrenal tissue (12/30) showed weak cytoplasmic reactivity, unlike all other tumors positive for CAIX which had membranous expression.

Conclusions: CAIX is a very sensitive marker for clear cell RCC, both in resections and core biopsies. However, CAIX also shows high expression in genitourinary tumors which can have a clear cell appearance such as urothelial and squamous cell carcinoma as well as adrenal cortical carcinoma and Sertoli cell tumor. Although non-neoplastic adrenal and adrenal cortical adenoma had CAIX reactivity, it was typically weak and cytoplasmic, unlike the expression seen in clear cell RCC.

794 Clear Cell Papillary Renal Cell Carcinoma: Clinicopathologic, Immunohistochemical, and Molecular Analysis.

L Duan, RF Youssef, V Margulis, Y Lotan, P Koduru, W Kabbani, P Kapur. University of Texas Southwestern Medical Center, Dallas.

Background: Clear cell papillary renal cell carcinoma (ccPRCC) is a recently described entity documented to occur both in end stage renal disease (ESRD) kidneys and sporadically. It is composed exclusively of cells with clear cytoplasm arranged in tubular and papillary pattern. Few series have been reported in literature but most contain small number of cases with the largest published case series consisting of 5 cases. These report ccPRCC as a distinctive renal cell carcinoma (RCC) with unique morphologic and molecular features.

Design: We reviewed over 632 RCC cases diagnosed during the past 10 years at our institution and selected 10 cases that morphologically fit ccPRCC. Two to five 1.0 mm cores of representative tissue was obtained from each case to construct a tissue microarray. A comprehensive analysis of standardized immunohistochemical (IHC) markers and fluorescence in-situ hybridization for chromosomes 3,7,17,Y were obtained.

Results: There were 5 male and 5 female patients, with age ranging from 33 to 80 years (median 62). Five patients had BMI ≥ 30; 4 had elevated serum creatinine, 2 had ESRD, and 1 had von Hippel-Lindau Disease. The tumors were predominantly solitary (60%), small (median 1.5cm), with stage less than pT1b (80%), and Fuhrman nuclear grade less than G2. None of the patients had lymph node metastasis or recurrence (median follow up 24 months). The tumor cells were positive for CK7 (100%), PAX2 (90%), PAX8 (90%), CAM5.2 (70%), CK903 (70%), vimentin (100%), GLUT-1 (90%), and EMA (90%); and negative for racemase (90%), RCC (80%), CD10 (70%), TFE3 (100%), and cathepsin K (100%). Five cases showed polysomy 7, two cases showed polysomy 17, and five cases showed loss of chromosome Y. Deletion of 3p was not detected.

Conclusions: Our study supports that ccPRCC is a distinct histologic entity and has unique IHC and molecular profiles. This unique IHC profile should help differentiate this entity from its histologic mimics, which have different therapeutic targets. ccPRCC appears to be a renal carcinoma with low risk for recurrence or metastasis. The IHC expression profile of sporadic and ESRD associated tumors appears similar.

795 Renal Cell Carcinoma with Extensive Clear Cell Component and Papillary Architecture: Value of Immunohistochemistry.

L Duan, RF Youssef, V Margulis, Y Lotan, P Koduru, W Kabbani, P Kapur. University of Texas Southwestern Medical Center, Dallas.

Background: The current classification of renal epithelial tumors is based on morphology and recognizes their distinct cytogenetic abnormalities. However, tumors with overlapping morphologic features can sometimes be encountered. We aim to further characterize renal cell carcinomas (RCC) with extensive clear cell changes and papillary architecture that are distinct from the previously described entity of clear cell papillary RCC (ccPRCC).

Design: We reviewed over 632 RCC cases diagnosed during the past 10 years at our institution and identified 15 cases that had extensive tubulo-papillary architecture lined exclusively with clear cells. Of these, 10 cases that morphologically fit ccPRCC were excluded. Two to five 1.0 mm cores of representative tissue was obtained from each case to construct a tissue microarray. A comprehensive analysis of standardized immunohistochemical (IHC) markers and fluorescence in-situ hybridization (FISH) for chromosomes 3, 7, 17, and Y were obtained.

Results: The patients included 2 African Americans and 3 Caucasians (age 25-72 yr, median 53 yr) with normal baseline creatinine (except in 1 case with ESRD). Compared to ccPRCC, these tumors were predominantly large (range 2.5 to 8.5 cm, median 5.5 cm) and had high pathologic stage (3 cases were pT3a) and high Fuhrman nuclear grade (G2-G4). Positive lymph nodes were present at time of surgery in 1 case. None of the cases showed recurrence (median follow up time 17 months). The tumors were negative for CK7 (100%), HMWCK (100%), PAX2 (80%), EMA (60%), TFE3 (100%), and cathepsin K (100%), and positive for racemase (100%), CD10 (100%), vimentin (60%), weak PAX8 (80%), GLUT-1 (40%), RCC (80%), and CAM5.2 (60%). Four cases showed polysomy 7, three cases showed polysomy 17, and four cases showed loss of chromosome Y. Deletion of 3p was not detected.

Conclusions: These tumors with papillary architecture and exclusive clear cell cytology show IHC and molecular profile similar to papillary RCC. Our study emphasizes the utility of IHC and molecular studies in making accurate diagnosis of renal cell tumors.

796 Histology-Radiology Correlation in Metastatic Clear Cell Renal Cell Carcinoma Treated with Pre-Operative Sorafenib and Nephrectomy.

W Dubinski, TK Kim, JJ Knox, A Finelli, AJ Evans. University Health Network, Toronto, ON, Canada.

Background: The role for pre-operative tyrosine kinase inhibitor (TKI) therapy prior to cytoreductive nephrectomy (CN) in patients presenting with metastatic clear cell renal cell carcinoma (mCCRCC) is under investigation. While reports on tumor response to TKI therapy, as assessed by dynamic contrast-enhanced ultrasound (DCE-US) and CT (DCE-CT) exist, the effects of TKI therapy on the histomorphology of CCRCC have not been described. We present these findings in patients presenting with mCCRCC.

Design: Patients at University Health Network presenting with mCCRCC were entered into a clinical trial comprising pre-operative Sorafenib followed by CN. After confirming a diagnosis of CCRCC by core needle biopsy, each patient received Sorafenib for 12 weeks followed by CN and resection of metastatic deposits. Fresh CN specimens were bivalved coronally and compared with DCE-US/CT findings pre- and post-TKI.

Results: Sixteen patients (mean 55 years, range 40-70) presenting with mCCRCC (mean primary tumor diameter 10.9cm, range 6.5-15.8) were enrolled. The full spectrum of Fuhrman grades (FG) was observed in the pre-treatment biopsies, including one case with rhabdoid features. Following TKI therapy, mean tumor diameter fell to 9.6cm by DCE-US/CT (range 5.4-14.7cm) (p=.005). In all patients, post-TKI DCE-US/CT showed a pattern of central necrosis (~90% vs. ~30% pre-treatment) with a peripheral rim of viable tumor. Extensive histologic sampling (mean # of sections 19.9, range 8-52) of the CN specimens showed excellent correlation with DCE-US/CT and confirmed the impression of extensive central necrosis and viable tumor localized to the periphery. The H&E morphology of the viable tumor in the CN specimens was essentially unchanged from that observed in the pre-treatment biopsies. In 15 patients, the FG of the viable CCRCC in the CN specimens agreed with the biopsy FG to within 1 point. One patient with a FG 1 at biopsy was found to have FG 1-2 tumor at CN with admixed foci of FG 4 with rhabdoid features. The morphology of all resected metastatic deposits (17 from 8 patients) matched that of their primary tumors.

Conclusions: This study provides histologic confirmation of the treatment response typically observed radiologically following TKI therapy. Based on a comparison with pre-TKI tumor morphology in needle core biopsies, viable post-TKI tumor (in both the CN specimens and metastatic deposits) showed no significant morphologic or FG changes which could be interpreted as "treatment effects" resulting from TKI therapy.

797 Automated Image Analysis of Endoglin and Microvascular Density in Clear Cell Renal Cell Carcinoma and Its Prognostic Significance.

W Dubinski, M Gabril, V Iakovlev, Y Youssef, K Kovacs, S Metias, F Rotando, M Moussa, C Streutker, GM Yousef. St. Michael's Hospital, Toronto, ON, Canada; London Health Sciences Center, ON, Canada.

Background: The metastatic potential of clear cell renal cell carcinoma (ccRCC) is related to tumor angiogenesis. Assessment of angiogenesis by quantifying intratumoral microvascular density (IMVD) may prove to be a useful prognostic parameter in ccRCC. Endoglin is a novel vascular marker that correlates with prognosis in numerous tumors. In this study, we provide the first automated digital assessment of IMVD in ccRCC using endoglin and CD31 and compare our findings with clinical outcome data. This automated approach overcomes many of the limitations of manual quantification.

Design: Fifty cases of ccRCC were immunostained for endoglin and CD31 to highlight tumor vasculature. Immunostained slides were scanned using an Aperio CS Scanner at 20× magnification, and image analysis was used to count IMVD and nuclear density within tumoral and adjacent normal kidney. Clinicopathologic parameters (age, tumor size, follow–up time, nuclear grade and tumor stage) were collected and correlated statistically with IMVD.

Results: Increased expression of endoglin and CD31 was associated with advanced tumor stage (p=0.026 and p=0.039, respectively). There was no correlation between tumor grade and endoglin or CD31 expression (p=0.30). Using a binary cut-off, endoglin-positive patients had significantly lower progression-free survival (p=0.017) compared to endoglin-negative patients. Using endoglin as a continuous variable, increased endoglin expression was associated with reduced survival (HR: 1.87, CI 1.39-2.53, p= <0.001). CD31 positive patients had a tendency for shorter progression-free survival but this was not statistically significant (p=0.13). There was no correlation

between CD31 and endoglin expression (r= -0.120, p=0.536). Receiver operating characteristic (ROC) curves showed that the combination between CD31 and CD34 showed the best performance (AUC = 0.81, 95%CI=0.64-0.99; p<0.028), followed by CD34 and Endoglin (*AUC*= 0.79).

Conclusions: Automated image analysis of endoglin and CD31 expression in ccRCC showed that increased IMVD is associated with higher tumor stage and decreased survival. The advances in digital assessment of immunohistochemical expression can be helpful in evaluating and establishing the clinical significance of new prognostic markers for renal cell carcinoma.

798 Cytokeratin 5/6 Distinguishes Reactive Urothelial Atypia from Carcinoma In Situ and Non-Invasive Urothelial Carcinoma.

A Edgecombe, EC Belanger, B Djordjevic, BN Nguyen, KT Mai. The Ottawa Hospital and University of Ottawa, ON, Canada.

Background: Cytokeratin 5/6 (CK5/6) is commonly used to differentiate epithelial hyperplasia from atypical hyperplasia and ductal carcinoma in situ in breast. The utility of CK5/6 to distinguish reactive urothelial atypia (RA) from urothelial carcinoma in situ (CIS) and the non-invasive component of papillary urothelial carcinoma (PUC) is not known, and is the focus of this study. CK5/6 performance is compared to that of cytokeratin 20 (CK20) and p16, which have been previously reported as useful markers in this differential.

Design: Twenty consecutive surgical specimens of reactive urothelial atypia (RA) with or without papillary hyperplasia, 40 high grade and low grade papillary urothelial carcinomas (PUC) and 20 CIS were submitted for immunostaining with CK5/6, CK20 and p16. The immunostaining pattern was documented as full urothelial thickness, basal cell layer or umbrella cell layer. The intensity/extent of immunoreactivity was recorded as negative, weak/focal (less than 20% of cells) and strong/diffuse (more than 50% of cells).

Results: Diffuse and strong reactivity involving the full thickness of urothelium was observed with CK5/6 in all cases of RA (100%). p16 and CK20 were negative in all the RA cases (no reactivity or reactivity in the umbrella cell layer). CK5/6 reactivity for CIS and high grade PUC was negative (no reactivity or reactivity in the basal cell layer) in all cases. CK20 was strongly positive (full thickness of urothelium) in 85% of CIS cases and 85% of high grade PUC cases. Strong positive staining for p16 was present in 90% of CIS cases and 80% of high grade PUC cases. Low grade PUC displayed variable reactivity for CK5/6, CK20 and p16.

Conclusions: Strong and diffuse CK5/6 reactivity in RA and negative CK5/6 reactivity (no reactivity or reactivity in the basal cell layer) in CIS and non-invasive PUC may be helpful in distinguishing between these two entities, especially in the setting of negative or weak/focal reactivity for CK20 and p16.

799 Comparison of Immunohistochemistry with FISH for Detection of TMPRSS2-ERG Rearrangement in Prostate Cancers in African American and Caucasian Populations.

RM Elliott, MA Leversha, JM Satagopan, QC Zhou, M Dudas, Y-B Chen, H Al-Ahmadie, S Fine, S Tickoo, JA Eastham, PT Scardino, M Koscuiszka, P Lee, I Osman, WL Gerald, VE Reuter, A Gopalan. Memorial Sloan-Kettering Cancer Center, New York; New York University, NY.

Background: Gene rearrangements of TMPRSS2 and ERG occur in approximately 13% of prostate cancers in African-Americans (AA) and 30-50% of those in Caucasians (CA). Screening for the rearrangement may provide prognostic information and may be used for patient stratification to guide treatment. Because screening by FISH may be expensive and time consuming, an immunohistochemical method for screening would be advantageous, especially in the AA population, which has a significantly lower prevalence of TMPRSS2-ERG rearrangement.

Design: The study cohort included 87 AA and 71 CA men. Gene rearrangement status was determined by interphase FISH using a 3 color break-apart probe containing BAC clones against 3'ERG, 3' and 5' TMPRSS2. FISH data were available for 78 AA and 67 CA men. Overexpression of the truncated ERG protein product was assessed using a primary monoclonal antibody (dilution 1:250) obtained from Epitomics (San Diego, CA). ERG antibody (ERG AB) data were available for 87 AA and 71 CA men. FISH was not evaluable in 9 AA and 4 CA cases due to technical difficulties. A pathologist blinded to the results of the FISH analysis assessed nuclear reactivity in tumor cells and scored reactivity as positive or negative.

Results: ERG expression by IHC was shown in 22% (19 of 87) of AA men and 42% (30 of 71) of CA men. Gene rearrangement was shown by FISH in 13% (10 of 78) of AA men and 37% (25 of 67) CA men. All AA cases were rearranged through deletion. IHC data were available for all 78 AA men who had data by FISH, and in these, 10 cases were positive by both ERG AB and FISH, while 7 cases were positive by ERG AB and negative by FISH. Both IHC and FISH data were available for 67 CA men, and in these, 25 cases were positive by both ERG AB and FISH, while 5 were positive by ERG AB and negative by FISH. None of the ERG AB negative cases were positive by FISH in either group. There was no difference in intensity of staining between tumors with translocation and those with deletion. FISH and ERG AB were discordant in 41% of AA cases.

Conclusions: 1. In patients with positive FISH, 100% showed ERG AB expression.
2. Fewer cases were 'not evaluable' by the ERG AB assay.
3. The value of FISH is in the distinction between translocation and deletion; however in the AA population this is probably unnecessary because all cases are rearranged through deletion.
4. Our study validates the difference in ERG expression between AA and CA patients.

800 Do Patients with Multiple Positive Cores of Gleason Score 6 (GS6) Adenocarcinoma on Biopsy Have Unfavorable Findings at Radical Prostatectomy (RP)?

CL Ellis, JI Epstein. The Johns Hopkins Hospital, Baltimore.

Background: While the presence of GS6 on biopsy is a relatively favorable finding, it is unknown is whether its good prognosis is maintained in the setting of multiple involved cores.

Design: We identified 6,156 men (4/1/00-4/30/07) with GS6 on biopsy who underwent RP at our institution. A "cure rate" was determined by a >75% probability of tumor showing no evidence of biochemical recurrence 10 years after RP as calculated by the Han tables (based on pre-operative PSA, GS at radical prostatectomy and status of organ confinement). We also evaluated the fraction of positive cores (positive cores/total cores); positive cores and fraction of positive cores were so tightly correlated (R=0.94) that there was no meaningful difference between the two variables and the number of positive cores was utilized.

Results: The number of positive cores averaged 2.5 (1-16). More positive cores statistically correlated with lower cure rate (p<0.0001), less organ-confined disease (p<0.0001), positive margins (p<0.001), and increasing RP grade (p<0.001).

Table

# of Positive Cores	Cure Rate > 75%	Percent OC	Negative Margins	RP GS6
1-6	90.5%	82.5%	89.3%	77.2%
>6	84.0%	68.3%	85.2%	66.4%
1	93%	88%	93%	82%
2	90%	83%	88%	75%
3	89%	77%	88%	75%
4	88%	77%	86%	70%
5	86%	70%	80%	72%
6	84%	67%	82%	73%
7	85%	64%	83%	70%
8	85%	77%	87%	64%
9	81%	62%	89%	68%
>10	83%	71%	85%	63%

Non-focal extra-prostatic extension (EPE) was seen in 7.9% and 13.1% of cases with 1-6 vs. >6 positive cores, respectively. Positive seminal vesicles or lymph nodes were seen in 1.5% and 3.5% of cases with 1-6 vs. >6 positive cores, respectively. However, even with multiple positive cores of GS6, the majority of patients had a relatively favorable outcome such that RP remains a viable option in this setting [Table]. Tables were also generated based on clinical stage (T1c vs T2), number of positive cores, and preoperative PSA level to predict organ confined disease as a guide for urologists to perform nerve sparing surgery. For example with nonpalpable disease (T1c), there was a ≥75% likelihood of organ confined disease with 1-3 positive cores regardless of PSA and with 4-6 positive cores & PSA 0-4 ng/ml.

Conclusions: Low Gleason score on biopsy is such a powerful prognostic finding, such that this favorable outcome is maintained even in the setting of multiple positive cores with GS6.

801 Not All Xp11 Translocation Renal Cell Carcinomas (RCC) Are the Same: *ASPL-TFE3* RCC Are More Likely To Present at Advanced Stage Than Are *PRCC-TFE3* RCC.

CL Ellis, JN Eble, AP Subhawong, G Martignoni, M Ladanyi, GJ Netto, P Argani. The Johns Hopkins Hospital, Baltimore, MD; Indiana University School of Medicine, Indianapolis; University of Verona, Italy; Memorial Sloan-Kettering Cancer Center, New York, NY.

Background: Xp11 translocation RCC are a characterized by chromosome translocations involving Xp11, resulting in gene fusions involving the *TFE3* transcription factor gene. The most common subtypes of Xp11 translocation RCC are the *ASPL-TFE3* RCC, resulting from a t(X;17)(p11;q25), and the *PRCC-TFE3* RCC, resulting from a t(X;1)(p11;q21). As most cytogenetically or molecularly confirmed cases have been described in case reports or small series, a formal clinical comparison of these two subtypes of Xp11 translocation RCC has not been performed.

Design: We report two novel cytogenetically confirmed Xp11 translocation RCC, one with an *ASPL-TFE3* gene fusion and the other with a *PRCC-TFE3* gene fusion. We review the literature for all published cases of *ASPL-TFE3* RCC (32 cases, 16 publications) and *PRCC-TFE3* RCC (34 cases, 16 publications) and contacted all corresponding authors to obtain or update published follow-up information.

Results: The novel *ASPL-TFE3* RCC case is a 16 year old female who presented with distant metastasis and developed progressive disease after one year. The novel *PRCC-TFE3* case is a 14 year old male who presented with a ruptured but localized 7cm neoplasm. Review of these cases and the composite literature revealed that 7/7 patients who presented with distant metastasis had *ASPL-TFE3* RCC (p=0.03), and all these patients either died of disease or have progressive disease. Regional lymph nodes were involved by metastatic carcinoma in 18 of the 24 *ASPL-TFE3* RCC in which nodes were resected, compared to 4 of 11 *PRCC-TFE3* RCC (p=.057). However, no patient with *ASPL-TFE3* RCC who presented with N1M0 disease developed recurrence at mean follow-up of 5 years. Two *PRCC-TFE3* RCC recurred late (20 and 30 years, respectively).

Conclusions: *ASPL-TFE3* RCC are more likely to present at advanced stage than are *PRCC-TFE3* RCC. However, while systemic metastases portend a grim prognosis, regional lymph node involvement does not in short term follow-up. The potential for *PRCC-TFE3* RCC to recur late warrants caution and long term follow-up. The clinical differences observed in the present study may reflect subtle functional differences between the ASPL-TFE3 and PRCC-TFE3 fusion proteins, of which further evidence may be the recently demonstrated difference in cathepsin-K expression between these two neoplasms.

802 Fine Needle Aspiration (FNA) Cytology of Metastatic Prostate Carcinoma. Is Cytoplasmic Vacuolization a Morphologic Feature of Anti-Androgen Effect and an Aid in the Differential Diagnosis?

CL Ellis, QK Li. The Johns Hopkins Hospital, Baltimore, MD.

Background: Anti-androgen therapy has been used for the treatment of prostate cancer for decades. Its major usages include preoperative shrinkage of tumor, symptomatic relief of obstructive effects and prophylaxis of tumor progression. This therapy also has a profound morphological effect on tumor, such as loss of glandular architecture and cytoplasmic degeneration. These features have been well documented in the surgically resected tumor; however, they have not been studied in FNA cytologic material, particularly in metastatic prostate cancers. The androgen deprivation treatment-induced morphological changes may cause diagnostic difficulty in the FNA specimen. In this study, we have reviewed the cytomorphology on FNA of metastatic prostate cancer and potential anti-androgenic treatment effect on tumor cells.

Design: A computer search of cytopathology specimens for a 20 year period in the archives of our academic medical center yielded 32 FNA cases with the diagnosis of metastatic prostate cancer. The cytomorphology of the metastatic tumor was correlated with immunohistochemical studies, morphology of the primary tumor and clinical information.

Results: The patients' ages ranged from 51 to 84 years, with a mean age of 71.5 years. The most common metastatic site in descending order is: lung (7 cases), regional LN (6 cases), liver (5 cases), pleura (4 cases), soft tissue (3 cases), bone (2 cases), adrenal (1 case) and others (4 cases). Among 32 cases, 24 had documented androgen deprivation therapy ranging from 2 months to more than 10 years of duration. Of 24 cases, the most notable feature is cytoplasmic vacuolization which occurs in 37% of cases (9/24) in greater than 50% of the cytoplasm. This feature is not present in the primary tumors. The clinical information for these cases is summarized in Table 1.

Table 1

Case	Age	Treatment	GS of Primary	Metastatic Site
1	75	Leuprolide	4+4	Lung
2	74	Leuprolide, Flutamide	3+4	Lung
3	81	Goserelin, Bicalutamide	3+4	Lung
4	61	Goserelin	4+4	Sacrum
5	72	Leuprolide	Ductal ADC	Lymph Node
6	75	Leuprolide	4+3	Retroperitoneum
7	69	Leuprolide, Zoledronic acid	4+3	Liver
8	68	Leuprolide, Zoledronic acid	3+3	Lymph Node
9	75	Leuprolide	5+5	Perirectum

GS = Gleason Score, ADC = Adenocarcinoma

Conclusions: The finding of high frequency of cytoplasmic clearing in metastatic tumor suggests a previously well-documented anti-androgenic effect. The awareness of this phenomenon may aid in the diagnosis and differential diagnosis of metastatic prostate cancer in difficult cases.

803 Prostate Cancer Gene Expression Adds Prognostic Information beyond Clinical and Pathological Criteria Such as Stage, Gleason Score, PSA, AUA Criteria, and CAPRA Score.

S Falzarano, C Magi-Galluzzi, T Maddala, D Cherbavaz, FL Baehner, C Millward, E Klein. Cleveland Clinic, OH; Genomic Health, Inc, Redwood City, CA.

Background: Prognosis of localized prostate cancer is estimated using clinical and pathological features including PSA, stage, Gleason score (GS), AUA criteria, and CAPRA score. These criteria do not yet fully account for individual tumor biology. We hypothesized that quantitative gene expression would add prognostic information beyond that provided by clinical and pathological features.

Design: All pts with clinical stage T1/T2 prostate cancer treated with RP at a single institution from 1987 to 2004 were identified (n~2,600). A cohort sampling design was used to select 127 pts with clinical recurrence (cR) and 374 pts without cR after RP. Surgical GS and clinical data were centrally reviewed. RNA was extracted from 6 manually dissected 10 µm FFPE tissue sections obtained from RP specimens and expression of 732 cancer-related and reference genes was quantified using a standardized RT-PCR assay. Univariate/multivariate analyses of cR, PSA recurrence, and prostate cancer-specific survival (PCSS) were performed using Cox PH regression.

Results: Blocks from 431 pts were evaluable by pre-specified criteria. Median f/up was 5.8 yrs. Pts were mostly Caucasian (83%), <70 yrs old (93%), clinical stage T1 (66%), had baseline PSA <10 ng/mL (82%), and had surgical GS≤7 (87%). In univariate analysis, many genes were significantly (unadj. $p<0.05$) associated with cR, PSA recurrence, and PCSS, 295, 235, and 203 genes respectively. The number of associated genes was much greater than that expected by chance and the associations were very strong, many with hazard ratios greater than 1.7 per standard deviation change in gene expression. Many genes remained significantly associated with each of the outcomes in multivariate analyses adjusting for pathologic T-stage, tumor specimen Gleason pattern (GP), GS, AUA group and CAPRA score (221, 194, 99, 244, and 271 genes respectively). For the strongest 20 genes, the magnitude of association was diminished by less than 20% after adjustment for stage, GP, AUA, and CAPRA, and less than 50% after adjustment for GS.

Conclusions: This genomic study was notable for the large number of cR events, the use of a standardized quantitative assay, and rigorous central review of pathology and clinical data. These results indicate that quantitative gene expression using RT-PCR adds prognostic information beyond traditional clinical and pathological features.

804 *ERG* Rearrangement Status in Prostate Cancer Detected by Immunohistochemistry.

SM Falzarano, M Zhou, P Carver, H He, C Magi-Galluzzi. Cleveland Clinic.

Background: *TMPRSS2:ERG* is the most common gene fusion in prostate cancer (PCA). It has been associated with expression of a truncated protein product of the oncogene *ERG*. A novel anti-ERG monoclonal antibody has been recently characterized which specifically recognizes all *ERG* gene fusion related isoforms. We investigated the correlation between *ERG* rearrangement assessed by fluorescence *in situ* hybridization (FISH) and ERG expression detected by immunohistochemistry (IHC) in a large cohort of patients from a single institution.

Design: 345 tumor foci from a cohort of 307 patients treated with radical prostatectomy for clinically localized PCA were included in the study. 13 tissue microarrays (TMAs) comprising all tumors and a subset of non neoplastic tissue samples were assessed for *ERG* rearrangement status by FISH and ERG expression by IHC. The accuracy of ERG detection by IHC in predicting *ERG* status as assessed by FISH (gold standard) was calculated in terms of sensitivity, specificity, positive predictive value (PPV) and negative predictive value (NPV).

Results: 305 (88%) tumor samples were informative for both FISH and IHC. 40 cases were not evaluable by either FISH (34) or IHC (6). Of the 103 (34%) *ERG* rearranged cases, 49 (47%) were positive by deletion, 47 (46%) by translocation and 7 (7%) by both mechanisms. ERG detection by IHC demonstrated a sensitivity and specificity of 96% and 99%, respectively, with a PPV of 99% and a NPV of 98% (Table 1). We identified 1 case with positive ERG expression and no identifiable *ERG* rearrangement by FISH and 4 rearranged cases with no expression of ERG. None of the 112 informative non neoplastic tissue samples was rearranged by FISH or showed any ERG expression.

Conclusions: ERG detection by IHC in PCA was highly predictive of *ERG* rearrangement as assessed by FISH in a large cohort of RP patients. Given the high yield and the easier task of performing IHC vs. FISH, ERG assessment by IHC may be useful for characterizing *ERG* status in PCA. Although a rare event (4%), the inefficient transcription/translation of the gene fusion product may be responsible for cases with gene rearrangement by FISH which do not express ERG, whereas ERG synthesis and overexpression may occur in absence of gene rearrangement detected by the FISH break-apart system.

Table 1. FISH and IHC data for tumor samples

	FISH Positive	FISH Negative	Total
IHC Positive	99 (32%)	1 (0%)	100 (33%)
IHC Negative	4 (1%)	201 (66%)	205 (67%)
Total	103 (34%)	202 (66%)	305 (100%)

805 Clinical Significance of miR-21 in Renal Cell Carcinoma.

H Faragalla, Y Youssef, B Kahalil, NMA White, S Mejia-Guerrero, C Streutker, M Jewett, G Bjarnason, L Sugar, MI Attalah, GM Yousef. Li Ka Shing Knowledge Institue St. Michael's Hosptial, Toronto, ON, Canada; Princess Margaret Hospital, Toronto, ON, Canada; Sunnybrook Health Sciences Center, Toronto, ON, Canada; University of Toronto, ON, Canada.

Background: Renal cell carcinoma (RCC) is the most common neoplasm of the adult kidney. Increasing evidence suggests that microRNAs (miRNAs) are dysregulated in RCC and are important players in RCC pathogenesis. MiR-21 is a known oncogene with tumor promoting effect in many types of cancer. The aim of this study was to examine miR-21 expression in RCC and to identify its potential clinical significance.

Design: We analyzed miR-21 expression in 105 cases of RCC and eight normal kidneys. More specifically, we analyzed 65 primary clear cell RCCs, 10 papillary RCCs, 10 chromophobe RCCs, 10 oncocytomas and 10 metastatic RCCs. Total RNA was extracted from formalin fixed paraffin embedded tissues and the expression of miR-21 was analyzed by real time PCR using TaqMan miR-21-specific probes. Results were normalized using RNU44 as an endogenous control. miRNA expression was analyzed in correlation with other clinicopathological parameters including tumor grade, stage, and progression-free survival.

Results: The expression of miR-21 was significantly increased in primary RCC when compared to normal kidney tissue. There was also differential expression between RCC subtypes and between RCC and oncocytoma. The highest levels of expression were found in clear cell and papillary RCC when compared to chromophobe RCC and oncocytoma. Also, there were significant differences of miR-21 expression among different stages of RCC with higher miR-21 expression being associated with later stage. There was an increase in miR-21 expression in metastatic RCC when compared to primary tumors. This, however, did not reach statistical significance. Survival analysis by Kaplan Meier showed patients with positive miR-21 tumors were more likely to have a recurrence than patients with tumors negative for miR-21 expression.

Conclusions: There is increased expression of miR-21 in kidney cancer which suggests it may play a role in the pathogenesis of RCC. Its level of expression can be used as a diagnostic marker, to distinguish between RCC tumor subtypes, and also as a prognostic marker in RCC. miR-21 can also be a therapeutic target for RCC.

806 Focal Positive PSMA Expression in Ganglionic Tissues Associated with Prostate Neurovascular Bundle: Implications for Novel Intraoperative PSMA Based Fluorescent Imaging Techniques.

SF Faraj, J Solus, J Eifler, T Alhussain, A Chaux, M Pomper, R Rodriguez, GJ Netto. Johns Hopkins Medical Institution, Baltimore, MD.

Background: Prostate specific membrane antigen (PSMA) is a type II transmembrane glycoprotein that is primarily expressed in glandular prostate tissue. We previously demonstrated occasional PSMA expression in peripheral nerve sheath tumors. A real time intra-operative imaging technique using a newly developed low molecular weight urea-based compound that binds to PSMA and fluoresces in the NIR spectrum is being pursued at our institution. Such intra-operative techniques could help decrease the rate of positive surgical margins of radical prostatectomy (RP). In the current study we evaluated PSMA expression in neurovascular bundle elements including peripheral nerve, ganglion and lymphovascular tissue in order to assess the feasibility of the above intraoperative technology.

Design: Twenty consecutive RP specimens were retrieved from our surgical pathology archives. PSMA immunoexpression was assessed in a representative section from each specimen containing neurovascular bundle elements using a PSMA monoclonal antibody (Clone 3E6, DAKO, Denmark). PSMA expression was evaluated by two pathologists. An intensity (1 = weak, 2 = moderate, 3 = strong) and extent (1 = <25%, 2 = 25%-75%, 3 = >75%) score was assigned in each RP for available prostate carcinoma (PCa) neurovascular bundle elements and associated ganglion tissue.

Results: As expected, PSMA membranous and cytoplasmic expression was documented in 100% (11/11) of examined PCa tumors. None of the peripheral nerve and lymphovascular components of 19 examined neurovascular bundles were positive for PSMA. However, focal weak to moderate staining was detected in associated ganglionic tissue in 3/15 (20%) examined RPs.

Tissue	PSMA Positive (%)	PSMA Intensity (n)			PSMA Extent (n)		
		1	2	3	1	2	3
PCa	11/11 (100%)	5	0	6	2	2	7
Nerve	0/19 (0%)	0	0	0	0	0	0
Ganglion	3/15 (20%)	2	1	0	3	0	0
Vessels	0/19 (0%)	0	0	0	0	0	0

Conclusions: We found focal positive PSMA expression in ganglionic elements adjacent to prostate neurovascular bundle tissue. This pattern of expression should be taken into consideration to distinguish prostate tissue from neurovascular bundle element during real time intra-operative imaging techniques using PSMA binding florescent compounds.

807 Comedonecrosis Revisited: Assocations with Intraductal Carcinoma of the Prostate.

SW Fine, K Udo, HA Al-Ahmadie, Y-B Chen, A Gopalan, SK Tickoo, VE Reuter. Memorial Sloan-Kettering Cancer Center, New York, NY.

Background: Within the current Gleason grading system, comedocarcinoma or cancer displaying intraluminal necrotic cells and/or karyorrhexis within cribriform/solid architecture, is assigned Gleason pattern 5. Intraductal growth of carcinoma resembles high grade adenocarcinoma architecturally and cytologically and may also show central necrosis, yet due to the presence of basal cells at the duct periphery is not graded in the Gleason system. We hypothesized that comedonecrosis was more commonly seen in intraductal than in invasive disease.

Design: From a large series of consecutively mapped radical prostatectomy specimens (n=386) from a single year, we selected 51 high grade, high volume tumors with available slides for review. All slides were examined for the presence of unequivocal comedonecrosis, utilizing strict criteria to exclude dense pink secretions, crush/cautery artifact as well as foci of large cribriform masses exhibiting perineural invasion. Standard immunohistochemistry for basal cell markers, 34βE12 and 4A4/p63, was performed to detect basal cell labeling in these foci.

Results: 10 of 51 cases showed some degree of comedonecrosis – 6 cases with one focus and 4 cases with ≥ 2 foci. Immunohistochemical stains revealed moderate to strong labeling for 34βE12 and 4A4/p63 in a basal cell distribution for all cancer foci displaying comedonecrosis, such that these foci were interpreted as intraductal carcinoma.

Conclusions: These initial results suggest that comedonecrosis is closely associated with intraductal growth of prostatic carcinoma. Although further studies are underway with a larger cohort of cases, if these findings are confirmed, routine assignment of Gleason grade 5 to comedocarcinoma should be reconsidered.

808 Prognostic Impact of Subclassification of Radical Prostatectomy Positive Margins by Linear Extent and Gleason Grade.

SW Fine, K Udo, AM Cronin, LJ Carlino, HA Al-Ahmadie, A Gopalan, SK Tickoo, PT Scardino, JA Eastham, VE Reuter. Memorial Sloan-Kettering Cancer Center, NY.

Background: The finding of a positive surgical margin (+SM) is an independent adverse prognostic factor in patients who have undergone radical prostatectomy for prostate cancer. A few studies have highlighted the prognostic significance of length of +SM and Gleason grade at the site of a +SM, yet the impact of these factors remains unclear. Utilizing detailed pathologic review, we aimed to evaluate the relationship between the linear extent of and Gleason grade at a +SM with progression following radical prostatectomy.

Design: We studied 2150 prostatectomies with pT2 or pT3a disease for grade, stage, and margin status. In +SM patients, location, number and linear extent of and highest Gleason grade at margins were recorded.

Results: 207 (10%) cases displayed a +SM with 45% (n=93) having pT2+ and 55% (n=114) having pT3a disease. pT3a +SM patients had higher PSA, tumor volumes and rates of Gleason score ≥ 7 compared to pT2+ patients. 45 patients with +SM progressed. Sub-categorization of +SM revealed most patients with 1 +SM (79%, n=164) and total margin length ≤ 1mm for 104 patients (50%), 1.1 to 3mm for 55 patients (27%), and >3mm for 48 patients (23%). 2-year progression-free probabilities were 95%, 91%, 83% and 47% for patients with negative margins, ≤ 1mm, 1.1 to 3mm and >3mm linear extent, respectively (p<0.001). 154 (74%) cases had highest Gleason grade 3 at +SM, while 53 (26%) had Gleason grade 4/5. The latter group were significantly more likely to progress (p<0.001). Concordance index of overall margin status was 0.636 and was not considerably enhanced with categorization by linear extent (concordance index 0.643).

Conclusions: Length of and Gleason grade at a positive surgical margin are associated with progression. However, categorization by linear extent did not add importantly to a model using margin status only. More robust markers are needed in positive surgical margin patients to warrant routine reporting and identify patients at risk for biochemical recurrence.

809 Affymetrix Genechip Microarray Analysis of Renal Cell Carcinoma in Formalin Fixed Paraffin Embedded Tissue.

K Fisher, AN Young, Q Yin-Goen, AO Osunkoya. Emory University Scool of Medicine, Atlanta.

Background: The classification of RCC is important because the different subtypes are associated with distinct clinical behavior, and patients may benefit from type-specific therapeutic modalities. Previously, we used high-density microarrays to discover biomarker profiles for diagnostic classification, characterized by differential expression in RCC subtypes. However, high-density arrays are difficult to apply for clinical diagnosis due to cost, complexity and challenges with quality control. In this study, we tested the utility of Ziplex(R) Tipchip arrays (Xceed Molecular/Axela) for diagnostic classification of renal cell carcinoma (RCC) in formalin fixed paraffin embedded tissue. The Ziplex platform is designed to enable array-based testing in clinical laboratories; it is an integrated system for simple, automated hybridization to Tipchips containing ~100 probes, followed by automated imaging in the same instrument.

Design: Gene expression was measured in formalin fixed paraffin embedded tissue from different RCC subtypes using custom Tipchip arrays, containing ~100 biomarkers identified from our previous study using high-density arrays. The renal tumors (6 cases of clear cell RCC, 3 cases of papillary RCC, and 6 cases of chromophobe RCC) were analyzed. Total RNA was extracted from the tumors, and cRNA was synthesized and hyridized to Ziplex(R) arrays. Results were normalized against the Geomean of 44 controls genes shown to be relatively invariant among the RCC subtypes.

Results: Most biomarkers on the Ziplex(R) arrays showed gene expression patterns among the RCC subtypes that were similar to our previous results in formalin fixed paraffin embedded tissue. The following diagnostic gene expression patterns were verified with the Ziplex(R) platform: Clear cell RCC overexpressed CA9, CAV1, CP, CXCR4, IL10RA, LY6E, NNMT, PLIN2 / ADPF, TGFB1 and vimentin; Papillary RCC over expressed AMACR, BAMBI, LAMB1, SCHIP1, SLC34A2;and Chromophobe RCC over expressed ACAT1, ACSL1, BLNK, CLDN8, COX5A, BDF1, GOT1, KIT, PVALB, and SLC25A4.

Conclusions: Our study demonstrates that Affymetrix Genechip microarray analysis can be utilized in the subtyping of RCC with comparable results in formalin fixed paraffin embedded tissue. This technology delivers similar results with high-density microarrays in formalin fixed paraffin embedded tissue, and lacks the complexity and quality control challenges encountered with high-density microarrays.

810 SPINK1 Protein Expression and Prostate Cancer Progression.

R Flavin, W Hendrickson, L Krunz, G Judson, R Lis, D Bailey, M Fiorentino, S Finn, N Martin, J Stark, A Pettersson, J Sinnott, K Penny, K Fall, E Giovannucci, M Rubin, P Kantoff, M Stampfer, M Loda, L Mucci. Dana Farber Cancer Institute/Harvard Cancer Center, Boston; Weill Cornell Medical College, New York.

Background: Overexpression of SPINK1 (which is an inhibitor of serine proteases) has recently been described in prostate cancer. SPINK1 expression has been associated with poor prognosis in endocrine treated prostate cancer and in prostatectomy treated patients. Some groups suggest that SPINK1 outlier expression is a unique molecular subtype for men with *TMPRSS2:ERG* negative tumours identifying a separate mechanism of prostate cancer progression. The objective of this study was to characterize the aggressive phenotype (defined as PSA/biochemical recurrence) in SPINK1 positive prostate cancer in a large, prospective study.

Design: Protein expression of SPINK1 was evaluated semiquantitatively following immunohistochemistry using mouse monoclonal antibody (Abnova) on archival FFPE TMAs which included 962 cases of prostate cancer among men diagnosed in two large, prospective cohorts. *TMPRSS2:ERG* status, by chromosomal translocation or intronic deletion, was assessed by an ERG break-apart FISH assay(n=270). The men were followed for cancer progression and mortality through March 2010. Multivariable Cox regression models were used to estimate associations of SPINK1 and prostate cancer outcomes, adjusted for clinical factors.

Results: 15.5% of tumors were SPINK1 positive. SPINK1 protein expression was predominately mutually exclusive to the presence of the *TMPRSS2:ERG* fusion (97.5% of cases; p=0.0003; chi-square test). SPINK1 positive tumors had higher PSA at diagnosis (p=0.015) and higher Gleason score (p=0.04). SPINK1 protein expression had a small positive association with biochemical (PSA) recurrence on age adjusted analysis; Hazard Ratio 1.30(0.85-2.00; p>0.05). There was no association with lethal prostate cancer; Hazard Ratio 0.98(0.54-1.78; p=0.96).

Conclusions: SPINK1 protein tends to be exclusively expressed in tumours without the *TMPRSS2:ERG* fusion and is found in ~15% of prostate cancers. SPINK1 positive prostate cancers may have a modest increased risk of prostate cancer progression.

811 Prognostic Relevance of the Revised pN Stages in the 7th TNM Classification for Bladder Cancer.

A Fleischmann, GN Thalmann, R Seiler. University of Bern, Switzerland; , Bern, Switzerland.

Background: The recently published 7th TNM staging system substantially changed the pN stages in bladder cancer. However, the prognostic relevance of the revised pN3 category (metastases in the common iliac region) is obscure.

Design: One hundred and sixty two bladder cancer patients were preoperatively staged N0M0, underwent cystectomy and standardized extended bilateral pelvic lymphadenectomy and showed lymph node metastases upon pathological examination. They were followed prospectively. The prognostic categories of the new TNM system and other risk factors (extracapsular extension of lymph node metastases, largest diameter of lymph node metastases) were evaluated in terms of survival.

Results: Median age at surgery was 67 years (range 35-89); median follow-up was 7.1 years (range 0.1-19.9); 96 patients relapsed and 115 died. A median of 27 lymph nodes

(range 10-56) and 3 lymph node metastases (range 1-46) were identified per patient. Five-year recurrence-free (RFS) and overall (OS) survival of the cohort was 34% and 33%, respectively. In univariate analysis extracapsular extension of nodal metastases (RFS: p<0.001; OS: p<0.001), primary tumor stage (RFS: p<0.003; OS: p<0.004) and the revised pN stages (RFS: p<0.05; OS: p<0.02) were significantly related to survival. The three survival curves separated completely showing a significant decline from pN1 to pN2 to pN3. Largest diameter of metastasis failed to predict survival. In multivariate analyses, only extracapsular extension (RFS: p=0.04, OS: p=0.004) and primary tumor stage (RFS: p=0.01, OS: p=0.04) added independent prognostic information.
Conclusions: The discriminatory ability of the revised pN stages is high showing poorest outcome for patients with pN3 disease. However, of all tested nodal tumor parameters only extracapsular extension of lymph node metastases added independent prognostic information.

812 High Nuclear Cyclin D1 Expression in Lymph Node Metastases from Bladder Cancer Is an Independent Risk Factor for Early Death.

A Fleischmann, D Rotzer, GN Thalmann, R Seiler. University of Bern, Switzerland.
Background: CyclinD1 not only promotes proliferation but also mediates invasion and metastasis of cancer cells thus contributing to a malignant phenotype. With increased understanding of its diverse functions CyclinD1 has been suggested to be interesting therapeutic target in cancer. The prognostic impact of CyclinD1 expression in lymph node positive bladder cancer has never been determined.
Design: One hundred and fifty lymph node positive patients with urothelial bladder cancer underwent cystectomy and pelvic lymphadenectomy and were followed prospectively for a median of 7.1 years (range 0.1-19.9). A tissue microarray was constructed with samples from all primary tumors and matched lymph node metastases. Immunohistochemical stains showed CyclinD1 expression in the nucleus and the cytoplasm. In each patient, percentage of stained cancer cells was determined in the primary tumor and the metastases considering the sub-cellular expression compartment. Expression data were correlated with tumor characteristics and survival.
Results: Nuclear and cytoplasmic CyclinD1expression were significantly (p<0.05) up-regulated in metastases (median nuclear/cytoplasmic expression: 50%/15%) compared to primary tumors (median nuclear/cytoplasmic expression: 30%/0%). High nuclear CyclinD1 expression in the metastases predicted early death significantly (p=0.003; 5-year overall survival: 14% vs. 37%) and independent from other risk factors (TNM stages, extranodal extension). These patients had a 1.7 fold elevated risk of dying compared to patients with low CyclinD1 expression (p=0.017). CyclinD1 expression in all other tumor cell compartments failed to add significant prognostic information and CyclinD1 expression was not correlated with specific tumor characteristics (TNM stage; number, total diameter and extracapsular extension of metastases).
Conclusions: Nuclear CyclinD1 expression in nodal metastases of bladder cancer is significantly up-regulated and predicts early death independently. This may help to identify high-risk patients and personalize adjuvant therapies, thus improving patient management.

813 Her2 Gene Status but Not Protein Expression Stratifies Survival Significantly in Lymph Node Positive Bladder Cancer.

A Fleischmann, D Rotzer, R Seiler, GN Thalmann. University of Bern, Switzerland.
Background: Fluorescence in-situ hybridization (FISH) and immunohistochemistry (IHC) are the most widely used tests to determine Her2 status in cancer. However, there is a controversy about the performance of both tests. Corresponding data in bladder cancer are still limited.
Design: One hundred and fifty lymph node positive patients with urothelial bladder cancer underwent cystectomy and pelvic lymphadenectomy. A tissue microarray was constructed with samples from all primary tumors and matched lymph node metastases. Her2 status was determined on genetic level by FISH and on protein level by IHC using ASCO criteria.
Results: Her2 amplification (15.3%) and borderline amplification (8.8%) are significantly (p=0.003) more frequent in nodal metastases than in primary bladder cancers (8.8% and 5.1%). The same is true for Her2 protein overexpression (score 2+/3+: 25.2% vs. 9.4%, p<0.001). FISH and IHC results are only moderately correlated (kappa in primary tumors: 0.566, in metastases: 0.673) with 38.5% of the amplified primary tumors being immunohistochemically Her2 negative but amplification in all immunohistochemically strongly positive (3+) primary tumors; corresponding data from the metastases are 19% and 91.5%. Patients with Her2 amplification in the metastases have more (median 5 vs. 3, p=0.262) and larger metastases (max. diameter median 1.5 cm vs. 1.0 cm, p=0.263), however, these differences are not significant. Corresponding data based on IHC always have higher p-values. Her2 amplification in the primary tumor significantly predicts poor outcome (p=0.044) but misses to add independent prognostic information (p=0.074). IHC based survival stratification is unsuccessful.
Conclusions: Her2 FISH data are only moderately correlated with IHC results, which do not detect a substantial part of the amplified tumors. Together with successful survival stratification by FISH but not by IHC this suggests an advantage of FISH for patient selection for anti-Her2 therapies.

814 Comparative Study of 3.0T MRI and Whole-Mount Prostatectomy Sections for Prostate Cancer Detection.

LV Furtado, M Heilbrun, C Dechet, M Schabel, B Foster, LJ Layfield, T Liu. University of Utah Health Sciences Center, Salt Lake City.
Background: Radical prostatectomy, as the standard of care for surgical treatment of clinically resectable and significant prostatic adenocarcinoma, is associated with significant morbidity. Less invasive, yet curative procedures are highly desirable. Such procedures would require accurate preoperative assessment of extent and localization of prostatic adenocarcinoma. 3.0T magnetic resonance imaging (MRI) has high signal and spatial resolution and may increase accuracy of assessment for presence of, size, and location of prostatic adenocarcinoma. In this study we correlated histopathologic findings on whole-mount prostatectomy specimens with 3.0T MRI to evaluate the performance of high resolution (3.0T) MRI for prostatic carcinoma.
Design: The study group consisted of twelve cases of prostate adenocarcinomas from patients (mean age: 61 years) for whom 3.0T MRI data were available. All of the prostatectomy specimens were entirely submitted in a whole-mount (approximately 4.5 mm section thickness) fashion, from apex to base. Slides were reviewed to determine location, size and Gleason scores of carcinoma of each plane, independent of radiology evaluation. Prostate MRI was performed with a pelvic surface coil at 3.0T strength. The high resolution T2-weighted images (TR3300/TE125, 3.0mm section thickness) were interpreted, independent of pathologic results. The prostate was divided into sextants, and scored for the presence or absence of disease. For each sextant, imaging and histopathologic findings were compared. Chi-square test was used for analysis.
Results: Compared to histopathologic findings from whole-mount prostatectomy sections, 3.0T MRI showed sensitivity of 66.7% (52.9% -78.6%), specificity of 86.7% (59.5% – 98.3%), positive predictive value of 95% (83.1% – 99.4%), and negative predictive value of 40.6% (23.7% – 59.4%).
Conclusions: 3.0T MRI performance without endorectal coil is comparable to that of standard 1.5T imaging for the detection of prostatic adenocarcinoma. Unfortunately, single parameter T2 signal abnormality still fails to detect some significant disease. Integrating information from additional MRI pulse sequence appears to be required to improve accuracy for prostate cancer detection. Currently, accuracy of MRI evaluation in the detection of prostatic disease is insufficient to allow its use for guidance of focused, limited prostatic resections.

815 Risk of Prostatic Carcinoma Following a Diagnosis of Atypical Small Acinar Proliferation: A Multicenter Retro-Respective Study.

MY Gabril, B Moussa, S Metias, MS Moussa, GM Yousef. London Health Sciences Center/ University of Western Ontario, ON, Canada; St Michael's Hospital/University of Toronto, ON, Canada.
Background: The clinical significance of the diagnosis of Atypical Small Acinar Proliferation (ASAP) is questionable. Though previous studies showed that ASAP has high predictive value for prostatic adenocarcinoma (Pca) in subsequent biopsies, still the follow up of these cases is a matter of controversy. In this study, we aim to investigate the incidence of Pca after initial diagnosis of ASAP. Also, we elucidate the criteria of adenocarcinoma developed after that ASAP diagnosis.
Design: 127cases of needle core prostate biopsy with isolated initial diagnosis of ASAP (with at least one subsequent follow up biopsy) at London Health Sciences Center and St. Michael's Hospital, Ontario, Canada, were included in this study (2000-2008). All slides from the cases were re-reviewed by uropathologists. The number of cores with ASAP, age, serum PSA, prostate volume, abnormal DRE, number of biopsy cores in the initial biopsy and also in re-biopsy specimens were evaluated. Clinico-pathological features were assessed in radical prostatectomy specimens for the 40 pateint who developed Pca after ASAP (Cancer volume, Gleason score, extraprostatic status, margins status, seminal vesicles invasion and laterality).
Results: Out of 127 cases with initial diagnosis of ASAP, 40 cases developed Pca. In univariate and multivariate analyses, PSA level was a significant predictor for predicating the presence of prostate cancer in cases with initial diagnosis of ASAP (p = 0.26 and p = 0.095 respectively). There was a statistically significant correlation between the site of ASAP and the site of developing carcinoma on follow-up biopsies (p = 0.019). Data extracted from radical prostatectomies for developed Ca showed cancer volume was > 5% (64.7%) and <5% in (35.3%) and Gleason score was 3+3 = 6/10 in 77% and 7/10 in rest of cases with comparable results of these parameters on initial core biopsies. No evidence of extraprostatic extension, seminal vesicles invasion or lymph nodes metastasis in all 40 cases was confirmed.
Conclusions: Our study showed that ASAP diagnosis is a significant predictor of subsequent Pca, and re-biopsy should be considered in these cases. Pca developed after a diagnosis of ASAP can have a more than a minimal cancer volume but has low tumor stage.

816 Reproducibility of Grading Papillary Urothelial Carcinoma of Bladder. Utility of RB, P53 and KI-67.

Y Gong, JS Hou, X Chen, RT Ownbey, BL Mapow, FU Garcia. Drexel University College of Medicine, Philadelphia, PA.
Background: Two histopathological features stratify Bladder Cancer treatment in its initial phase. Histological grade: Low (LG) and high (HG) and the status of lamina propria invasion. Interobserver variability in grading papillary urothelial carcinoma (PUC) is well documented (Miyamoto, 2010). The aim was to assess the reproducibility of grading PUC and to assess the utility of a panel expression (P53, RB and Ki-67).
Design: 92 consecutive cases (TURB and biopsies), with primary PUC of the bladder diagnosed from 1/2001 to 6/2010 were retrieved from the University Hospital. 20 additional cases were not included due to different diagnosis and slides not being available. Five pathologists graded de-identified H&E slides using WHO/ISUP 2004 criteria for the first review (R1). On the second review (R2) (interval 3-4 weeks), image analysis % expression for panel was provided. A weighted Kappa (κ) coefficient was generated against the original pathology diagnosis (R1 and R2) and between pathologists using PASS software. Unpaired t-test was used to analyze panel expression.
Results: 59 men (64.1%) and 33 women (35.9%) with age range 39 to 93 years (mean 68±13) constituted the study group. 50 LG (39 non-invasive (NI) and 11 invasive (IN)) and 42 HG (7 NI and 35 IN) were reviewed. Consensus is reached in 67.4% and 64.1% on R1 and R2. Reproducibility with original diagnosis is high for R1 (κ ranging 0.678 to 0.770, mean 0.745±0.039) and R2 (κ ranging 0.682 to 0.758, mean 0.718±0.041).

The intra-observer reproducibility for each pathologist is 0.827, 0.855, 0.734, 0.854 and 0.674. Agreement amongst pathologists is high in the R1 (κ ranging 0.741 to 0.841, mean 0.796±0.036) & R2 (κ ranging 0.764 to 0.829, mean 0.786±0.030). HG-IN has the highest agreement in R1 and R2 (80%, 85.7%), followed by LG-NI (71.8%, 61.5%). HG-NI and LG-IN have the lowest agreement in R1 and R2 (14.3%, 28.6% & 45.5%, 27.3%). The panel increased agreement with original diagnosis in the HG-NI by 14.3% and HG-IN by 5.7%. Expression of each panel marker was studied for HG and LG groups. In HG, RB expression is decreased (52.8±33.0% to 35.6±38.9%, $p<0.05$), P53 expression is increased (21.8±28.4% to 43.4±37.7%, $p<0.05$) and Ki-67 expression is increased (29.1±23.0% to 61.1±25.7%, $p<0.05$).

Conclusions: 1) WHO/ISUP 2004 classification of PUC grading is highly reproducible in a non-specialized academic department. 2) Panel expression information did not increase grading reproducibility overall but did improve it in HG group. 3) Loss of RB and increased P53 and Ki-67 expression correlates with HG tumor.

817 Validation of AJCC 2009 Tumor Staging of 681 N0M0 Clear Cell Renal Cell Carcinoma Treated by Radical Nephrectomy.

JM Gonzalez-Berjon, LD Truong, JY Ro, AG Ayala, SS Shen. The Methodist Hospital and Weill Medical College of Cornell University, Houston, TX.

Background: The recent 2009AJCC staging system had a number of changes for pathologic staging of renal cell carcinoma (RCC), including substaging pT2 and combining perirenal/sinus fat invasion with renal vein invasion as pT3a. Clear cell RCC is the most common type of RCC and has a propensity to spread hematogenously through the renal vein. This study attempts to validate the prognostic significance of the 2009 AJCC system in a radical nephrectomy series.

Design: A total of 681 patients with N0M0 clear cell RCC treated by radical nephrectomy with a mean follow up time of 59.9 months were analyzed. The overall survival was calculated using the Kaplan-Meier method and the log rank test was used to compare the survival difference between different staging groups.

Results: Of the 681 patients, the stage distribution was: pT1a – 206 (30.2%), pT1b -153 (22.5%), pT2a – 62 (9.1%), pT2b – 30 (4.4%), pT3a – 220 (32.3%), pT3b/pT3c – 4 (0.6%), and pT4 – 6 (0.9%). A total of 238 patients (34.9%) died during the follow-up period. In univariate analysis, there were significant differences of the overall survival between pT1/T2 vs. pT3, and pT3 vs. pT4 tumors. There was no significant difference between pT1b vs. pT2 ($p=0.29$) tumors or between pT2a vs. pT2b ($p=0.8$) tumors. More importantly, there was a significant difference in overall survival between the pT3a with perirenal/sinus fat invasion (n=136) and pT3a with renal vein invasion (with or without fat invasion, n=84), with a 5-year survival of 56% and 36%, respectively (Figure 1) ($p=0.001$).

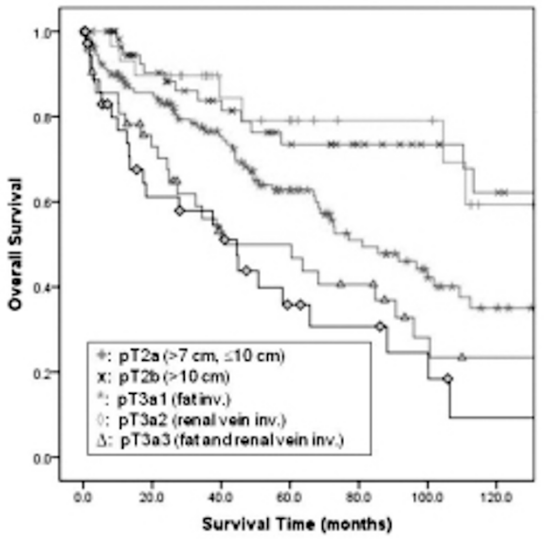

Conclusions: Out data prove that recent 2009 TNM staging system is a powerful predictor of survival for clear cell RCC. However, our findings suggest that 1) the value of substaging of pT2 tumors is limited; and 2) renal vein invasion carries a significantly worse prognosis than perirenal/sinus fat invasion, therefore, lumping together perirenal/sinus fat invasion with renal vein invasion as a single substage is unwarranted.

818 Evaluation of a Novel ERG Antibody in Prostate Cancer and Correlation with TMPRSS2-ERG Gene Rearrangement Status by FISH, ACGH and ERG mRNA Expression.

A Gopalan, M Dudas, MA Leversha, BS Taylor, N Schultz, H Hieronymous, Y Chen, H Al-Ahmadie, SW Fine, SK Tickoo, CL Sawyers, WL Gerald, VE Reuter. MSKCC, New York.

Background: TMPRSS2-ERG gene rearrangements are present in 30-50% of prostate cancer (PC) and lead to overexpression of a truncated ERG protein. The presence of the rearrangement may have prognostic significance and assist in patient stratification to guide therapy. An antibody based test for detection of rearrangement would therefore have significant clinical utility. We studied a recently characterized ERG antibody on a well annotated set of prostate cancer samples in which FISH, copy number and ERG mRNA expression data were available.

Design: Immunohistochemistry for ERG protein using a monoclonal antibody (clone EPR3864; Epitomics, Burlingame, CA) was performed on tissue microarrays containing 145 cases of PC. Positive or negative nuclear expression and intensity of staining (1-3) was recorded. TMPRSS2-ERG gene rearrangement status was determined by interphase FISH using a 3 color breakapart probe containing BAC clones against 3'ERG, 3' and 5' TMPRSS2. FISH data were available in 95 cases. In 50 cases with both ERG antibody (ERG AB) and FISH data, TMPRSS2-ERG rearrangement status derived using combined aCGH and whole-transcript outlier expression inferred from exon expression arrays was also available for correlation.

Results: Of 94 cases where FISH and ERG AB data were available, 3 (3%) were ERG (+) and FISH (-). One of these had expression and copy data available, both of which supported the ERG AB result. None of the ERG AB (-) cases were FISH (+). No difference in staining intensity was observed between cases rearranged by translocation or deletion. ERG mRNA overexpression was present in 48 cases in the dataset. 45 were evaluable, of which 37 were ERG AB (+) and 8 ERG AB (-). Four of the 8 ERG AB (-) cases were evaluable by FISH and all were negative for the rearrangement while all 8 were fusion positive by aCGH. The discrepancy between ERG AB/ FISH and aCGH/ expression is likely due to tumor heterogeneity and sampling.

Conclusions: Antibody based detection of TMPRSS2-ERG rearrangement shows a high concordance with FISH

The greater discordance between ERG AB and mRNA/ aCGH likely reflects tumor heterogeneity and different areas sampled for genomic studies and TMA based assays

819 Usual and Unusual Histologic Patterns of Gleason Score 8-10 Adenocarcinoma of the Prostate.

S Gottipati, JC Warncke, PA Humphrey. Washington University Medical Center, MO.

Background: The 2005 International Society of Urological Pathology (ISUP) modified Gleason grading scheme defines several gland arrangements of Gleason patterns 4/5. For pattern 4 these are fused microacinar glands, ill defined glands with poorly formed glandular lumina, large cribriform glands, cribriform glands with an irregular border, and hypernephromatoid. For pattern 5 these are solid sheets, cords, or single cells and comedocarcinoma. Scant data exist on the frequency of occurrence of these patterns. This aim of this study was to ascertain the frequency of the defined patterns in needle biopsy tissue, to determine the common admixtures, and to define patterns not in the 2005 ISUP report.

Design: 136 needle biopsy cases with a Gleason score (GS) of 8-10 were examined. We quantitated the number and type of ISUP patterns present for each case, determined extent of core involvement, and assessed for patterns not described in the 2005 ISUP system.

Results: A mean of 3.6 patterns (range 1-8) was identified per case. Fused microacinar glands (52.9% of cases) and ill defined glands with poorly formed glandular lumina (50.7%) comprised the predominant and most frequently admixed patterns. Also detected were single cells (48.5%), single signet ring cells (34.6%), cribriform glands (31.6%), sheets of cells (22.8%), chains (4.4%), comedonecrosis (2.2%), and hypernephromatoid (0.7%) patterns. GS 8-10 carcinoma was typically extensive, with a mean of 4.6 positive cores (range 1-15) per case. Only two cases (1.5%) had a very small carcinoma focus (1-2 mm), with ill-defined glands with poorly formed lumina and single cell patterns being present in these two cases. Patterns not present in the ISUP report include single file growth, nested, and solid cylinder patterns. The single file pattern, similar to that seen in lobular breast carcinoma, was present, usually focally, in 35.3% of the cases. The small solid nested pattern was detected in 22.8% of the needle biopsy cases. Only one case (0.7% of cases) had solid cylinders.

Conclusions: The results show that patterns of Gleason score 8-10 prostatic adenocarcinoma can be stratified based on their frequency of occurrence in needle biopsy. We characterize the frequency of the ISUP-defined and additional patterns including single file, small nested, and solid cylinder arrangements. For diagnostic recognition purposes it is important to be aware of the frequency of various patterns encountered in Gleason score 8-10 adenocarcinoma, the types of admixtures, and the histomorphological presentation of unusual variants.

820 Immunohistochemical (IHC) Expression of Carbonic Anhydrase IX (CA9) in Papillary (PRCC) and Chromophobe (CHRCC) Renal Cell Carcinoma Is Associated with Necrosis.

R Goyal, B Zhu, V Parimi, S Bishu, X Lin, XJ Yang, SM Rohan. Northwestern University, Chicago, IL.

Background: The modern classification of renal cell carcinoma (RCC) recognizes numerous subtypes of which clear cell (CRCC), PRCC, and CHRCC are the most common. Many IHC markers useful in differentiating RCC subtypes have been described. CA9 protein expression is induced by hypoxia or in the case of CRCC abrogation of the VHL / HIF pathway. In a recent phase III clinical trial radiolabeled CA9 was used with imaging techniques to preoperatively identify CRCC with high specificity. In the pathology literature it has been suggested that CA9 expression is often seen in PRCC and other renal tumors. We evaluated CA9 IHC in different RCC subtypes focusing on tumors with necrosis.

Design: H&E sections of RCC were evaluated for necrosis. IHC for CA9 was performed on whole sections from 17 RCC with necrosis (10 PRCC, 7 CHRCC) and 17 RCC without necrosis (10 PRCC, 7 CHRCC). Ten CRCC were included as controls. Qualitative (intensity 0-3+) and quantitative (% of cells) CA9 labeling was evaluated. The distribution of staining within a tumor (peri-necrotic vs. viable areas) was recorded. Only membranous CA9 labeling was considered positive. Statistics were performed using the Student's t-test.

Results: CA9 staining was seen in a larger percentage of cells and was more intense in necrotic areas compared to non-necrotic areas in PRCC (necrotic mean cell % = 5%; non-necrotic mean cell % = 1% [p value = 0.03]; mean intensity in necrotic areas = 2.1; mean intensity in non-necrotic areas = 0; p value < .001). A difference was also seen between mean intensity CA9 staining in necrotic versus non-necrotic areas in CHRCC (1.17 vs 0; p value = 0.02). Necrotic areas of PRCC and CHRCC when compared to each other showed no significant differences in either percentage of cells staining or intensity of staining (p value = 0.17 and p value = 0.75 respectively). All of the CRCC evaluated exhibited >90% of cells staining with 3+ intensity.
Conclusions: PRCC and CHRCC can exhibit expression of CA9 albeit at a much lower level relative to CRCC. Non-clear cell carcinomas with areas of necrosis show greater and more intense CA9 staining compared to non-clear cell carcinomas without necrosis. Caution should be taken when interpreting CA9 IHC in difficult to classify RCC cases exhibiting necrosis, particularly in small biopsies. The relevance of CA9 expression in necrotic non-clear cell RCC renal tumors as it relates to new preoperative imaging modalities warrants further investigation.

821 The Diagnosis of Clear Cell Renal Cell Carcinoma (CRCC) on Needle Core Biopsies (NCB) of the Kidney: How Specific Is Carbonic Anhydrase IX (CA9) Immunohistochemistry (IHC)?

R Goyal, B Zhu, S Bishu, V Parimi, X Lin, XJ Yang, SM Rohan. Northwestern University Feinberg School of Medicine, Chicago, IL.
Background: NCB of renal masses are becoming more common in clinical practice. NCB are often done in patients with contraindications to surgery prior to ablative therapies or in clinical trials of neoadjuvant targeted therapies. In the latter case, trial enrollment is often dependent on proper subclassification of a tumor. The modern classification of renal cell carcinoma (RCC) recognizes numerous subtypes of which CRCC is the most common. Many IHC markers useful in differentiating RCC subtypes have been described. IHC expression of CA9 is seen in most CRCC secondary to alteration of the VHL/HIF pathway. The expression of CA9 in CRCC is well known in the clinical literature in which the use of radiolabeled CA9 and PET/CT for the preoperative diagnosis of CRCC with high specificity has been documented. In the pathology literature it has been suggested that CA9 is not specific for CRCC and that CA9 expression is often seen in papillary RCC (PRCC) and other renal tumors. The aim of our study was to evaluate the utility of CA9 IHC in the diagnosis of CRCC on NCB.
Design: Thirty-two cases of renal tumors that had undergone NCB and then subsequent resection were evaluated. CA9 IHC was performed on the NCB in each case. Only membranous CA9 labeling was considered positive. The staining was graded from 0 to 3+ (0, no staining; 1+, 1-25% cells positive; 2+; 26-50%; and 3+, >50%). The final pathology of the resection specimen was used as the "gold standard" diagnosis. The presence or absence of necrosis was noted in each case.
Results: The final pathologic diagnoses included 21 CRCC, 4 PRCC, 4 chromophobe RCC, 2 unclassified RCC, and 1 oncocytoma. 95% (20/21) CRCC exhibited 3+ CA9 IHC. Three cases had discordant NCB and final pathology diagnoses (table 1). The sensitivity and specificity for CA9 labeling in CRCC were: 95% and 73% respectively.

Cases with discordant NCB diagnoses (DX)

	NCB DX	Final DX	CA9	Necrosis
Case 1	Unclassified RCC	PRCC	2+	Present
Case 2	Unclassified RCC	PRCC	2+	Present
Case 3	CRCC	Unclassified RCC	3+	Present

Conclusions: Most CRCC can be correctly subclassified on NCB by morphology alone. CA9 IHC has high sensitivity but only moderate specificity for a diagnosis of CRCC on NCB. The expression of CA9 in non-clear cell RCC is often seen when necrosis is present. Thus, caution should be taken in interpreting and reporting CA9 IHC results on NCB in morphologically ambiguous cases with histologic or radiographic evidence of tumor necrosis.

822 Frozen Section (FS) Analysis of Cancer Containing Bladder Transurethral Resection Specimens (TURB) for the Presence of Muscularis Propia (MP) Invasion.

R Goyal, S Bishu, V Parimi, XJ Yang, SM Rohan. Northwestern University Feinberg School of Medicine, Chicago, IL.
Background: The use of FS for intra-operative consultation and management can be an extremely powerful tool. However, surgical pathologists are commonly confronted with specimen types which are not amenable to FS or clinical questions which can be better addressed on permanent section (PS). At our institution, we are frequently asked to assess TURB specimens at FS for the presence of MP invasion. Given the lack of studies in the literature addressing this specific issue it is difficult to make an evidence based argument against this practice. This study documents the experience of a single academic center in evaluating cancer containing TURB specimens at FS for MP invasion.
Design: Thirty-two cases of cancer containing TURB specimens sent for FS from 2008-2010 were identified in our files. The FS and PS diagnosis were reviewed for discrepancies in regards to the presence or absence of invasive carcinoma, tumor grade, and MP invasion. Cases that were excluded from the calculation of test performance included: 1) cases with FS diagnosis deferred 2) cases without muscularis propria on the FS and subsequent PS slides. The sensitivity (SEN), specificity (SPEC), positive predictive value (PPV), and negative predictive value (NPV) for identifying MP invasion at FS were then calculated.
Results: In 5 cases (16%) the FS diagnosis was deferred. In all of the remaining cases the FS diagnosis of carcinoma and the tumor grade was concordant with the PS diagnosis. In 7 cases MP was not present in the FS or the subsequent PS slides. Of the remaining 20 cases, 2 false positive and 6 false negative diagnoses of MP invasion were identified (60% concordance rate). The test performance for FS assessment of MP invasion in TURB were SEN = 45%, SPEC = 77%, PPV = 71%, and NPV = 53%.
Conclusions: The diagnosis of carcinoma and the tumor grade can be determined accurately on TURB specimens at FS. The diagnosis of MP invasion on PS can be difficult and our results suggest that this diagnosis is even more difficult at FS. Though this study is based on small numbers at one academic center, the results strongly point to the conclusion that the examination of TURB specimens for MP invasion is best done on PS. This conclusion is also supported by our experience that the FS diagnosis in TURB cases rarely, if ever, changes intraoperative management.

823 Selective Immunohistochemical Markers To Distinguish between Metastatic High Grade Urothelial Carcinoma to the Lung and Primary Poorly Differentiated Invasive Squamous Carcinoma.

AM Gruver, D Westfall, CF Farver, DJ Luthringer, AO Osunkoya, JK McKenney, MB Amin, DE Hansel. Cleveland Clinic, OH; Cedars-Sinai Medical Center, Beverly Hills, CA; Emory University School of Medicine, Atlanta, GA; Stanford University School of Medicine, CA.
Background: The distinction between primary lung carcinomas and lung metastases from other sites, especially the urinary tract, is a common diagnostic dilemma in surgical pathology. As urothelial carcinomas (UCCs) can demonstrate a broad range of morphology, and frequently demonstrate squamous differentiation, the distinction between metastatic UCC to the lung and primary pulmonary invasive squamous cell carcinoma (SCC) can often be challenging. Individual immunohistochemical (IHC) markers are often not especially helpful in these situations, as both p63 and high molecular weight cytokeratin, which are often used in the diagnosis of UCC, are expressed in SCCs from various anatomic locations.
Design: We examined a panel of 12 established and emerging IHC markers in 30 patients with paired urinary tract and presumed metastatic lung tumors to establish a useful diagnostic panel.
Results: The best markers to aid in the distinction between poorly differentiated metastatic UCC and primary pulmonary SCC were CK7, CK20, GATA-3, S100-A1 and UROIII, with the utility of the latter dependent upon the quantity of tissue available for analysis. The observed percent positive staining in non-metastatic UCC and primary pulmonary SCC with these markers was CK7 (100% vs. 33%), CK20 (54% vs. 7%), GATA-3 (78% vs. 23%), S100-A1 (0% vs. 20%) and UROIII (14% vs. 0%) respectively.
Conclusions: When interpreted in close correlation with clinical history and routine H&E histomorphology, these markers (CK7, CK20, GATA-3, S100-A1 and UROIII) may be a useful adjunct in the distinction of metastatic high grade UCC to the lung.

824 Immunohistochemical (IHC) Profile To Distinguish Urothelial from Squamous Differentiation in Carcinomas of Urothelial Tract.

C Gulmann, GP Paner, RS Parakh, DE Hansel, SS Shen, JY Ro, C Annaiah, A Lopez-Beltran, P Rao, K Arora, YM Cho, R Alsabeh, MB Amin. Beaumont Hospital, Dublin, Ireland; University of Chicago, IL; Cedars-Sinai Medical Center, Los Angeles, CA; Cleveland Clinic, OH; The Methodist Hospital, Houston, TX; Faculty of Medicine, Cordoba, Spain; MD Anderson Cancer Center, Houston, TX.
Background: Urothelial neoplasms with squamous morphology raise the differential diagnosis between pure primary squamous cell carcinoma (SCC), urothelial carcinoma (UC) with squamous differentiation, and secondary involvement by SCC, e.g. from uterine cervix or anal canal. Accurate identification between these entities is critical due to differing prognosis and therapeutic strategies and the diagnostic dilemma may be compounded in limited samples.
Design: We evaluated the utility of an IHC panel of three urothelial-associated antibodies (Uroplakin III, S100P and GATA3) & two squamous-associated antibodies (CK14 and Desmoglein-3) in 50 primary urothelial neoplasms: 15 pure UC, 12 pure SCC and 23 UC with squamous differentiation. Squamous differentiation was defined by intercellular bridges or evidence of keratinization.
Results: Pure SCC were positive for CK 14 (100%) & Desmoglein-3 (75%), negative for GATA3 (0%) & Uroplakin III (0%); one case was S100P positive (9%). Pure UC had an opposite pattern & were positive for S100P (93%), GATA3 (93%) & Uroplakin III (73%) & were negative for Desmoglein-3 (0%); CK 14 was positive in 27% of cases. 74% of UC with squamous differentiation had expression of urothelial & squamous associated markers (S100P 83%, GATA3 35%, Uroplakin III 13%, CK14 87% and Desmoglein-3 70%); although reactivity for individual markers within some tumors did not always correspond with morphologic differentiation. Of the remaining 26%, 4 showed an overall 'squamous' immunoprofile whilst 2 cases showed a 'urothelial' immunoprofile.

	Pure SCC (n=12)	Pure UC (n=15)	UC with SCC diff (n=23)
CK14	100%	27%	87%
Desmoglein-3	75%	0%	70%
GATA3	0%	93%	35%
Uroplakin III	0%	73%	13%
S100P	9%	93%	83%

Conclusions: 1) A panel of five antibodies reliably distinguishes carcinomas of the urothelial tract with squamous & urothelial differentiation suggesting potential utility due to management implications. 2) Immunostaining in tumors with both urothelial & squamous differentiation showed mixed profile. 3) Lack of correlation of some IHC markers with morphologic differentiation in a few tumors with mixed differentiation suggests that changes at the protein level precede phenotypic manifestation.

825 ERG Oncoprotein Overexpression in Matched Primary and Metastatic Prostate Adenocarcinomas.

B Gurel, H Fedor, JL Hicks, AM De Marzo. Johns Hopkins University School of Medicine, Baltimore.

Background: Gene fusions of Ets family members to the androgen-regulated TMPRSS2 gene is a common occurrence in prostate cancer. The most common fusion is between TMPRSS2 and ERG, which occurs in roughly 50% of prostate cancers. Until recently, little was known regarding the expression of the ERG protein. Two recent reports indicate robust staining for ERG protein in a subset of prostate cancers and that this correlates highly with FISH-verified rearrangements (Prostate Cancer and Prostatic Diseases, 13:228–237,2010; Neoplasia, 12:590-598,2010). However, whether untreated metastatic prostate cancers are also ERG protein positive has only been examined in 7 cases thus far.

Design: For this study, we constructed a TMA using primary prostate adenocarcinoma tissues from 37 radical prostatectomy specimens and matched, hormone-naïve metastatic prostate carcinoma tissues from accompanying pelvic lymph node dissections, using the largest tumor nodule from each case. The TMA slide was stained with a rabbit monoclonal antibody (Epitomics), digitized and uploaded into TMAJ for web-based analysis. Each TMA spot was then visually assessed for ERG oncoprotein immunopositivity in the carcinoma lesion.

Results: As shown previously, there was strong staining in virtually all endothelial cells yet no staining was present in normal prostate epithelium. In most positive cases, virtually all of tumor cells showed robust nuclear staining. Of the 37 primary carcinomas, 27 (73%) were positive for ERG. Of these 27, 24 (88.9%) of the matched lymph node metastases were positive, whereas 3 were negative. Of the primary tumors that were negative for ERG, all corresponding lymph nodes were negative. There were no cases where only the lymph node metastasis was positive with the primary being negative.

Conclusions: Our results show that ERG protein positivity in a primary index tumor is mirrored to a large extent in corresponding untreated lymph node metastases. Since there were no cases of positively staining lymph node metastases without a corresponding primary tumor being positive, these results support prior studies indicating that ERG alterations resulting in ERG protein overexpression occur early during prostate carcinogenesis. Thus, unlike other molecular alterations in prostate cancer that occur more frequently in progressive disease (e.g. PTEN loss and 8q24 gain), a given prostatic adenocarcinoma lesion either does or does not have ERG protein overexpression, and if it does, it occurs very early in the process and is maintained across disease states.

826 The Utility of Novel Immunohistochemical Marker ERG in Detecting Prostate Cancer Following Atypical Prostate Biopsies: Will New Tumor Markers Be of Value in Such Circumstance?

H He, C Magi-Galluzzi, P Carver, S Falzarano, K Smith, M Rubin, M Zhou. Cleveland Clinic; Weill Cornell Medical College, New York; Peking University, Health Science Center, Beijing, China.

Background: A diagnosis of 'Atypical glands suspicious for cancer' (ATYP) in prostate biopsy (PBx) is associated with an average of 42% risk of detecting prostate carcinoma (PCa) in subsequent PBx. Many studies have failed to identify any clinical, histological or molecular characteristics of ATYP that could predict which patients would have PCa in the follow-up. *TMPRSS2*: *ERG* gene rearrangement is highly specific and is present in approximately 50% of PCa. Recently, a novel anti-ERG monoclonal antibody, when used as an immunohistochemical (IHC) marker, has been found to highly correlate with *TMPRSS2*: *ERG* gene rearrangement status. We evaluated the utility of this antibody on PBx with initial ATYP diagnosis to determine whether ERG expression could help improve PCa detection in subsequent PBx.

Design: ERG protein expression was evaluated by IHC on 103 cases of PBx with initial ATYP diagnosis. The pathological features of ATYP and ERG expression were correlated to the PCa detection in follow-up PBx.

Results: ERG expression was detected in 16/103 (15.5%) PBx with an initial ATYP diagnosis. Of the 16 ERG positive cases, the atypical glands were positive for ERG in 9 cases. In remaining 7 cases, positive ERG staining was found in the glands other than ATYP glands, including low and high grade prostatic intraepithelial neoplasia, and morphologically benign glands. In 49 cases with confirmed PCa diagnosis, 7 (14.2%) was positive for ERG in ATYP biopsy. PCa was detected in 7/16 (43.8%) of ERG-positive cases, and in 42/87 (48.3%) of ERG-negative cases in subsequent PBx (p=0.841 by x^2 test). ATYP was categorized as "favor cancer", "indeterminate" and "favor benign". PCa was detected in 18/29 (62.1%), 24/42 (57.1%) and 7/32 (21.9%) (p=0.002 by x^2 test) in the 3 categories. Addition of ERG IHC results did not improve the cancer detection in the 3 categories.

Conclusions: ERG-positive glands were present in 15.5% of ATYP PBx. However, the positive ERG stain did not correlate with increased cancer detection in subsequent PBx. The most likely explanation is that while positive ERG IHC identifies patients who harbor PCa, PCa in these patients is under-detected by the current PBx protocols. Our results suggest that new PCa markers have limited contribution to the ultimate PCa detection as long as the diagnosis of PCa depends on the detection of cancer tissue by PBx which currently has significant false negative rate.

827 Carbonic Anhydrase IX Is an Independent Prognostic Predictor for Clinically Localized Clear Cell Renal Cell Carcinoma.

H He, P Elson, H Aydin, S Campbell, B Rini, C Magi-Galluzzi, M Zhou. Cleveland Clinic; Peking University, Health Science Center, Beijing, China.

Background: Carbonic anhydrase IX (CAIX) is a membrane glycoprotein regulating pH and serves as a marker for hypoxia. It is expressed in the majority of clear cell renal cell carcinomas (CCRCC) and high level of expression (in $\geq$85% of tumor cells) has been reported to correlate with better prognosis in patients with metastatic CCRCC. Its prognostic significance in localized CCRCC, however, is uncertain due to conflicting results from only a few studies. We investigated the expression and prognostic significance of CAIX in a large cohort of localized CCRCC with long-term follow-up.

Design: A tissue microarray was constructed from 552 unilateral, clinically localized CCRCC treated surgically between 1990 and 2003 and was immunostained for CAIX expression (antibody clone NB100-417). The membranous CAIX staining was evaluated as positive. The staining intensity (0-negative, 1-weak, 2-moderate, 3-strong) and the percentage of cells with each staining intensity were recorded. A composite score was calculated by adding together the products of each staining intensity and its corresponding percentage of positive cells. The CAIX expression, measured as composite score, maximum intensity and percentage of positive cells, was correlated with pathological parameters and clinical outcomes.

Results: CAIX was expressed in 80.4% (444/552) cases with staining intensity 1, 2 and 3 seen in 16.5%, 42.4% and 21.5% of cases. The median percentage of positive cells was 67% (range 2-100%) and the median composite score was 90 (range 4-300). CAIX composite score inversely correlated with Fuhrman nuclear grade and necrosis (p=0.02 and 0.04). In univariate analysis, presence of strong staining intensity (staining intensity 3) and percentage of positive cells were both associated with overall survival, p=0.002 and 0.004, respectively. Using the Cox proportional hazards model, the presence of any strong staining (intensity 3) was a significant independent predictor for better survival (hazard Ratio=2.82, p=0.003) as were the other known bad prognosis markers including age, presence of perinephric fat invasion, nuclear grade, and necrosis.

Conclusions: The CAIX expression is associated with overall survival in patients with localized CCRCC. Strong CAIX expression is significantly associated with better survival independent of other known clinicopathological parameters. Our study confirms the prognostic significance of CAIX expression in clinically localized CCRCC.

828 Gain of Chromosome 12 Is an Adverse Prognostic Factor for Clinically Localized Clear Cell Renal Cell Carcinoma: A Chromogenic In-Situ Hybridization (CISH) Study.

H He, P Elson, H Aydin, S Campbell, B Rini, C Magi-Galluzzi, R Tubbs, M Zhou. Cleveland Clinic; Peking University, Health Science Center, Beijing, China.

Background: The role of tumor suppressor gene *p53* and its major negative regulator *MDM2* in clear cell renal cell carcinoma (CCRCC) has only been addressed recently. A few studies have generated conflicting data regarding MDM2 expression and its prognostic significance in CCRCC. This study examined the quantitative alteration of *MDM2* gene and chromosome 12 and their correlation with clinical outcomes.

Design: Dual-color chromogenic in situ hybridization using probes for *MDM2* (12q15) and centromeric region of chromosome 12 was performed on a tissue microarray containing 333 clinically localized CCRCC treated surgically between 1990 and 2003. The copy number of *MDM2* gene and chromosome 12 was quantified under a bright field microscopy. An *MDM2*/chromosome 12 ratio $\geq$2.0 indicated amplified, and a ratio <2.0 indicated nonamplified *MDM2* gene. Simultaneous Cases displaying >2 signals of both probes and the *MDM2*/chromosome 12 ratio <2.0 indicated the gain of chromosome 12. Results were correlated to the clinicopathological parameters, recurrence-free survival (RFS) and overall survival (OS).

Results: Gain of chromosome 12 was present in 22.5 % (75/333) clinically localized CCRCC. *MDM2* amplification was only observed in 2.7% (9/333) cases. The gain of chromosome 12 was significantly associated with adverse pathological factors, including higher Fuhrman grade and pathological stage, and the presence of necrosis (all $p\leq$0.01), but not with age or sarcomatoid differentiation. Patients with chromosome 12 gains showed significantly worse 5-year RFS (64$\pm$6% vs 87$\pm$2%, p<0.0001) and OS (64$\pm$6% vs 85$\pm$2%, p<0.0001) in univariable models. In multivariable Cox models, chromosome 12 gain, pathologic stage, Fuhrman grade and necrosis all significantly correlated with RFS. The hazard ratio for chromosome 12 gain was 2.86 (p=0.002).

Conclusions: Isolated *MDM2* gene amplification is rare in clinically localized CCRCC. However, gain of chromosome 12 is present in 22.5% of CCRCC and is an independent predictor for poor prognosis. Studies are ongoing to identify candidate genes on chromosome 12 that confer adverse prognosis.

829 Pathologic Characteristics and Clinical Outcome of Renal Epithelioid Angiomyolipoma: A Multi-Institutional Experience Based on Primary Tumor Resections.

W He, JC Cheville, PM Sadow, A Gopalan, SW Fine, HA Al-Ahmadie, Y Chen, E Oliva, P Russo, VE Reuter, SK Tickoo. Memorial Sloan-Kettering Cancer Center, New York, NY; Mayo Clinic, Rochester, MN; Massachusetts General Hospital, Boston.

Background: Cases of metastases/recurrences in some renal epithelioid angiomyolipomas (E-AML) are well documented; hence E-AML is regarded as potentially malignant. The overall true incidence of aggressive behavior among all cases of E-AML remains undetermined. While the reported incidences of metastasis have ranged from 0 to >45%, the studies with high incidence have mainly consisted of cases received in consultation, or derived from case reports. To determine the true overall biologic behavior among all cases, we studied cases of E-AML from the time of resection of the primary tumors at 3 institutions with high nephrectomy volumes.

Design: Material from all renal AMLs, for which primary resection was performed at the 3 institutions over periods of 18, 30 and 30 years, respectively, was reviewed. Only the cases with pure or almost pure epithelioid histology were considered as E-AML for this study. Cases received in consultation were not included. Gross findings were obtained from the pathology reports, and clinical follow-up from medical records/prospectively maintained clinical renal data-base.

Results: Material was available on 435 renal AML cases with primary resections at these institutions. Eighteen (4.1%) of these were E-AML (80-100% epithelioid). The F:M ratio was 10:8, and the mean age, 51 years (range, 31-80 yrs). Mean tumor

size was 7.5 cm (range, 1-19 cm). Other morphologic features currently available on 9 cases from 1 institution include, gross and microscopic tumor necrosis (5/9; 56% cases), mitotic rate <1 to 5/10 HPFs, and presence of pleomorphic giant cells (8/9; 89%). Over a mean follow-up of 55 months (range, 1-192 mths) available on 17/18 cases, none developed recurrence or metastasis. Sixteen of the patients were alive with no-evidence-of-disease (NED) at the time of last follow-up; one patient died of unrelated causes while NED.

Conclusions: 1. Pure/virtually pure epithelioid AML constitute approximately 4% of all resected AMLs. 2. While aggressive behavior in some E-AMLs is well-reported in literature, we observed no metastasis or recurrences in cases with primary resection over a period of long follow-up. 3. Our data indicates that the rate of aggressive clinical behavior of E-AML, as defined by the WHO classification, is lower than what the literature suggests; most cases follow a benign clinical course.

830 Evaluation of TMPRSS2-ERG Fusion Protein in Prostate Cancer Pathogenesis across Continents.

R Henshall-Powell, C Yu, R Bremer, IA Sesterhenn, D Tacha. Biocare Medical, Concord, CA; AFIP, Washington, DC.

Background: The incidence of prostate cancer is 30-50 times more prevalent in North American vs. Asian populations. Chromosomal translocations involving ETS transcription factors, such as ERG and ETV1, are frequent events in human prostate cancer pathogenesis. In particular, the TMPRSS2-ERG fusion gene was discovered to be the most frequent proto-oncogene present in 45-65% (North American) and 15-20% (Asian) of prostate cancers. The TMPRSS2-ERG fusion is associated with a more aggressive phenotype. Given the ease of performing IHC vs. FISH, ERG protein expression in FFPE tissue may be an extremely useful tool for the molecular subtyping of prostate cancer. This study evaluated the sensitivity and specificity of a mouse ERG mAb on human prostate tissues; comparing North American and Asian cases. A wide variety of normal and neoplastic tissues were tested to establish specificity.

Design: Tissue microarrays (TMA's) of human prostate adenocarcinoma (Grades 1-4 and Gleason Scores 2-10), normal prostate and other normal and neoplastic tissues were analyzed. TMA's were processed according to standard IHC protocols. Samples were incubated with mouse anti-ERG mAb for 30mins followed by chromogenic visualization (DAB-HRP).

Results: Only 19% (32/169) of tissues from patients of Asian descent showed high expression of ERG compared to 45% (15/33) of North American prostate TMA's. Gleason Score or tumor grade were not dependent upon ERG expression. 744 normal and neoplastic tissues analyzed: only 0.4% (3/744) showed positive staining for ERG: one each of a T-Cell Lymphoma, B-Cell Lymphoma and Melanoma; thereby demonstrating 99.6% specificity for prostate tissues.

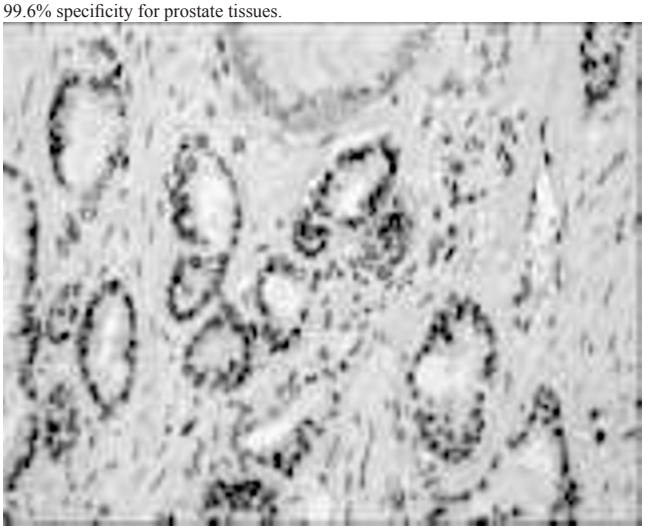

Conclusions: High specificity of TMPRSS2-ERG expression (99.6%) in prostate cancer tissue was demonstrated with this mAb by examining normal and neoplastic tissues. ERG expression was independent of Gleason Score or tumor grade. The frequency of ERG expression was higher in North American vs. Asian patients, correlating to a higher incidence of prostate cancer in North American populations. Considering the association of TMPRSS2: ERG rearrangement with a more aggressive phenotype and a 96.5% correlation between ERG-positive PIN and ERG-positive carcinoma, the evaluation of ERG expression may be a valuable diagnostic tool.

831 High Frequency of KRAS Mutation in Penile Squamous Cell Carcinomas.

J Hernandez-Losa, CM Valverde, C Ferrandiz-Pulido, R Somoza, I de Torres, S Ramon y Cajal. Hospital University Vall d´ Hebron, Barcelona, Spain; Hospital University Vall d´Hebron, Barcelona, Spain.

Background: Several risk factors have been associated with the carcinogenesis of penile squamous cell carcinomas (PSCC), most of them related to poor hygiene and HPV infections. The molecular biology of these carcinomas is not well understood, and the treatment of metastatic disease remains undefined. Recently, EGFR overexpression arises as a good molecular marker present in almost 90% of PSCC, and patients treated with EGFR directed therapies have shown promising results. The aim of this study was to analyze somatic mutations downstream of this receptor that could be activated and associated with resistance to EGFR inhibitors.

Design: We analyzed the somatic mutation of BRAF and KRAS in a total of 28 samples of PSCC including 17 usual type SCC, 10 verrucous carcinomas and 1 basaloid carcinoma. The samples were collected from de archives of the Pathology Department of our institution from 1996 to 2009. The DNAs were extracted from FFPE blocks by Biorobot EZ1 following the manufacturer protocol of the EZ1-DNA Tissue kit (Qiagen). KRAS and BRAF mutations were amplified with specific primers, and sequenced by Sanger with Bigdye terminator v3.1 Cycle Sequencing Kit

Results: No BRAF mutations were found in our series. However, we identified somatic missense mutations in the KRAS gene in 6 out of 26 penile cancer samples (23%). Two samples could not be evaluated for KRAS status. All mutants were activating G12D mutations. The histopathological characteristics of the tumors bearing KRAS mutations were studied, observing 3 out of 6 mutations in usual SCC tumours, 2 in verrocous and 1 in basaloid carcinoma. The grade of these tumors was as follows: 3 Stage III, 1 Stage II and 2 Stage I carcinomas.

Conclusions: BRAF mutations are not involved in the signalling downstream of EGFR in this type of carcinomas. KRAS mutations, in contrast, were found in 23% of PSCC analyzed. These mutations don't seem to strongly correlate to any histology type of carcinoma, although they tend to be more present in advanced stages (II and III) in comparison with earlier stages. These results suggest a role of KRAS mutation in the prognosis and progression of these carcinomas and support the importance to determine KRAS status in the selection of patients to be treated with anti-EGFR based therapies

832 Clear Cell-Papillary Renal Cell Carcinoma (CP-RCC) Not Associated with End Stage Renal Disease: Clinicopathologic Analysis of 50 Tumors Confirming a Novel Subtype of Renal Cell Carcinoma (RCC) Occurring in a Sporadic Setting.

LP Herrera, O Hes, M Hirsch, E Comperat, P Camparo, P Rao, M Picken, R Montironi, C Annaiah, K Arora, P Tamboli, DE Westfall, FA Monzon, MB Amin. Cedars-Sinai Medical Center, Los Angeles, CA; Charles Univesity, Plzen, Czech Republic; Brigham and Women's Hospital, Boston, MA; l'Hotel-Dieu, Place du Parvis, Paris, France; Hôpital Foch, Suresnes, France; MD Anderson Cancer Center, Houston, TX; Loyola University Hospital, Chicago, IL; Polytechnic University of the Marche Region, Ancona, Italy; The Methodist Hospital, Houston, TX.

Background: RCC with clear cell & papillary features includes numerous distinctive subtypes including a recently described subtype arising in end-stage kidneys. Accurate subtyping of RCC is essential as each represents a distinctive clinicopathologic entity associated with prognostic & predictive significance.

Design: A detailed clinicopathologic study of 50 tumors occurring in 48 patients was performed.

Results: The mean age of the pts. was 63 (range 32-83) yrs. with slight male predominance (1.3:1). All tumors were well circumscribed, averaged 2.2 (range 0.5-6) cm. Tumors had relatively typical morphology with encapsulation & tubular, tubulopapillary, tubulocystic & cystic morphology. The papillary architecture was unique in that it occurred secondarily within tubules and cysts, occasionally with branching. The cytoplasm was variable although all tumors had clear cytoplasm with distinct nuclear arrangement aligned circumferentially, resembling secretory endometrium. The nuclei of all cases were low grade, mostly Fuhrman nuclear grade 2 with only focal areas showing prominent nucleoli. Necrosis, mitotic activity, vascular invasion, or sarcomatoid change were not observed in any case. The stroma varied from being hyalanized to occasionally fibromuscular. 94% of tumors were pT1a & 6% were pT1b. Immunostudies showed CK7 (100%), HMCK (96%), PAX-2 (100%), PAX-8 (100%), vimentin (100%), CAIX (97%) positivity, & negativity for racemase, TFE3 & RCC Ag. Follow up in 25 pts.; mean 19 (range 1-91) mos. showed no evidence of local recurrence, distant metastasis or death due to disease.

Conclusions: 1) CP-RCC may occur in a sporadic setting and is distinctive from other unique subtypes of RCC. 2) The tumors are frequently small and invariably of low nuclear grade and low pathologic stage with extremely favorable prognosis. 3) Its distinctive immunoprofile has utility in the accurate distinction from other RCC with clear and papillary features.

833 Detailed Immunohistochemical Characterization in the Spectrum of Sex Cord Stromal Tumors (SCST) of the Testis Using Novel and Established Immunohistochemical (IHC) Markers: A Study of 41 Cases.

LP Herrera, M Amin, JD Schwartz, SS Shen, DE Hansel, GP Paner, P Tamboli, K Arora, C Annaiah, RS Parakh, MB Amin. Cedars-Sinai Medical Center, Los Angeles, CA; William Beaumont Hospital, Detroit, MI; The Methodist Hospital, Houston, TX; Cleveland Clinic, OH; University of Chicago, IL; MD Anderson Cancer Center, Houston, TX.

Background: SCSTs of the testis are rare accounting for 4% of all testicular neoplasms. They present with a range of architectural & cytologic patterns & a spectrum of differentiation overlapping in their morphology with germ cell tumors, metastatic tumors & paratesticular neoplasms. Immunohistochemistry is a potentially useful diagnostic adjunct in these rare tumors with multiple patterns. SF1-steroidogenic factor 1, a nuclear transcription factor controlling steroidogenesis & development of the gonads, has recently shown to be of value in ovarian tumors – its expression in SCSTs of the testis is largely unknown.

Design: 41 SCSTs encompassing the range seen in the testis were evaluated using traditionally used (inhibin, melanA, calretinin, CD99, S100 and synaptophysin) & novel (SF1) IHC markers.

Results: IHC expression (in percentage) in different SCST subtypes is summarized in the table. Synaptophysin had the lowest positivity rate (17%) amongst all markers studied.

IHC expression (%) in different SCST subtypes

Type*	SF1	MelanA	Inhibin	Calretinin	WT1	S100	CD99
LCT (n=17)	94	94	94	94	5	11	41
SCT (n=6)	50	83	16	50	33	50	16
MSCST (n=5)	40	60	20	60	20	20	20
USCST (n=5)	100	80	40	80	50	60	40
GCT (n=4)	100	50	50	50	100	100	50
% (+)	71	73	63	74	31	33	40

* LCT – Leydig Cell Tumor, SCT – Sertoli Cell Tumor, MSCT – Mixed SCST, USCST – Unclassified SCST, GCT – Granulosa Cell Tumor. Data not shown for large cell SCST, signet ring cell SCST and adrenogenital syndrome tumors (n=4).

Conclusions: 1) SF1 is a sensitive marker for testicular SCST, however, its sensitivity is lower than reported for ovarian tumors (100%). 2) WT1 is less commonly expressed in testicular (31%) in contrast to ovarian (80-100%) SCSTs. 3) SF1, calretinin & melanA should constitute markers in a screening panel for testicular tumors in which SCST is in the differential diagnosis. 4) Depending on histological complexity, other useful SCST markers in the testis include inhibin and CD99.

834 Prostatic Diseases in the Elderly Men: Glandular Microenvironment Signaling of IGFR-1, Steroid Hormone Receptors, Matrix Metalloproteinases and Dystroglycans.

A Hetzl, W Favaro, F Montico, U Ferreira, A Billis, V Cagnon. UNICAMP/Institute of Biology, Campinas, Sao Paulo, Brazil; UNESP, Campinas, Sao Paulo, Brazil; UNICAMP, Campinas, Sao Paulo, Brazil.

Background: Senescence is a determining factor for the occurrence of morphological changes in the prostate. Thus, the objective of this work was to characterize and correlate the α and β-dystroglycans (αDG, βDG), androgen receptor (AR), α and β-estrogen receptors (αER, βER), matrix metalloproteinases 2 and 9 (MMP-2, MMP-9) and insulin-like growth factor receptor (IGFR-1) reactivities in both stromal and epithelial compartments of elderly men without prostatic lesion and with Benign Prostatic Hyperplasia (BPH), High Grade Prostatic Intraepithelial Neoplasia (HGPIN) and Prostatic Cancer (PC).

Design: Sixty samples from the prostatic peripheral zone of autopsies and/or radical prostatectomies of 60-90 year old patients were divided into standard (no lesions), HGPIN, PC and BPH groups and analyzed by means of immunohistochemistry and Western Blotting analyses.

Results: The results showed increased IGFR-1, MMP-2 and MMP-9 protein levels in the PC and HGPIN groups in relation to other groups. Decreased αDG and βDG protein levels were verified in the PC and HGPIN groups in relation to the BPH and standard groups. Intensified AR immunoreactivity was verified in the epithelial compartment in all studied groups. αER immunoreactivity was more intense in the epithelial compartment in the PC and HGPIN groups than in the other groups. βER immunoreactivity was weaker in the epithelial compartment of the HGPIN and PC groups than in the BPH and standard groups.

Conclusions: Abnormal αDG, βDG, IGFR-1, MMP-2 and MMP-9 protein levels certainly compromised the glandular epithelial-stromal interaction in the senescence. The differential steroid hormone receptor reactivities in the glandular lesions in both prostatic compartments indicated different paracrine signals to the dynamics of the prostate and pointed out the importance of estrogenic pathways in the activation of these changes. Also, these findings indicated that there was a direct association between IGFR-1, MMPs and steroid hormone receptors, pointing towards IGFR-1 as a target molecule in prostate therapy and a possible factor for MMPs positive signaling.

835 Effect of Robotic-Assisted Laparoscopic Prostatectomy on Surgical Pathology Specimens.

H Hong, L Mel, J Taylor, Q Wu, H Reeves, A Allan. Brody School of Medicine at East Carolina University, Greenville, NC; Eastern Urological Associates, P.A., Greenville, NC; College of Allied Health Sciences at East Carolina University, Greenville, NC.

Background: Robotic-assisted laparoscopic prostatectomy (RALP) is a technique evolved over the last decade with significant efforts in improving functional outcomes following surgery. Currently, it is estimated that about 80% of prostatectomies in the USA are performed using RALP. It is interesting for pathologists and urologists to compare RALP with conventional open radical retropubic prostatectomy (RRP), and evaluate their effect on surgical pathology specimens.

Design: RALP and RRP procedures performed from 2007 to 2010 in our institution were retrospectively reviewed. Relevant data were collected from surgical pathology reports, and statistically analyzed.

Results: RALP group contains 104 patients with average age 61.4, Gleason score 6.60, tumor volume percentage 29.7%, and 63% of the patients at T2c stage; RRP group contains 42 patients with average age 60.6, Gleason score 7.05, tumor volume percentage 38.6%, and 68% of the patients at T2c stage. Comparison of these two groups shows that 28.9% of RALP and 66.7% of RRP have positive surgical margins, with statistically significant difference (P<0.001). If only patients at T2c stage are compared, the positive surgical margin is 25.4% for RALP and 60.7% for RRP (P<0.002). We further used a logistic regression model to adjust the difference in cancer stage, tumor volume percentage and Gleason score between these two groups in comparing the positive surgical margin rates. The odds ratio of RALP versus RRP is 0.20 with a 95% confidence interval (0.08, 0.52), suggesting highly significant difference in the two procedures (P<0.001). No significant difference is noted for tumor involvement in apex and bladder base margins between two groups (P>0.05). The size of seminal vesicles in RALP specimen (average 5.12 cm^3) is interestingly larger than that of RRP (1.20 cm^3, P<0.001), although this probably has no considerable effect on patient management. Comparison of RALP performed by different surgeons shows no significant difference in positive surgical margin rates (P=0.83).

Conclusions: RALP has become a new technique widely accepted by urologists and patients. The major change brought to surgical specimens by RALP is reduced positive surgical margins. This conclusion is made after adjusting the cancer stage, tumor volume percentage and Gleason score in patients from both RALP and RRP groups.

836 Renal Epithelial Tumors with Clear Cell Morphology Encompass a Heterogeneous Group of Renal Cell Carcinomas.

M Hosseini, M Tretiakova, A Chang, J Taxy, T Antic. University of Chicago, IL.

Background: Clear cell renal cell carcinoma (CRCC) is the most common kidney malignancy. In recent years, immunohistochemistry (IHC) and molecular methods have identified other new entities with clear cell morphology, e.g., clear cell papillary (CPRCC) and translocation RCC (TRCC), mostly in young patients. This study investigated the occurrence of these entities among cases previously diagnosed as RCC.

Design: A review of surgical pathology archives from 2005-2010 revealed 109 cases of RCC in individuals 20-50 years of age. Based on morphology 13 were chromophobe RCC, 21 papillary, 1 medullary and 1 adult Wilms. 27 cases were not available for review and 46 had clear cell morphology. The H&E sections were reviewed and supplemented by an IHC panel of AMACR, TFE3, CK7 and CAIX.

Results: The original diagnoses in the 46 cases were: 41 CRCC, 4 TRCC and 1 case unclassified. The revised interpretations based on morphology and IHC profile were: 27 CRCC, 5 CPRCC, 12 TRCC and 2 unclassified RCC. Of the 27 CRCC cases, 12 were AMACR, TFE3 and CK7 negative, positive for CAIX; 9 were AMACR and CAIX positive, negative for CK7 and TFE3; 6 were AMACR, CK7 and CAIX positive, TFE3 negative. Of the 5 CPRCC cases, all were AMACR and TFE3 negative, positive for CK7 and CAIX. All 12 TRCC were TFE3 positive but only 10 and 9 were positive for AMACR and CAIX respectively. Of the 2 unclassified cases, both demonstrated TRCC morphology; however they were negative for TFE3 and positive for CAIX.

Conclusions: Clear cell morphology is not restricted to conventional CRCC as the newly described entities of CPRCC and TRCC demonstrate. A histologic and IHC review of 46 clear cell tumors in patients ranging from 20-50 years old within a 5 year period resulted in a change of diagnosis in 12 cases (26%) to the newly described entities. The potential heterogeneity of CRCC is presently of uncertain clinical significance, although the subtypes do affect a younger population. In addition, the reported evolution of these clear cell carcinoma subtypes suggests a more indolent course for PCRCC and more aggressive for TRCC. Awareness of these entities as supplemented by immunostaining may impact the implementation of partial nephrectomy, non surgical treatments and focused clinical surveillance.

837 Measuring Dimension of Tumor Invasion of Urothelial Carcinoma (UCa) in Transurethral Resection Predicts Time of Recurrence.

Z Hu, GP Paner, K Mudaliar, GA Barkan. Loyola University, Maywood, IL; University of Chicago Hospital, IL.

Background: Over time, there have been improvements in diagnosis and treatment of UCa of the bladder by transurethral resection of bladder tumor (TURBT). However, recurrence rate still remains significantly high and thus, additional predictive variables in TURBT specimens are necessary to further enhance patient's management.

Design: A total of 110 TURBT specimens (1997-2005) of UCa were reviewed by 2 genitourinary pathologists. Amount of tumor invasion by UCa was measured in terms of percentage, focality (focal vs. non-focal), and dimension (DI, aggregate length of invasion). Correlating amount of tumor invasion to recurrence was quantified using SAS and Origin.

Results: A total of 39/110 (35%) patients with invasive UCa [9 females (23%), 39 males (77%)], were identified. Patient age ranged from 56 to 94 years old (mean 70 years). Recurrence rate in these patients was 96% (22 of 23); 1 patient had no recurrence (1 of 23). 95% of recurrence (21 of 22) occurred in less than 1 year post TURBT.

Table-1 The Characteristics of Invasive Urothelial Carcinoma

Dimension of tumor invasion (% of all recurrences)	<0.1 cm (14%)	0.1-0.5 cm (45%)	>0.5cm (41%)
The time for recurrence (% of all recurrences)	<4 months (32%)	4-6 months (23%)	>6 months (27%)

UCa with large DI (≥0.5 cm) had recurrence in less than 6 months. Conversely, tumor recurrence that occured more than 6 months had smaller DI (< 0.3 cm).

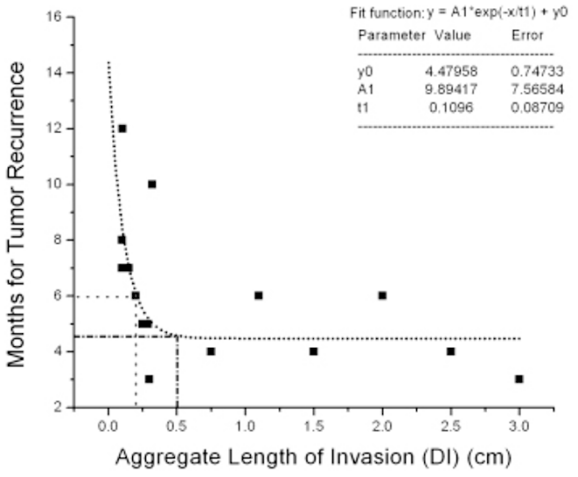

Statistical analysis showed that there was negative correlation of DI with time to recurrence ($p<0.05$, correlation coefficient: -0.47). Percentage or focality of invasion did not show similar correlation observed in DI.

Conclusions: There is a high correlation between DI and time to recurrence of UCa. Our study indicates that UCa with DI of ≥0.5 cm is likely to recur in less than 6 months and UCa with DI ≤0.3 cm may recur after 6 months. Thus, dimension of tumor invasion as a predictive variable could be considered as a possible variable in surgical pathology reporting of TURBT for UCa.

838 Subcellular Localization and Quantification of Androgen Receptor in Hormone-Naïve Prostatic Adenocarcinoma and Clinical Correlation.

W Huang, C Hoyt, T Pier, D Fletcher-Holmes. University of Wisconsin-Madison; Cambridge Research and Instrumentation, Inc., Woburn, MA.

Background: Androgen receptor (AR) is primarily located in the nucleus in an androgen-bound form and functions as a transcription factor. Recent studies have shown that AR shuttles between the nucleus and cytoplasm, and that cytoplasmic membrane AR initiates signal transduction. However, limited quantitative and clinical correlation studies of AR at subcellular levels are available.

Design: Two prostatic adenocarcinoma (PCa) outcome tissue microarrays (TMA) are constructed, each consisting of duplicate cores of PCa tissues from 183 PCa patients (174 hormone-naïve, 9 castration resistant) and 48 benign prostatic tissue (BPT). Two TMA slides with 4 cores representing each patient's PCa or BPT were stained using an immunofluorescent assay. The epithelial/membrane compartment was defined with mouse anti-e-cadherin monoclonal antibody (mAb) (Dako, 1:50) and visualized with Alexa Fluor 488. AR was detected with rat anti-AR mAb (Abcam, 1:200, with tyramide amplification) and visualized with Alexa Fluor 647. The nuclear compartment was defined and visualized with DAPI. Vectra™ platform (CRI) was used to scan TMA slides, segment subcellular compartments and quantify AR in each compartment. AR expression levels in the nucleus (nAR), cytoplasm (cAR) and membrane (mAR) compartments from the 174 hormone-naïve patients were included for analysis and their correlation with Gleason scores, PCa pathological stages and recurrence status was studied. One-way Anova was used to compare means.

Results: AR was detected in all three compartments in both PCa and BPT: highest in nucleus, lowest in cytoplasm. AR levels in the three compartments were generally lower in PCa than BPT. Significantly lower nAR, cAR and mAR levels were only found in patients with cancer recurrence (CRecur) ($p\leq0.05$) compared to recurrence-free (RF) patients. No significant differences of AR levels in any of the three compartments were found between RF patients and patients with biochemical recurrence (BRecur) or between BRecur patients and CRecur patients. Also, the mAR and nAR but not the cAR levels were significantly lower in the GS8 group compared to the GS6 and GS7 groups. The AR levels in all three compartments were not significantly correlated with PCa stages.

Conclusions: Our study confirms that AR is expressed not only in the nucleus but also in the cytoplasm and cytoplasmic membrane of prostatic epithelium. mAR and cAR could also be used as markers to predict PCa progression and outcome.

839 microRNA Associated with Aggressive Prostate Cancer in Racial Disparity.

H Huang, X Wu, L Zhou, Y Li, O Basturk, H Ostrer, S Freedland, I Osman, V Reuter, J Melamed, P Lee. New York University Medical Center, NY; Memorial Sloan Kettering Cancer Center, New York, NY.

Background: African American (AA) men have the highest rates of prostate cancer (PCA) in the world and a worse prognosis when compared to *Caucasian American (CA) men***.** The reason for the ethnic disparity between AA and CA men in PCA risk, incidence, clinical progression, and disease specific death includes genetic differences between the two populations. These genetic differences may occur in microRNAs (miRNAs), a class of small, non-coding RNAs regulating the expression of genes, including tumor suppressor genes and oncogenes, at the level of translation. It has been reported that subsets of miRNAs are strongly associated with racial disparity in tumors such as uterine leiomyoma. In this study, we determined the association between altered expression and function of miRNA in prostate cancer, especially in relation to its racial disparity.

Design: To test the hypothesis that altered expression of miRNAs is associated with racial differences in prostate cancer patients, we first examined the expression of miRNAs in benign and cancerous prostate with a miRNA microarray of 700 miRNAs using prostatectomy specimens of AA (n=8) and CA (n=7) PCA. Next, we determined the association of altered miRNA expression on a racial tissue microarray within these two populations (n=71 for AA and n=56 for CA). We also tested whether increased expression of specific miRNAs promotes cell growth, invasion and metastasis in prostate cancer cell lines *in vitro* by using WST colorimetric cell proliferation and Matrigel invasion assays.

Results: The miRNA microarray analysis of the 15 macrodissected matched benign and cancer tissue revealed differences in distribution of a number of miRNAs in AA versus CA prostate cancer when compared against corresponding expression in benign AA and CA prostate tissue. Among the dysregulated miRNAs, with confirmation by miRNA in-situ hybridization, let7c was decreased in prostate cancer with a greater decrease in AA prostate cancer. We also observed a racial difference for miR30c. Let-7c overexpression in in vitro studies reduced the growth of prostate cancer cells.

Conclusions: Certain miRNA types are associated with prostate cancer in African American patients, and based on biologic function may contribute to aggressive behavior.

840 Invasive Urothelial Carcinomas of the Renal Pelvis Show Immunohistochemical Expression for PAX8 and PAX2 in a Subset of Cases.

J Hughes, AR Sangoi, JK McKenney. Stanford, Stanford, CA; El Camino Hospital, Mountain View, CA.

Background: Previous studies have reported discrepant staining results with anti-PAX antibodies in invasive urothelial carcinomas of the upper urinary tract. Knowledge of the PAX immunoreactivity pattern in these urothelial tumors is particularly important for the differential diagnostic distinction from renal cell carcinoma in small image guided biopsies, which is critical to the subsequent planning of clinical management.

Design: We identified invasive urothelial carcinomas of the upper urinary tract (i.e. ureter and renal pelvis primaries) with available H&E stained glass slides and paraffin blocks from our surgical pathology archives. All slides were reviewed to confirm diagnoses and a representative slide was stained with anti-PAX8 (polyclonal, 1:20, Proteintech, Chicago, IL) and anti-PAX2 (Z-RX2, 1:100, Zymed, San Francisco, CA) antibodies using standard citrate retrieval techniques. Immunohistochemical expression was scored as positive if any nuclear staining was present and the percentage of neoplastic cells with positive staining was recorded.

Results: 30 total invasive urothelial carcinomas of the upper tract were identified (10 ureter and 20 renal pelvis primaries). Four of 20 invasive urothelial carcinomas of the renal pelvis (15%) had nuclear staining with anti-PAX antibodies [1 PAX8+/PAX2- (80% of neoplastic cells); 1 PAX8+/PAX2- (50% of neoplastic cells); 1 PAX8+/PAX2+ (20 and 15% of neoplastic cells, respectively); 1 PAX8-/PAX2+ (5% of neoplastic cells)]. Nuclear immunoreactivity for PAX2 was generally weaker than PAX8 and had higher cytoplasmic background staining. None of the 10 invasive urothelial carcinomas of the ureter expressed PAX-8 or PAX-2.

Conclusions: In this study, PAX8 was expressed in 15% and PAX2 in 10% of primary invasive urothelial carcinomas of the renal pelvis by immunohistochemistry, but the ureteral primary tumors were negative. This potential staining should be considered when facing the differential diagnostic distinction of renal cell carcinoma from invasive urothelial carcinoma of the renal pelvis, particularly in small image guided biopsy samples where the histologic appearance may be distorted.

841 microRNA Expression and mRNA Transcripts in Clear Cell (Conventional) Renal Cell Carcinoma.

AH Hughes, G Sharma, S Roy, JM Krill-Burger, CM Sciulli, MA Lyons, LA Kelly, AV Parwani, R Dhir, T McHale, WA LaFramboise, SI Bastacky. UPMC, Pittsburgh, PA.

Background: MicroRNAs (miRNA) are small non-protein-coding RNAs which post-transcriptionally regulate gene expression by targeting specific messenger RNAs (mRNA) for degradation. Previous studies have shown altered expression levels of miRNAs in renal cell carcinoma. The aim of this study was to simultaneously interrogate clear cell (conventional) renal cell carcinoma (ccRCC) and normal renal tissue (NRT) across the entire miRNA and mRNA transcriptomes in parallel using microarrays to identify unique miRNA and mRNA transcripts in ccRCC.

Design: We interrogated precisely annotated and classified ccRCC and NRT across the entire single nucleotide polymorphism (SNP) genome (Affymetrix 6.0 Arrays) and miRNA/mRNA transcriptomes in parallel using microarrays (Affymetrix Hu 133-2.0 plus, Exiqon MicroRNA Array), and frozen ccRCC and NRT (n=5). The data were subjected to statistical analyses and hierarchical clustering (Partek Genomics Suite) to produce discrete sets of miRNAs with increased and decreased levels in ccRCC compared to NRT. Correlational analysis of the miRNA and mRNA profiles was performed to identify reciprocal changes in miRNA linked to changes in their targets, identified using the Sanger miRBase. The mRNA targets were functionally annotated using GeneCards (Weizmann Institute of Science) and the National Institute of Health Database for Annotation, Visualization and Integrated Discovery (DAVID) program.

Results: Six miRNAs were identified with significantly altered expression levels in ccRCC compared to normal renal tissue (NRT): miR-141 ($p<5.3\times10^{-9}$), miR-200c ($p<9.2\times10^{-7}$), and miR-624 ($p<2.9\times10^{-3}$) were decreased, and miR-21 ($p<2.1\times10^{-7}$), miR-105 ($p<1.8\times10^{-6}$), and miR-361-3p ($p<7.6\times10^{-3}$) were increased. The mRNA transcripts representing targets of these miRNAs displayed significant correlated expression changes, including FAIM2, GAL3ST1, and VEGFA. Other targeted genes

included transcripts encoding protein binding proteins, potassium and calcium ion channels, kinases, and transcription factors. MiRNAs encoded by chromosome 3 were found to be decreased in ccRCC, correlating with recognized chromosome 3 deletions in ccRCC, and further supported by concurrent SNP analysis.

Conclusions: In summary, this study contributes to the growing understanding of the role that miRNAs play in renal cell carcinoma, specifically ccRCC. The data identified six miRNAs with altered expression in ccRCC compared to NRT which target gene products relevant to tumorigenesis. Both the miRNAs identified and the gene products they regulate represent potentially important therapeutic and diagnostic targets in patients with ccRCC.

842 PAX8 Is a Sensitive Marker for Papillary Renal Cell Carcinoma: Comparison with PAX2.

A Husain, S Liu, A Yilmaz, K Trpkov. University of Calgary and Calgary Laboratory Services, AB, Canada.

Background: PAX8 and PAX2 are transcription factors which have been implicated in the oncogenesis of the renal, Müllerian and thyroid neoplasms. Recent studies suggested that PAX8 and PAX2 can be useful diagnostic markers in the evaluation of primary and metastatic renal tumors. In particular, PAX8 has been shown to be a highly sensitive marker for papillary renal cell carcinoma (96%; *Mod Pathol* 2010;23 suppl1;178A). To our knowledge, PAX8 and PAX2 immunohistochemistry (ICH) profiles have not been compared in PRCC and other common renal tumors.

Design: We compared the ICH staining of PAX8 and PAX2 in a tissue microarray (TMA) generated to evaluate 85 PRCC. In addition, 13 common renal tumors were included in the TMA: 5 clear cell (CcRCC), 3 chromophobe (ChRCC) and 5 oncocytomas. Staining intensity, which typically demonstrates nuclear pattern for both markers, was scored as 0 (negative), 1+ (weak), 2+ (moderate), 3+ (strong). The extent of staining was scored as focal (≤25% of cells) or diffuse (>25% of cells).

Results:

PAX8 and PAX2 expression: comparison in PRCC and other common renal tumors

		PRCC (n=85)	CcRCC (n=5)	ChRCC (n=3)	Oncocytoma (n=5)
PAX8	0	2 (2%)	0 (%)	0 (0%)	0 (0%)
	1+	24 (28%)	2 (40%)	2 (67%)	2 (40%)
	2+	37 (44%)	2 (40%)	1 (33%)	3 (60%)
	3+	22 (26%)	1 (20%)	0 (0%)	0 (0%)
PAX2	0	11 (13%)	1 (20%)	2 (67%)	1 (20%)
	1+	42 (50%)	2 (40%)	1 (33%)	3 (60%)
	2+	25 (29%)	2 (20%)	0 (0%)	1 (20%)
	3+	7 (8%)	0 (0%)	0 (0%)	0 (%)

PAX 8 was positive in 98% of PRCC. Overall, PAX8 demonstrated moderate to strong (2-3+) staining in 70% of PRCC (vs. 37% for PAX2) and 60% of CcRCC (vs. 20% for PAX2). PAX8 was diffusely positive in all evaluated renal tumors. Although PAX2 was positive in 87% of PRCC, 42/74 (57%) of positive PRCC showed 1+ intensity. PAX2 was focally positive in 11/74 (15%) PRCC and in 1/5 (20%) oncocytomas and it was diffusely positive in all evaluated CcRCC and ChRCC.

Conclusions: PAX8 is a sensitive marker for PRCC and demonstrated superior profile than PAX2 regarding the ICH staining frequency, intensity and the extent of staining. PAX8 may be a useful addition to the ICH panel when evaluating a possible PRCC in a limited biopsy core or in the differential diagnosis of an unknown metastatic carcinoma with papillary differentiation. PAX8 was also a more reliable marker than PAX2 in the evaluation of CcRCC. Both PAX8 and PAX2 appear to be of limited diagnostic utility in the evaluation of ChRCC and oncocytoma.

843 Kidney Biopsy for Tumors: Pathologic Interpretation and Clinical Significance.

JM Huss, S Raman, J Huang. UCLA David Geffen School of Medicine, Los Angeles, CA.

Background: Kidney tumors have traditionally been treated with nephorectomy. The current trend is to observe benign tumors while ablating those that are small. In these situations, a kidney biopsy is critical to document the tumor type for management and prognosis, but diagnosis can be challenging as different types of renal tumor have overlapping features and the samples are usually smaller than what most pathologists are used to working with. This study was performed to summarize our experience in interpreting such biopsies.

Design: From 2002 to 2010, 138 renal mass biopsies were performed in our institution. Patient demographics, final pathology diagnosis, immunohistochemical studies used and if available, subsequent nephrectomy specimens were analyzed.

Results: 1. The patients consisted of 102 men and 36 wemen, between 29-88 years of age. Of them, 93 cases (67%) were malignant, 30 (22%) were benign including 16 oncocytomas and 4 angiomyolipomas, 9 (7%) were inconclusive and 6 (4%) were non-diagnostic.

2. Immunohistochemistry was performed in 92 (67%) cases.

3. Of the 93 malignancies, 85 (91%) were renal cell carcinomas (RCC). The remaining cases were metastatic tumors, lymphomas, and poorly differentiated carcinoma NOS.

4. RCCs consisted of 60 cases (71%) of clear cell type, 10 cases (12%) of papillary type (8 type I and 2 type II), 2 cases (1.4%) each of chromophobe and the newly described oncocytic papillary type, 1 case (0.7%) each of multilocular cystic RCC and collecting duct carcinoma. 9 cases (6.5%) were unclassified.

5. The majority of the patients received ablation at the time of biopsy with biopsy tissue the only material documenting the tumor type.

6. 16 cases diagnosed as malignant had subsequent nephrectomy, of which 15 cases (94.4%) had identical diagnosis as biopsy. 1 case of RCC was changed from clear cell type on biopsy to papillary type II on nephorectomy.

7. 2 cases with inclnclusive biopsy diagnosis also had sebsequent nephorectomy and both showed benign lesions.

Conclusions: 1. Renal biopsy for mass lesions is increasingly used, particularly for small lesions that can be safely ablated and for lesions that are possibly benign by radiology.

2. Using the same criteria for nephorectomy specimens, a definitive diagnosis can be rendered in the majority of the renal tumor biopsies with remarkable accuracy.

3. Immunohistochemistry is a valuable tool in helping the diagnosis and subclassification of renal tumors.

4. Used properly, renal biopsy is an important modality to arrive at a definitive tissue diagnosis without subjecting patients to major surgery.

844 Digital Quantification of the Cribriform and 7 Other Patterns of Prostate Cancer and Their Association with PSA Failure.

KA Iczkowski, KC Torkko, GR Kotnis, RS Wilson, W Huang, TM Wheeler, AM Abeyta, FG La Rosa, S Cook, PN Werahera, MS Lucia. University of Colorado Denver, Aurora; University of Wisconsin, Madison; Baylor College of Medicine, Houston, TX.

Background: Grading of large acinar (LA) prostate cancer--cribriform and papillary patterns--is controversial. Most pathologists have grown to accept cribriform cancer as grade 4, not 3, but outcome-based data to support proper grading were lacking.

Design: Among 157 men, 76 with PSA failure (≥0.2 ng/mL) were matched to 81 without failure in nearly equal proportions from each of 3 institutions. Primary matching criterion was follow-up interval; secondary criteria were stage, Gleason grade, and patient age. Tumor slides from entire radical prostatectomies were scanned as virtual slides and 9 histologic patterns were digitally traced. Cribriform cancer foci that were small (≤12 lumens) were analyzed separately.

Results: Gleason score (≤6 versus ≥7) was associated with failure (p=0.023), as were stage, margin status, and tumor volume and preoperative PSA, but not patient age or gland volume. Highest pattern frequencies were single, separate acini (98% of specimens), and fused small acini (83%); those of LA patterns were: papillary, 65%, large cribriform, 38%, and small cribriform, 17%. On multivariate analysis, the high-grade pattern whose presence had the highest odds ratio (OR) for PSA failure was cribriform at 6.21 (95% C.I. 2.67 – 14.41, p≤ 0.0001), then papillary (p=0.04) and individual tumor cells (p=0.004), but not fused small acini (p=0.58). Cumulative area sum of cribriform pattern, per additonal mm^2, held a 1.18 odds ratio for failure (p=0.007), higher than 1.00 to 1.02 for other high-grade patterns. Men without failure never had > 11.8% cribriform cancer; all 8 men with cribriform area sum ≥25 mm^2 had failure (range 33-930).

Presence of both large and small cribriform patterns was linked to failure (p<0.0001, and p=0.0015). For 17 men with >1/3 of cancer area composed of LA cancer, OR was 11.60 (p<0.003), and seminal vesicle invasion was more frequent (p=0.0047). A hypothetical re-grading of cribriform cancer (though non-necrotic) as grade 5 strengthened grade associations with failure.

Fused small acini and individual cells co-occurred significantly, as did papillary and cribriform foci.

Conclusions: Cribriform and papillary cancer should, at least, be graded higher than Gleason 3, regardless of size, to correlate properly with PSA failure, and a cribriform pattern should be mentioned in reports when present. LA patterns may represent a divergent pathway of high-grade tumor development as opposed to fused small acini/ individual cells.

845 FOXA1 a Poor Prognostic Marker in Prostate Cancer: A Validation Study.

RK Jain, R Mehta, J Ro, H Nakshatri, YM Cho, S Badve. Indiana University School of Medicine, Indianapolis; Methodist Hospital, Houston, TX; University of Ulsan College of Medicine, Asan Medical Center, Seoul, Korea.

Background: Forkhead box protein A1 (FOXA1), a transcription factor, is important for normal development of the prostate gland. We have previously demonstrated that FOXA1 is marker of poor prognosis that is associated with development of metastasis. The aim of this study was to validate the results of prior exploratory study in a cohort with long term follow up data.

Design: Expression of FOXA1 was analyzed by immunohistochemistry (IHC) in a series of 117 prostate cancers patients selected from the period of 2000 to 2003. Ten tissue microarrays (TMAs) were prepared using 0.6μ triplicate cores from these patients along with one core from corresponding normal tissue adjacent to the tumor foci. All TMAs were stained for FOXA1 using previously described methods and the nuclear expression was noted in primary tumor as well as in normal prostatic tissues using the Histoscore method. Statistical methods used for analyses included Spearman's correlation, Chi-square, and Fisher's exact tests.

Results: High FOXA1 expression in primary prostate tumors correlated positively with positive metastatic status that included cases with nodal and/or distant metastases at surgery or metachronously after surgery (p= 0.010). It also positively correlated with extra-prostatic extension (p = 0.037), seminal vesicle invasion (p=0.048), perineural invasion (p=0.008) and T stage (p= 0.030). It did not correlate with age, PSA level at diagnosis, Gleason score and angiolymphatic invasion.

Conclusions: High FOXA1 expression is related to the development of metastasis. This validation study suggests that FOXA1 expression could be used to identify cancers with a propensity to metastasize fulfilling an unmet need for a predictor of biologic behavior of prostate cancer. In addition, modulating FOXA1expression in prostate cancer may be a potential therapeutic approach.

846 Urinary Bladder Sinuses. A New Pathological Finding with Clinical and Pathological Significance.

T Jayasinghe, B Djordjevic, EC Belanger, SJ Robertson, BN Nguyen, KT Mai. The University of Ottawa, ON, Canada.

Background: We studied the changes in the urinary bladder in radical cystectomy specimens characterized by segmental mucosal invaginations into the submucosa and muscularis propria. We termed these lesions as urinary bladder sinuses (UBS).

Design: 50 consecutive radical cystectomy specimens (49 for carcinoma with history of BCG/radiation/chemotherapy and 1 for neurogenic bladder) and 20 transurethral resections of the bladder (TURBT) specimens were reviewed. UBS were classified into the superficial and deep types. Superfical UBS was defined as invaginations of the mucosa (including the urothelium, the lamina propria and the muscularis mucosa) extending into the submucosa, while deep UBS was defined as mucosal invaginations extending into the muscularis propria.

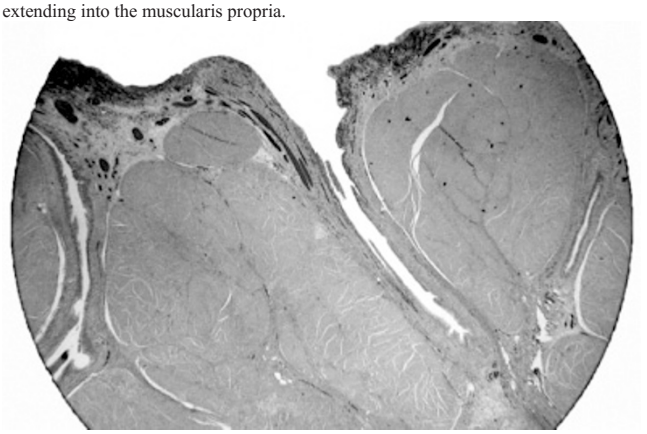

Results: Superficial UBS were distinguished from cystitis cystica due to the cleft-like structures and deep UBS distinguished from the intramural ureters by the multiple cleft-like structures. UBS were often associated with cystitis cystica and proliferation of Von Brunn's nests. In TURBT specimens, superficial UBS were identified in 3 out of 20 cases. In radical cystectomy specimens, superficial UBS were identified in 35 cases (including one neurogenic bladder), while deep UBS (all with associated superficial UBS) were seen in 4 cases. Superficial UBS were more often seen at the borders of scars or outside the invasive carcinoma and were often identified at the base of the bladder. All deep UBS were identified in areas without invasive carcinoma. Intraepithelial neoplasia was seen involving the mucosa of the superficial sinuses in 2 of 4 radical cystectomy specimens and in 1 of 3 TURBT specimens. Furthermore, deep UBS were often associated with increased thickness of the muscularis propria.

Conclusions: UBS may pose diagnostic problems with deeply invasive carcinoma, as they may mimic muscle invasive cancer on pelvic examination and imaging techniques. Recognition of this type of lesion is important, both pathologically and clinically, to avoid over-staging of the tumor.

847 Assessment of Tumor Volume by Frozen Section Examination of the Radical Prostatectomy Specimen: Correlation with Long-Term Follow-Up.

RE Jimenez, JC Cheville, RJ Karnes, JL Hilderbrand, CM Lohse, TJ Sebo. Mayo Clinic, Rochester, MN.

Background: While tumor volume (TV) in radical prostatectomy (RP) specimens (RPS) is considered a significant prognostic factor in prostate cancer (PCa), few studies have included enough follow-up (f/u) to evaluate its long-term impact on prognosis. We describe our experience in assessing this parameter on frozen section (FS) examination on a cohort of PCa patients (pts) followed for over a decade.

Design: 451 consecutive RPS from 1995-98 with no neoadjuvant therapy were evaluated at time of surgery by a standardized, limited sampling protocol using FS technique, followed by reevaluation next day with permanent sections (sct). Average number of sct evaluated per RPS was 14 (range 13-63). Crude estimates of TV were calculated after correlation of microscopic exam results with gross locations where sct were taken. F/u data was obtained during routine clinical f/u and/or via questionnaires to pts no longer followed at our institution.

Results: Mean time from RP to last f/u was 11.3 years (y) (median 12.5; range 0.1-15.1). Mean and median TV was 6.69 and 2.6 cc, respectively (range 0.0005-131.25). 49% of tumors had a Gleason score (GS) of ≤6, 77% were organ confined, and 59% had negative surgical margins (mgn). 90.4% of cases were signed-out the same of surgery. 7.7% were amended/addended to correct/supplement information rendered at time of FS. 135 pts experienced cancer progression at a mean of 4.3 y after RP. Progression-free survival (PFS) rates at 5 and 10 y were 80% and 69%, respectively. 18 of 440 pts died from PCa at a mean of 6.9 y after RP. Cancer-specific survival (CSS) rates at 5 and 10 y after RP were 99% and 97%. GS, mgn status and pathologic stage correlated with PFS, while all of them but mgn status correlated with CSS. TV correlated with PFS and CSS.

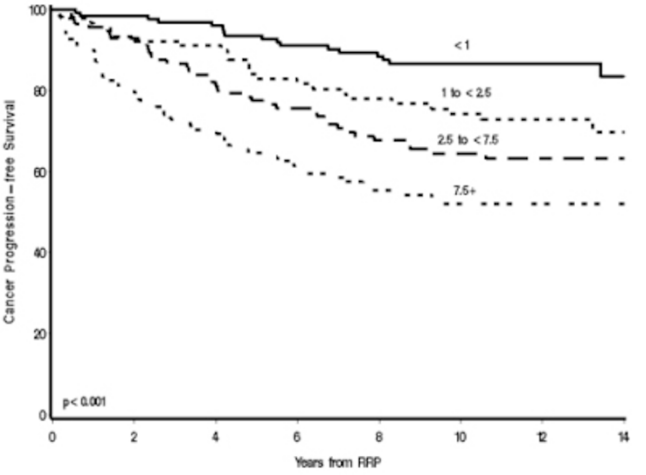

C indexes for TV were 0.675 and 0.802 for PFS and CSS, respectively, compared to those of GS (0.698 and 0.711) and stage (0.639 and 0.775).

Conclusions: TV, as estimated by a combination of careful gross assessment and microscopic examination at time of FS, is a strong predictor of both PFS and CSS and, in our study actually outperforms pathologic staging categories. FS examination of the RPS is highly efficient, as it provides accurate diagnostic and prognostic information with excellent turnaround time.

848 Do Robotic Prostatectomy Positive Surgical Margins Occur in the Same Location as Extraprostatic Extension?

MT Johnson, GN Box, DS Sharp, A Shabsigh, R Abaza, DL Zynger. The Ohio State University Medical Center, Columbus.

Background: The frequency of positive surgical margins (PSM) is higher in prostatectomies with extraprostatic extension (EPE). In some cases with organ confined tumor, PSM may reflect incomplete surgical resection. EPE could indicate that complete tumor resection is difficult, therefore resulting in PSM. The goal of this study was to evaluate cases with both EPE and PSM to determine if the locations are concordant.

Design: We conducted a retrospective review of 997 robotic prostatectomies performed at our institution between March 2007 and July 2009 and identified prostatectomy specimens with both EPE and PSM. Prostates had been entirely submitted and processed in whole mount format per our institutional standard protocol. All whole mount slides were then re-reviewed by a genitourinary pathologist. The prostate was subdivided into 8 regions (anterior apex, posterior apex, anterior mid, anteriolateral mid, posterior mid, posteriolateral mid, anterior base and posterior base) and all locations of EPE and PSM were recorded, as well as the size of the largest focus of EPE and PSM.

Results: 5% (50/997) of robotic prostatectomy specimens had both EPE and PSM. In this subset, the predominate Gleason score was 7 (Gleason 7, 74%; 8, 10%; 9, 16%), average volume of carcinoma was 41% (range 15-95%) and pathologic stage was pT3 (pT3a, 62%; pT3b, 38%). Analysis of cases with concurrent EPE and PSM revealed that EPE occurred most commonly at the mid prostate (apex, 11%; mid, 56%; base, 33%), particularly mid posterolateral (29%). In contrast, PSM was most frequent at the base (apex, 27%; mid, 24%; base, 49%). 66% of cases had EPE and PSM in discordant locations, 20% had EPE and PSM in the same location, and 14% had areas in which EPE and PSM were in the same location but also had other areas of discordant EPE and PSM. The average largest focus of EPE was 0.35 cm (range 0.005-1.2 cm, median 0.2 cm) and the average PSM was 0.33 cm (range 0.0015–1.2 cm, median 0.1 cm).

Conclusions: In this study of robotic prostatectomy specimens with concomitant EPE and PSM, PSM more frequently occurs in a location without EPE. EPE was most frequent in the posterolateral mid prostate, while the PSM was most common in the prostatic base. A better understanding of where PSM occur may help guide surgical technique to decrease residual tumor.

849 Expression of the Hedgehog Family of Proteins in Prostatic Adenocarcinomas (PACS): Hedgehog Signaling Is Associated with High Grade, Advanced Stage and Biochemical Disease Recurrence.

BVS Kallakury, GM Sheehan, CE Sheehan, HAG Fisher, RP Kaufman, T Nazeer, JS Ross. Georgetown Univ Hospital, Washington, DC; Albany Medical College, NY.

Background: The hedgehog signaling pathway plays an important role in cell proliferation, differentiation, stem cell maintenance and tissue regeneration. This pathway is also implicated in carcinogenesis and in promoting tumor cell growth of several cancers including those arising from skin, liver, brain, pancreas, breast, colon, soft tissue and bladder. The role of HH pathway in prostate carcinogenesis is contradictory; a mouse model study shows no evidence of its involvement in tumor development while a human tissue study demonstrates expression of HH ligands at different stages of prostate cancer development. In this study, we report the prognostic significance of HH signaling in human PACs.

Design: Formalin-fixed, paraffin embedded sections from 138 PACs were immunostained by automated methods (Ventana) with goat polyclonal Shh, Dhh, Smo, and GLI-1 and rabbit polyclonal patched (Santa Cruz) antibodies. Cytoplasmic and/or nuclear immunoreactivity was scored for intensity and percentage of positive cells

in both tumor and adjacent benign epithelium. Cases were assessed as tumor = benign (T = B), tumor > benign (T > B) and tumor < benign (T < B). Results were correlated with clinicopathologic variables.
Results: Tumor immunoreactivity was predominantly cytoplasmic for all proteins. Cytoplasmic protein expression was noted as: Shh [T = B 62%, T > B 38%, T < B 0%]; Dhh [T = B 73%, T > B 24%, T < B 3%]; patched [T = B 34%, T > B 66%]; GLI-1 [T = B 72%, T > B 27%, T < B 1%], and Smo [T = B 84%, T > B 10%, T < B 6%]. Increased Shh and GLI-1 expression each correlated with high grade [$p < 0.0001$; $p = 0.004$], advanced stage [$p = 0.007$; $p = 0.005$], and biochemical disease recurrence [$p = 0.046$, $p = 0.038$], respectively. Increased Dhh expression correlated with high grade [$p < 0.0001$] and biochemical disease recurrence [$p = 0.044$]. Increased patched expression correlated with high grade [$p < 0.0001$] and advanced stage [$p = 0.006$]. Increased Smo expression correlated with advanced stage [$p = 0.042$]. On multivariate analysis, increased Shh expression ($p = 0.029$) independently predicted biochemical disease recurrence.
Conclusions: The hedgehog signaling pathway appears to play an important role in prostate carcinogenesis with increased expression of this family of proteins correlating with adverse prognostic variables, warranting further studies of this pathway as a therapeutic target in the management of patients with prostate cancer.

850 Anterior Fat Pad Lymph Node Evaluation in Robot-Assisted Radical Prostatectomy (RARP) Specimens.

SH Kang, HS Hwang, SH Yoo, DS Yoo, H Ahn, YM Cho, E McQuitty, JY Ro. University of Ulsan College of Medicine, Asan Medical Center, Seoul, Korea; The Methodist Hospital, Weill Medical College of Cornell University, Houston, TX.
Background: Urologists dissect the anterior fat pad (AFP) during RARP because this facilitates visualization of the prostate apex and bladder neck. AFP evaluation may be essential procedure during RARP, because lymph nodes in AFP may harbor metastatic tumor. Then, not only pelvic lymph node metastasis, but also the metastatic status of AFP lymph nodes, can be a prognostic factor and influence tumor stage grouping.
Design: 439 patients underwent RARP at the Asan Medical Center from July, 2007 to August, 2010. Of these, 221 included AFP excision. We reviewed the final reports and H&E slides to assess presence and number of lymph nodes in the AFP, as well as rates of metastasis to these lymph nodes.
Results: Among the 221 cases with AFP dissection, 18 (8.1 %) had one each AFP lymph node and 203 (91.9 %) had no lymphoid tissue in the AFP. Two of the 18 cases with AFP lymph nodes had metastatic carcinoma in a completely effaced node. All 18 cases with AFP lymph nodes had pelvic lymph node dissection, and 1 of the cases with AFP nodal metastasis also had pelvic lymph node metastasis. The case with metastatic carcinoma in AFP and pelvic lymph nodes had a preoperative PSA of 48.8 ng/ml, and a Gleason score 7 (4+3); in the case with metastatic AFP lymph node but negative pelvic lymph nodes, these values were 34 ng/ml and 9 (4+5), respectively
Conclusions: In our study, AFP lymph nodes were found in 18 of 221 RARP specimens with AFP dissection (8.1 %), with metastatic carcinoma in 2 of these 18 cases. One case also had pelvic lymph node metastasis, but the other was negative for pelvic lymph node metastasis. In this case, tumor stage grouping would be falsely low in the absence of AFP lymph node evaluation. Since AFP excision is regarded as routine during RARP, a careful evaluation for the presence of lymph node (s) in the AFP specimens is recommended because lymph node status in AFP may have a significant impact on tumor stage.

851 Xanthogranulomatous Pyelonephritis (XGP) of Kidney: Another IgG4 Associated Pseudotumor?

SH Kang, SA Kim, S Jung, YM Cho, AG Ayala, JY Ro. Universitiy of Ulsan College of Medicine, Asan Medical Center, Seoul, Korea; Pusan University Hospital, Pusan, Korea; Weill Medical College of Cornell University, The Methodist Hospital, Houston.
Background: XGP is an uncommon chronic inflammatory disorder with uncertain histogenesis. During routine sign out, a case of XGP showed significant plasma cell infiltration (≥50 plasma cells/1hpf) with sclerotic inflammation and a subsequent IgG4 staining demonstrated numerous IgG4 positive plasma cells. This case prompted us to study the relationship between XGP and IgG4 associated sclerotic disease.
Design: We retrieved 15 cases diagnosed as XGP from the Surgical Pathology file of Asan Medical Center, Seoul, Korea from 1999 to 2010. Histologically an attempt was made to separate areas with predominance of inflammatory components (neutrophils, foamy histiocytes, lymphocytes, plasma cells) from areas predominantly depicting the sclerotic component. Immunohistochemical studies for IgG4 and IgG were performed. The number of IgG4 positive plasma cells was counted on 1 high power field and IgG4/IgG ratio was evaluated in both inflammatory component and sclerotic areas separately.
Results: Of the 15 patients with XGP, 13 were women and 2 were men. Their mean age was 55.8 years with a range of 34 to 74 years. All cases showed a mass forming lesion with clinical diagnosis of RCC. The lesions averaged in size 3.9 cm with a range of 1.5 cm to 13cm. Overall all cases showed numerous plasma cells and sclerotic reaction. The inflammatory component was significantly more abundant in the central areas than in the periphery of the XGP ($P<0.001$), while the sclerotic component was the reverse ($P<0.001$). Neutrophils and foamy histiocytes were more frequently observed in the center of the lesion ($P=0.002$, <0.001), but the distribution of lymphocytes and total plasma cells were not different between the center and the periphery of the lesions. However, the number of IgG4-positive plasma cells and IgG4/IgG ratio were significantly higher in the peripheral sclerotic areas compared to the central area ($P=0.001$, <0.001, respectively).
Conclusions: Based on our study, 1) not all but most of XGP seem to be related to IgG4 associated sclerotic disease. 2) The peripheral distribution of IgG4 positive plasma cells suggests that IgG4 positive plasma cells have an active role for a sclerotic phase of the disease. Lastly 3) to establish XGP being another IgG4 positive pseudotumor, more studies are required for the histogenesis and potential treatment.

852 The Role of MUC1, MUC2 and MUC7 in the Outcome of Superficial (Ta, T1) Urinary Bladder Cancer (SBC).

D Kankaya, S Kiremitci, S Baltaci, Z Biyikli, O Tulunay. Medical School of Ankara University, Turkey.
Background: SBC can be cured in most cases however, it also has a very high incidence of recurrence. Therefore, there is a need for molecular markers that may identify patients at risk for recurrence and progression that would benefit from early and additional therapeutic modalities.
Design: Immunohistochemistry was performed on 99 TUR materials of SBC, using antibodies against MUC1, MUC2 and MUC7. Apical membranous ($MUC1_{ap}$), superficial stratified ($MUC1_{st}$), scattered ($MUC1_{sc}$) and full thickness ($MUC1_{fth}$) MUC1 staining patterns were evaluated and the extent of the patterns was determined on papillary (p) and inverted (i) areas of the tumors. The extent of complete membranous staining ($MUC1_{m}$) was also established. Cytoplasmic ($MUC2_{c}$), membranous ($MUC2_{m}$), and golgi zone ($MUC2_{gz}$) MUC2 staining and the extent of staining were evaluated. MUC2 expression was also evaluated for the presence of apical staining as $MUC2_{ap-}$ or $MUC2_{ap+}$. The extent of cytoplasmic ($MUC7_{c}$) and membranous ($MUC7_{m}$) MUC7 staining was determined. The MUC7 distribution in the areas with papillary and inverted growth pattern as well as with high nuclear grade (HNG) were recorded for each tumor.
Results: Tumors with $MUC1_{m}$ positivity of ≥ 30% showed higher invasion rate ($p=0.001$) and more areas with HNG ($p=0.006$). $MUC1_{pfth}$ ($p= 0.003$) and $MUC1_{ifth}$ ($p=0.024$) positivity increased from Ta to invasion suspicious and T1 SBC, in spite of the decrease of $MUC1_{pst}$ ($p= 0.009$), $MUC2_{ap}$ ($p= 0.046$), $MUC2_{m}$ ($p=0.001$) staining patterns. A positive correlation was found between the extent of HNG areas and $MUC1_{m}$ ($p=0.002$), $MUC7_{c}$ ($p=0.039$) positivity whereas, a negative correlation was found with duration of tumor relapse ($p=0.049$). $MUC2_{m}$ ($p=0.033$), $MUC2_{ap}$ ($p=0.009$), $MUC1_{ap}$ ($p=0.049$) expressions of the tumors were correlated with prolonged duration of tumor relapse though, shortening of duration of tumor relapse with expression of $MUC7_{c}$ ($p=0.034$) was found. $MUC1_{m}$ expression ($p=0.015$) and inflammation in the tumor ($p=0.025$) were correlated with decreased survival rates.
Conclusions: This study demonstrates that MUCs may have a role in the assessment of the course of SBCs. $MUC1_{fth}$ and $MUC1_{m}$ expressions predict progressive course moreover, $MUC1_{m}$ staining, 30% or more, indicates poor survival. $MUC7_{c}$ expression indicates shorter duration of relapse. On the contrary, $MUC2_{m}$ and $MUC2_{ap}$ expressions identify patients with favorable prognosis.

853 Solid Pattern of Testicular Yolk Sac Tumor: A Morphologic and Immunohistochemical Study of 52 Cases.

C-S Kao, MT Idrees, RH Young, TM Ulbright. Indiana University School of Medicine, Indianapolis; Massachusetts General Hospital & Harvard Medical School, Boston.
Background: Yolk sac tumors (YST) may exhibit numerous patterns, including microcystic/reticular, papillary, glandular, and solid. The solid pattern is prone to misinterpretation, particularly in small biopsy specimens, as other testicular neoplasms, most commonly seminoma. Distinguishing solid pattern YST from seminoma is of critical importance since they are treated differently.
Design: 52 cases of solid YST were confirmed by reviewing H&E stained sections. A solid pattern was defined as a sheet-like arrangement that could have rare foci of microcysts and that occupied more than 2 mm^2. The following features were assessed: cytoplasmic quality, associated YST patterns, necrosis, lymphocytic infiltrate, hyaline globules, intercellular basement membrane deposits, microcysts, sinusoidal vascularity, myxoid background, degree of nuclear pleomorphism and an appliqué pattern. Immunohistochemical stains were performed on 36 cases and evaluated by a modified Allred scoring method for proportion and intensity of positivity.
Results: Solid YST was mostly comprised of sheets of cells with abundant pale to clear cytoplasm (85%) and almost always (98%) associated with other patterns, most commonly microcystic/reticular (75%), glandular (35%) and myxoid (25%). Intercellular basement membrane (75%), focal microcysts (67%), significant nuclear pleomorphism (65%) and hyaline globules (65%) were common, whereas a myxoid background (39%), lymphocytic infiltrate (17%) and an appliqué pattern (8%) were less frequent. AE1/AE3 cytokeratin and glypican 3 provided the most intense and diffuse staining of solid YST, whereas AFP was negative in 38%. CD117 stained 59% whereas podoplanin was positive in only 1 case (3%) and OCT3/4 was uniformly negative.
Conclusions: Solid YST can generally be recognized by careful morphologic evaluation, especially its association with other patterns, the presence of band-like deposits of basement membrane, occasional microcysts, nuclear pleomorphism and intracellular hyaline globules and usual absence of lymphocytes. In difficult cases an immunohistochemical panel including AE1/AE3, glypican 3, OCT3/4 and podoplanin aids in its distinction from other neoplasms. Frequent positivity of solid YST for CD117 indicates it has little value in the differential diagnosis with seminoma. AFP stains are commonly negative or weak and focal and should not solely be relied on for diagnosis.

854 Prognostic Significacne of MTORC1 Immunoexpression in Clear Cell (Conventional) Renal Cell Carcinoma.

P Kapur, D Rakheja, RF Yousse, V Margulis, W Kabbani, Y Lotan. UT Southwestern Medical Center, Dallas, TX.
Background: The mammalian target of rapamycin complex 1 (mTORC1) signaling controls key cellular processes such as survival and proliferation, is dysregulated in many human cancers, and drugs targeting this pathway are in clinical development. We undertook this study to ascertain if clear cell (conventional) renal cell carcinoma

(ccRCC) demonstrates significant expression of mTORC1 pathway components and if the expression of activated mTORC1 has any prognostic significance.
Design: Standard immunohistochemical analysis was performed for phospho-(Ser235/236)-S6 ribosomal protein (pS6), phospho-(Ser2448)-mTOR (p-mTOR), and mTOR using tissue microarrays constructed from 288 primary ccRCC treated at our hospital with nephrectomy (1998-2008). Duplicate 1.0 mm cores of representative tumor were obtained from each case to construct the tissue microarrays. Cytoplasmic staining intensity was scored as 0 (absent), 1 (weak), 2 (moderate), or 3 (strong). The percentage of positively staining cells was scored as 0 (none), 1 (<10%), 2 (10-70%), or 3 (>70%). A final Histo-score was calculated in each tumor as the product of intensity and percentage, and was correlated with clinico-pathological parameters and outcome using the nonparametric van der Waerden test. Two-tailed P<0.05 was considered significant.
Results: In our cohort, M:F ratio was 1.48 and mean age at diagnosis was 62 years. Mean tumor size was 5.7 cm. 27 (9%) patients had bilateral tumors, 107 (37%) had high Fuhrman grade (G3-4), 79 (27%) had high pathologic stage (pT3-4), 46 (16%) developed subsequent metastases / recurrence, and 17 (6%) died of the disease. P-S6 staining was weak in 76 (26%) and strong in 61 (21%) cases; p-mTOR was weak in 82 (28%) and strong in 129 (45%) cases; mTOR was weak in 96 (33%) and strong in 60 (21%) cases. Stronger expression of p-S6 was associated with high Fuhrman grade (p<0.0001), high pathologic stage (p=0.0016), and the development of metastases / recurrence (p=0.0478). The staining pattern of all antibodies was essentially similar in nature and consisted of granular cytoplasmic staining.
Conclusions: The significant association of strong p-S6 immunoexpression with higher grade, higher stage, and subsequent development of metastasis / recurrence in ccRCC suggests that the rapamycin-sensitive mTORC1 pathway is hyperactive and therefore an attractive therapeutic target in these tumors.

855 Clinicopathologic Characteristics and Outcomes of Renal Cell Carcinoma: A Single Center Experience.

P Kapur, R Youssef, F Alhalabi, V Margulis, Y Lotan, W Kabbani. UT Southwestern Medical Center, Dallas, TX.
Background: Renal cell carcinoma (RCC) forms 4% of all adult cancers with an increasing incidence. Although rate of metastases at presentation remains high (30%), the incidence of localized RCC has also increased. About 20%-30% of patients develop local recurrence or distant metastasis after resection. This study aimed to redefining clinicopathologic features of RCC based on a single specialized center experience.
Design: We retrospectively reviewed medical records of patients who underwent resections for RCC between 1997 and 2008 at UTSW. Clinical and pathologic data were extracted. All H&E stained slides of all available cases were reviewed.
Results: 632 resections were done; 427 (68%) were conventional (ccRCC), 79 (12.5%) papillary (pRCC), 34 (5%) chromophobe (cRCC), 49 oncocytoma (7.5%), 13 (2%) clear cell papillary renal cell carcinoma (ccPRCC), 5 (1%) acquired cystic renal disease associated renal cell carcinoma (ACDK-RCC), 12 (2%) unclassified, 3 (0.5%) cases were a translocation-associated carcinoma and one case (0.3%) of renal mucinous tubular and spindle cell carcinoma. Median age for ccRCC was 59 years (range 18-94; M:F ratio is 1.5:1). Of 421 ccRCC patients with follow-up, there were 397 (94.3%) alive, 377 (90%) had no evidence of tumor and 20 (10%) had confirmed recurrences/metastases. Twenty-four (5.7%) died within the follow-up period (mean time 4.9 years), of which, nine patients (2.1%) died of metastatic/ recurrent tumor and 15 died by other causes. On the other hand, of 77 patients with pRCC with available follow up, 5 died (Two (2.5%) died of disease), and 73 were alive at last follow-up (with 2 patients (2.5%) with recurrence/metastases). Advanced pathologic tumor stage (>=pT3) was more frequent for ccPRCC than pRCC (30% vs. 4%, p=0.0004); however, pRCC tended to demonstrate a higher Fuhrman nuclear grade (G3-4) (53% vs. 41%, p=0.07) and more frequent lymph node involvement at presentation (4% vs. 1%, p=0.06). Amongst the newly described group of RCC (ccPRCC, ACDK-RCC, translocation-associated RCC and mucinous tubular and spindle cell carcinoma), all patients were alive with no evidence of disease within the follow-up period.
Conclusions: This data is compatible with the literature incidence of RCC, yet, the frequency of recurrence and metastases following surgery is lower. In addition, while pRCC tended to show a higher nuclear grade and more frequent nodal involvement, ccRCC had a higher pathological stage at presentation and relatively worse disease-free survival.

856 OCT4 Staining in Diagnosis of Micrometastasis in Retroperitoneal Lymph Node Dissections.

T Kieffer, L Cheng, M Idrees. Indiana University, Indianapolis.
Background: Immunohistochemical staining with OCT4 is a sensitive and specific marker for seminoma and embrynal carcinomas. Patients with stage I seminoma post orchiectomy may choose surveillance, adjuvant therapy, or retroperitoneal lymph node dissection (RPLND) to manage occult metastasis. RPLND has staging and therapeutic value, and proper staging is extremely important. We developed a study to assess the utility of OCT4 staining in identifying micrometastasis in RPLND in seminoma patients.
Design: Forty-five RPLNDs with primary or metastatic seminoma were identified in the archives. The cases were subdivided into virgin RPLND with clinical suspicion (VRPLND+CS), virgin RPLND without clinical suspicion (VRPLND-CS), and postchemotherapy RPLND (PC RPLND). H&E slides were reviewed and representative blocks were chosen that were initially read as negative or containing multiple benign nodes. Sections were stained with polyclonal goat anti-OCT4 antibody and viewed with light microscopy. Additional positive lymph nodes were identified.
Results: 262 lymph nodes from 45 RPLND cases were reviewed: 13 VRPLND+CS, 11 VRPLND-CS, and 21 PC RPLND. Clinical suspicion was defined as adenopathy or elevated germ cell serum markers. 21 additional positive lymph nodes were identified in 12 cases (Table 1). There was no change in diagnosis after OCT4 immunostaining. The greatest difference between pre OCT4 staining and post OCT4 staining was seen in VRPLND+CS (12.6%) followed by PC RPLND (7.4%) then VRPLND-CS (4.1%).

1 RPLND data

	Metastasis/Total cases		Positive nodes/Total nodes	
	Pre-OCT4	Post-OCT4	Pre-OCT4	Post-OCT4
Virgin RPLND with clinical suspicion	11/13 (84.6%)	11/13 (84.6%)	4/79 (5.1%)	14/79 (17.7%)
Virgin RPLND without clinical suspicion	5/11 (45.5%)	5/11 (45.5%)	0/74 (0%)	3/74 (4.1%)
Postchemotherapy RPLND (Clinically evident disease)	18/21 (85.7%)	18/21 (85.7%)	2/109 (1.8%)	10/109 (9.2%)
Total	34/45 (75.6%)	34/45 (75.6%)	6/262 (2.3%)	27/262 (10.3%)

Conclusions: There is a significant difference between the number of positive lymph nodes before and after OCT4 staining (2.3% to 10.3%, respectively) with virgin RPLND with clinical suspicion accounting for most total and proportional additional positive nodes. All differences arose from cases in which positive nodes had already been identified thus there was no change in diagnosis. Multiple cases were identified where single cells had metastasized. We recommend diligence when examining RPLND and routine OCT4 staining for diagnosis of micrometastasis and precise staging especially in patients with adenopathy or elevated serum markers.

857 Expression of Putative Stem Cell Markers CD133 and Oct-4 in Papillary Renal Cell Carcinoma and Its Prognostic Significance.

K Kim, JY Ro, YM Cho. Kangbuk Samsung Hospital, Sungkyunkwan University School of Medicine, Seoul, Republic of Korea; University of Ulsan College of Medicine, Asan Medical Center, Seoul, Republic of Korea.
Background: Papillary renal cell carcinoma (PRCC) is the second most common malignant tumor of the kidney. Except for tumor stage and histologic type, its prognostic parameters remain controversial. Recently, cancer stem cells (CSCs) have been a focus of growing attention because of their implication in therapeutic resistance and poor prognosis. CD133 is a cell surface marker being widely used to identify CSCs in various organs. Oct-4 is a transcription factor serving as a key regulator of stemness of stem cells. However, their expression pattern and its prognostic significance have not been evaluated in PRCC.
Design: The expressions of CD133 and Oct-4 were examined in a tissue microarray constructed from 124 cases of PRCC by immunohistochemistry and correlated with clinicopathologic prognostic factors.
Results: CD133 was expressed at the apicolateral membrane of tumor cells in 45 cases (36.9%). CD133-expressing PRCCs showed favorable prognostic features such as type 1, small tumor size, kidney-confined disease, low tumor stage, no distant organ metastasis, and prolonged disease-specific survival rate compared to CD133-negative PRCCs. Oct-4 showed nuclear staining and was expressed in 26 cases (21.1%) of PRCCs. In contrast to the CD133 expression, high expression of Oct-4 (cut-off value of 12.5%) was associated with frequent lymphovascular invasion and shorter disease-specific survival. In multivariate analysis, tumor stage, histologic type, and high Oct-4 expression were independent prognostic factors for disease-specific survival. CD133 expression was an important prognostic marker in univariate analysis, however, was not independent prognostic factor in multivariate analysis.
Conclusions: These results indicate that besides being stem cell markers, CD133 and Oct-4 expression can be used as prognostic markers in PRCC with CD133 expression as a favorable prognostic marker and especially Oct-4 over-expression as a poor prognostic marker.

858 Hedgehog Pathway Gene Product Expression in Renal Cell Carcinomas (RCC).

KA Kim, JL Garbaini, CE Sheehan, RP Kaufman, JS Ross, AM Hayner-Buchan. Albany Medical College, NY.
Background: The hedgehog signaling pathway is involved in embryonic development and stem cell renewal in a variety of tissues. Recent studies demonstrate reactivation of this normal developmental signaling pathway in RCC, suggesting a role for the hedgehog pathway in RCC tumorigenesis. This study investigates the expression of these and other hedgehog pathway gene products in RCC.
Design: Tissue sections from 94 formalin-fixed, paraffin-embedded cases of RCC were immunostained by an automated method (Ventana Medical Systems Inc., Tucson, AZ) using Santa Cruz goat polyclonal antibodies to Desert hedgehog (N-19) and Sonic hedgehog (N-19), and Santa Cruz rabbit polyclonal antibodies to Fox M1 (K-19) and patched (H-267). Cytoplasmic immunoreactivity based on intensity and distribution was semiquantitatively scored and the results were correlated with clinical and morphologic variables.
Results: Sonic hedgehog (SHH) overexpression was noted in 39/94 (42%) tumors, including 26/77 (34%) clear cell carcinomas and correlated with high grade (p=0.035 for all tumors, p=0.007 for clear cell carcinomas). Patched overexpression was identified in 52/94 (55%) tumors, including 36/77 (47%) clear cell carcinomas and correlated with high grade (p=0.002 for all tumors, p=0.01 for clear cell carcinomas), shortened length of survival (p=0.04) and showed a trend toward association with advanced stage (p=0.06). Fox M1 overexpression was noted in 52/94 (55%) tumors and showed a trend toward correlation with high grade (p=0.071 for all tumors, p=0.085 for clear cell carcinomas). Desert hedgehog (DHH) was overexpressed in 43/94 (46%) tumors and showed a trend toward correlation with advanced stage (p=0.09). There was significant coexpression of each of the proteins with one another (p≤0.002). In addition, there was significant co-overexpression of SHH and patched within high grade tumors (p=0.024 for all tumors, p=0.037 for clear cell carcinomas). On multivariate analysis, tumor grade (p=0.01) and stage (p=0.012) independently predicted overall survival.

Conclusions: The hedgehog signaling pathway appears to be upregulated in high grade RCCs and associated with aggressive disease (advanced stage and shortened survival). Further, these pathway members (SHH, DHH, patched and Fox M1) appear to be co-expressed. Additional studies to further characterize the role of the hedgehog pathway in RCC are indicated.

859 Incidence of Reclassification in Patients Undergoing Active Surveillance for Favorable-Risk Prostate Cancer.

J Kim, JW Davis, J Ward, X Wang, C Pettaway, L Pisters, S Matin, D Kuban, SJ Frank, AK Lee, IN Prokhorova, VT Brown, CJ Logothetis, P Troncoso. The University of Texas MD Anderson Cancer Center, Houston.

Background: Morphologic characterization of prostate cancer (PC) in ultrasound-guided biopsies (BXs) has been used to determine risk stratification and need for therapy (Tx). BX schemes have evolved to ensure adequate sampling of the prostate. In a prospective cohort trial of active surveillance (AS), patients (pts) with early-stage PC are stratified into 3 groups: Gr I (low risk), Gr II (AS is pt's choice), and Gr III (competing comorbidities prevent local Tx). To standardize data, we began requiring all pts to have a repeat BX (re-BX) within 6 mo of study entry according to an 11-core BX scheme that is also used during surveillance. We report our experience with an emphasis on BX findings in Gr I.

Design: Eligibility criteria: Gr I pts: Gleason score (GS) 6 (3+3), one positive (pos) core (<3 mm), and a total prostate-specific antigen (PSA) level <4 ng/mL or GS 7 (3+4), one pos core (<2 mm), and PSA level <4 ng/mL. Gr II and Gr III pts must have clinically localized disease. Pts are monitored every 6 mo by PSA, testosterone, and digital rectal exam. At yr 1, all pts must undergo re-BX and thereafter follow a predetermined BX scheme based on pathologic findings. Definitive Tx is offered for unequivocal clinical and/or radiographic progression or when ≥1 of the following is detected at postenrollment Bx: increased tumor length in pos core, ≥2 pos cores, or upgrading of tumor. An increase of >30% in surveillance PSA from baseline level is also considered reclassification.

Results: From February 2006–May 2010, 378 pts enrolled; 376 met eligibility criteria (92 before June 2007 re-Bx requirement). Of 136 Gr I pts, 42 were enrolled before and 94 after the re-BX requirement. During surveillance, 17 (12.5%) pts met the reclassification criteria on re-BX, 10/42 (24%) before and 7/94 (7.4%) after re-BX requirement (*before:* 1 yr, 6; 1.5 yr, 1; 2 yr, 3; *after:* 1 yr, 6; 2 yr, 1). Of the 17 reclassified pts, 4 chose Tx. No pt met PSA reclassification criterion in Gr I. Of 228 Gr II pts, 45 were enrolled before and 183 after the re-BX requirement. Included in the 183 were 45 (24.6%) pts who were restratified to Gr II because of a re-BX; 14 of these pts chose to have Tx.

Conclusions: For appropriate risk stratification, repeat extended BX should be considered for men choosing AS. Prostate BXs in favorable-risk PC have a high sampling bias rate and should be accounted for in AS protocols. Reclassification owing to sampling bias on re-BX vs true disease progression needs further investigation.

860 Clear Cell Renal Cell Carcinoma with Tubular-Follicular-Cystic Architecture.

Z Kos, EC Belanger, SJ Robertson, B Djordjevic, KT Mai. The University of Ottawa, ON, Canada.

Background: Clear cell renal cell carcinoma (CRCC) usually displays variable architecture, including alveoli, acini, tubules, follicles, cysts, papillae, solid nests and sheets. Large solid nests and sheets are usually associated with high nuclear grades, while areas with low Furhman nuclear grades (1-2/4) often display alveolar or tubulo-follicular-cystic (TFC) architecture, with or without papillae. We present an immunohistochemical and fluorescence in situ hybridization (FISH) study of CRCC with a predominant TFC architecture.

Design: 12 CRCC with TFC architectures were reviewed. Tumors with an alveolar architecture accounting for more than 10% of the tumor were excluded. Representative sections were submitted for immunostaining with cytokeratin 7 (CK7), alpha-methyl-acyl-CoA racemase (AMACR) and for FISH for loci 3p25 (Von Hippel Lindau gene) and 3p14 (fragile histidine triad gene), as well as for centromeres of chromosomes X, Y, 7 and 17.

Results: Male to female patient ratio was 5:1. Patient age ranged from 33-68 (54±8). All tumors were stage I and ranged in size from 1.2-3.5 cm (2.1±0.4). No recurrence or metastases occurred during the period of follow-up (up to 5 years with a mean of 3 years). Grossly, all tumors were encapsulated.

Focal areas of alveolar architecture were seen in 3 tumors. Focal areas with features of tubular cystic renal cell carcinoma with clear cell changes were identified in 4 tumors. Immunostaining showed positive CK7 reactivity ranging from diffuse in 7 tumors, focal in 3 tumors to negative in 2 tumors. AMACR reactivity was extensive in 2 and focal in the remaining 10 tumors.

FISH revealed 7 tumors with loss of 3p, 2 tumors with loss of 3p and gain of chromosome 7, and one tumor with loss of 3p and gain of chromosomes 7 and 17. The remaining 2 tumors showed no detectable chromosomal changes. Tumors without loss of 3p displayed strong and extensive CK7 reactivity. Tumors with trisomy 7/17 showed focal papillary formations.

Conclusions: We propose that CRCC with a TFC architecture is a distinct type of renal cell carcinoma (RCC), characterized grossly by encapsulation and microscopically by a predominant TFC architecture. The chromosomal findings suggest that these tumors do not always present with typical chromosomal changes of CRCC or papillary RCC.

861 Does the Percentage of Involvement of Prostate Base Needle Core Biopsies by Prostatic Adenocarcinoma Predict Potential Risk of Seminal Vesicle Invasion?

C Kovach, AO Osunkoya. Emory University School of Medicine, Atlanta.

Background: Prostatic adenocarcinoma is the most common non-cutaneous cancer in men and is the second leading cause of cancer related deaths in men in the U.S. Unilateral or bilateral seminal vesicle invasion by prostatic adenocarcinoma (pT3b) is typically characterized by poor clinical outcome. Identification of patients who are potentially at increased risk of having seminal vesicle invasion is therefore critical. To date, very few studies have been published regarding the prediction of seminal vesicle invasion at radical prostatectomy based on prostate needle core biopsy findings.

Design: A search was made through the surgical pathology files at our institution for radical prostatectomy cases signed out as prostatic adenocarcinoma with unilateral or bilateral seminal vesicle invasion. Only cases with available prostate needle core biopsies for review were selected. Two groups were established based on the presence or absence of ipsilateral seminal vesicle invasion on radical prostatectomy. The percentage of tumor involvement in each prostate needle core obtained from the base was documented, with emphasis on the core with the greatest tumor volume. The latter was then correlated with the status of the ipsilateral seminal vesicle. A two-tailed t-test was performed to compare the data between the two groups.

Results: A total of 27 cases were selected**.** Mean patient age was 60 years (range: 46 – 70 years). 7/27 cases (26%) had bilateral seminal vesicle invasion, 12/27 cases (44%) had only right seminal vesicle invasion, and 8/27 cases (30%) had only left seminal vesicle invasion. A total of 54 data points were generated based on the number of cases analyzed and laterality of seminal vesicle involvement. Mean percentage of involvement in the base needle core biopsies that had subsequent ipsilateral seminal vesicle invasion was 66.9% (CI: +/- 8.1%). Mean percentage of involvement in the base needle core biopsies that had no subsequent ipsilateral seminal vesicle invasion was 27% (CI: +/- 16.28%). The differences between the two groups were statistically significant (p = 0.00007).

Conclusions: This study demonstrates a statistically significant correlation between the percentage of involvement of the prostate base needle core biopsy by prostatic adenocarcinoma, and the presence of ipsilateral seminal vesicle invasion. In addition, this study highlights one of the advantages of accurately reporting the percentage of individual cores involved by prostatic adenocarcinoma on prostate needle core biopsies.

862 Gleason Score (GS) 7 Prostate Cancer with Lymph Node Metastases (LN+): Findings at Radical Prostatectomy (RP).

ON Kryvenko, NS Gupta, N Virani, Z Lane, JI Epstein. Henry Ford Hospital, Detroit; Jefferson Medical College, Philadelphia; Johns Hopkins University, Baltimore.

Background: Prostate cancers with LN+ are relatively rare in contemporary practice and typically seen with GS8-10 disease. Little is known about the morphology of GS7 prostate cancer with LN+.

Design: RPs with GS7 LN+ without prior therapy from 2000 to 2010 composed the study group. A control group (at least two times in number) without LN metastases (LN-) was Gleason and stage-matched. Remote tumor foci were classified as satellites when they had the same morphology as the dominant nodule; otherwise they were interpreted as multifocal.

Results: The study group was composed of GS347 (n=11), GS437 (n=14), GS347 with tertiary 5 (n=2), and GS437 with tertiary 5 (n=8). No difference in age was seen between study and control. A higher proportion of the LN+ patients were black compared to the percentage of LN-, 42.9% vs. 13.4%, respectively (p=0.0004). Mean preoperative PSA was higher in those with LN+ (13.8) vs. those with LN- (7.9) (p=0.03). The percentage of positive biopsy cores almost reached statistical significance with a mean of 55.4% for LN+ compared to 45.3% for LN- (p=0.055). At RP, there were no differences seen in prostate weight, focal vs. non-focal EPE, or Gleason 4 pattern (poorly formed glands vs. fused vs. cribriform vs. glomeruloid). Graded subjectively as 1-3, nuclei (p=0.007) and nucleoli (p=0.0005) were larger with LN+ vs. LN-, with no difference in nuclear pleomorphism or nucleoli distribution. Other morphologic findings are listed in table (LVI = lymphovascular invasion; IDC = intraductal carcinoma).

	Tumor Vol., % (<0.0001)	pT3a/pT3b, % (0.0006)	LVI, % (<0.0001)	IDC, % (<0.0001)	Satellites, % (0.001)
LN+	31.1	51.4/45.7	65.7	51.4	22.8
LN-	15.0	85.4/14.6	25.6	9.8	3.7

Conclusions: Within GS7 prostatic carcinoma, there are significant differences in cases with LN+ vs. LN- in ethnicity, preoperative PSA, tumor volume, stage, LVI, intraductal spread, satellite tumor foci, nuclear enlargement and size of macronucleoli. These variables may be worthwhile to assess as prognostic markers in GS7 disease on biopsy (ie. IDC, cytology) or at RP (all variables) even in men with LN-.

863 Molecular Assessment of Clonality in Mixed Epithelial and Stromal Tumors of the Kidney: Evidence for a Single Cell of Origin with Capacity for Epithelial and Stromal Differentiation.

JB Kum, M Wang, DJ Grignon, M Zhou, R Montironi, S Shen, A Lopez-Beltran, JN Eble, L Cheng. Indiana University, Indianapolis; Cleveland Clinic, OH; Polytechnic University of the Marche Region, Ancona, Italy; The Methodist Hospital, Houston, TX; Cordoba University, Spain.

Background: Mixed epithelial and stromal tumors of the kidney (MESTK) are uncommon biphasic tumors of the kidney with cystic and solid areas composed of ovarian-like stroma and an epithelial component with variable morphology. Little is known about the pathobiology and molecular features of these tumors. There are two theories regarding the development of the tumor. One theory proposes that the stroma is neoplastic but the epithelium represents "trapped" structures and is not clonal. Another

theory proposes that both the stroma and epithelium are neoplastic and arise from a common cell of origin.
Design: A total of 21 MESTK tumors from female patients who underwent radical or partial nephrectomies were examined. The epithelial and stromal components of MESTK, as well as adjacent non-neoplastic renal parenchymal tissues were separately laser microdissected from sections prepared from formalin-fixed and paraffin-embedded tissues. X-chromosome inactivation analysis was performed by examination for random or nonrandom inactivation methylation patterns of exon 1 of the human androgen receptor gene on chromosome Xq11-12.
Results: Nineteen of the 21 tumors were informative. Seven of these informative cases showed random X chromosome inactivation pattern in both epithelial and stromal component of MESTK. Nonrandom inactivation of the X-chromosome was found in 12 of 19 informative tumors. The same pattern of nonrandom inactivation of the X-chromosome was seen in both epithelial and stromal components in all 12 of the tumors with nonrandom X-chromosome inactivation.
Conclusions: MESTK are clonal tumors with the stroma and epithelium showing the same pattern of X-chromosome inactivation. Our data support the theory that the stroma and epithelium arise from a common cell of origin.

864 Metastatic Teratomas with Secondary Malignant Components: Molecular Genetic Evidence That Somatic-Type Malignancies Arise from the Same Progenitor Cells as the Teratomatous Component.

JB Kum, M Wang, TM Ulbright, SDW Beck, RS Foster, DJ Grignon, JN Eble, L Cheng. Indiana University, Indianapolis.
Background: Occasionally, testicular teratomas have been observed to develop secondary somatic-type malignant components. Such components may be seen in the primary germ cell tumor or, more commonly, within metastatic sites after chemotherapy with cisplatin-based agents. The molecular genetic relationship between teratoma and the secondary malignant component is uncertain.
Design: We examined 23 metastatic teratoma and secondary malignant component pairs of metastatic tumors. Interphase florescence in situ hybridization analysis for 12p overexpression and i(12p) were performed on formalin-fixed, paraffin-embedded specimens. Additionally, we compared the pattern of allelic loss between the teratoma and the secondary malignant component using four microsatellite DNA markers (D1S508; IFNA; D13S317 and D18S543). A laser capture microdissection technique was used to procure separate tumor components.
Results: The histologies of the secondary malignant components included adenocarcinoma (11), primitive neuroectodermal tumor (3), sarcoma (5), squamous cell carcinoma (1), chondrosarcoma (1) and rhabdomyosarcoma (2). Two of the 23 (8.7%) tumor pairs showed i(12p) in the teratomatous component only and 3 of the 23 (13%) tumor pairs showed no abnormalities of chromosome 12p by interphase FISH. Eighteen of 23 tumor pairs (78%) showed either overexpression of 12p and/or i(12p). Seven of the 8 (88%) tumor pairs tested, had identical patterns of loss of heterozygosity in both the teratoma and the secondary malignant component. One case showed allelic loss at the IFNA locus in the secondary malignant component only.
Conclusions: Our data show that the secondary malignant components which develop in germ cell tumors have the same genetic alterations detectable by florescence in situ hybridization and loss of heterozygosity studies as in the corresponding teratoma. These findings suggest that the somatic-type malignancies and the teratomas are clonally related and likely derived from a common progenitor cell. Interphase florescence in situ hybridization that can be performed on formalin-fixed, paraffin-embedded is a sensitive method for detecting 12p overexpression and i(12p), thus aid in establishing germ cell origin.

865 Perineal Mapping Biopsy of Prostate: Experience from a Single Academic Institution and Impact on Prostate Cancer Management.

LP Kunju, R Siddiqui, M Rowley, D Miller, S Meyers, D Wood, JT Wei. University of Michigan, Ann Arbor.
Background: Appropriate patient selection for active surveillance is crucial. We evaluated the utility and morbidity of perineal prostate mapping biopsy prior to making a decision for definitive therapy of prostate cancer (PCa).
Design: 116 patients with elevated/rising PSA and/or previous diagnosis of PCa with at least 1 prior transrectal prostate biopsy underwent restaging with perineal template mapping prostate biopsy at a single academic institution between Sept 2007 and June 2010. Seventy five (64%)patients had a previous PCa diagnosis while 41 (36%)patients had no previous history of PCa. All biopsies were performed by two experienced urologists using transrectal ultrasound and brachytherapy implant grid under spinal or general anesthesia. Samples were taken every 5 mm throughout the volume of the prostate and labeled separately.
Results: The mean age was 62.5Y (SD ±9). The mean number of cores obtained was 61 (SD ±14) and mean number of positive cores was 4.9 (SD±5). PCa was identified in 81/116 (70%) patients, including 59 (51%) patients with a previous PCa diagnosis vs. 22 (19%) with no history of PCa. Significant PCa (Gleason Score ≥7) was noted in 42 /116 (36%) patients including 27 (23%) and 15 (13%) of patients with and without history of PCa respectively. Seven of 116 (6%) patients had high-grade PCa (Gleason score ≥8), of which 5 (4%) were diagnosed in patients with no previous history of PCa. Complications were limited and included 18 patients (8%) with urinary retention (10) or hematuria (8). Twenty eight patients (24%) underwent definitive therapy for PCa including robotic radical prostatectomy (19%), radiation therapy (4%) and cryosurgery (1%). Eighty-four (72%) patients are on active surveillance.
Conclusions: Perineal mapping biopsy of the prostate is well tolerated and can be safely used to provide accurate staging information for PCa management. It is potentially a very useful tool in selecting patients for active surveillance and can profoundly impact personalized management of PCa.

866 Viability of Glomeruli and Proximity to Tumor in Partial Nephrectomy Specimens for Renal Cell Carcinoma.

ET Lam, A Mortazavi, GS Phillips, D Sharp, D Zynger. The Ohio State University Medical Center, Columbus.
Background: The optimal surgical margin size for partial nephrectomy has not been clearly defined. Current surgical technique attempts to preserve the maximum amount of non-neoplastic renal tissue although it is unknown whether closer surgical margins translate into improved preservation of renal function. Mechanical compression from the tumor may lead to glomerular injury and the kidney surrounding the tumor may not be functional. Therefore, the goal of preserving all non-neoplastic renal parenchyma with a surgical margin of nearly zero may not be necessary and could increase positive surgical margins. In this study, the viability of glomeruli adjacent to renal cell carcinoma in partial nephrectomy specimens was evaluated.
Design: We retrospectively reviewed 53 partial nephrectomy cases containing renal cell carcinoma. Tumor size and minimum/maximum resection margins were measured. Glomeruli within 0-0.25 cm, 0.25-0.5 cm, 0.5-0.75 cm, and 0.75-1.0 cm from the tumor were quantified and categorized as 1) nonviable (matrix occupying >90% of the glomerular space), 2) minimally viable (including matrix 50-90% or markedly disrupted glomeruli) and 3) viable (all other glomeruli). Spearman's rank-method was used to evaluate the correlation between tumor size and minimum/maximum margins. Random-effects linear regression was used to test the association between percent of viable glomeruli and closeness to tumor. Wilcox rank-sum method was used to compare the size of the resected margin and margin status.
Results: The mean percentages of viable glomeruli in successive 0.25 cm distances from the tumor were: 0-0.25 cm, 58%; 0.25-0.5 cm, 80%; 0.5-0.75 cm, 90%; 0.75-1.0 cm, 92%. The absolute percent of viable glomeruli was 24.4% higher in the region >0.5 cm from the tumor compared with the region ≤0.5 cm from the tumor ($p = < 0.001$). Median tumor size was 2.5 cm (range 0.7-8.7 cm, mean 2.9 cm) with median minimum margin of 0.15 cm (range 0-0.9 cm, mean 0.2 cm) and maximum margin of 0.7 cm (range 0.3-1.7 cm, mean 0.8 cm). There was no significant correlation between tumor size and minimum or maximum margin, tumor size and glomerular viability or margin size and incidence of positive margins.
Conclusions: Our findings demonstrate that the immediate peri-tumoral rim of non-neoplastic tissue is abnormal and populated with a mixture of nonviable, minimally viable and viable glomeruli. Distance from the tumor correlates with increased viability of glomeruli which should be considered to define the optimal surgical margin size for partial nephrectomy.

867 Identification and Characterization of Two Novel Testicular Germ Cell Markers, Glut3 and cyclinA2.

BE Lane, SB Jones, JD Brooks, J Higgins. Stanford University School of Medicine, Palo Alto, CA.
Background: Testicular germ cell tumors (TGCT) are the most common type of testicular tumor, and encompass different histologic types that carry great significance for prognosis and treatment. Though diagnoses are often made on hematoxylin and eosin (H&E) stained sections alone, immunohistochemical studies are often required for more accurate diagnosis and when these tumors present at extragonadal sites. Traditional markers for identifying and distinguishing testicular germ cell tumors include PLAP, CD117, AFP, and CD30. More recently, the addition of OCT4 and SALL4 have increased sensitivity on immunohistological detection of germ cell tumors. Despite these recent breakthroughs in TGCT immunohistochemistry, there is still the need for additional ancillary markers to add to the repertoire.
Design: We examined gene expression data from a previously published microarray study that compared normal testis mRNA expression to various testicular germ cell tumors. We also performed a search of the literature to identify less well characterized, putative markers. Glut3 and cyclinA2 expression was evaluated by immunohistochemistry using tissue microarrays (TMA).
Results: Of 66 seminomas included in the TMA, 64 (97%) showed positive nuclear staining for cyclinA2, and 58 (88%) were strongly positive. Strong positive staining for cyclinA2 was also seen in the spermatocytic seminoma. All twenty of the embryonal carcinomas stained positively with cyclinA2, and 19 of these (95%) displayed strong nuclear staining for cyclinA2. Twenty of 20 embryonal carcinomas stained for glut3 in a membranous pattern. Of 8 yolk sac tumors, 100% stained with glut3; and in all but one, the staining pattern was strong and diffuse. We evaluated glut3 and cyclinA2 staining on a general tumor array containing 486 samples representing 156 different tumors. CyclinA2 did stain a number of other tumor types, but the majority of these were weak or focal staining. Glut3 was positive only in a handful of other tumors, interestingly, most of these were of ovarian origin.
Conclusions: Glut3 is a sensitive (96%) and specific (92%) marker for embryonal carcinomas and yolk sac tumors. While cyclinA2 is a sensitive marker of seminomas and embryonal carcinomas (98%), its specificity is lower if focal and weak staining of non germ cell tumors is considered positive. The sensitivity and specificity of Glut3 are comparable to that seen for SALL4.

868 Utility of CD34 and CD31 in the Distinction between Invasive Micropapillary Urothelial Carcinoma and Invasive High Grade Urothelial Carcinoma with or without Pseudo-Micropapillary Features.

SR Lauer, AO Osunkoya. Emory University School of Medicine, Atlanta, GA.
Background: Micropapillary urothelial carcinoma is an aggressive variant of urothelial carcinoma. The distinction between this entity and usual type urothelial carcinoma or urothelial carcinoma with pseudo-micropapillary features has become increasingly important in view of therapeutic and prognostic implications. Unfortunately, recent studies have shown some degree of lack of interobserver reproducibility even amongst

urologic pathologists. To date, only very few immunohistochemical stains such as MUC1 which is not readily available in most academic institutions or private laboratories have been proposed to aid in the distinction between micropapillary urothelial carcinoma and usual type urothelial carcinoma or urothelial carcinoma with pseudo-micropapillary features. In this study, we demonstrate the utility of CD34 and CD31 in this regard.

Design: A search was made through the surgical and consultation files at our institution for cases of micropapillary urothelial carcinoma. A control group of usual type urothelial carcinoma and urothelial carcinoma with pseudo-micropapillary features was also identified. A representative slide/block of each case was selected and immunohistochemical stains for CD34 and CD31 were performed. The immunohistochemical stains were reviewed for the presence of positive staining within the center of the tumor papillae or invasive nests, and the results were documented. Areas of angiolymphatic invasion were excluded.

Results: 23 cases with a diagnosis of micropapillary urothelial carcinoma of the bladder with available tissue blocks were identified from 2002 to 2010. 30 cases of usual type urothelial carcinoma and urothelial carcinoma with pseudo-micropapillary features were selected. 23/23 cases (100%) of micropapillary urothelial carcinoma lacked expression of CD34 and CD31 within the center of invasive tumor micropapillae. In contrast, 30/30 cases (100%) of usual type urothelial carcinoma and urothelial carcinoma with pseudo-micropapillary features demonstrated positive expression of CD34 and CD31 within the center of invasive tumor papillae.

Conclusions: To the best of our knowledge, our study is the first to examine the utility of readily available markers CD34 and CD31 in the distinction between invasive micropapillary urothelial carcinoma and invasive usual type urothelial carcinoma or urothelial carcinoma with pseudo-micropapillary features. CD34 and CD31 may aid in the distinction between these entities when confronted with equivocal cases.

869 Clinicopathologic Analysis of Prostate Cancer in Men Age 45 or Younger: A Review of a Single Institution.

JA Laurini, T Lopez, JC Cheville, RJ Karnes, TJ Sebo, RE Jimenez. Mayo Clinic, Rochester, MN.

Background: Some prior studies of prostate cancer in men age 45 years or younger (PCa≤45) suggested that these patients (pts) had a less favorable outcome. However, most of these studies were performed before PSA screening programs. We studied a cohort of PCa≤45 treated by radical prostatectomy (RP) and analyzed pathological and clinical differences between PCa≤45 and older pts.

Design: RP specimen slides from cases of PCa≤45 that underwent RP at our institution from 1987 to 2007 were reviewed for Gleason score (GS), tumor location, and histologic subtype. Original GS, PSA level, pathologic stage, margin status (and a score combining these factors – GPSM score), pre- and post RP therapy, were compared with the remaining (older) pts in the registry. Biochemical failure (BCF) rates were compared using Kaplan-Meier (KM) analysis. Cox regression model was used for multivariate analysis.

Results: Of 16,551 RP at our institution in the study period, 181 (1.09%) were for PCa≤45. 168 had available slides for review, on which 72.6 % had a GS ≤6, 9 and 3 cases showed mucinous and ductal features, respectively, and 14 cases showed involvement of the anterior/transition zone. 82.3 % had negative margin status and 88.9 % were organ-confined. Over the study period, a significant increase in the number of PCa≤45 undergoing RP was noted (1 pt in 1987 vs 17 in 2007; p<0.0001). PCa≤45 when compared to older men had a lower median preoperative PSA (4.4 vs 6.2 ng/ml; p <0.0001); seminal vesicle involvement (4.4% vs 11.8%; p=0.0022); lymph node metastases (2.3% vs 6%; p=0.0370); positive surgical margins (17.7% vs 28.6%; p=0.0012); lower pathologic stage (p=0.0001); GS (p=0.0248); and were less likely to receive hormonal (5% vs 13.9%; p=0.0005) or radiation (5.5% vs 10.6%; p=0.0274) therapy for recurrent disease. KM analysis revealed a lower rate of BCF in PCa≤45.

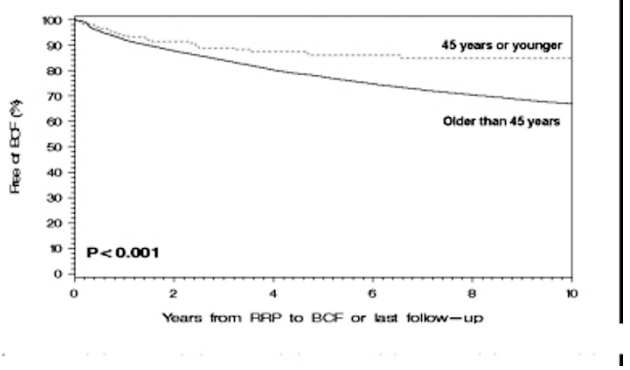

On multivariate analysis, this difference was not significant once age at diagnosis was controlled for year of surgery and GPSM score.

Conclusions: Diagnosis of PCa≤45 has increased steadily over the years. PCa≤45 is not associated with unique morphologic or topographic features; however, pts with PCa at this young age are more likely to be associated with favorable pathologic findings upon diagnosis.

870 Renal Mucinous Tubular and Spindle Cell Carcinoma: Expanding Our Knowledge of Immunohistochemical and Cytogenetic Findings.

AR Laury, M Riveros-Angel, VS Sabbisetti, P Dal Cin, MS Hirsch. Brigham and Women's Hospital, Boston, MA.

Background: Mucinous tubular and spindle cell carcinoma (MTSCC) is a recently described rare subtype of renal cell carcinoma (RCC). It is a heterogenous tumor composed of epithelioid cells forming tubules and cords, admixed with spindle cell foci, typically associated with a mucinous/myxoid stroma. The differential diagnosis of MTSCC includes papillary RCC (PRCC) due to overlapping architectural and immunohistochemical findings. The few previously reported karyotypes have described multiple monosomies; however, fewer than typically seen in chromophobe RCC (ChRCC). The goal of this study was to better characterize the immunoprofile and chromosomal abnormalities (as determined by conventional karyotype and FISH) in MTSCCs, particularly as compared to PRCC, ChRCC, and oncocytoma (ONC).

Design: 22 cytogenetically confirmed renal epithelial neoplasms (5 MTSCCs, 6 PRCCs, 5 ChRCCs, & 6 ONCs) were immunostained for RCC, CK7, CK20, CD10, AMACR, hKIM-1, S100A1, Galectin3, WT1, HMB45, CD15, cKit, and E-cadherin. Staining was scored as negative (0), rare (1+, <10%) or positive (2+, 10-50% or 3+, >50%). All analyses were interpreted blind to morphologic and karyotypic diagnoses.

Results: Conventional cytogenetics demonstrated that the MTSCCs contained multiple monosomies, including losses of 1, 6, 14, 15 and 22. Positive immunohistochemical findings are presented in Table 1. The presence of Galectin3, cytoplasmic (cy) WT-1, and E-cadherin plus the absence of CD10 support the diagnosis of MTSCC over PRCC. The absence of AMACR, S100A1 and KIM-1 can help distinguish ChRCC from MTSCC when overlapping cytogenetic findings (multiple monosomies) are present; Galectin-3 is not helpful for this distinction. CK7, CK20, RCC, CD15, cKit, and HMB45 are less useful discriminators.

Neoplasm (N)	Galectin3	E-Cadherin	WT1 (cy)	CD10	AMACR	S100A1	KIM-1
MTSCCA (5)	3	3	2	1	4	4	3
PRCC (6)	0	0	0	5	6	5	2
ChRCC (5)	5	5	0	0	0	0	0
ONC (6)	6	1	0	1	0	5	0

Conclusions: This study presents the karyotypic findings of 5 additional MTSCCs, confirming that multiple chromosomal monosomies (esp. 1, 6, 14, 15, and 22) are common in MTSCC. It also demonstrates a new and unique immunohistochemical panel (Galectin3+, WT1+, E-cadeherin+/CD10-) which can aid in the diagnosis of MTSCCA over PRCC. The presence of AMACR, S100A1, and KIM-1 also support a diagnosis of MTSCC over ChRCC. FISH, in combination with morphologic and immunophenotypic findings, is predicted to aid in the diagnosis of MTSCC, especially when conventional cytogenetics is not available.

871 Lysophosphatidylcholine Acyltransferase 1 (LPCAT1) Is Associated with the Progression of Prostatic Adenocarcinoma Independent of Race and Age.

TJ Lawrence, X Zhou, Z He, C Pound, SA Bigler. The University of Mississippi Medical Center, Jackson.

Background: There is not yet a satisfactory biomarker in predicting the progression of prostate cancer. Lysophosphatidylcholine acyltransferase 1 (LPCAT1) is a recently characterized enzyme that converts lysophosphatidylcholine into phosphatidylcholine. Increased LPCAT1 activity has been reported in adenocarcinomas of the colon and prostate (PCa). The current study is designed to determine if there is correlation of LPCAT1 expression with various clinical features of prostate cancer.

Design: Tissue micro arrays (TMA) were made from 183 selected prostatic tissues from 123 patients accessioned over the past 20 years at The University of Mississippi Medical Center and used for the immunohistochemistry (IHC) study of LPCAT1. A scoring system was created by a combination of percentage of positive cells and intensity of staining recorded as 0, 1, 2 or 3. All specimens were divided into 4 groups: benign, high grade prostatic intraepithelial neoplasia (HGPIN), primary PCa, and metastatic PCa. Primary PCa was further sub-grouped as low grade, intermediate grade, and high grade according to Gleason scores (2-6, 7, and 8-10, respectively). The IHC combined score was also analyzed in relation to patient age and race.

Results: One-way analysis of variance (ANOVA) showed statistically significant difference in staining scores among groups (p < 0.0001). The mean staining score was 3 in metastatic PCa group, which was significantly higher than that in primary PCa, HGPIN, and benign groups (2.15, 1.13, 1.45, respectively; p=0.001981, p<0.0000001, p<0.0000001, respectively). There was a significant increase in staining of primary PCa as compared to PIN (p=0.00243) and to benign (p =0.000381). ANOVA also showed statistically significant difference among grades of primary PCa (p<0.0001); however, this difference was significant only between high and low grade primary cancers (p=0.001206). Also, LPCAT1 IHC scores were higher in primary tumors from patients who subsequently developed metastasis than in patients not known to have developed metastasis over the follow-up period, and this difference was independent of Gleason score. The results suggested that IHC scores for LPCAT1 did not correlate with patient's age and race in this study cohort.

Conclusions: The results of this study suggest that LPCAT1 is associated with the progression of prostate cancer independent of age and race. Primary prostate adenocarcinoma with higher LPCAT1 staining score predicts risk of distant metastasis.

872 Ras Pathway Activated by Loss of ARL11: A Missing Link in Cancer Initiation.

S Lee, S Lee, J Bondaruk, T Majewski, H Wang, S Zhang, M Bar-Eli, P Black, Y Wang, CC Guo, C Dinney, HB Grossman, M Knowles, K Baggerly, B Czerniak. UT MD Anderson Cancer Center, Houston, TX; St. James's University Hospital, Leeds, United Kingdom.

Background: Our previously reported mapping studies of bladder cancer provided evidence that a new class of genes, referred to as forerunner (FR) genes (ITM2B, P2RY5, GPR38 and ARL11), located near known tumor suppressors such as RB1, drive early clonal expansion of neoplasia. (S Lee, *et al.* PNAS 104: 13732-13737, 2007) These studies suggested three major steps for the involvement of the RB1 locus in tumor development. In the first step, one allele of FR gene and RB1 is inactivated by deletions. Secondly, homozygous inactivation of the FR genes is accomplished by hypermethylation or less frequently by mutations and is associated with the expansion of early *in situ* precursor lesions. Finally the contiguous tumor suppressor, such as RB1, is inactivated most commonly by a mutation. This step is associated with clonal evolution into carcinoma *in situ* progressing to invasive cancer.

Design: Recently, we concentrated our efforts on the ARL11 candidate FR gene, which encodes ADP-ribosylation factor-like 11 protein, a ras-related member of the small GTPases, that functions as GDP/GTP nucleotide interswitch for signal transduction. Our studies focused on ARL11 expression, promoter methylation and cell cycle analysis with emphasis on ARL11's relationship to the ras signaling pathway.

Results: We have shown that ARL11 has been silenced by hypermethylation in approximately 40% of urothelial carcinomas of the bladder and the silencing was associated with *in situ* expansion of intraurothelial neoplasia. Moreover, loss of ARL11 expression was almost mutually exclusive with the FGFR3 mutations (<5% of bladder tumors showed a co-existence of mutant FGFR3 and methylated ARL11). Functional studies conducted on immortalized normal urothelial cells grown *in vitro* showed that ARL11 reduced cell proliferation, which was mediated by the inhibition of the ras pathway. This effect was associated with the down-regulation of the active ras and ERK1/2 phosphorylation as well as with the up-regulation of negative cell cycle regulator proteins such as $p27^{kip1}$ and parallel down-regulation of cyclins D1 and E. Conversely, the silencing of ARL11 conferred a tumor suppressor effect promoting cell proliferation via the activation of the ras signaling pathway.

Conclusions: Recessive events in the RB1 locus associated with the loss of ARL11 promote expansion of intraurothelial precursor lesions by activating the ras pathway in early phases of bladder carcinogenesis.

873 ALDH1 Expression Is Associated with Low Tumor Grade and Stage in Renal Cell Carcinomas (RCC).

JA Levesque, JS Ross, CE Sheehan, RP Kaufman, A Hayner-Buchan. Albany Medical College, NY.

Background: ALDH1 is a member of the aldehyde dehydrogenase family that plays a major role in the biosynthesis of retinoic acid, a regulator of cellular proliferation, differentiation and survival. ALDH1 is overexpressed in many head and neck squamous cell carcinomas, predicts poor clinical outcome in breast cancer and correlates with a favorable prognosis in ovarian cancers. This study examines ALDH expression in renal cell carcinoma (RCC).

Design: Formalin-fixed, paraffin-embedded tissue sections from 74 renal cell carcinomas were immunostained by automated methods (Ventana Medical Systems Inc., Tucson, AZ) using mouse monoclonal ALDH1 (clone 44/ALDH; BD Biosciences). Cytoplasmic, membranous, and nuclear immunoreactivity were semiquantitatively scored based on staining intensity and distribution and the results were correlated with morphologic and prognostic variables.

Results: Membranous ALDH1 overexpression was observed in 55/74 (74%) RCC; and correlated with tumor type [79% clear cell vs 45% other subtypes, p=0.018] and low tumor grade [82% low grade vs 58% high grade, p=0.029]. Cytoplasmic ALDH1 overexpression was observed in 38/74 (51%) tumors; and correlated with early stage [60% early stage vs 35% advanced stage, p=0.040]. Nuclear ALDH1 overexpression was noted in 31/74 (42%) RCC and showed a trend toward correlation with low tumor grade [48% low grade vs 28% high grade, p=0.094]. There was correlation between nuclear and membranous immunoreactivity (90% of RCC overexpressing nuclear ALDH1 protein also exhibited a membranous pattern of overexpression, p=0.007). On multivariate analysis, advanced tumor stage and disease recurrence independently predicted survival.

Conclusions: ALDH1 overexpression in renal cell carcinoma correlates with low tumor grade (membranous and nuclear staining) and early pathologic stage (cytoplasmic staining). ALDH1 expression may exert a favorable impact in renal cell carcinomas.

874 Comparison of PAX-2 and PAX-8 Expression in Primary Neoplastic and Metastatic Tumors of Wolffian Duct and Mullerian Origin.

A Lewis, S Shen, J Ro, A Ayala, L Truong. Methodist Hospital, Houston, TX.

Background: PAX-2 and PAX-8 are homologous and complementary members of the pair box gene family. They are known to control the development of organs derived from the Wolffian and Mullerian ducts. Individual studies suggest a similar expression of PAX-2 and PAX-8 in normal and neoplastic tissue. However, direct comparison of their tissue expression, which may imply both biologic and diagnostic importance, is not available.

Design: Immunostaining for PAX-2 and PAX-8 on *consecutive* formalin-fixed, paraffin embedded tissue sections from samples of non-neoplastic tissue (n=202), primary tumors (n=500), and metastatic tumors (n=275) was performed. Staining frequency (% of cases), extent (% of stained cells), and intensity (0-3+) were compared.

Results: For *non-neoplatic tissue*, virtually identical (constant, strong, diffuse) expression of PAX-2 and PAX-8 was noted in epithelial cells of uterine cervix, endometrium, fallopian tube, seminal vesicle, testicular efferent duct, and distal renal tubules. PAX-8, but not PAX-2, was present in all thyroid tissue samples and 85 % of pancreatic islet cells. *For primary neoplasms*, PAX-2 and PAX-8 were expressed in renal cell carcinoma (RCC) and tumors of Mullerian origin. Among RCC (n=166), expression was 63.25% and 87.35% of tumors, extent of staining was 56.19% and 71.99% of tumor cells, and the intensity scores were 1.49 and 1.8 for Pax-2 and Pax-8 respectively. Among tumors of Mullerian origin, the expression of Pax-2 and Pax-8 was: 43.40% and 90.56% of tumors, staining extent 24.47 % and 85.88% of tumor cells, and intensity scores 1.1 and 2.57, respectively. PAX-8, but not PAX-2, was noted in all 67 papillary or folicular thyroid neoplasms and 75% of 15 well-differentiated pancreatic neuroendocrine tumors. Focal weak staining for both PAX-2 and PAX-8 was noted in a few parathyroid lesions. The stronger and more extensive PAX-8 expression noted in primary tumors was also noted for *metastases* (2 and 2.59; mean intensity scores, Pax-2 and Pax-8, respectively).

Conclusions: There is significant overlapping expression of PAX-2 and PAX-8 in both normal and neoplastic tissue, in keeping with their similar genetic ontogeny. However, remarkable differences are also noted including more expression of PAX-8 over PAX-2 for both primary and metastatic RCC and Mullerian tumors, and frequent PAX-8, but not PAX-2, expression in other tumors including thyroid follicular tumors and pancreatic neuroendocrine tumors. PAX-8 provides better diagnostic yield than PAX-2 and perhaps may supersede PAX-2 in selecting a diagnostic panel.

875 *PTEN* Deletion and Heme Oxygenase-1 Overexpression Are Associated with Adverse Clinical Outcome and Cooperate in Prostate Cancer Progression.

Y Li, S Jack, X DingZhang, M Yoshimoto, S Liu, K Bijian, A Gupta, JA Squire, J Zhang, M Alaoui Jamali, TA Bismar. University of Calgary and Calgary Laboatory Services, AB, Canada; McGill University, Montreal, QC, Canada; Guangdong General Hospital, Guangdong Academy of Medical Sciences, Guangzhou, Guangdong, China; Queen's University, Kingston, ON, Canada; University of Calgary, AB, Canada.

Background: Over-expression of heme oxygenase-1 (HO-1), a sensor and regulator of oxidative stress and tissue redox homeostasis, and deletion of *PTEN*, a tumor suppressor gene, has been reported in prostate cancer (PCA).

Design: We assessed HO-1 expression and *PTEN* deletion, and their prognostic values, in two cohorts of men with localized PCA and castration resistant prostate cancer (CRPC). HO-1 expression was scored semi-quantitatively and *PTEN* status was assessed by a four-color interphase FISH.

Results: There was a significant difference between HO-1 epithelial expression between benign, high-grade prostatic intraepithelial neoplasia (HGPIN), localized PCA, and CRPC ($p<0.0001$). The highest epithelial HO-1 expression was noted in CRPC (2.00 ± 0.89) followed by benign prostate tissue (1.49 ± 1.03), localized PCA (1.20 ± 0.95) and HGPIN (1.07 ± 0.87). *PTEN* deletions were observed in 66% and 42.6% of CRPC and localized PCA, respectively. Although neither HO-1 overexpression nor *PTEN* deletion by itself in localized PCA showed significant association with PSA relapse, the combined status of both markers correlated with disease progression (Log-rank test, $p= 0.01$). In preclinical prostate cancer model, inhibition of HO-1 by shRNA in PC3M cells where *PTEN* is restored, strongly reduced cell growth and invasion *in-vitro* and inhibited tumor growth and lung metastasis formation in mice compared to control cells or to where only HO-1 is inhibited or PTEN is restored.

Conclusions: We provide novel evidence for strong correlation between epithelial HO-1 expression and *PTEN* deletions in relation to PCA patient's outcome. This cooperation is supported by data using PCA preclinical model where both HO-1 and *PTEN* were manipulated. These findings open-up novel cooperative genetic pathways associated with PCA progression and could potentially lead to discovery of novel therapeutic modalities for advanced PCA.

876 Macroscopic Features of Prostate Cancer.

C Lindh, L Egevad. Karolinska Institutet, Stockholm, Sweden.

Background: Prostate cancer is notoriously difficult to see at gross examination. This makes cutting of surgical specimens and biobanking more challenging than for tumors of other sites. This is to our knowledge the first systematic report on macroscopic features of prostate cancer in a large series of unfixed specimens.

Design: A set of 515 radical prostatectomy specimens were examined macroscopically by a trained pathologist (LE) at the Karolinska University Hospital 2002-2010. Unfixed prostates were bisected horizontally through the level of palpable nodules, positive preoperative biopsies or the junction of mid-apical thirds. Findings suggestive of cancer on cut surfaces were noted on a schematic drawing. Distinct findings were classified as conclusive for cancer and described as tan, white, yellow or orange while more subtle changes were classified as suspicious. Specimens were totally embedded. Tumor was outlined, all slides digitized and tumor maps were compared with gross descriptions. Tumor foci at the level of inspection were classified as minimal (<2 mm) or substantial (>2 mm).

Results: At gross examination, areas conclusive or suspicious for cancer were seen in 52% and 24%, respectively. Substantial cancers were found in 94% of conclusive foci and in 69% of suspicious foci. When no cancer was seen grossly, substantial cancers were found somewhere on the cut surface in 56%. In the entire series, substantial and minimal cancers were found anywhere at the level of macroscopic inspection in 85% and 9%, respectively. Of substantial tumors 58% had distinct gross findings (29% tan, 31% white, 16% yellow and 24% orange) and 20% were macroscopically suspicious. Among substantial cancers that were not seen at gross examination, 56% were PZ tumors and 35% TZ tumors compared to 73% and 18%, respectively, of all tumors ($p = 0.005$).

Conclusions: Findings conclusive for cancer at gross examination predict microscopic cancer in 94%. Of cancers larger than 2 mm 58% have distinct gross findings. TZ tumors are more difficult to see macroscopically than PZ tumors.

877 Biomarker Expression in Sarcomatoid Renal Cell Carcinoma: Comparison with Non-Sarcomatoid Components, and Renal Cell Carcinoma Unclassified.

L Liu, Q Yin-Goen, AN Young, AO Osunkoya. Emory University School of Medicine, Atlanta.

Background: The biomarker expression of the various subtypes of renal cell carcinoma (RCC) continues to be an area of great interest with clinical, diagnostic and therapeutic significance. The comparison of biomarker expression of sarcomatoid RCC with non-sarcomatoid component has hitherto not been well characterized.

Design: A search was made through the surgical pathology files of an academic institution for cases of RCC with sarcomatoid differentiation. 15 cases were selected; 6/15 (40%) clear cell CCRCC, 6/15 (40%) chromophobe CHRCC, 2/15 (13%) papillary PAPRCC, and 1/15 (7%) clear cell papillary CCPRCC. A case of RCC unclassified (UC) was also included in the study. Tumor cells obtained from separate FFPE tissue blocks of the sarcomatoid and non-sarcomatoid components were microdissected in each case. The relative expression of tumor biomarkers was measured by quantitative RT-PCR. RCC biomarkers were chosen from our previous microarray studies, and included: CCRCC markers CA9 and NNMT; PAPRCC markers AMACR, BAMB1 and SLC34A2; and CHRCC markers PVALB and BDF1. Results were analyzed using bioinformatics software.

Results: The non-sarcomatoid and sarcomatoid CCRCC components showed increased expression of NNMT compared to CA9. The non-sarcomatoid and sarcomatoid CHRCC components showed increased expression of parvalbumin compared to BDF1. The non-sarcomatoid and sarcomatoid PAPRCC components showed increased expression of BAMB1 and AMACR compared to SLC34A2. The non-sarcomatoid component of CCPRCC showed increased expression of CA9, AMACR and BAMB1, while the sarcomatoid component showed only slightly increased expression of SLC34A2. In most cases, the biomarker expression levels were higher in the non-sarcomatoid components compared to the sarcomatoid components. In all cases, the positive tumor biomarker expression levels in the non-sarcomatoid areas were relatively lower than in our previously studied RCC subtypes that had no sarcomatoid component. Expression of NNMT, parvalbumin and BAMB1/AMACR tended to distinguish sarcomatoid CCRCC, CHRCC and PAPRCC respectively from sarcomatoid RCC of other subtypes. The RCCUC case showed broad increased expression of NNMT, BDF1 and BAMB1, confirming a truly mixed phenotype.

Conclusions: Our study suggests that NNMT, parvalbumin and BAMB1/AMACR, are markers of choice for cases of CCRCC, CHRCC and PAPRCC respectively. These markers may have a critical diagnostic role in cases of sarcomatoid RCC in which subtyping is precluded by the absence of the non-sarcomatoid component, especially on needle core biopsies.

878 Characterization of *ERG* Gene Rearrangements and *PTEN* Deletions in Unsuspected Prostate Cancer of the Transition Zone.

S Liu, M Yoshimoto, K Trpkov, JA Squire, Q Duan, TA Bismar. Univerity of Calgary and Calgary Laboratory Services, AB, Canada; Kingston General Hospital and Queen's University, AB, Canada; Tom Baker Cancer Center, Calgary, AB, Canada.

Background: It was proposed that ERG gene rearrangements and PTEN deletions signify a distinct molecular subtype of prostate cancer (PCA) with adverse prognostic implications. SPINK1 over-expression was also found to be associated with disease progression. Systematic analysis of the incidence of ERG rearrangements, PTEN deletions and SPINK1 over-expression has not been performed in the prognostically favorable transition zone (TZ) PCA.

Design: We interrogated 54 unsuspected PCA tumors obtained by transurtetheral resection of the prostate using fluorescence in-situ hybridization for *ERG* rearrangements and *PTEN* deletions. SPINK1 over-expression was assessed by immunohistochemistry.

Results: *ERG* rearrangements were detected in 6/47 (12.7%) cases with 4/6 occurring by deletion. *PTEN* deletions were detected in 9/47 (19.1%) cases with only 3/47 (6.4%) having both *PTEN* losses and *ERG* rearrangements (p=0.07). SPINK1 over-expression was present in 8/49 (16.3%) and was exclusively restricted to non-*ERG* rearranged tumors. Only *ERG* rearrangements were associated with higher tumor volume >5% (p=0.04); *PTEN* deletions showed similar trends (p=0.06). No assocation was observed between SPINK1 and tumor volume. None of the markers showed association with Gleason score.

Conclusions: ERG rearrangements and PTEN deletions are infrequently found the PCA from the TZ and appear to be less common than in the peripheral zone tumors. TZ and peripheral zone tumors share similar molecular etiologies with different biological behavior based on the rate of *ERG* and *PTEN* detection. The infrequent detection of ERG and /or PTEN genetic aberrations in tumors from the TZ may however delineate a subset of tumors with more aggressive behavior. In this cohort, no major differences existed in the incidence of SPINK1 tumors between transition and peripheral zone.

879 ERG Protein Expression in Prostatic Small Cell Carcinoma Cases with Known *ERG* Gene Rearrangement Status.

T Lotan, A Chaux, W Wang, N Gupta, J Epstein, A De Marzo, G Netto. Johns Hopkins University School of Medicine, Baltimore, MD.

Background: *ERG* gene rearrangements occur frequently in prostatic carcinoma and are specific to this tumor type. Previously, we showed that *ERG* gene rearrangements occur in nearly half of all prostatic small cell carcinoma (SCC) cases making *ERG* rearrangement a promising marker of prostatic origin in this tumor type. Here, we looked at ERG protein expression by immunohistochemistry (IHC) in prostatic SCC and associated acinar carcinoma (ACa) with known *ERG* gene rearrangement status.

Design: IHC for ERG was performed on a TMA constructed from 30 cases of prostatic SCC. Fluorescence in situ hybridization (FISH) was performed on the same TMA using a break-apart probe for 5' and 3' *ERG*. Cases were scored for nuclear ERG protein expression and a case was considered to express ERG protein if greater than 10% of cells expressed ERG at a 1+ or greater intensity. Cases were scored for the presence or absence of *ERG* gene rearrangement through deletion or translocation in at least 50 cells.

Results: Overall, 20% of prostatic SCC cases (6/30) expressed ERG protein by IHC. FISH results for *ERG* gene rearrangement were available in 73% of SCC cases (22/30). Of the cases with known *ERG* rearrangement by FISH, 40% (4/10) were positive for ERG protein by IHC. The specificity of ERG IHC for gene rearrangement was high, with 92% of cases (11/12) that were negative for rearrangement also negative for ERG protein expression. Similarly, all normal prostate epithelium adjacent to SCC tumors spotted on the TMA was negative for ERG protein (6/6 cases). The sensitivity of ERG IHC for *ERG* gene rearrangement was considerably higher in the concurrent ACa tumors. 27% of SCC cases (6/22) had a concurrent ACa tumor component present on the array with evaluable FISH results. Of these, 67% (4/6) had *ERG* gene rearrangement present and 100% of these cases (4/4) were positive for ERG protein by IHC. Interestingly, 50% of cases (2/4) with *ERG* rearrangement in both the ACa and SCC components were negative for ERG protein expression in the SCC component and positive for ERG protein in the concurrent ACa component.

Conclusions: The sensitivity of ERG IHC for *ERG* gene rearrangement is relatively low in prostatic SCC. The lack of ERG protein expression in more than half of SCC cases with known *ERG* gene rearrangement may be in part due to the fact that this tumor type is often androgen-insensitive. Finally, the high specificity of ERG IHC for *ERG* gene rearrangement makes ERG IHC a promising marker for establishing prostatic origin in SCC cases of unknown primary.

880 Immunohistochemical Study of Clear Cell Papillary Renal Cell Carcinoma.

S Lu, P Lal, JE Tomaszewski, Z Bing. University of Pennsylvania, Philadelphia.

Background: Clear cell papillary renal cell carcinoma (CCPRCC) is a recently described renal neoplasm that has morphologic features of both clear cell renal cell carcinoma and papillary renal cell carcinoma. Due to its rarity, the morphologic and immunohistochemical features of CCPRCC need to be further defined.

Design: Potential CCPRCC cases were identified by a natural language computer search for the diagnostic description of both "clear cell" and "papillary" over a 4-year period on pathology reports from kidney tumor specimens from the Department of Pathology in our hospital. H&E stained slides were reviewed. A panel of immunohistochemical stains with appropriate controls was performed, including RCC, CD10, vimentin, CK7, EMA, E-cadherin, TFE-3, CK903, and AMACR. Demographic data, clinical information, Fuhrman nuclear grade and tumor stage were correlated.

Results: 18 out of 236 renal cell carcinomas had diagnostic description of both clear cell morphology and papillary architectures during the 4-year period. Out of these 18 cases, one needle biopsy and four nephrectomy specimens were confirmed to be CCPRCC based on the histologic features described in the literature. Of these, one was male and four female, with age ranged from 38-68 years (mean 61).Three patients had end stage renal disease, while the others had kidneys with normal function. Tumor could arise in either the native or the transplanted kidney. Tumor size varied from 0.1 cm to 3.6 cm. Two patients had multiple tumor nodules involving either unilateral or bilateral kidneys, one patient had concurrent papillary renal cell carcinoma, and another patient had multiple renal papillary adenomas. Tumor could be either solid or predominantly cystic. The nuclei of clear cells lining the papillary architecture were either located towards the luminal side or in the center. Immunostains for CK7, EMA, CK903 and E-cadherin were positive in all the cases tested, while RCC was consistently negative. AMACR, CD10, vimentin and TFE-3 immunostains were variably positive. All tumors were of low Fuhrman nuclear grade (I or II), at low tumor stage (pT1a), and organ confined.

Conclusions: Although rare, CCPRCC is not that uncommon among renal tumors with both clear cell morphology and papillary architecture. It can arise in kidney of end stage disease as well as of normal function. Bilateral kidneys can be involved simultaneously, and other concurrent renal cell neoplasms can be seen as well. CCPRCC has distinct histologic and immunophenotypic characteristics that can be reliably employed to separate it from close mimickers.

881 Pathological Features of Contemporary Radical Prostatectomy Specimens for Prostate Cancer.

C Magi-Galluzzi, SM Falzarano, K Streator Smith, EA Klein, M Zhou. Cleveland Clinic.

Background: Prostate cancer (PCA) disease has changed substantially over the last 20 years due to the introduction of prostate-specific antigen (PSA) blood test in PCA screening. The present study was carried out to analyze the pathological features of contemporary PCA in radical prostatectomy specimens (RP) and compare them with RP from 1987-2004.

Design: We analyzed the pathological features of 1109 consecutive RP performed for clinically localized prostate cancer (PCA) at our institution between 2005 and 2010 (Group1). Pathologic features were compared with a cohort of 471 patients who underwent RP at the same institution between 1987 and 2004 (Group 2). All cases were reviewed by a single genitourinary pathologist, mapped, staged and graded according to the 2005 ISUP consensus conference on Gleason grading. For purposes of analysis, GS was subdivided in three categories: GS ≤6, GS=7 and GS≥8.

Results: Patients mean age was 59 (range 39-81) and 62 years (range 42-77) for Group 1 and 2, respectively. Pathological characteristics for the two groups are reported in table 1. Number of patients who underwent lymph node dissection, lymph node metastases (LN+), margin of resection (MOR) status, microscopic bladder neck (BN) involvement and lymphovascular invasion (LVI) were significantly different between groups (Table 1). PCA was mostly bilateral (88% and 83%). Tumor volume distribution in Group 1 was as such: low (<0.5 cc) in 19%, medium (0.5-2.0 cc) in 50%, and extensive (>2.0cc) in 31% of cases. A single focus PCA was detected in 13%, 2 distinct PCA in 17%, multifocal PCA in 62% of cases. In 4% and 3% of cases, respectively, PCA involved half of or the entire prostate.

Conclusions: There is a significant shift towards more favorable pathological parameters in RP specimens in contemporary series (2005-2010)compared to 1987-2004. This shift may result from a change in patient selection or PCA biology. PCA continues to be predominantly a bilateral and multifocal disease, with extensive volume in approximately 1/3 of cases.

Table 1

	2005-2010	1987-2004	p (Chi Square)
# RP	1109	471	
Age, mean	59	62	
GS≤6	24%	17%	<0.001
GS7	57%	46%	
GS≥8	20%	37%	
Tertiary pattern 5	6%	11%	0.001
LN dissection	59%	71%	<0.001
LN+	4%	8%	0.018
pT2	53%	38%	<0.001
pT2+	11%	9%	
pT3a	29%	35%	
pT3b	6%	17%	
MOR+	27%	32%	0.036
BN+	6%	10%	0.006
LVI	25%	29%	0.004
Bilateral PCA	88%	83%	0.008

882 Evaluation of UroVysion™ FISH and Cytology Testing – Concordance and Cost Effectiveness Comparison between Cotesting vs. Non-Cotesting Samples.

N Manglik, P Wasserman, S Sheikh-Fayyaz, N Morgenstern. North Shore Long Island Jewish Health System, New Hyde Park, NY.

Background: FISH is widely used in urothelial cancer patients however, there are no strict guidelines for ordering this expensive test. Some clinicians order it only in cases with equivocal cytology whereas others use it more liberally. Combined FISH and cytology may guide clinicians well in straight forward cases but in fair number of cases they will give conflicting results making it difficult to plan treatment. This problem is further complicated by the fact that the amount/quality of cells might be different in each urine specimen due to variable shedding of urothelium. We hypothesize that if these tests are done on the same urine sample (cotesting); they will have a better concordance and hence will be easier to interpret for clinicians, as opposed to when they are done on different urine specimens (non-cotesting).

Design: We studied 203 patients (410 samples) who had urine cytology and FISH tests at our institution during 2006-2009 and divided their samples in two groups: Cotesting and Non-Cotesting. Cotesting category had urine cytology and FISH on same sample. Non Co-testing group had these tests on different urine samples. We compared concordance of cytology with corresponding FISH results in both groups to evaluate if it was different in two groups. By concordance we mean that when cytology was abnormal corresponding FISH was positive and vice a versa.

Results: Concordance between cytology and FISH was 84% (174) in the Cotesting group (total 208) whereas it was lower in the Non-Cotesting group 74% [(75), (from the total of 101)]. The FISH and cytology results in the Cotesting group were concordant in 10% more cases than in the non-cotesting group. We had 399 FISH studies in our institution during 2009 out of which 100 (25%) were uninformative (insufficient number of cells). We had surgical follow up in 84 cases in which sensitivity and specificity for cytology was 42%, 65%; and for was FISH 29%, 79% respectively.

Conclusions: Our study shows that when FISH and cytology were ordered on different urine sample they showed 10% lower concordance. Based on our results we propose an algorithmic approach for ordering FISH testing. Cytology should always be ordered when ordering FISH. If cytology does not show sufficient number of cells then a repeat sample for FISH analysis should be requested. This practice will not only give a better concordance between cytology and FISH, but will also eliminate FISH testing on sparsely cellular specimens with uninformative results.

883 A Comparison of Proliferation Markers in Urothelial Carcinomas of the Urinary Bladder.

OM Mangrud, BD Hidle, R Waalen, E Gudlaugsson, EAM Janssen, JPA Baak. Stavanger University Hospital, Norway; University of Bergen, Norway; Innlandet Hospital Trust, Lillehammer, Norway.

Background: In Norway, 1218 new urinary bladder cancer patients were diagnosed in 2008. Treatment depends heavily on grade and TaT1 stage, but observer prognostic variability in staging and grading is considerable which may have strong implications for patients. A URO-QP model consisting of the following features: proliferation associated biomarker Ki67, mitotic activity index (MAI), and the mean area of the 10 largest nuclei (MNA10) has been developed. Lately we have added Phosphohistone H3, a marker of cells in late G2 and M phase.

Design: Patients with primary urothelial carcinoma of the urinary bladder diagnosed at a university hospital 2002-2006 with long follow up were included into the study. All specimens were routinely graded according to the WHO 73 system and analyzed according to the URO-QP model. Grading according to the WHO 2004 system was performed after archival specimen retrieval. ROC analysis was used to calculate cut-off values for MNA10, MAI and PPH3. Kaplan-Meier curves and Cox regression analysis were used to analyse the prognostic value of the variables with recurrence or stage progression as end-points.

Results: 194 patients were included. Mean follow-up was 53.4 months (range 1-101). Nineteen of the patients (10 %) progressed to a higher stage; 6.8 % of the patients with grade 1 tumours, 4.1% of the patients with grade 2 tumours and 23.1 % of the patients with grade 3 tumours (p=0.001), or 4.2 % of the patients with low grade tumours and 18.7 % of the patients with high grade tumours (p=0.001).

In agreement with previous studies, ROC curve analysis showed the following thresholds: MNA10>136.4, Ki67>18 and MAI>4. PPH3 threshold was >23. Patients with MNA10>136.4 showed 24% stage progression, contrasting 5% of those with lower MNA10. (p<0.001). This was the strongest identifier of patients with progression (p<0.001, Hazard Ratio=6.2, 95% confidence interval 2.3 – 16.8). None of the morphological grading systems, Ki67, PPH3, or MAI had additional prognostic value.

Conclusions: None of the variables analyzed showed any significant prognostic value for recurrence. For stage progression all proliferation markers, MNA10, and grading had independent prognostic value. In multivariate analysis MNA10 with a threshold of 136.4 um was the only remaining factor overshadowing all the other factors.

884 Distribution of Human Papilloma Virus Genotypes and Dermatoses in Penile Carcinoma in a Low Incidence Area in Europe.

S Mannweiler, S Sygulla, E Winter, Y Razmara, K Pummer, S Regauer. Medical University Graz, Austria.

Background: Invasive penile squamous cell carcinoma (SCC) accounts for 0.4-0.6% of all male malignancies in the USA and Europe. Investigations on the presence of transforming HPV-infections, LS and LP in a low incidence area for penile SCC in a homogenous patient cohort are rare.

Design: The distribution of human papillomavirus virus (HPV), lichen sclerosus (LS) and lichen planus (LP) in archival formalin-fixed specimens of 30 basaloid high-grade penile intraepithelial neoplasia (PeIN) and 108 invasive penile SCC was analysed for 28 HPV-LR and HPV-HR-genotypes(Inno-Lipa HPV Genotyping Extra) and immunohistochemically for over-expression of p16, a "surrogate" marker for transforming HPV-infection.

Results: Of 30 PeIN with p16 overexpression, 23/30 PeIN revealed a single HPV-genotype: HPV-HR16 (22) and HPV-HR18 (1). 1 PeIN each with type-specific reaction products for HPV-HR 16, 18, 33 and 73 revealed additional reaction products indicating a possible co-infection. 2 PeIN revealed multiple type-specific HPV-HR genotypes including HPV-HR18, only 1 PeIN revealed multiple HPV-HR genotypes without HPV16/18. In 60 SCC with p16-overexpression, HPV-HR 16 was the single genotype in 42/53 pT1, 4/5pT2 and 2/2 pT3 SCC, HPV-HR 45 the single genotype in 1 SCC. HPV-HR18 was not detected as single genotype. 5/60 SCC revealed type-specific HPV-HR 33 with possible co-infection with HPV-HR 52 and HPV-LR 54. 2/60 SCC contained multiple HPV genotypes in addition to HPV-HR16. 4/60 SCC harboured multiple type-specific HPV-HR genotypes without HPV-HR16/18. Overall, a single HPV-genotype was identified in 80% HPV-induced penile lesions: HPV-HR16 (22 PeIN, 48 SCC), HPV-HR45 (1 SCC) and HPV-HR18 (1 PeIN). 7 SCC & 2 PeIN with type-specific product for HPV-HR 33, HPV-HR 16, HPV-HR 18 and HPV-HR 73 revealed additional reaction products suggestive of co-infection. 14/90 lesions (15%) showed multiple type-specific HPV-HR-genotypes: 4% with & 11% without HPV-HR16/18. 20/90 PeIN/SCC (22%) harboured type-specific HPV-HR-genotypes other than HPV-HR16/18. 46/48 p-16-negative SCC were HPV negative and associated with LS > LP in more than 50%. The two p16-neg. SCC were a HPV-LR6-positive condylomatous SCC and a HPV-HR45-positive SCC.

Conclusions: 60% of invasive SCC and all PeIN were HPV-induced, with HPV 16 being the sole genotype in 80%. HPV18 & other HR-genotypes were identified in 20%. 40% of invasive SCC were HPV-negative. LS was the predominant dermatosis in non-HPV-associated penile cancer. These cancers may be prevented by early recognition and appropriate treatment.

885 Differential Expression of Cathepsin-K in Neoplasms Harboring *TFE3* Gene Fusions.

G Martignoni, S Gobbo, P Camparo, M Brunelli, E Munari, D Segala, M Pea, F Bonetti, M Ladanyi, GJ Netto, M Chilosi, P Argani. University of Verona, Italy; Van Andel Research Institute, Paris, France; Hospital Orlandi, Bussolengo, Italy; Memorial Sloan-Kettering Cancer Center, New York; Johns Hopkins Hospital, Baltimore.

Background: Cathepsin-K is a papain-like cysteine protease whose expression is driven by microphthalmia transcription factor (MiTF) in osteoclasts. TFE3 and TFEB are related members of the same transcription factor subfamily as MiTF, and all 3 have overlapping transcriptional targets. We have previously shown that all t(6;11) renal cell carcinomas (RCC), which are known to harbor an *Alpha-TFEB* gene fusion, as well as a subset of the Xp11 translocation RCC, which harbor various *TFE3* gene fusions, express cathepsin-K, while no other common RCC subtype does (Mod Pathol 2009; 22:1106-1022). We have hypothesized that aberrant overexpression of TFEB or certain TFE3 fusion proteins essentially function like MiTF in these RCC, and thus activate cathepsin-K expression. However, the expression of cathepsin-K in specific subtypes of Xp11 translocation RCC, as well as alveolar soft part sarcoma (ASPS) which harbors the same *ASPL-TFE3* gene fusion as some Xp11 translocation RCC, has not been specifically addressed.

Design: We performed immunohistochemistry for cathepsin-K on the following neoplasms: 11 genetically confirms t(X;1)(p11;q21) RCC, which harbor *PRCC-TFE3* gene fusion; 8 genetically confirmed t(X;17)(p11;q25) RCC, which harbor the *ASPL-*

TFE3 gene fusion; and 7 ASPS, all of which harbor the *ASPL-TFE3* gene fusion. The percentage and intensity of neoplastic cells labeling was assessed.
Results: All 7 ASPS strongly expressed cathepsin-K in a mean of 85% of neoplastic cells (range 70-100%). In contrast, all 8 *ASPL-TFE3* RCC were completely negative for cathepsin-K. However, 11 of 13 *PRCC-TFE3* RCC expressed cathepsin-K in a mean of 80% of neoplastic cells (range 30-90%).
Conclusions: Diffuse expression of cathepsin-K distinguishes from ASPS from *ASPL-TFE3* RCC, which harbor the same gene fusion. The latter can be useful diagnostically, especially when ASPS presents in an unusual site (such as bone) or with clear cell morphology which raises the differential diagnosis of metastatic *ASPL-TFE3* RCC. The difference in expression of cathepsin-K between the *PRCC-TFE3* RCC and *ASPL-TFE3 RCC* together with the recently observed clinical differences between these subtypes of Xp11 translocation RCC, suggests the possibility of subtle functional differences between these two related fusion proteins.

886 Expression of Putative Stem Cell Markers ALDH1 and CD133 in Urothelial Carcinoma of the Bladder.

A Matoso, KT Sciandra, S Elsamra, K Singh, J Renzulli, R Jacob, R Tavares, G Haleblian, L Noble, G Pareek, MB Resnick, LJ Wang. Rhode Island Hospital/Brown University, Providence.
Background: Expression of the stem cells markers aldehyde dehydrogenase-1 (ALDH1) and CD133 have been detected in hematopoietic and solid tumors. This is the first study that evaluates the expression of ALDH1 and CD133 in bladder cancer and their associations with pathological stage and patient followup.
Design: Tissue microarrays were constructed with normal and tumor samples from 81 endoscopic bladder resections and cystectomy specimens. Immunohistochemistry for ALDH1 (1:400 dilution; clone44 BD Biosciences) and CD133 (dilution 1:200; ab19898 Abcam) was performed and scored using a quantitative system that assigned 1-4 points for extent and for intensity. A total score of 5 or higher was considered strong and 4 or lower weak.
Results: Normal urothelium expressed ALDH1 along the basal layer in 4% of samples while CD133 expression was present in the umbrella cells in 13 % of cases. Expression of ALDH1 and CD133 in tumors and its relationship with depth of invasion is summarized in Table 1.

Immunohistochemistry Results

		Strong		Weak		Negative	
	Total	Aldh1	CD133	Aldh1	CD133	Aldh1	CD133
All cases	81(100)	28 (35)	0(0)	12 (15)	22(27)	41 (50)	59(73)
Non-invasive	25(30)	4 (16)	0(0)	5 (20)	6(24)	16 (64)	19(76)
Invasion into lamina propria	23(28)	3 (13)	0(0)	1 (4)	8(35)	19 (83)	15(65)
Invasion into muscularis propria and beyond	33(40)	21 (64)	0(0)	6 (18)	8(24)	6 (18)	25(76)

Strong ALDH1 expression correlated with muscularis propria invasion when compared to non-invasive tumors and tumors invading the lamina propria (63.6 % vs. 12.5%; p<0.001). CD133 expression was weaker and more focal and there was no correlation with invasion into lamina propria or muscle. Among non-invasive tumors, expression of ALDH1 was detected in 30% (6/20) of high grade and 60% (3/5) of low grade tumors; expression of CD133 was present in 25% (5/20) of high grade and 20% (1/5) of low grade tumors indicating a lack of correlation with tumor grade for both markers. Survival at 100 months in patients with strong expression of ALDH1 was 15% vs. 50% in patients with weak or negative ALDH1 expression.
Conclusions: Our results demonstrate that expression of ALDH1, but not CD133, correlates with invasion into the muscularis propria. Although our results suggest that strong expression of ALDH1 correlates with overall shorter survival, a larger cohort of patients with a stage matched analysis is necessary to confirm this hypothesis.

887 Potential Impact of Gleason Grade Reproducibility on Active Surveillance Management in Prostate Cancer: A Multi-Institutional Study of Patients Enrolled in a Prospective Active Surveillance Study (PASS).

JK McKenney, J Simko, M Bonham, LD True, S Hawley, L Newcomb, PASS Pathology Group, PR Carroll, JD Brooks. Stanford, Stanford, CA; University of California, San Francisco; University of Washington, Seattle; Canary Foundation, Palo Alto, CA.
Background: The impact of Gleason grade reproducibility on the management of patients in an active surveillance protocol has not been fully addressed.
Design: Three sets of digital images, each comprised of 17 separate prostatic carcinomas on core needle biopsy, were constructed [set 1 (classic Gleason patterns), set 2 (tangential Gleason pattern 3 vs Gleason pattern 4), set 3 (intraobserver test with same cases as set 2). Eleven pathologists from the PASS study sites assigned Gleason scores for each case. Interobserver and intraobserver reproducibility was assessed for assignment of the highest Gleason pattern (3 vs 4 or higher). In addition, a set of prostate needle core biopsies from of 97 consecutive patients enrolled in an active surveillance study (Canary PASS) were identified and those with available glass slides (n=82) were re-reviewed to determine the frequency of cases requiring the distinction of tangentially sectioned well-formed glands (Gleason pattern 3) from focally poorly formed glands (Gleason pattern 4).
Results: Interobserver reproducibility for classic Gleason patterns was "substantial" (Light's kappa: 0.76). Varying interpretation of carcinoma glands as tangentially sectioned Gleason pattern 3 or small poorly formed glands of Gleason pattern 4 led to the rare discrepancy in this test set. Interobserver reproducibility in test set 2 was only "fair" (Light's kappa: 0.26). Intraobserver reproducibility between sets 2 and 3 for each observer ranged from 65% to 100% (mean 81.5%; median 82%). In the set of biopsies retrospectively reviewed from 82 patients on active surveillance, 61 patients had carcinoma. 15 (24.5%) of these 61 patients had a set of biopsies with at least one focus in which the distinction between tangentially sectioned Gleason pattern 3 glands and focal poorly formed Gleason pattern 4 glands had to be carefully considered.
Conclusions: Reproducibility of grading classic Gleason patterns is high. However, variability in grading occurred in making the distinction between tangentially sectioned pattern 3 glands and the subset of pattern 4 glands that are poorly formed glands. Developing universally accepted histologic and/or molecular criteria for distinguishing these patterns and, subsequently, characterizing their natural history would be useful in the management of patients on active surveillance.

888 MMSET Is Associated with Prostate Cancer Progression and Over-Expressed in Androgen Independent Metastatic Prostate Cancer.

R Mehra, I Asangani, R Lonigro, X Cao, NE Philips, K Suleman, S Varambally, MA Rubin, RB Shah, KJ Pienta, AM Chinnaiyan. University of Michigan, Ann Arbor; Weill Cornell Medical College, New York; Caris Life Sciences, Irving.
Background: MMSET has been extensively studied in several tumors and is known to be part of the recurrent t(4;14) (p16;q32) translocation in Multiple Myeloma. We sought to characterize MMSET in a cohort of benign prostate tissues, clinically localized prostate cancer (PCA) and a warm autopsy cohort of androgen independent lethal metastatic PCAs and investigate its correlation with prostate cancer progression and the clinical features of these patients.
Design: MMSET mRNA levels in prostate cancer datasets were obtained using Oncomine, a cancer microarray database (www.oncomine.org). A tissue microarray (TMA) was constructed representing 96 patients with clinically localized prostate cancers who underwent radical prostatectomy at the University of Michigan as the primary monotherapy. Two other tissue microarrays (TMAs) were constructed representing 156 tumor foci (metastatic PCA samples and primary PCA, when present) from 47 rapid autopsies of men died of androgen independent metastatic PCA. Immunohistochemical analysis was performed using antibodies against MMSET on these tissue microarrays.
Results: Meta-analysis using cDNA datasets in Oncomine revealed MMSET to be overexpressed in metastatic prostate cancer compared to benign and clinically localized prostate cancer (Varamally et al and Lapointe et al). Immunohistochemical evaluation and analysis of TMAs revealed MMSET to be over-expressed in clinically localized prostate cancer compared to benign prostate tissues and this difference was statistically significant (p = 0.0004). MMSET was further over-expressed in androgen independent metastatic prostate cancer compared to clinically localized prostate cancer. Further survival analysis is being carried out to investigate the role of MMSET in prostate cancer outcome.
Conclusions: Here we show the MMSET to be highly expressed in prostate cancer. Our results suggest that MMSET expression increases during the natural history of prostate cancer progression, in particular with androgen-independent state and metastatic disease. It underscores the importance of investigating the functional role of MMSET in prostate cancer and its usefulness as a potential therapeutic target of cancer therapy.

889 Prevalence and Pathology of Renal Tumors in Autosomal Dominant Polycystic Kidney Disease (ADPKD) Versus Acquired Cystic Kidney Disease in End-Stage Renal Disease (ACKD-ESRD).

V Mehta, MM Picken. Loyola University Medical Center, Maywood, IL.
Background: ACKD-ESRD is a known risk factor for the development of renal cell carcinoma (RCC). In contrast, the risk for RCC in ADPKD is perceived to be small. The current prevalance of RCC in the general population of the USA is approximately 0.4%. ADPKD occurs in approximately 1-2/1000 live births and accounts for 10% of patients requiring dialysis/renal transplantation. The objective of this study is to compare the prevalence/pathology of renal tumors in ADPKD vs ACKD-ESRD vs the general population.
Design: We reviewed, retrospectively, all nephrectomies done at our Institution between 1985-2010, in patients (pts) with ADPKD and ACKD-ESRD. We compared the prevalence and types of tumors in both groups of patients and compared the data with published epidemiological data.
Results: The ADPKD group comprised 73 kidneys from 42 pts (19 M/23F); in 7/42, both kidneys were removed, but not simultaneously. Mean age was 50.3 yrs (range, 31-71yrs). The ACKD-ESRD group comprised 97 kidneys/80 pts (44M/36F). Mean age: 47.1 yrs (range 19-78 yrs). Four ADPKD kidneys showed RCC (5.4%): clear cell in 3/4, papillary RCC in 1/4; all in male patients. 13 ADPKD kidneys (17%) showed benign tumors: papillary adenomas -8, cystic nephroma-mixed epithelial and spindle cell tumors (CN-MEST) – 4, angiomyolipoma (AML) -1. Out of 80 ACKD-ESRD pts, RCC was seen in 32 pts (25M/7F): clear cell RCC in 16/32 pts (50%), papillary RCC in 7/32 pts (21.8%), acquired cystic disease associated RCC in 7/32 pts (21.8%), sarcomatoid RCC and chromophobe RCC in 1 pt each (3.1%). Of 97 kidneys with ACKD-ESRD, 17 contained papillary adenomas, 2 CN, 1 oncocytoma and 1 collecting duct (CD) adenoma.

TABLE 1

	ADPKD	ACKD-ESRD
RCC PREVALANCE	5.4%	40%
PATHOLOGY	ADPKD	ACKD-ESRD
Clear cell RCC	3	16
PRCC	1	7
ACKD ASSOCIATED RCC	0	7
CHROMOPHOBE	0	1
SARCOMATOID RCC	0	1
PAPILLARY ADENOMA	8	17
CN-MEST	4	2
ONCOCYTOMA	0	1
AML	1	0
CD ADENOMA	0	1

Conclusions: In our series, the prevalence of RCC in ACKD-ESRD was 40% while, in APKD, it was 5.4%; this represents a 100-fold and 10-fold increase respectively, when compared with the general population. Patients with ACKD-ESRD and ADPKD were, on average, 1 decade younger than the general population with RCC. While ACKD-ESRD patients may harbor tumors that are unique to this entity, the spectrum of neoplasia in ADPKD appears to be similar to that in the general population. Further studies are needed to establish whether active surveillance of patients with ADPKD should be considered.

890 Does the Sextant Site of Atypical Small Acinar Proliferation on Initial Prostate Needle Biopsy Predict Sextant Site of Cancer on Follow-Up Prostate Needle Biopsy?

JL Merrimen, G Jones, A Rocker, JR Srigley. Dalhousie University, Halifax, Canada; McMaster University, Hamilton, Canada; Mount Sinai Hospital, Toronto, Canada.

Background: Prostate needle biopsies (PNBs) are routinely performed to evaluate patients with abnormal digital rectal exams or elevations in serum prostate specific antigens. A small percentage of cases show atypical small prostatic glandular proliferations (ASAP) and in these cases a repeat biopsy is recommended which yields a cancer diagnosis in 27-42% of cases.

Design: Using a database including data from the PNBs from 12304 men who underwent initial prostate sampling during an 8 year period (May 1999- June 2007), we identified 91 men who received an ASAP diagnosis and were found to have prostate cancer on a follow-up biopsy. Extended biopsy protocol strategies were reduced to traditional sextant sites. The site of ASAP on initial biopsy and site of cancer on follow-up biopsy were compared.

Results: In our study, the median duration between initial biopsy and follow-up biopsy with cancer diagnosis was 7.9 months. There is a significant correlation between the sextant site of an ASAP diagnosis and the sextant site of cancer in 43.4% (range 33.3-50%) of cases (p=0.014).

Conclusions: The sextant site of an ASAP on initial biopsy predicts the sextant site of cancer on follow-up biopsy in a moderate percentage of cases. The optimal repeat biopsy strategy in ASAP patients includes early, complete sampling of the prostate gland but additional samples from the sextant site of the ASAP may be useful in clarifying the diagnosis in these cases.

891 Strong and Diffuse Nuclear Staining for Phospho-c-Jun Distinguishes Clear Cell Renal Cell Carcinoma from Its Mimickers.

ET Miller, MB Rettig, CE Magyar, J Huang. UCLA David Geffen School of Medicine, Los Angeles, CA.

Background: Classification of renal epithelial tumors continues to present daily challenges to practicing pathologists as the major histologic types have overlapping architectural and cytologic features. Immunohistochemical markers have proven useful in certain cases but none is absolutely sensitive and specific. Therefore, a panel of markers is often required and novel markers are still being developed to increase our ability in the accurate classification of equivocal cases.

The loss of VHL gene function contributes to the majority of clear cell renal cell carcinomas (ccRCC). Our recent molecular study of the signaling pathway reveals that loss of VHL function results in hyper-phosphorylation of c-Jun. As a commercial anti-p-c-Jun antibody works well in paraffin-embedded tissue sections, we studied its utility in distinguishing the major histologic types of renal epithelial tumors.

Design: We selected from archival files 20 cases of ccRCC, 20 cases of chromophobe RCC (chRCC), 20 cases of oncocytoma, and 6 cases of papillary type I RCC (pRCC). One representative section from each case was stained with an anti-p-c-Jun antibody (Cell Signaling Technology, #9261, used at 1:30) which gives a nuclear staining pattern in positive cells. Five random fields on each slide were manually scored for staining intensity (0 to 3+) and percentage of positive cells. The two parameters were multiplied to arrive at a final staining score ranging from 0 to 300. One way ANOVA test was used to compare the mean staining scores between ccRCC and other tumor types.

Results: As expected from the results of our molecular analysis, the tumor cells of ccRCC showed diffuse and strong nuclear staining for phosphor-c-Jun, while the staining in other tumors was negative or only weakly and focally present in the periphery of the tumors adjacent to non-neoplastic kidney. The staining score was 129.3 ± 72.5 for ccRCC, 18.9 ± 36.6 for chRCC, 28.2 ± 25.9 for pRCC, and 3.3 ± 7.9 for oncocytoma. The difference between ccRCC and each of the other renal epithelial tumor types was statistically significant ($p<0.001$).

Conclusions: 1. The results of immunohistochemical study confirm those of molecular pathway study showing that loss of VHL gene function in ccRCC results in increased phosphorylation of c-Jun, a proto-oncogene and an important transcription factor.

2. Immunohistochemical study for phospho-c-Jun can be used to distinguish ccRCC from its common mimickers with high sensitivity and specificity thus has important value in the differential diagnosis of renal epithelial tumors.

892 Oxidative Damage Sensor in Atrophy and Adenocarcinoma in the Prostate.

AP Mogal, MA Watson, PA Humphrey. Washington University School of Medicine, St. Louis, MO.

Background: Chronic inflammation of long standing duration is thought to play a significant role in the pathogenesis of cancer in several organs and has been implicated as being potentially important in prostate cancer development. Proliferative inflammatory atrophy (PIA) has been proposed as a potential precursor lesion for prostate cancer. However, the precise molecular abnormalities in PIA vs carcinoma have not been fully defined. We have previously analyzed the molecular variability and differential genetic signatures within normal, atrophic, PIN and invasive carcinoma subgroups by microarray analysis. Here, we utilized an immunohistochemistry (IHC) approach to confirm expression of a biologically relevant 21 kDa protein (21kDaP), identified by differential microarray expression analysis, that plays a protective role against oxidative damage and thus, may have implications in the pathogenesis of the putative PIA to carcinoma pathway.

Design: Fifty radical prostatectomies were utilized, based on the presence of benign epithelium, atrophy, PIN, and invasive carcinoma in the same case. H&E sections were reviewed and peripheral zone non-atrophic benign epithelium (NABE, n=93), atrophy (n=93), PIN (n=34) and invasive carcinoma (n=61) lesions were selected. Different morphological subtypes of atrophy were included: simple (SA=68), simple with cyst formation (SACF=32), post atrophic hyperplasia (PAH=21), partial (P=4) and PIA (54). IHC was performed on sections from paraffin embedded tissue blocks for 21kDaP. IHC results were evaluated for proportion reactivity (% glands with positive staining), cytoplasmic vs nuclear reactivity and intensity (1+, 2+, 3+) of 21kDaP staining.

Results: 21kDaP expression was detected as follows: 92/93 atrophy, 23/61 cancer, 3/34 PIN, 57/93 NABE. All subtypes of atrophy showed heterogeneous reactivity for 21kDaP. The mean reactivity for atrophy lesions was 60% while cancer / PIN lesions showed 20% reactivity. 87/92 (94%) atrophy lesions showed strong (2+, 3+) granular cytoplasmic reactivity. By contrast, 13/23 (56%) cancer cases showed diffuse mild (1+) nuclear reactivity. NABE showed variable (1+) nuclear and cytoplasmic reactivity.

Conclusions: 21kDaP protein expression was elevated in almost all atrophy cases irrespective of morphological subtype, compared to non-atrophic benign epithelium. Our results suggest that molecular perturbations secondary to oxidative tissue damage may play a significant role in a relationship between PIA and carcinoma. Further studies are warranted to explore other genes involved in this damage process and putative progression pathway.

893 ERG-Mediated Repression of HPGD in Prostate Tumorigenesis.

A Mohamed, T Sreenath, S-H Tan, C Sun, S Shaheduzzaman, Y Hu, G Petrovics, Y Chen, D McLeod, A Dobi, S Srivastava, I Sesterhenn. Center for Prostate Disease Research, Uniformed Services University of the Health Sciences, Rockville, MD; Armed Forces Institute of Pathology, Washington, DC; Walter Reed Army Medical Center, Washington, DC.

Background: Activation of the ETS Related Gene (ERG) was originally identified in subsets of Ewing sarcomas, myeloid leukemias and, recently, in the majority of prostate cancers. Recent studies have indicated that 15-hydroxy-prostaglandin dehydrogenase (*HPGD*), a tumor suppressor, is down regulated in a majority of lung, colon, breast, and bladder cancers. However, the regulation of HPGD within the biological context of ERG expressing prostate tumors remain to be defined. The objective of this study was to evaluate effects of ERG on the prostaglandin pathway in prostate cancer.

Design: Correlation between HPGD and ERG expression was evaluated at the mRNA and protein levels in prostate cancer specimens. Small interference RNA against human ERG and HPGD were used to knock-down ERG and HPGD expressions. Functional consequences of ERG and HPGD knock-down were assessed in ERG expressing VCaP cells harboring TMPRSS2-ERG fusions.

Results: Comparison of HPGD expression in ERG positive and negative prostate tumors revealed a trend towards decreased HPGD expression. We found robust overexpression of HPGD in response to ERG knock-down in VCaP prostate tumor cells. Chromatin immunoprecipitation experiments revealed the recruitment of ERG protein to the HPGD core promoter.

Conclusions: Expression of ERG in prostate tumorigenesis may disrupt suggested tumor suppressor functions of HPGD.

894 Automated Tumor Volume Estimation Using Digitized Prostatectomy Specimens.

JP Monaco, JE Tomaszewski, A Madabhushi. Rutgers University, Piscataway, NJ; University of Pennsylvania, Philadelphia.

Background: Following prostatectomy, the prostate is sliced into histological sections (HSs) which are then analyzed to gather relevant biomarkers such as stage and grade. A promising potential biomarker is tumor volume (TV), which has been shown in some studies to be an independent predictor of recurrence. Unfortunately, the time-consuming nature of assessing TV precludes it from clinical practice. Additionally, the lack of a standard means for measuring TV has resulted in articles both extolling and challenging its prognostic value. For TV to have clinical utility, pathologists require a rapid means for accurately measuring it. Accordingly, we introduce an algorithm that automatically detects the spatial extent of cancerous regions in digitized prostatectomy specimens, providing a means for assessing TV.

Design: The algorithm proceeds as follows: Step 1) The glands are identified and segmented (Figures 1(b) and 1(c)). Step 2) Morphological features are extracted from the segmented boundaries. Step 3) A Markov Random Field based classifier labels each gland as either malignant or benign. The blue dots in Figure 1(d) indicate the centroids of those glands classified as malignant. Step 4) The cancerous glands are consolidated into regions (red polygons in Figure 1(d)). Having determining the cancerous regions, measuring tumor volume becomes trivial.

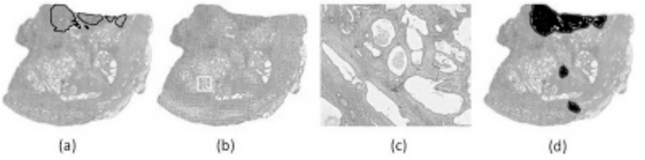

Figure1

Results: Figure 2 plots a receiver operator characteristic (ROC) curve indicating the performance (with respect to the area of CaP identified) of our cancer detection system over 40 HSs from 20 patients. Note that at a senstivity of 88% the specificity is 90%. The area under the ROC curve is 0.93.

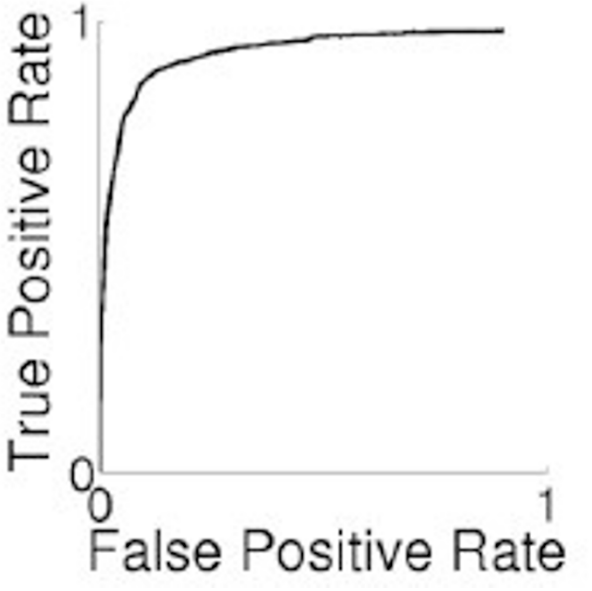

Figure2

Conclusions: We introduced an algorithm for automatically measuring TV from prostatectomy specimens. This algorithm could facilitate a large-scale investigation of the prognostic value of TV.

895 Chromosomal Imbalances Identify Pathways Associated with Resistance to Antiangiogenic Therapy in Clear Cell Renal Cell Carcinoma.

FA Monzon, K Alvarez, L Peterson, K Sircar, P Tamboli, E Jonasch. The Methodist Hospital, Houston, TX; The Methodist Hospital Research Institute, Houston, TX; MD Anderson Cancer Center, Houston, TX.

Background: Antiangiogenic agents are used to treat metastatic clear cell renal cell carcinoma (ccRCC). Currently there are no biomarkers of therapeutic efficacy with these agents. We have previously shown that chromosome copy number alterations are associated with poor (14q loss) or more favorable outcomes (5q31-ter gain). In this study, we evaluated candidate genes that might be responsible for therapeutic resistance in metastatic ccRCC (mRCC). The genes evaluated were miR-143, an anti-oncomir located in 5q; and HIF-1alpha (HIF1A), a proangiogenic molecule located in 14q and often deregulated in ccRCC.

Design: We obtained archival FFPE tumor specimens from 56 patients with mRCC treated with sorafenib (after tumor removal) or bevacizumab (neoadjuvant treatment). DNA from the FFPE blocks was analyzed with Affymetrix 250K Nsp SNP microarrays. We identified the presence of genomic imbalances and loss of heterozygosity (LOH) to obtain "virtual karyotypes". We then evaluated candidate genes in gain/lost chromosomal regions by qPCR and immunohistochemistry (IHC) in the bevacizumab treated specimens.

Results: Gain of 5q was strongly associated with longer progression free survival (PFS) in both sorafenib and bevacizumab treated cohorts (HR = 0.25, 95% CI 0.08 to 0.81, P = 0.021 and HR = 0.82 95% CI 0.65- 1, P < 0.0001 respectively). miR-143 showed higher expression in samples with 5q gain but it did not reach statistical significance (P > 0.05). In the bevacizumab cohort, 14q loss showed a significant association with worse response to treatment (CR or PR vs SD or PD, Fisher exact test, P = 0.0473). HIF1A mRNA expression was significantly reduced in specimens with loss of 14q and mRNA levels were associated with PFS (HR = 2.29, 95% CI = 1.01-5.16, P = 0.045). HIF-1alpha protein expression was also reduced in samples with 14q loss.

Conclusions: Our results show that chromosomal imbalances associated with outcomes in ccRCC lead to changes in the expression of miR-143 and HIF1A. Low HIF1A expression was strongly correlated with shorter PFS. We hypothesize that loss of 14q could lead to an imbalance in HIF-1α/HIF-2α activity, leading to increased HIF-2α and enhanced c-Myc expression, which improves tumor cell viability by altering DNA damage repair mechanisms, and by upregulating various pro-survival pathways.

896 Reflex UroVysion Testing in Abnormal Urine Cytology: Surveillance Versus Initial Evaluation.

JW Mooring, M Lowery-Nordberg, S Zhang. Louisiana State University Health Sciences Center, Shreveport, Shreveport; Feist Weiller Cancer Center, Shreveport, LA.

Background: Bladder cancer is the fourth most common cancer among men in the United States. Patients with bladder cancer require long-term surveillance for recurrence and progression, and cytoscopy and urine cytology are typically used for surveillance. However, cystoscopy often fails to detect flat tumors, and cytology has a low sensitivity for low-grade tumors. UroVysion is a FDA approved fluorescence in situ hybridization (FISH) probe set for surveillance of patients with a bladder cancer, and initial evaluation for bladder cancer in patients with urinary symptoms. However, the value of UroVysion has been under extensive debate.

Design: Cases with UroVysion testing during 2004-2009 were retrieved from the pathology database and were separated into two categories: surveillance, and initial evaluation. The follow-up histology results were retrieved.

Results: A total of 81 cases were included in this study and the cytology diagnoses were: 8 positive, 67 atypical and 6 negative. 36 cases had positive UroVysion test (44.4%, 36/81). The test was positive in 75% of positive, 41.8% of atypical, and 33.3% of cases with negative cytology. UroVysion was positive in one renal cell carcinoma and one metastatic colon carcinoma. There were 45 cases for surveillance and 36 cases for initial evaluation. The UroVysion positive rate was higher in the evaluation group (50%) than surveillance group (40%), but it was not statistically significant (p=0.33). For cases with abnormal urine cytology, UroVysion test had sensitivity, specificity, positive predicative value (PPV) and negative predicative value (NPV) 64.7%, 66.7%, 84.6% and 40% respectively.

Conclusions: The UroVysion test positive rate is slightly higher in the initial evaluation group than the surveillance group, but it is not statistically significant. For urine with abnormal cytology, UroVysion test has a good PPV (84.6%) but a poor NPV (40%). So, cases with abnormal urine cytology and negative UroVysion test should have further evaluation for possible urothelial carcinoma. Abnormal urine cytology with a positive UroVysion test has a high probability of urothelial carcinoma. The UroVysion test can also be positive in other non-urothelial lesions.

897 Immunohistochemical Study of Spermatocytic Seminoma of the Testes, with Special Reference to the Re-Assessment of C-Kit.

S Morinaga. Kitasato Institute Hospital, Tokyo, Japan.

Background: It has been believed that spermatocytic seminomas of the testes show exclusively negative reactions for immunohistochemical markers specific for classical seminomas and intratubular malignant germ cells, including c-kit, placental alkaline phosphatase (PLAP), OCT4, etc. However, a few reports contradicting this general opinion, which have demonstrated the expression of c-kit in some subsets of patients with spermatocytic seminomas, have also been published. Thus, the significance of c-kit immunohistochemistry in spermatocytic seminoma has not yet been clarified.

Design: Formalin-fixed paraffin-sections prepared from 10 patients of spermatocytic seminoma of the testes, including 1 patient from our own institution and 9 referred from other institutions, were immunohistochemically stained with 5 different commercially available antibodies against c-kit, including 2 monoclonal rabbit antibodies. In addition, the expressions of PLAP, OCT4, NANOG, D2-40, VASA and SALL4 were also simultaneously examined.

Results: Sections from seven to nine of the 10 patients showed positive staining for c-kit determined with each of the 5 antibodies to c-kit. The staining pattern was diffuse and predominant in the cell membrane. Non-neoplastic spermatogonia of the seminiferous tubules around the tumors also showed positive staining. Stainings for all of PLAP, OCT4, NANOG and D2-40 were negative in all cases. All of the 10 cases were positive for SALL4 and VASA.

Conclusions: Spermatocytic seminoma cells and non-neoplastic spermatogonia showed positive staining for c-kit with most of the currently available antibodies against c-kit. These findings could provide new insight into the histogenesis of spermatocytic seminoma.

898 Evaluation of the Epithelial Component of Stromal Tumor of Uncertain Malignant Potential (STUMP).

M Nagar, J Epstein. The Johns Hopkins Hospital, Baltimore, MD.

Background: STUMPs are rare tumors characterized by an atypical, unique stromal proliferation of the prostate. Various stromal proliferations of STUMPs have been described (degenerative atypia, cellular stroma, phyllodes, myxoid stromal predominant), however, epithelial proliferations occurring within STUMP have not been systematically described to date.

Design: We reviewed 82 cases of STUMP from our consultation service from 1990 through 2010. 18 cases without a glandular component were excluded. We next evaluated the glandular component of the remaining 64 cases of STUMP for glandular crowding and complexity, prostatic intraepithelial neoplasia (PIN), squamous metaplasia, urothelial metaplasia, basal cell hyperplasia, adenosis, and clear cell cribriform hyperplasia.

Results: Of the 64 cases of STUMP, the stromal components were as follows, degenerative atypia N=39, cellular/spindled N=16, and phyllodes N=9. In 53 cases (83%), the glandular component differed from glands on the same biopsy specimen uninvolved by STUMP. The most common abnormalities were glandular crowding in 32/64 (50%) and a very prominent basal cell layer in some glands in 32/64 (50%) cases. The next most frequent glandular variation from normal was prominent papillary infolding in 13/64 (20%). Less frequent epithelial changes within the STUMP were as followed: 8/64 (12%) showed cystically dilated glands; 6/64 (9%) had urothelial metaplasia; 6/64 (9%) had basal cell hyperplasia; 5/64 (8%) showed squamous metaplasia; 3/64 (3%) had cribriform hyperplasia; 2/64 (3%) had adenosis; and 1 case each with high grade PIN and low grade PIN. The glandular component of STUMP was histologically normal in 11 (17%) cases. There was a tendency towards urothelial and squamous metaplasia in STUMPs with a phyllodes pattern, as well as a prominent basal cell layer in STUMPs with degenerative and cellular stroma.

Conclusions: This is the first study to systematically describe the epithelial proliferations occurring in STUMP. This study suggests that within STUMPs, there is epithelial mesenchymal crosstalk as has been described in benign prostate and in prostatic carcinogenesis. In unusual cases of STUMP, the epithelial proliferation was so predominant that it masked the diagnosis of STUMP.

899 The Novel Vitamin D Analog ZK 191784 Inhibits Prostate Cancer Cell Invasion by Modulating Matrix Metalloproteinases and the Adhesion Molecule ICAM-1.

G Nesi, M Martinesi, C Treves, A Simoni, M Stio. University of Florence, Italy.

Background: Low serum levels of $1,25(OH)_2D_3$ (1,25D), thought to be the best indicator of vitamin D deficiency, have been associated with increased risk and a more aggressive biologic behavior of PCa. In this study, we examined the effects of 1,25D and its novel, low-calcemic analog ZK 191784 (ZK) on secreted matrix metalloproteinases (MMPs), as well as on the intercellular adhesion molecule-1 (ICAM-1) protein levels in human PCa cell lines LNCaP and DU-145. In order to assess the mechanisms of action of vitamin D derivatives, the expression of the vitamin D receptor (VDR) was estimated.

Design: Cells were incubated with vehicle (control), 1,25D or ZK, under serum-free conditions for 48 h. MMP-2 and MMP-9 activity was determined by gelatin zymography, while ICAM-1 and VDR levels were assessed by Western blot analysis and immunocytochemistry.

Results: 1,25D and ZK caused a marked decrease in the gelatinolytic activity of both MMP-2 and MMP-9 in DU-145 and LNCaP cell lines. Densitometric analysis showed a marked dose-dependent decrease in MMP activity compared to control, with a maximum reduction of MMP-2 and MMP-9 when ZK was used. VDR expression in cells treated with vitamin D derivatives was up-regulated over control. Contrariwise, ICAM-1 was down-regulated in the cells incubated with 1,25D or ZK.

Conclusions: These results support the possibility that vitamin D-based therapies may be beneficial in the prevention and management of advanced PCa.

900 Splicing Variants of Carbonic Anhydrase IX in Bladder Cancer and Urine Sediments.

G Nesi, F Malentacchi, S Vinci, D Villari, C Selli, C Orlando. University of Florence, Italy; University of Pisa, Italy.

Background: In human cancers, carbonic anhydrase IX (CAIX) influences cell proliferation and tumor progression, maintaining intracellular and extracellular pH under hypoxic conditions. An alternative CAIX isoform, lacking exons 8-9 (AS) and independent from the levels of hypoxia, was recently demonstrated in cancer cells. AS-CAIX competes with the full-length (FL) isoform in the regulation of extracellular pH, in a mainly mild hypoxic status. In the present study we evaluated mRNA expression of the two CAIX isoforms and their clinical relevance in bladder carcinomas and urine sediments.

Design: We measured mRNA expression of FL- and AS-CAIX isoforms in tumor tissues and benign mucosa from 45 patients with urothelial carcinoma of the urinary bladder. The expression of the two isoforms was also measured in the urine sediment of 81 bladder cancer patients and 93 control subjects.

Results: Expression of FL-CAIX mRNA was lower than AS-CAIX in benign mucosa ($p=0.006$) whereas in paired bladder cancers FL-CAIX mRNA was higher ($p=0.007$). Consequently, the percentage of FL-CAIX in bladder cancers (median: 62.6%) was significantly higher than in benign mucosa (15.0%) ($p<0.0001$). In the urinary sediments of bladder cancer patients, FL-CAIX mRNA was significantly higher in comparison to normal controls ($p=0.003$). FL-CAIX percentage appeared dramatically higher in urine sediments of bladder cancer patients (64.5%) in comparison to controls (7.5%) ($p<0.0001$). In addition FL-CAIX% was significantly different in sediments from pTa-pT1 and ≥pT2 patients (51.5% and 91.7%, respectively) ($p=0.016$). Stratification according tumor grade indicated that FL-CAIX% was significantly reduced in low-grade urothelial papillary carcinomas (33.3%) in comparison to high-grade (88.6%) ($p=0.005$) The clinical sensitivity for FL-CAIX% in urine sediments was 0.93, with a 0.76 specificity. Using the same cut-off, positive predictive value was 0.78, whereas negative predictive value was 0.93.

Conclusions: Our results seem to indicate that, in bladder cancers and related urine sediments, FL-CAIX is the prevalent and most accurate, clinically relevant variant surrogate of hypoxic stress.

901 Human Papillomavirus and Non-Muscle Invasive Urothelial Bladder Cancer: Potential Relationship from a Pilot Study.

G Nesi, T Cai, S Mazzoli, P Geppetti, R Bartoletti. University of Florence, Italy; Santa Chiara Hospital, Trento, Italy; Santa Maria Annunziata Hospital, Florence, Italy.

Background: Although the association between High-Risk Human Papilloma Viruses (HR-HPV) and urothelial bladder carcinoma has been extensively investigated, data on the role of HPV in bladder carcinogenesis are controversial. The aim of the present study was to assess the potential relationship between the presence of HR-HPV and non-muscle invasive urothelial bladder cancer (NMIBC).

Design: A total of 137 subjects (78 patients affected by NMIBC and 59 controls) were recruited in this prospective study. HR-HPV DNA was evaluated both in urine and tumour tissue. Data from patients were compared with data from controls. The difference between patients and controls in terms of the presence of HR-HPV was estimated. The association between pathological findings and the presence of HR-HPV in the patient group was analysed.

Results: HR-HPV DNA was found in 27 of 78 (34.6%) tumour samples and in 6 of 59 (10.1%) specimens from TUR-P, with a statistically significant difference ($p=0.0009$; dF=1; Chi square=10.98). HR-HPV DNA in urine was found in 36 of 78 (46.1%) patient samples, but in only 8 of 59 (13.5%) control samples ($p<0.0001$: dF=1; Chi square=16.37). A statistical significant difference in terms of HR-HPV frequency between high-grade and low-grade urothelial bladder cancer was found ($p=0.032$; RR=0.52 – 95% CI 0.27-0.93; OR=0.34 – 95% CI 0.13-0.90).

Conclusions: This study highlights the correlation between urothelial bladder cancer and HPV infection, suggesting that HR-HPV may play an aetiological role in the development of urothelial bladder cancer.

902 The Diagnostic Utility of CAIX, TTF-1 and TGB Immunopanel in the Diagnosis of Metastatic Renal Cell Carcinoma to the Thyroid.

G Netto, A Cimino-Mathews. The Johns Hopkins Hospital, Baltimore.

Background: Clear cell renal cell carcinoma (ccRCC) may occasionally present with metastatic lesions. The thyroid is not an uncommon site for metastatic RCC, where such lesion could be misinterpreted as a clear cell change in adenomatoid nodules, follicular adenomas, or parathyroid glands. PAX8 is a transcription factor expressed by thyroid and renal-lineage cells. No prior study has evaluated the diagnostic utility of PAX8 and ccRCC marker carbonic anhydrase IX (CAIX) in this setting.

Design: Twelve cases of metastatic ccRCC to the thyroid, six parathyroid glands and parathyroid adenomas with clear cell change, six papillary thyroid carcinoma, five thyroid follicularadenomas and five thyroid adenomatoid nodules with clear cell change were retrieved from our archives. All cases were assessed by standard immunohistochemistry for thyroid transcription factor-1 (TTF-1; Cell Marque), thyroglobulin (TGB; Cell Marque), PAX8 (Pharmingen) and CAIX (Bond-Lecia). Extent and intensity of nuclear or cytoplasmic immunoexpression was assessed in each sample with any labeling considered a positive result.

Results: All metastatic ccRCC were positive for PAX8 (moderate to strong, patchy or diffuse) and CAIX (strong, diffuse), and were negative for TTF-1 and TGB. All primary thyroid lesions (normal thyroid, papillary thyroid carcinomas, follicular adenomas, and adenomatoid nodules) labeled strongly and diffusely for TTF-1, TGB and PAX8 and were negative for CAIX. Parathyroid tissue and adenomas were all negative for TTF-1, TBG, PAX8 and CAIX.

Immunostaining pattern of clear cell RCC and primary thyroid lesions

		TTF-1	TGB	PAX8	CAIX
	Number	% Positive	% Positive	% Positive	% Positive
Metastatic clear cell RCC	12	0%	0%	100%	100%
Follicular Adenoma	5	100%	100%	100%	0%
Adenomatoid Nodule	5	100%	100%	100%	0%
Papillary Thyroid Carcinoma	6	100%	100%	100%	0%
Parathyroid gland and adenoma	6	0%	0%	0%	0%
Non-neoplastic Thyroid Tissue	34	100%	100%	100%	0%

Conclusions: An immunoprofile of **"TTF1(-)/TGB(-)/CAIX(+)"** was 100% sensitive and specific for metastatic ccRCC to thyroid. The reverse profile **"TTF1(+)/TGB(+)/CAIX(-)"** supported a primary thyroid lesion. As expected, immunostaining with PAX8 is not helpful in distinguishing between metastatic ccRCC and primary thyroid lesions.

903 ERG Protein IHC Expression as an Alternative Methodology for Evaluation of *ERG* Fusion Status in Prostate Adenocarcinoma.

GJ Netto, R Albadine, A Chaux, A Toubaji, J Hicks, A Meeker, AM Demarzo. Johns Hopkins Medical Institution, baltimore.

Background: We previously demonstrated the presence of *TMPRSS2-ERG* gene fusions in 46% of prostatic adenocarcinomas in a large cohort, using a break-apart fluorescence in situ hybridization (FISH) technique. In the current study, we assess expression of ERG fusion protein product using immumonhistochemistry (IHC) and correlate it with our previous FISH findings in the same cohort.

Design: The cohort consisted of 10 TMAs containing paired tumor and normal tissues from radical prostatectomies (RRP) performed at our hospital between 1993 and 2001. They included 441 cases. IHC was performed using a commercial rabbit anti-ERG monoclonal antibody (clone EPR 3864; Epitomics, Burlingame, CA), FISH analysis was previously performed using break-apart probes for 5' and 3' regions of *ERG* (Albadine, et al 2009). An IHC score (H score =intensity X percentage of positives cells) was assigned in each spot and averaged per tumor spots. When comparing fusion status by FISH and IHC techniques, any positive ERG expression on IHC was considered positive.

Results: ERG protein immunoexpression was detected in 202/441/ (46%) PCa and none of the paired benign prostate samples.

ERG expression by IHC vs ERG fusion by FISH in large cohort of prostatic adenocarcinoma

	No. cases	ERG =0 (%)	ERG>0 (%)	P value
Fusion by ERG split				<0.00001
Absent	327	219 (67.0)	108 (33.0)	
Present	114	18 (15.8)	96 (84.2)	
Fusion by ERG deletion				<0.00001
Absent	271	215 (79.3)	56 (20.7)	
Present	170	22 (12.9)	148 (87.1)	
ERG fusion				<0.00001
Absent	239	211 (88.3)	28 (11.7)	
Present	202	26 (12.9)	176 (87.1)	

Conclusions: We were able to demonstrate ERG fusion protein expression in 46% of prostate adenocarcinoma using EPR 3864 monoclonal anti-ERG antibody. A strong correlation between *ERG* rearrangement status by FISH and positive IHC expression of ERG fusion protein product is demonstrated. ERG protein IHC expression may offer an accurate alternative for evaluation of *ERG* fusion status in PCa. The significance and underlying mechanisms of our finding of a subset of tumors with discrepant ERG protein expression /*TMPRSS2-ERG* fusion status (IHC positive/FISH negative) warrants further investigation.

904 Frozen Section (FS) Evaluation of Margins in Radical Prostatectomy Specimens.

A Nunez, F Mukhtar, V Dailey, R El-Galley, O Hameed. University of Alabama at Birmingham.

Background: Intraoperative consultation during radical prostatectomy is sometimes performed to evaluate for the presence of adenocarcinoma ± benign prostatic glands at

surgical margins. However, the utility of routine FS analysis for this indication remains controversial as the literature shows mixed results.
Design: A retrospective search was conducted at our institution to identify all radical prostatectomy cases evaluated by FS over a 5-year period. Excluding those performed for lymph node evaluation, the original FSs and the corresponding permanent sections were reviewed to determine the presence/absence of prostatic adenocarcinoma and benign prostatic glands. Histological review of the remaining sections was used to determine the final margin status of the entire prostate gland.
Results: During the study period, 71/575 (12.3%) cases underwent FS evaluation of margins generating 192 individual FSs (range, 1-10/case; mean, 2.65±0.25). These FSs were labeled as from the bladder neck/base (90), posterolateral/neurovascular bundle (71), apex/distal urethra (20), or seminal vesicles (11). Eight FSs were diagnosed as atypical or suspicious because of significant freezing, crushing and/or thermal artifacts, 11 as positive for carcinoma, and the remaining 173 as benign, including 2 that had carcinomatous glands show up on permanent sections. This resulted in a sensitivity of 85%, specificity of 100%, positive predictive value (PV) of 100%, negative PV of 99% and accuracy of 99%. When the final margin status was considered as the gold standard, the sensitivity dropped to 71%, the negative PV to 87% and the accuracy to 81%. The mean number of FSs in cases with positive final margin(s) was not significantly different from that in cases with negative margins (3.1 vs. 2.5; P=.3). Benign prostatic glands were identified in 50 (27%) FSs, most frequently in those from the bladder neck/base (37/90); 41%) followed by those from the apex/distal urethra (8/20; 40%), seminal vesicle (1/11; 9%) and posterolateral/neurovascular bundle (4/71; 6%).
Conclusions: Evaluation of margins by FS in radical prostatectomy specimens is quite specific for the diagnosis of adenocarcinoma; however, potential histological artifacts and a lower sensitivity, especially for the prediction of final margin status, somewhat limit its diagnostic utility. Accordingly, only judicious use is recommended. Although a significant proportion of FSs harbor benign prostatic glands, the value of additional resection following such a finding in decreasing the risk of biochemical failure is yet to be determined.

905 Intravenous pT3 Renal Cell Carcinoma: The Challenge of Gross Recognition.

KO Ojemakinde, CX Zhao, A Bhalodia, SM Bonsib. Louisiana State University Health Sciences Center, Shreveport.

Background: Extrarenal extension of renal cell carcinoma (RCC) is usually by intravenous (IV) routes, renal sinus veins (SV), main renal vein (MRV) or retrograde into cortical veins (CV). Determination of primary tumor (PT) size requires distinguishing renal-limited disease from IV extension. This study examines the accuracy of gross evaluation for IV extension.
Design: Photographs of 28 RCCs with/without IV invasion were given to 10 pathologists instructed to outline PT with a pen but exclude SV, MRV, CV. These were compared to control photos marked by 2 authors (SMB and AB) who had examined all cases. Pathologists were divided into 5 faculty with 3-25 yrs. experience and 5 trainees (PGY4 residents/fellows). Correctly outlined PT were tabulated and analyzed by Fisher's exact test and p-values calculated.
Results: Twenty-eight photos marked by 10 pathologists resulted in 280 observations. All pathologists (50/50) correctly marked pT1/T2 PT. Substantial errors occurred with pT3 IV tumors with inclusion of IV tumor as PT (Fig1-correct; Fig2-IV included as PT). Only 70/230 pT3 tumors were correctly marked. Faculty correctly marked 23/130 pT3 PT. Trainees correctly marked 47/130 pT3 PT.

Distribution of the properly identified Primary Tumors.

pT-Stage	# Photograph Cases	Trainees = 5	Faculty = 5	p-Value.
pT1/2	5	100%	100%	NS
pT3-SV	5	40%	36%	1.0
pT3-SV+CV	8	35%	20%	0.21
pT3-MRV+SV	1	40%	20%	1.0
pT3-MRV+SV+CV	9	47%	11%	0.0004
Total pT3	23	40.9%	20.0%	0.0009

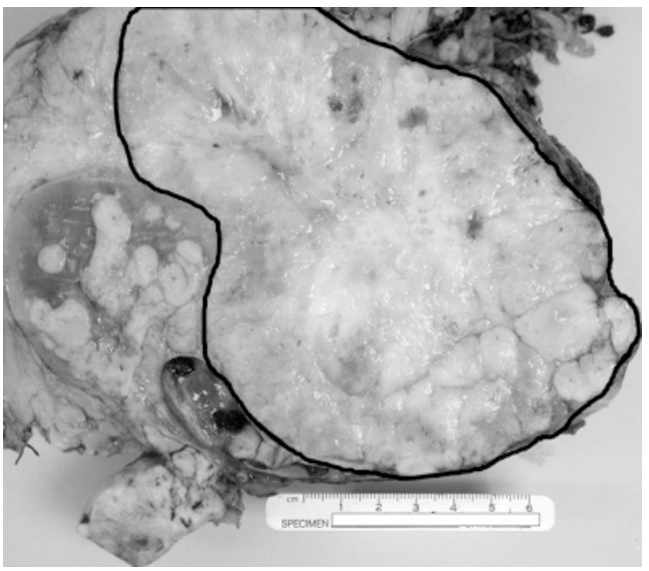

Conclusions: 1) Pathologists correctly identify pT1/2 but often misinterpret pT3 IV RCC. 2) Trainees out performed faculty attributed to training by SMB and AB. 3) Tumor size may be over estimated and pT3 tumors understaged if prosectors are not trained in recognizing IV extension. 4) The importance of tumor size is lost if inaccurate gross evaluation is widespread.

906 Biologic Significance of Axonogenesis in Prostate Cancer Measured by PGP 9.5.

A Olar, R Li, D He, D Florentin, G Ayala. Baylor College of Medicine, Houston, TX.

Background: Cancer related axonogenesis (increase in nerve density) and neurogenesis (increased number of ganglion cell bodies) is a recently described biologic phenomenon. Our previously published data showed that nerve density in prostate cancer (PCa) and the number of neurons in the parasympathetic ganglia are increased with prostate cancer (PCa) progression. Protein gene product 9.5 (PGP 9.5) is a member of the ubiquitin hydrolase family of proteins, confined to the cytoplasm of the nerves and neurons. It is a cytoplasmic neuron-specific protein structurally and immunologically distinct from neuron-specific enolase.
Design: Tissue microarrays were constructed from 435 radical prostatectomy specimens with PCa. Anti-PGP 9.5 antibodies were used to identify and quantify nerve density. Protein expression was objectively analyzed using image deconvolution, segmentation and computerized digital image analysis. Data was correlated with clinico-pathological variables and tissue biomarkers available in our database.
Results: Of all of the analyzed clinico-pathological parameters, only the lymph node status had a weak but significant positive correlation with nerve density as measured by PGP 9.5 expression (rho=0.106; p=0.0275). By Cox univariate analysis, PGP 9.5 was a predictor of time to biochemical recurrence (p=0.05). However, it was not an independent predictor of biochemical recurrence on multivariate analysis. Increased nerve density correlated with increased proliferation of PCa cells, highlighted by Ki67 (rho=0.186, p=0.0019). It also correlated positively with expression of proteins involved in survival pathways such as pAKT (rho=0.191, p=0.0015), pNFKB p536 (rho=0.217, p=0.0060), GSK2 (rho=0.152, p=0.0131), PIM2 (rho=0.198, p=0.0017), CMYC (rho=0.134, p=0.0463), SKP2 (rho=0.157, p=0.0029), SRF (rho=0.320, p=0.0000), P27 (rho=0.197, p=0.0007), and negatively with PTEN (rho=-0.178, p=0.0356). Increased nerve density correlated with increased levels of hormonal regulation elements: AR (rho=0.148, p=0.0100), ER Alpha (rho=0.296, p=0.0409); and with co-regulators and repressors: SRC1 (rho=0.164, p=0.0060), TIF2 (rho=0.164, p=0.0064), AIB-1 (rho=-0.399, p=0.0392), DAX (rho=0.163, p=0.0050).
Conclusions: Increase in nerve density or axonogenesis is a recently described phenomenon of paramount importance in the biology of prostate cancer. It is implicated in the regulation of different cancer signaling pathways and is associated with high proliferation rate prostate cancer and decreased survival.

907 Semaphorin 4F Expression and Its Role in Axonogenesis and Aggressive Behavior of Prostate Cancer.

A Olar, R Le, Y Ding, D He, D Florentin, G Ayala. Baylor College of Medicine, Houston, TX.

Background: Cancer related axono-neurogenesis is a recently described biologic phenomenon. Semaphorin 4F (S4F) is a member of a family of proteins with roles in embryological axon guidance and continues to be expressed in adulthood. S4F produced by prostate cancer (PCa) cells is a key regulator of the interactions between nerves in the tumor microenvironment and cancer cells. S4F is also expressed in the reactive stroma.
Design: Tissue microarrays from 350 radical prostatectomy specimens with PCa were immunostained with antibodies against S4F developed at our institution. Slides were digitized using image deconvolution imaging and analyzed using image segmentation technology. Data was provided on a cell per cell basis (nuclear vs. cytoplasmic), per tumor compartment, per patient. Data was correlated with pertinent clinico-pathological parameters and biomarkers. Survival analysis was performed. To understand the

heterogeneity of S4F expression we used an unsupervised clustering algorithm. Each patient was represented to a row, and the expression bins were columns. Color-coding showed the percentage of cells present in each expression bin, with blue representing low % and orange high % of expressing cells.
Results: S4F expression was found in the cytoplasm and nuclei of epithelial PCa and reactive stromal cells and was increased in high grade preneoplastic lesions and PCa compared to normal epithelium. Nuclear and cytoplasmic PCa, as well as stromal S4F expression had different patterns of heterogeneity. Patients with high values of S4F in PCa cytoplasm were at significantly higher risk of biochemical recurrence, by univariate and multivariate analysis [p=0.0007, HR=7.551 (2.34-24.31)]. It was also significant for time to PCa specific death on univariate analysis. S4F cytoplasmic expression in PCa cells also correlated with nerve density in PCa (p=0.04) and perineural invasion diameter (p=0.004), corroborating evidence of S4F's involvement in PCa induced axonogenesis and perineural invasion. Significant correlations were identified with NFkB and inversely with PCa apoptosis in perineural invasion.
Conclusions: By using state of the art quantitative methods we studied S4F biomarker expression within the cancer compartments as well as within the reactive prostatic stroma. Our cumulated data demonstrates that S4F is significantly involved in human PCa progression and regulates the interaction between cancer and nerves.

908 Immunohistochemical Expression of Renal Markers in Matched Primary and Metastatic Renal Cell Carcinomas.

Z Pan, WE Grizzle, O Hameed. University of Alabama at Birmingham.
Background: The diagnosis of metastatic renal cell carcinoma (RCC) may be challenging, especially due to its broad morphologic spectrum and potential histologic mimicry of other tumors. Thus immunohistochemistry (IHC) has become an invaluable tool for the diagnosis. Recent studies, however, have found that many proteins are up- or down-regulated in metastasis and it is unknown whether this affects the utility of IHC in the diagnosis of metastatic RCC.
Design: A retrospective review was performed to identify RCCs in which materials from both primary and metastatic sites were present. After histologic review, the primary and metastatic tumors were punched (1.0 mm) in triplicate and plated on tissue microarrays. IHC was then performed with antibodies directed against the RCC antigen (RCCA), kidney-specific cadherin (KSC), carbonic anhydrase-IX (CA-IX), PAX2, and PAX8. The intensity (0-3) and percentage of positive cells (0-100%) were used to calculate the H-score for each immunostain.
Results: Our search identified 16 cases. There was significant variation (P<0.0001; paired ANOVA) in marker expression when primary and metastatic RCCs were grouped together (Fig 1) with RCCA having the lowest average H-score (P value <0.001; paired t-test). In comparing primary and metastatic tumors there was also significant variation (P<0.0001; ANOVA) with greater CA-IX, PAX2 and PAX8 expression in metastases (Fig 2). Moreover, out of 8 originally PAX8-ve tumors (H-score < 10), 7 expressed this marker in corresponding metastases. The expression of KSC was very similar in primary and metastatic RCCs, whereas a significant proportion of originally RCCA+ve tumors lost such expression in metastases (44% vs. 2% for all other markers; P<0.0001; X^2).

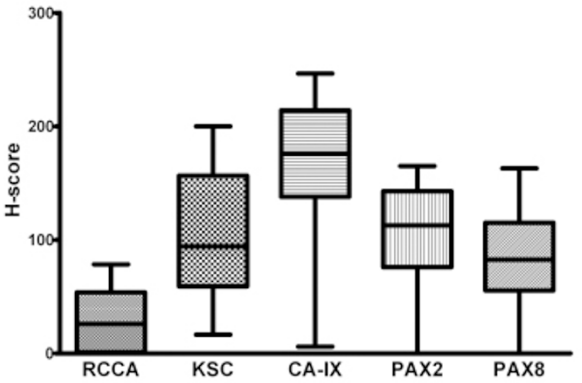

H-scores of Different Markers in Renal Cell Carcinoma

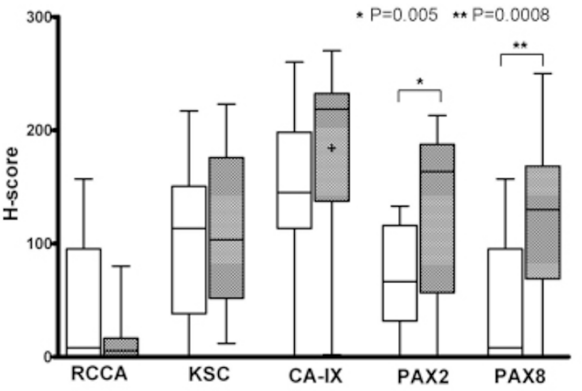

H-scores in Primary and Matched Metastatic (shaded boxes) RCCs

Conclusions: Although there is significant variation in the expression of renal markers in primary and metastatic RCC, loss of RCCA expression in metastatic lesions appears to be the only finding of potential clinical consequence.

909 Mesenchymal Neoplasm of the Penis: Clinicopathological Analysis of 19 Cases.

GP Paner, MB Amin, JY Ro, JR Srigley, DJ Grignon, DE Hansel, JD Schwartz, RE Jimenez, MB Amin. University of Chicago Hospital, IL; Cedars-Sinai Medical Center, Los Angeles, CA; Methodist Hospital, Houston, TX; Credit Valley Hospital, Mississauga, ON, Canada; Indiana University School of Medicine, Indianapolis; Cleveland Clinic, OH; William Beaumont Hospital, Royal Oak, MI; Mayo Clinic, Rochester, MN.
Background: Primary sarcomas of the penis are extremely rare and clinicopathological features of these tumors are not fully explicated.
Design: We report our experience with 19 primary mesenchymal tumors of the penis.
Results: These included 11 leiomyosarcoma (LMS), 2 epithelioid sarcoma (ES), 2 fibrosarcoma (FS), 1 low grade sarcoma, NOS, 1 angiosarcoma (AS), 1 Kaposi's sarcoma (KS), and 1 glomus tumor. Patients with LMS were 44 – 82 yrs old (mean 61 yrs). The LMSs measured 1.5 – 5 cm (mean 2.6 cm) and included 7 superficial and 4 deep tumors, the latter situated below the tunica albuginea or/and involved the corpus spongiosum. By FNLCC system, LMSs were grade 1 (1), 2 (9), and 3 (1). 1 LMS had focal epithelioid and 1 had focal rhabdoid features. 1 patient with deep grade 2 LMS presented with lung metastasis. Follow-up was available in 8 LMS patients (range 5-144 mos). 1 patient with deep grade 2 LMS had recurrence 24 mos after diagnosis and no evidence of disease (NED) 84 mos after diagnosis. 1 patient with deep grade 2 LMS died of disease (DOD) within 1 yr of diagnosis. 1 patient with deep grade 3 LMS died of other cause 5 mos after diagnosis. 4 patients with superficial grade 2 LMS had NED at 12, 36, 42, and 48 mos follow-up and 1 with superficial grade 1 LMS has NED at 144 mos follow-up. ES occurred in 54 yrs old (proximal type) and 18 yrs old (features of conventional type) that presented as penile ulceration. The 18 yr old ES patient presented with lung metastasis and DOD 5 mos after diagnosis. FS occurred in 70 yrs old (1.6 cm, deep, grade IV) and 74 yrs old (2.5 cm, deep, grade III). Follow-up in 1 showed recurrence 45 mos after diagnosis. The low grade sarcoma occurred in a 51 year old patient as a penile urethral mass and had NED 21 mos after transurethral resection. The AS occurred in 53 years old as deep penile lesion and the KS in 61 yrs old as superficial nodular phase lesion.
Conclusions: 1) Penile sarcomas present with a range of histology and are most commonly LMS. 2) Depending on the histologic subtype tumors maybe associated with poorer prognosis. 3) This series shows that aggressive behavior in penile LMSs occurred only in deep tumors, supporting the prognostic importance of the proposed histoanatomic stage.

910 Antibody-Based Detection of ERG Rearrangement-Positive Prostate Cancer.

K Park, SA Tomlins, KM Mudaliar, Y-L Chiu, R Esgueva, R Mehra, K Suleman, S Varambally, JC Brenner, T MacDonald, A Srivastava, AK Tewari, U Sathyanarayana, D Nagy, G Pestano, LP Kunju, F Demichelis, AM Chinnaiyan, MA Rubin. Weill Cornell Medical College, New York, NY; University of Michigan, Ann Arbor; Roche Group, Tucson, AZ.
Background: TMPRSS2-ERG gene fusions occur in 50% of prostate cancers and result in the over-expression of a chimeric fusion transcript that encodes a truncated ERG product. Previous attempts to detect the product have been hindered by a lack of specific antibodies.
Design: We characterize a rabbit anti-ERG monoclonal antibody (clone EPR 3864, Epitomics) using immunoblotting on prostate cancer cell lines, synthetic TMPRSS2-ERG constructs, chromatin immunoprecipitation and immunofluoresence. We correlated ERG protein expression with the presence of ERG gene rearrangements in prostate cancer tissues using a combined IHC and FISH analysis. We independently evaluated two patient cohorts and observed ERG expression confined to prostate cancer cells and high-grade prostatic intraepithelial neoplasia associated with ERG-positive cancer, as well as vessels and lymphocytes.

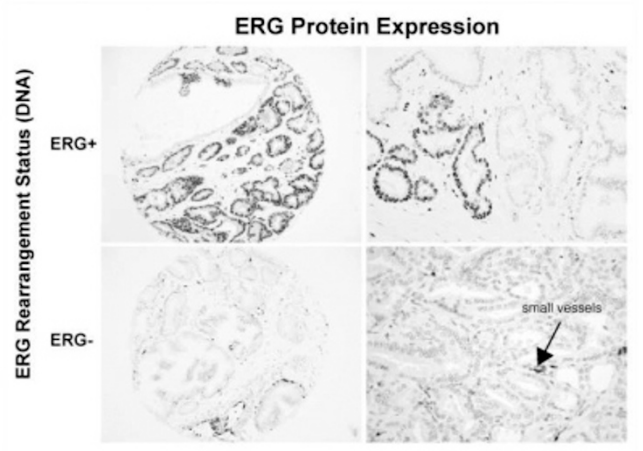

Results: Image analysis of 131 cases demonstrated nearly 100% sensitivity for detecting ERG rearrangement prostate cancer, with only 2 of 131 cases demonstrating strong ERG protein expression without any known ERG gene fusion. The combined pathology evaluation of 207 patient tumors for ERG protein expression had 95.7% sensitivity and 96.5% specificity for determining ERG rearrangement prostate cancer.
Conclusions: This study qualifies a specific anti-ERG antibody and demonstrates exquisite association between ERG gene rearrangement and ERG protein expression. Given the ease of performing IHC versus FISH, ERG protein expression may be useful for molecularly subtyping prostate cancer based on ERG rearrangement status and suggests clinical utility in prostate needle biopsy evaluation.

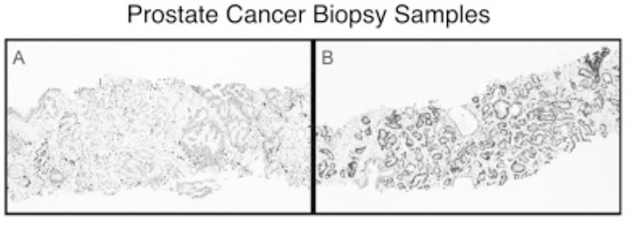

911 Discovery of Novel Drug Targets for Small Cell Prostate Cancer.
K Park, H Beltran, D Rickman, TY MacDonald, S Terry, F Demichelis, DM Nanus, MA Rubin. Weill Cornell Medical College, New York.
Background: Small cell carcinoma of the prostate is a rare but an aggressive cancer with poor prognosis. It is believed that small cell carcinoma can arise *de novo* or from existing adenocarcinoma although no molecular studies have documented this transition. We sought to better understand the molecular transformation of small cell carcinoma and identify novel drug targets.
Design: We used Next Generation RNA sequencing and oligonucleotide arrays to extensively profile small cell prostate tumors, prostate adenocarcinomas, and benign prostate tissue, and validated findings on tumors from a large cohort of patients using immunohistochemistry (IHC) and Fluorescence In Situ Hybridization (FISH).
Results: ERG rearrangement was present in 47% of small cell prostate cancer, but ERG protein expression was absent and corresponded directly with lack of androgen receptor expression. We sequenced 7 small cell prostate tumors, 30 adenocarcinomas, and 5 benign samples. We identified the cell cycle kinases, Aurora kinases A and B, as significantly overexpressed and Aurora A amplified in small cell prostate cancer compared to adenocarcinoma or benign ($p<0.001$). Evaluation of Aurora kinase expression by IHC of tumors revealed that the majority of small cell cancers (21/28) displayed strong cytoplasmic staining with Aurora A antibody and strong nuclear staining with Aurora B antibody, and IHC was positive in > 50% of tumor cells. In comparison, only 15/118 of adenocarcinoma cases had positive cytoplasmic staining with Aurora A antibody and 34/118 were positive for speckled nuclear and nuclear membrane staining with Aurora B antibody. In these cases, IHC positive cells made up less than 5% of cells. None of the 21 benign samples had Aurora kinase overexpression. FISH evaluation revealed significant copy number gain of Aurora A in 8/28 small cell cancers, 7/118 adenocarcinoma, and none of the benign cases. The small cell prostate cancer cell line and xenografts (NCI-H660), was preferentially sensitive to Aurora kinase inhibition, compared to the prostate adenocarcinoma (VCaP, LnCaP).
Conclusions: There is likely clonal origin of small cell prostate cancer from adenocarcinoma (with ERG fusion positivity seen in both), but ERG expression is limited to adenocarcinoma and driven by AR signaling. Aurora kinase A and B are significantly overexpressed, and Aurora A is amplified, in small cell prostate cancer compared to adenocarcinoma and benign prostate. In vitro and in vivo data confirms that these are novel drug targets for small cell prostate cancer.

912 Towards the Development of a Multiplex Prostate Cancer Specific Biomarker.
K Park, S Banerjee, F Demichelis, MA Rubin. Weill Cornell Medical College, New York.
Background: Trefoil factor 3 (TFF3), polypeptides secreted by normal human intestinal mucosa, is associated with various cancers and found to be over-expressed in a subset of prostate cancers. Previous work suggests that the common TMPRSS2-ERG fusion can down-regulate TFF3 expression in hormone-naïve prostate cancer. Given this inverse expression relationship, we wanted to test if a combined marker could serve as a prostate cancer specific biomarker.
Design: Double staining with immunohistochemistry (IHC) produced protein expression data of nuclear ERG and cytoplasmic TFF3 on a tissue microarray composed of cases with known mRNA expression data generated by Next Generation RNA sequencing (RNA-Seq).
Results: 41% of the cases had positive nuclear staining for ERG and 71 % had positive cytoplasmic staining for TFF3 with more than 50% of the cells. Out of 63 cases, 13 had both ERG and TFF3 staining in the same cancer cells with inversely correlated intensities ($p=0.00827$, Generalized Fisher test). The relationship between ERG and TFF3 expression was confirmed by ERG gene rearrangement status with FISH ($p=2.6e-05$, Fisher's test). Out of 34 tumors without ERG gene rearrangement, 22 had moderate or strong TFF3 expression. 21 out of 23 ERG rearranged tumors had no or weak TFF3 expression. It was 18 times more likely to have high TFF3 protein expression in tumors without ERG rearrangement. 7% of the cases had neither ERG gene rearrangement (4/57) nor ERG/TFF3 protein expression (5/63). When the protein expression was compared to mRNA transcript level, there was a linear correlation for both ERG ($p=0.004$) and TFF3 ($p=3.8e-06$). 6 tumor cases had matching benign tissues: 3 had weak and focal (less than 10% of the cells) positivity with TFF3 IHC.
Conclusions: This study demonstrates that the protein expression of ERG and TFF3 corresponds to the mRNA expression. 92% of tumors had over-expression of either ERG or TFF3 so the feasibility of combining ERG and TFF3 as biomarker for primary prostate cancer should be further explored.

913 Subtyping of Papillary Renal Cell Carcinoma (PRC) by Fine Needle Aspiration (FNA): A Reliable Approach To Providing Valuable Prognostic Information.
GE Parks, SJ Sirintrapun, KR Geisinger. Wake Forest University School of Medicine, Winston-Salem, NC.
Background: Studies have shown prognostic value in the subclassification of PRC. Type 1 has papillae with single layers of small cells with minimal cytoplasm, and type 2 has papillae lined by cells with ample, eosinophilic cytoplasm. Poor prognosis has been associated with high stage, high nuclear grade, subtype 2, absence of foam cells, and abundant fibrous stroma. Histologic subtyping and recognition of high grade features on FNAs thus provides valuable and immediate prognostic information. While the features of PRC in FNAs have been described, little has been done to determine whether subtyping or grading may be possible on FNA alone. In many cases, corresponding core needle biopsy (CB) or cell block material may not be obtained.
Design: Case files were searched from 2000 – 2010 for renal FNAs with the diagnosis PRC; 65 cases were identified, 43 had corresponding CBs, with 24 available for review. The FNA (DiffQuick and Papanicolau-stained) was reviewed by a cytopathologist, and CBs by a genitourinary pathologist in an independent, blinded review. Each case was evaluated for subtype (1-2), nuclear grade (1-4), and high vs. low grade.
Results: CB and FNA were identified with type 1 (upper panels), and type 2 features (lower panels).

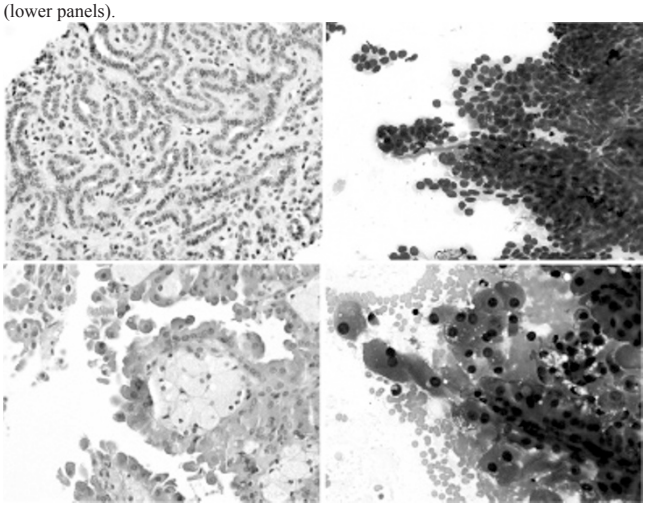

Nine CB (36 %) were found to be type 2. The sensitivity and specificity for type 2 on FNA were 66.7% and 93.3% respectively. When nuclear grades were grouped as high (3 & 4) and low (1 & 2), the sensitivity and specificity for high grade features on FNA were 100% and 83.3% respectively. Good correlation was observed with quantitative (1-4) grading as well: in 70.8% of cases the nuclear grade was an exact match, and in 20.8% of cases the grade on FNA was higher (four cases higher by one, one case higher by 2). There were only two cases (8.3%) in which grade on FNA was lower than that determined with the CB.
Conclusions: Based on a limited sample set, recognition of histologic subtype 2

and high grade features in FNAs of PRC is possible, reliable, and provides valuable, rapid prognostic information. These initial findings suggest that a larger study may be informative, and that FNAs of PRC have value complementary to CB.

914 Total Submission of Pelvic Lymphadenectomies Performed at Radical Prostatectomy Increases Lymph Node Yields and Detection of Microscopic Metastases.

JL Perry-Keene, H Samaratunga, V Vyas, B Delahunt. Royal Brisbane and Women's Hospital, Brisbane, QLD, Australia; Aquesta Pathology, Brisbane, QLD, Australia; Wellington School of Medicine and Health Science, University of Otago, Wellington, New Zealand.

Background: Lymph node metastasis in prostate cancer is associated with poor prognosis, being indicative of stage 4 disease. Studies indicate up to a median of 16 lymph nodes are identified in pelvic lymphadenectomies, while a minimum of 13 nodes is required to accurately identify lymph node metastases. The 2009 ISUP consensus conference found less than 10% of respondents detected more than 10 lymph nodes per case, although only 41% blocked the entire specimen, including fat. Currently there is no consensus as to the optimal handling of lymphadenectomy specimens received with radical prostatectomies.

Design: 110 consecutive radical prostatectomies with pelvic lymph node sampling were examined. All tissue from the lymphadenectomies was submitted with macroscopically palpable lymph nodes blocked separately. The following parameters were recorded: number of macroscopically identified palpable lymph nodes, number of microscopically identified impalpable lymph nodes, number of blocks submitted, number of nodes involved by metastatic adenocarcinoma, size of metastasis and whether the involved node was palpable or impalpable.

Results: As shown in figure 1, submission of all tissue from pelvic lymphadenectomy specimens increased the lymph node yield from an average of 3.75 to 10.8 lymph nodes. Metastatic prostate cancer was identified in 8 of 110 cases (7.3%). 5 (63%) of the metastases were identified in palpable lymph nodes alone. In two cases, metastases were identified in both palpable and impalpable lymph nodes. In one case, the metastasis was identified in an impalpable lymph node only.

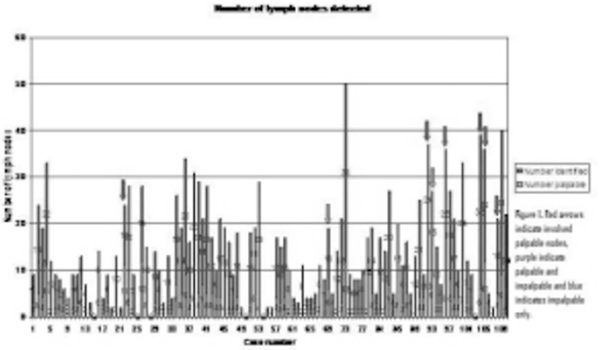

Conclusions: Submission of all tissue from pelvic lymphadenectomies markedly improved lymph node yields and facilitated identification of macroscopically undetectable lymph nodes, some of which were demonstrated to contain metastases. We conclude that submission of the complete lymphadectomy specimen improves staging accuracy and prognostication.

915 Renal Small Cell Oncocytoma with Pseudosettes – A Histomorphologic, Immunohistochemical, Ultrastructural and Molecular Genetic Study of 10 Cases.

FB Petersson, T Vanecek, M Michal, N Kuroda, M Hora, O Hes. Charles University and University Hospital, Plzen, Czech Republic; National University Health System, Singapore, Singapore; Red Cross Hospital, Kochi, Japan.

Background: A clinicopathological characterization of a rare subtype of renal oncocytoma (RO), the small cell oncocytoma with pseudorosettes (SCOP) is presented. This subset of SCO may present differential diagnostic problems, especially on core biopsies.

Design: 10 cases of SCOP were identified out of 391 ROs from our registry. Detailed morphologic immunohistochemical studies and molecular genetic (FISH and CGH) analyses were performed.

Results: The cohort comprised of 6 females and 4 males, age 51 to 84 years. The tumors were composed of small basophilic cells ("oncoblasts") with scant cytoplasm and monomorphic nuclei. No necrosis or mitotic activity were discerned. In all cases, a varying number of pseudorosettes were identified. The pseudorosettes were composed of small globules of (PAS-positive) hyaline basal membrane-like material surrounded by small oncoblastic cells. The immunohistochemical profile of the neoplastic cells was: positivity for AE1-3 (10/10), EMA (10/10), c-kit (6/10), MIA, Pax 2 (9/10), AMACR (6/10), CD10 (5/10), parvalbumin (8/10), claudin 7 (10/10) and claudin 8 (3/10). No immunoreactivity for carbonic anhydrase IX, HMB-45, S100A1, TFE3. Using CGH, no chromosomal changes were identified in 3 examined cases. No numerical changes of chromosomes 7 and 17 were revealed on FISH analysis.

Conclusions: 1, SCOP constitute a morphologically homogenous subset of tumors group within SCOs. 2, The immunohistochemical profile of SCOP was variable and differed in significant respects from that of conventional renal oncocytoma. 3, No genetic abnormalities were detected on CGH analysis. 4, All tumors behaved in a benign fashion.

916 Renal Translocation t(6;11) Carcinoma: A Study on 5 Cases Using Histomorphology, Immunohistochemistry, Ultrastructure and Molecular Genetic Techniques.

FB Petersson, T Vanecek, M Michal, G Martignoni, M Brunelli, D Spagnolo, N Kuroda, X Yang, I Alvarado Cabrero, M Hora, O Hes. Charles University and University Hospital, Plzen, Czech Republic; National University Health System, Singapore, Singapore; University of Verona, Italy; PathWest Laboratory Medicine WA, Nedlands, Australia; Red Cross Hospital, Kochi, Japan; North West University Chicago, IL; Centro Medico, Mexico City, Mexico.

Background: To date, only few cases of "rosette forming t(6;11), HMB45 positive renal carcinoma" have been published. In this paper we contribute further data on 5 cases.

Design: All cases were examined histologically and immunohistochemically. In 3 cases ultrastructural studies were performed. Molecular genetic studies using aCGH, RT- PCR and FISH were employed on 3 cases where fresh tissue was available.

Results: Patients were 4 females and 1 male, age range 20 to 39 years. Follow up (range 3-5 years) did not reveal any metastatic events or recurrences. All tumors were mostly encapsulated. No necrosis was seen. Tumors displayed a solid or solid/alveolar architecture and contained (occasionally long and branching) tubular structures composed of dyscohesive neoplastic cells and, more frequently, pseudorosettes. 5/5 cases displayed focal immunoreactivity for HMB-45, Cathepsin K. Melan A and MiTF was positive in 3/5 cases, respectively. Tyrosinase and vimentin positivity was found in 4/4 cases, respectively. Cytokeratins and CD10 were positive in 4/5 cases, respectively. On ultrastructural examination, numerous electron-dense secretory granules resembling melanosomes were present in the cytoplasm. Psedorosettes were composed of reduplicated basement membrane-like material. aCGH revealed multiple chromosomal changes, especially losses. In 2/3 cases there was loss of chromosome 22. Using RT-PCR, 2/3 tumors were positive for theAlpha -TFEB-fusion transript. No *VHL* mutation, LOH 3p, or promotor methylation of the *VHL* gene was found in 2 cases studied.

Conclusions: 1, "rosette forming t(6;11), HMB45 positive renal carcinoma" displays some morphologic heterogenity, e.g. characteristic pseudorosettes are not always conspicuous. 2, Immunoreactivity for HMB-45 (but not Melan A or MitF) and Cathepsin K appears to be constant finding and expression of cytokeratins is a frequent finding. 3, Loss of chromosome 22 was the most common numerical aberration, no mutation of the *VHL*-gene or LOH 3p were present. 4, All cases appear to pursue a benign clinical course.

917 *TMPRSS2:ERG* Rearrangement and Markers of Metabolic Signaling Pathways Implicated in Prostate Carcinogenesis.

A Pettersson, R Flavin, J Stark, M Fiorentino, M Pollak, K Penney, HD Sesso, M Gleave, TA Bismar, S Perner, S Finn, MA Rubin, J Ma, E Giovannucci, M Stampfer, P Kantoff, M Loda, L Mucci. Dana Farber/Harvard Cancer Center, Boston, MA.

Background: The common gene fusion *TMPRSS2:ERG* may act in concert with other key molecular events in the initiation and progression of prostate cancer. We examined if perturbation of metabolic signaling pathways, including expression of the Insulin receptor (IR), IGF-1 receptor (IGF1R), Adiponectin receptor 2 (AdipoR2), and fatty acid synthase (FASN), is associated with *TMPRSS2:ERG* rearrangements.

Design: We studied 392 men with prostate cancer. *TMPRSS2:ERG* status, by chromosomal translocation or intronic deletion, was assessed by an *ERG* break-apart FISH assay on tissue microarrays. Protein expression of IR, IGF1R, AdipoR2 (manual assessment), and FASN (semi-automated assessment) was evaluated by immunohistochemistry. We used the Wilcoxon rank-sum test to assess the differences in intensity of expression of these biomarkers among rearrangement positive versus negative tumors.

Results: In total, 40% of the tumors were rearrangement positive, with two-thirds occurring through deletion. Tumors harboring the *ERG* rearrangement had higher protein tumor expression of IR (P<0.001), IGF1R (P<0.001), AdipoR2 (P=0.03) (Figure 1), and FASN (P=0.009) (Figure 2). All these associations were more pronounced for rearrangement through deletion. There were no alterations in expression of these markers noted in the adjacent normal in rearrangement positive versus negative tumors.

Conclusions: *TMPRSS2:ERG* rearrangement is associated with upregulation of the IR, IGF1R, AdipoR2, and FASN. These observations suggest that *TMPRSS2:ERG* rearrangement, particularly through deletion, is associated with altered metabolic signaling pathways implicated in prostate carcinogenesis.

* Shared senior authorship

Figure 1. Protein tumor expression of IGF-1 receptor (IGF1R), Insulin receptor (IR), and Adiponectin receptor 2 (AdipoR2) by *TMPRSS2:ERG* fusion status

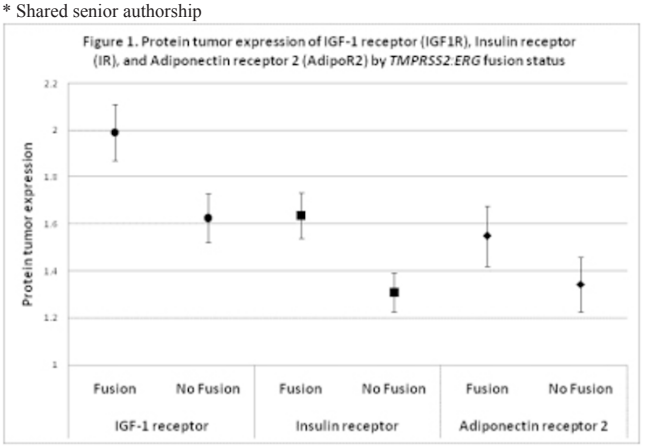

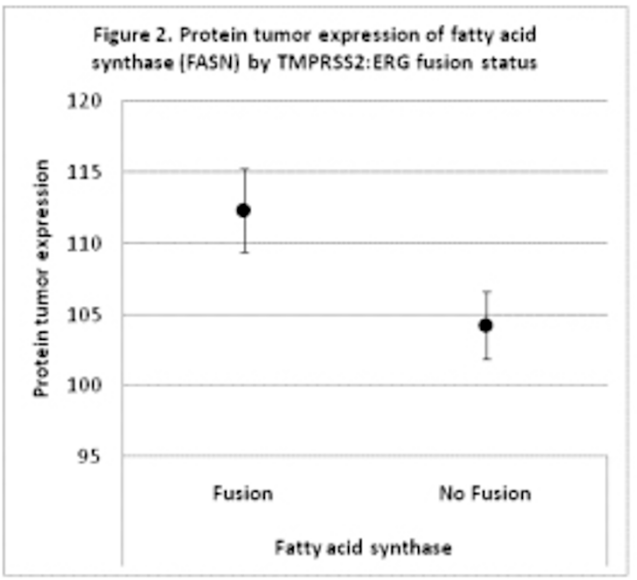

918 Comparison of the Pathologic Spectrum of Neoplasia in Autosomal Dominant Polycystic Kidney Disease (ADPKD) and Acquired Cystic Kidney Disease in End-Stage Renal Disease (ACKD-ESRD).

MM Picken, V Mehta. Loyola University Medical Center, Maywood, IL.

Background: ACKD-ESRD and ADPKD are characterized by the development of multiple cysts in the kidneys. The development of renal cell carcinoma (RCC) is a recognized risk factor in ACKD-ESRD and patients are therefore subjected to active surveillance. In contrast, the risk of RCC in ADPKD is perceived to be small and not warranting surveillance. The objective of this study was to compare and contrast the pathologic spectrum of neoplasia as seen in ACKD-ESRD versus ADPKD versus the general population.

Design: We reviewed, retrospectively, all the nephrectomies performed in our department between 1985 and 2010 in patients with ADPKD and ACKD-ESRD. We compared the incidence and types of tumors encountered in ADPKD and ACKD-ESRD, and compared the results with published epidemiological data.

Results: 43 patients (19M/23F) with ADPKD underwent 73 nephrectomies; in 7/42, both kidneys were removed but not simultaneously. Mean age was 50.3 years (range, 31-71years). A review of the pathology revealed that 4 nephrectomies contained malignant tumors (prevalence = 5.4%). The histological subtype of the cancers was as follows: 3/4 clear cell RCC and 1/4 papillary RCC. All carcinomas were seen in males. Of 73 kidneys, 13 (17%) showed benign tumors: papillary adenomas (8), cystic nephroma (2), angiomyolipoma (1), and mixed epithelial and stromal tumor of the kidney (2). Eighty patients with ACKD-ESRD (44 males and 36 females) underwent 97 nephrectomies. Renal cell carcinoma was seen in 32 patients (25 males and 7 females), prevalence = 40%. The histological subtype of the cancers was as follows: clear cell RCC 50% (16/32), papillary RCC 21.8% (7/32), acquired cystic disease-associated RCC 21.8% (7/32), sarcomatoid RCC 3.1% (1/32), and chromophobe RCC 3.1% (1/32). Benign tumors were also identified as follows: Papillary adenomas in 17, cystic nephroma in 2, oncocytoma in 1 and collecting duct adenoma in 1 case.

Conclusions: Renal cell carcinoma arising in the setting of ADPKD as well as ACKD-ESRD is much more common in males. While, among neoplasms arising in ACKD-ESRD, there are tumors that are unique to this condition, tumors arising in APKD are similar to those seen in the general population; this includes both malignant and rarer, benign entities. While the risk of malignancy in ADPKD is smaller than in ACDK-ESRD, it is nevertheless 10x higher than in the general population. In both groups (ADPKD and ACKD-ESRD) the pts with RCC are a decade younger than the median age of pts with RCC in the general population.

919 Calcium Oxalate Crystals Are Present in Acquired Cystic Kidney Disease in End-Stage Renal Disease (ACKD-ESRD) but Not in Autosomal Dominant Polycystic Kidney Disease (ADPKD) – Does This Signify a Role in Cancer Development?

MM Picken, V Mehta. Loyola University Medical Center, Maywood, IL.

Background: In both ACKD-ESRD and ADPKD, numerous cysts develop and renal failure ensues. When compared with the general population, in ACKD-ESRD there is a 100-fold increase in renal cancer risk, while in ADPKD the risk is much lower. The pathogenesis of malignancy in ACKD-ESRD is not well understood, but certain cancers that are unique to ACKD-ESRD are associated with calcium oxalate crystals. Hence, their presence has been implicated in the pathogenesis of these cancers. The aim of this study was to asses the prevalence of calcium oxalate crystals in nephrectomies from patients with ACKD-ESRD versus ADPKD.

Design: We reviewed, retrospectively, all the nephrectomies performed in our department between 1985 and 2010 in patients with ADPKD and ACKD-ESRD. We compared the pathology of tumors in ADPKD and in ACKD-ESRD and evaluated the specimens for the presence or absence of calcium deposits. In H&E slides, calcium oxalate crystals were identified under polarized light, while calcium apatite crystals showed only a bluish color and no polarization.

Results: 42 patients (19 M/23F) with ADPKD underwent 73 nephrectomies; in 7/42, both kidneys were removed but not simultaneously. Mean age was 50.3 yrs (range, 31-71yrs). 4 nephrectomies showed RCC (5.4%): 3/4 clear cell RCC and 1/4 papillary RCC; all in male patients. There was also fibrosis and hemorrhages in the cyst wall. Blue crystals of calcium apatite were seen in 33/42 ADPKD nephrectomies, while none showed calcium oxalate crystals. Eighty patients with ESRD (44 M/36F) underwent 97 nephrectomies. RCC was seen in 32 patients (25M/7F): clear cell RCC in 16/32, papillary RCC in 7/32, acquired cystic disease associated RCC in 7/32, sarcomatoid and chromophobe RCC in one each. Calcium oxalate crystals were identified in 42 ACKD-ESRD; 2 tumors with abundant calcium oxalate crystals were classified as calcium-oxalate associated RCC. Only 4 ACKD-ESRD kidneys, all without malignancy, showed blue crystals of calcium apatite.

Table 1

	ADPKD	ACKD-ESRD
Ca apatite	33/42	4/80
Ca oxalate	0/42	32/80
RCC	4/42	32/80

Conclusions: In our study, kidneys with ACKD-ESRD showed a high prevalence of calcium oxalate crystals, while kidneys with APKD showed none. In 2 kidneys, the tumors were classified as calcium oxalate associated RCC. Whether the presence of calcium oxalate crystals is reponsible for a higher rate of cancers in ACKD-ESRD remains to be established. The prevalence of RCC is 10 fold higher in ACKD-ESRD than in ADPKD.

920 Renal Tumors in End Stage Renal Disease.

JD Pimentel, ON Kryvenko, NS Gupta, BA Jones. Henry Ford Hospital, Detroit, MI.

Background: Historically the majority of renal tumors reported in end-stage renal disease were papillary renal cell carcinoma (PRCC) but, it has been recently proposed that acquired cystic disease-associated RCC (ACDRCC) and clear cell papillary RCC (CCPRCC) are more common in ESRD. Therefore, we decided to characterize renal tumors from patients with ESRD at our institution.

Design: We performed a text-based search for ESRD and renal tumors in our pathology information system. After cases were retrieved, clinical data was reviewed and hematoxylin and eosin stained slides were characterized morphologically by a genitourinary pathologist. Immunostains for CK7, CD10, EMA and AMACR were performed on representative blocks.

Results: We evaluated 23 tumors from 20 ESRD patients, retrieved from 2005 to early 2010. 17 patients had radical nephrectomy for tumor. 3 patients had tumors diagnosed at autopsy. By morphology and immunohistochemistry 8/23 (34.8%) of tumors were CCPRCC, 7/23 (30.4%) PRCC, 3/23 (13%) clear cell RCC (CCRCC), 3/23 (13%) ACDRCC and 2/23 (8.7%) chromophobe RCC (CH-RCC). In the subset of tumors from patients with acquired cystic disease, 6/16 (37.5%) were CCPRCC, 3/16 (18.8%) CCRCC, 3/16 (18.8%) PRCC, 3/16 (18.8%) ACDRCC and 1/16 (6.3%) CH-RCC. The majority of the tumors were pT1a (18/23), three were pT1b and two were pT2. 18/20 (90%) patients were African-American. The male-to-female ratio was 3:1.

Immunostain Reactivity

	CK7 +, f, neg	CD10 +, f, neg	EMA +, f, neg	AMACR +, f, neg
CCRCC	0/3, 0/3, 3/3	3/3, 0/3, 0/3	2/3, 1/3, 0/3	3/3, 0/3, 0/3
PRCC	6/7, 1/7, 0/7	5/7, 1/7, 1/7	5/7, 1/7, 1/7	7/7, 0/7, 0/7
CCPRCC	8/8, 0/8, 0/8	1/8, 2/8, 5/8	8/8, 0/8, 0/8	0/8, 0/8, 8/8
ACD	1/3, 0/3, 2/3	3/3, 0/3, 0/3	1/3, 2/3, 0/3	3/3, 0/3, 0/3
CH-RCC	2/2, 0/2, 0/2	0/2, 2/2, 0/2	2/2, 0/2, 0/2	0/2, 2/2, 0/2

+, positive; f, focal; neg, negative

Immuno-morphologic features

	CK7	CD10	EMA	AMACR	Papillary feat.	Other feat.
PRCC	+	+	+	+	+	
PRCC	+	+	+	+	+	
PRCC	+	+	+	+	+	
PRCC	+	+	+	+	+	
PRCC	+	f	+	+	+	
PRCC	+	+	-	+	+	
PRCC	f	-	f	+	+	
CCPRCC	+	-	+	-	+	
CCPRCC	+	-	+	-	+	
CCPRCC	+	-	+	-	f	
CCPRCC	+	-	+	-	f	
CCPRCC	+	f	+	-	+	
CCPRCC	+	f	+	-	+	
CCPRCC	+	+	+	-	+	
CCPRCC	+	-	+	-	f	
CCRCC	-	+	+	+	-	HG
CCRCC	-	+	f	+	-	
CCRCC	-	+	+	+	-	HG
ACDRCC	+	+	+	+	-	C
ACDRCC	-	+	f	+	-	C
ACDRCC	-	+	f	+	-	C
CH-RCC	+	f	+	f	-	
CH- RCC	+	f	+	f	-	

f-focal, HG-hyaline globules, C-Oxalate crystals

Conclusions: In our cohort of ESRD patients, CCPRCC was the most frequent renal tumor. CCPRCC was also the most frequent tumor in the patients with acquired cystic disease.

921 Chromophobe Renal Cell Carcinoma: A Clinicopathological Study of 203 Cases with Primary Resection at a Single Institution.

CG Przybycin, A Gopalan, HA Al-Ahmadie, Y-B Chen, SW Fine, AM Cronin, P Russo, VE Reuter, SK Tickoo. Memorial Sloan-Kettering Cancer Center, New York, NY.

Background: Chromophobe renal cell carcinoma (C-RCC) is known to have less aggressive biologic behavior than clear cell RCC. In spite of multiple studies (including the more recent one on 145 cases), many clinicopathologic issues about C-RCC remain contentious. Issues that need to be further addressed or confirmed include; the biologic behavior as compared to other types of renal tumor, the incidence of sarcomatoid features, and the clinical impact of pathologic features like necrosis, nuclear grade and tumor stage. To address these and other issues, we studied 203 consecutive C-RCCs with primary resection performed at our institution.

Design: Slides in our files were reviewed on all cases. Gross findings were obtained from pathology reports, and follow-up data from a prospectively maintained clinical renal tumor data-base.

Results: From 1980 to 2005 we identified 203 C-RCCs in 200 patients, resected by partial or total/radical nephrectomy at our institution. There was a significant progressive decrease in tumor size (p=.047) and stage (p=.001) from 1980-2000. Both these trends were completed by the year 2000. Five patients had metastasis at presentation while progression after the initial surgery (recurrence, metastasis or death due to disease) occurred in 8 more. Only 4 of 203 (1.97%) tumors showed sarcomatoid features. Over a median follow-up of 6.1 years (range, 0.1-18 yrs), 5 and 10 year disease-specific progression were 3.7 and 4.6%, respectively. Such outcomes were significantly association with tumor size >7 cm, sarcomatoid differentiation, small vessel angiolymphatic invasion, and microscopic necrosis (p = <0.05 each). Tumor stage (pT) or lymph node metastasis tended to show some association, but did not reach statistical significance (p= 0.05 and 0.06, respectively). Conventional Fuhrman and a modified grading scheme similar to that proposed in the literature recently, mitotic index, cytologic eosinophilia and architectural patterns were not associated with outcome.

Conclusions: 1.Sarcomatoid differentiation is less common in C-RCC, compared to that reported in clear cell RCC. 2. Tumor size, sarcomatoid differentiation, small vessel invasion, and microscopic necrosis are the only features associated with adverse outcome. 3. Based on this long follow-up on a large number of cases, C-RCC appears to have better clinical outcomes than clear cell and papillary RCC. 4. The decrease in tumor size and stage seen during the last two decades seems to have stabilized.

922 Rb, PTEN and p53 Tumor Suppressor Loss Is Common in Prostatic Small Cell Carcinoma.

H Rahimi, W Wang, NS Gupta, JI Epstein, GJ Netto, AM De Marzo, TL Lotan. Johns Hopkins University School of Medicine, Baltimore, MD; Henry Ford Health System, Detroit, MI.

Background: Small cell carcinoma (SCC) of the prostate is a rare subtype with an aggressive clinical course which often occurs with an associated acinar prostatic adenocarcinoma (ACa) component. To date, the frequency of tumor suppressor loss in prostatic SCC has not been extensively studied. Here, we systematically examined expression of retinoblastoma (Rb), PTEN, and p53 proteins by immunohistochemistry (IHC) in prostatic SCC and the associated ACa component.

Design: IHC for Rb, PTEN and p53 was performed on a TMA constructed from 30 cases of prostatic SCC spotted in quadruplicate. 20 cases (66%) were transurethral resections of the prostate (TURP), 8 (27%) were bladder, prostate or rectal biopsies, and 2 (7%) were radical prostatectomies. In 73% (22/30) of cases, a concurrent or prior history of prostatic ACa was established, while 7% (2/30) of cases were diagnosed by positive PSA immunostaining and 7% (2/30) had a documented negative cystoscopy. 23% (7/30) of cases had a concurrent ACa component present on the TMA. Cases were scored for nuclear Rb/p53, and cytoplasmic PTEN using a binary scoring system (+/-). A case was considered to have lost Rb or PTEN protein if any TMA spot showed loss in >95% of tumor cells. Positive p53 expression was scored if any spot in a case showed strong expression (3-4+) in >50% of tumor cells.

Results: 90% (26/29) of SCC cases and 43% (3/7) of concurrent ACa cases showed Rb protein loss. 57% (4/7) of cases showed concordance of the SCC and ACa components for Rb status, while 43% (3/7) showed presence of Rb protein in the ACa component with loss of Rb in the SCC component. 63% (17/27) of SCC cases and 71% (5/7) of concurrent ACa cases had PTEN protein loss. 86% (6/7) of cases showed concordance in SCC and ACa components for PTEN status. 56% (14/25) of SCC cases and 66% (4/6) of concurrent ACa cases showed positive p53 expression. 66% (4/6) of cases showed concordance in the SCC and ACa components for p53 status.

Conclusions: Tumor suppressor loss at the protein level is common in prostatic SCC. Similar to previous studies of lung SCC, we found Rb protein loss in the vast majority of prostatic SCC cases, suggesting that loss of this tumor suppressor is critical to the development of this tumor type in multiple organ systems. Loss of PTEN and expression of p53 were also seen in more than half of prostatic SCC cases. Overall, this data suggests that future therapies targeting these tumor suppressor pathways may be beneficial in the treatment of this aggressive tumor.

923 Immunohistochemical Expression of OCT 3/4 in Renal Medullary Carcinoma – A Potential Diagnostic Pitfall.

P Rao, P Tamboli. University of Texas MD Anderson Cancer Center, Houston.

Background: Renal medullary carcinoma (RMC) is a rare aggressive renal tumor that classically afflicts young men with sickle cell trait. The tumor shows overlapping pathologic & clinical characteristics with collecting duct carcinoma (CDC) & urothelial carcinoma (UC) which often results in a diagnostic conundrum. When the tumor presents in a metastatic site in the absence of a history of a renal tumor, germ cell tumor (GCT) is a diagnostic consideration given the young age of most patients (pts). OCT3/4 is an immunohistochemical marker that is routinely used in clinical practice & is widely considered to be a specific marker for GCT. Although OCT3 gene expression has been previously reported in the mammalian kidney the immunohistochemical expression of OCT3/4 in renal tumors has not been studied.

Design: We studied the pathologic & immunohistochemical characteristics of 12 RMCs. Immunohistochemical stains for OCT3/4, Ulex Europeaus lectin, CK7, PIN dual, PAX8 & PAX2 were performed & the expression of these same markers were compared in a group of 5 CDCs & 10 UCs

Results: Pts with RMC ranged in age from 21- 39 yrs (mean 31.8). All had sickle cell trait. There were 8 men & 4 women. Tumor size ranged from 3.8-17.5 cm (mean 8.1 mos). OCT3/4 staining was noted in 8/12 RMC's & was absent in all cases of CDC & UC. 7/12 RMC cases also stained for Ulex Europaeus lectin. Interestingly all but 1 case of CDC were negative for this marker. The immunohistochemical results are summarized below.

Distribution of positive immunohistochemical stains in RMC, CDC & UC.

	OCT3/4	Ulex Europaeus	Vimentin	CK7	PINdual	PAX8	PAX2
RMC	8/12	7/11	8/12	9/12	4/12	9/10	7/11
CDC	0/5	1/5	NA	0/5	0/5	3/5	NA
UC	0/10	1/10	0/10	7/10	7/10	0/10	0/10

NA- Not available

Follow up was available in all cases (range 3-24 mos). 7/12 pts were DOD (mean time to death 12.5 mos) & 5 pts were AWD (mean FU 7.6 mos).

Conclusions: OCT3/4 expression is not specific for GCT & may be noted in a subset of RMC's. Caution must be employed in interpreting the presence of OCT3/4 staining in a poorly differentiated neoplasm at a metastatic site as a GCT, especially when a clear history of sickle cell trait is not available as this may represent a potential diagnostic pitfall. The expression of OCT3/4 may have a role in discriminating RMC from CDC & UC however further studies with a larger number of cases are required to establish the utility of this marker in routine clinical practice.

924 Plasmacytoid Carcinoma of the Urinary Bladder: An Invasive Urothelial Carcinoma Subtype with Important Staging and Follow-Up Implications.

R Ricardo, M Nguyen, N Gokden, A Sangoi, J Presti, Jr, J McKenney. Stanford, Stanford, CA; University of Arkansas for Medical Sciences, Little Rock; El Camino Hospital, Mountain View, CA.

Background: Plasmacytoid carcinoma of the urinary bladder is a urothelial carcinoma subtype/variant that has been emphasized in the literature for its morphologic overlap with both plasma cells and metastatic carcinomas from other anatomic sites. Our experience with plasmacytoid urothelial carcinomas suggests that they may have unusual patterns of disease spread that are not typical of urothelial carcinoma.

Design: We identified cases of plasmacytoid urothelial carcinoma diagnosed on radical cystectomy. All H&E stained glass slides were reviewed to confirm diagnoses. Patient age, sex, AJCC stage, and sites of metastatic spread/recurrence were recorded.

Results: 14 patients with plasmacytoid urothelial carcinoma diagnosed on radical cystectomy were identified. The patient ages ranged from 42 to 81 years (mean: 66.7; median: 69.5); 10 were male and 4 were female. 1 tumor was pT2, 9 were pT3, and 4 were pT4. 6 of 14 (43%) patients presented with lymph node metastases and 4 of 14 (29%) had unusual patterns of metastasis at the time of cystectomy and staging. These sites of metastatic spread included: 1 pre-rectal space; 1 ovary and vagina; 1 bowel serosa; and 1 omentum and bowel serosa. 3 patients are known to have had subsequent metastases involving: 1 pre-rectal space, 1 pleural fluid and small bowel serosa, and 1 bowel serosa.

Conclusions: In this study, 29% of patients with the plasmacytoid variant of urothelial carcinoma presented with atypical patterns of disease spread. The possibility of non-contiguous intra-abdominal spread that may involve serosal surfaces should be emphasized to ensure proper intraoperative staging and follow-up.

925 Do the Tables and Nomograms Commonly Used by Clinicians To Predict Pathological Stage in Men with Biopsy Gleason Score (GS) 8-10 Adenocarcinoma of the Prostate Match What Is Seen at Radical Prostatectomy (RP)?

B Robinson, N Diana Gonzalez Roibon, B Trock, J Epstein. The Johns Hopkins Hospital, Baltimore.

Background: The Partin Tables and the Kattan Nomogram are the two most commonly used tools to predict the pathological stage at RP based on preoperative clinical findings and biopsy pathology. These tools use mathematical equations (logistic regression) which are primarily based on the majority of men with prostate cancer (ie. biopsy GS ≤7) to predict the outcome for all men, including those with higher grade cancer on biopsy. It is unknown how accurate these predictions are which can have significant implications for deciding therapy.

Design: 411 men with GS 8-10 prostate cancer on biopsy (2004-2010) who under RP at our institution were studied. All RPs were serially sectioned and submitted in their entirety. Clinical stage, biopsy GS, and serum PSA for each patient was inputted into both the Partin Tables and the Kattan Nomograms to generate a predicted probabilities of each stage which was then compared to the actual findings at RP.

Results: For the Partin Table there were no significant differences between observed and predicted organ confined (n=175 and 178.5, respectively, p=0.898), seminal vesicle invasion (SVI) (n=55 and 56.2, respectively, p=0.224), or lymph node metastases (LN met.) (n=32 and 26.3, respectively, p=0.142). Using the Kattan Nomograms, it predicted 215 organ confined cases compared to 175 RPs which had organ confined disease (p=0.022). The Kattan nomograms also predicted 75 cases with SVI, whereas there were 80.5 RPs with SVI (p=0.0002). There were no difference between observed and predicted

LN met. using the Kattan nomogram (n=32 and 31.0, respectively, p=0.395).
Conclusions: Utilizing a large number of cases with high grade cancer at biopsy and matched entirely submitted RP specimens, the current study was able to assess the accuracy of the two most commonly predictive tools used by clinicians to predict pathological stage. Whereas the Partin Tables accurately estimated pathological stage, the Kattan Nomogram underestimated stage at RP. Using the Kattan Nomograms, men with GS 8-10 disease on biopsy may be counseled that they have more curable disease than they in fact do. Some men may choose RP based on these overly optimistic predictions as opposed to other therapies, such as radiation therapy. Pathologists can play a key role in the treatment and prognostication of prostate cancer by testing the validity of commonly used clinical tools using RP data.

926 Cancer/Testis (CT) Antigen Expression Correlates with Non-Response to BCG Therapy and Invasive Disease in Human Bladder Cancers.

BD Robinson, TM D'Alfonso, R Chiu, EC Kauffman, DS Scherr, LJ Old, Y-T Chen. Weill Cornell Medical College, New York; Ludwig Institute for Cancer Research, New York.

Background: CT antigens comprise a group of immunogenic proteins normally expressed only in germ cells but aberrantly activated in a variety of cancers, including urothelial carcinoma. Previous studies have shown that CT antigen expression is more common in high grade bladder tumors, and some CT antigens have been shown to weakly correlate with pathologic stage. Given the likely role of the immune system in the effectiveness of Bacillus Calmette-Guérin (BCG) therapy in superficial urothelial carcinoma, we investigated whether CT antigen expression would correlate with BCG therapy response. Possible correlations between CT antigen expression, tumor invasion (pTa/Tis v. pT1) and p53 expression were also examined.
Design: Protein expression of 7 CT antigens (MAGEA, NY-ESO-1, CT7, CT10, CT45, GAGE, SAGE1) and p53 was immunohistochemically evaluated in a tissue microarray containing 125 urothelial carcinoma samples in triplicate from 78 BCG-treated patients (32 pTa, 11 pTis, 35 pT1). Pre- and post-BCG samples were available in 16 patients, pre-BCG only in 37, and post-BCG only in 25 patients. For CT antigens, unequivocal nuclear or cytoplasmic staining in any tumor cells was considered positive. Only nuclear staining was considered positive for p53.
Results: CT antigen positivity strongly correlated with invasive disease (any CT+ seen in 60% of pT1 v. 23% of pTa/Tis; p=0.001) and also correlated with non-response to BCG immunotherapy (p=0.03). Invasive carcinomas (pT1) showed a trend toward BCG failure when compared to non-invasive tumors (pTa/Tis; p=0.06). In the 16 cases with both pre- and post-BCG samples, no change was seen in CT antigen expression before and after treatment. CT antigen positivity correlated with p53 overexpression (p=0.03); however, p53 positivity did not correlate with BCG response.
Conclusions: Expression of any CT antigen correlates with BCG failure. One explanation may be that CT antigens are more frequently expressed in invasive tumors, a group less likely to respond to BCG treatment than non-invasive tumors in our cohort. Alternatively, it may be that CT+ tumors, already presenting "foreign" antigens to the immune system and escaping cell death, are likewise impervious to the immunomodulatory effects of BCG instillation. Our findings suggest that CT antigen expression may be useful in deciding whether to treat a patient with BCG or a more aggressive therapy. CT antigen expression may also help identify those non-invasive tumors at high risk for progression to invasion.

927 Clinical and Pathologic Features of Prostate Cancer with Prostatic-Specific Antigen (PSA) Less Than 2.5 ng/ml. A Study of 209 Cases.

L Roquero, O Kryvenko, S Sukumar, M Diaz, M Menon, N Gupta. Henry Ford Hospital, Detroit, MI.

Background: A PSA level of 4.0 ng/mL or greater is the recommended threshold for further evaluation or biopsy; however, recent screenings have suggested the use of a set point of a PSA level > 2.5 ng/mL to trigger a prostate biopsy. Men who undergo biopsy with a PSA level of less than 2.5 ng/mL have other significant prostate cancer risk factors, including suspicious findings on digital rectal examination (DRE), a strong family history, or an increasing PSA velocity.
Design: Pathology files of our hospital were searched for patients who had undergone radical prostatectomy (RP) with initial PSA of less than 2.5 ng/mL between the periods of 2001 to 2008. All cases with prior hormonal therapy were excluded. Clinical parameters recorded were age, race, initial PSA at diagnosis, clinical presentation, family history of prostate cancer and biochemical recurrence (BCR). Pathologic parameters noted were Gleason score (Gl), prostate weight, tumor volume, presence or absence of extraprostatic extension (EPE), seminal vesicle invasion (SVI) and lymph node metastasis (MET).
Results: 209 patients were identified with a mean age of 59 years (38-74) and mean PSA of 1.7 ng/mL (0.18-2.49), 102 (48.8%) presented with an abnormal DRE and 57 (27.2%) had strong family history of prostatic carcinoma. Increasing PSA velocity was only seen in 9 (4.3%) of patients. Race was known in 115 patients, 97 were Caucasians, 15 African American and 3 Asians. Clinical T stage was available in 175 cases, 91 (52%) were cT1 and 84 (48%) were cT2.
Following RP with a mean prostatic weight of 39 grams (16.44-86.16), 121 (59%) showed Gl 6, 70 (33%) showed Gl 7 and 18 (8%) were Gl 8 and above. EPE was observed in 30 (14%), SVI in 4 (2%) and MET in 2 (1%). BCR was seen in 4% of patients (8/182) with a average follow up of 23 months and all were pathologic stage T3.
Out of 46 patients with PSA $\leq$ 1.0 ng/mL, 43 (93.5%) were Gl 6 and 3 (6.5%) were Gl 7; EPE was seen in 3 (6.5%) and SVI in 1 (2.1%). 36 patients recieved lymph node dissection, none showed MET.
Conclusions: In spite of adverse clinical parameters of abnormal DRE and strong family history, our data show that majority of prostate cancer in PSA < 2.5 ng/mL are organ confined and low grade. BCR was only seen in patients with higher Gleason's score (Gl 8 and above) with non organ confined disease. We did not find adverse pathologic outcome in patients with very low PSA values ($\leq$1.0 ng/mL).

928 Primary Versus Secondary Bladder Adenocarcinoma: A Diagnostic Challenge.

S Roy, AV Parwani. UPMC, Pittsburgh, PA.

Background: Primary bladder adenocarcinoma (PBA) is a rare tumor characterized by malignant glandular proliferation with varying degrees of differentiation. These tumors are difficult to distinguish from colonic adenocarcinomas based on morphological features, especially on limited specimens. There is limited data available about the role of immunohistochemical (IHC) markers in distinguishing PBA from secondary bladder adenocarcinomas (SBA). In this study we have attempted to analyze a set of immunohistochemical markers and in distinguishing the two groups.
Design: A total of nine cases of bladder adenocarcinomas (5 PBA & 4 SBA) were studied. The control group included 5 cases each of urothelial carcinoma (UC) and colonic adenocarcinoma (CA). Morphological features were assessed on Hematoxylin and eosin stained sections. IHC by Streptavidin-biotin method using DAB chromogen was performed for cytokeratin 7 (CK7), cytokeratin 20 (CK20), beta-catenin, E-Cadherin, Villin and CDX-2. Cytoplasmic/membranous (CM) versus nuclear staining was assessed for beta-catenin and cytoplasmic and/or membranous staining was assessed for the other immunomarkers. Florescence in-situ hybridization (FISH) studies targeting chromosomes 3, 7, 9 and 17 are underway to further investigate possible differences between the tumor types.
Results: Nine cases of bladder adenocarcinomas included 5 males and 4 females in the age range of 25-87 years. All cases of PBA were characterized by infiltrating intestinal type malignant gland. Two tumors had mucinous features and one had signet ring cells. Three of 4 SBA were metastatic from the GI tract and one represented a divergent glandular differentiation in an UC. IHC staining for beta-catenin demonstrated CM staining in all PBA and additional strong nuclear staining in 3 of 4 SBA. The control cases of CA showed strong nuclear as well as CM expression of beta-catenin in 4 of 5 cases. No difference in staining pattern was observed with CDX2, villin, E-Cadherin and CK20. CK7 expression was restricted to benign and malignant urothelium and only one case of PBA.
Conclusions: In summary, the above findings suggest that beta-catenin can be used in conjunction with morphological and clinical information to aid in distinguishing PBA from SBA. This may help support the hypothesis that the dysregulation in the Wnt signaling pathway due to beta-catenin is operative in SBA and CA, unlike PBA. Although CK7 may help in distinguishing colonic from urothelial tumors, it cannot differentiate between glandular neoplasms of both organs. CK20, CDX2, Villin and E-cadherin do not appear to be of diagnostic use in this scenario.

929 Differential Chromosomal Copy Number Variations in Chromophobe Renal Cell Carcinoma and Oncocytoma Using High Resolution SNP Array.

S Roy, AH Hughes, G Sharma, MA Lyons, MJ Krill-Burger, LA Kelly, AV Parwani, S Bastacky, WA LaFramboise, R Dhir. UPMC, Pittsburgh, PA.

Background: Chromophobe renal cell carcinoma (ChRCC) and oncocytoma (Onc) are biologically distinct renal tumors; however subsets of these tumors exhibit overlapping morphological and immunohistochemical features. High-density single nucleotide polymorphism (SNP) arrays allow genome-wide interrogation of chromosome copy number variation (CNV) and loss-of-heterozygosity at resolutions of 1-2kb. This study investigates CNV in these tumors to identify molecular changes as potential discriminants between these RCC classes.
Design: Five ChRCCs and 4 Onc with classic histologic features and non-neoplastic renal tissue from nephrectomy specimens were evaluated. DNA was purified from flash-frozen specimens. Five hundred nanograms were cut with restriction endonuclease Nsp I or Sty I followed by adaptor ligation and PCR based whole genome amplification. PCR products were purified, fragmented, denatured, labeled and hybridized to Affymetrix 6.0 SNP arrays. Results were processed to detect CNV using Genotype Console and Partek Genomics Suite (hMM modeling) to derive results between tumor and normal samples and in comparison to an in-house reference library of normal tissues (n=10).
Results: The analysis revealed significant CNV changes affecting 6116 genes in ChRCC as compared to 721 genes in Onc samples. In the ChRCCs, there was a predominance of deletions (83%, 441 CNV) over amplifications (17%, 88 CNV) detected in at least 3 of the 5 specimens. These deletions were specifically clustered on chromosomes 1 (267 CNV) and 10 (174 CNV) only, signifying loss of large portions of these structures. The amplifications were fewer and distributed among chromosomes 4, 5, 7, 8, 11, 12, 14, 15, 16, 20 and 22. In contrast, Onc demonstrated amplifications in chromosomes 2, 4, 5, 6, 7, 10, 12, 18, and 21 but at a lower frequency compared to ChRCC specimens. Unlike ChRCC, deletions in Onc specimens were atypical and unshared across this tumor class.
Conclusions: The distinct patterns of CNV including the large numbers associated with ChRCC compared to Onc may reflect different mechanisms of tumorigenesis. The prominent deletions in chromosomes 1 and 10 were specifically seen in ChRCCs. Furthermore, the amplifications were mainly clustered in chromosomes 12, 15 and 22 in ChRCCs, in contrast to Onc. These findings support the hypothesis of significant differences in the pattern of gain and loss of genetic material in the two tumor groups which can be potentially exploited to establish clinically useful diagnostic markers and identify therapeutic targets.

930 Lack of FISH Abnormalities in Bladder Biopsies from Patients with History of Pelvic Radiation: A Pilot Study.

K Rumilla, M Campion, T Oberg, J Voss, J Zhang, K Halling, T Sebo. Mayo Clinic, Rochester, MN.

Background: Radiation therapy is part of the clinical armamentarium used to treat pelvic malignancies in men and women. The radiated field often includes the bladder and may induce mucosal alterations which can be mistaken in urine cytology specimens and bladder biopsies for urothelial cancer. We conducted a pilot study to investigate whether FISH abnormalities were detected in patients with bladder biopsies exhibiting radiation treatment effect.

Design: 17 bladder biopsy samples from 14 patients who have undergone radiation therapy for prostate, bladder, rectal, cervical or ovarian cancer were selected. Of these, 13 were benign and 4 contained urothelial cancer (2 high-grade, 2 low-grade papillary). Of these 4, 3 were from patients with a corresponding benign biopsy. Specimens were analyzed using FISH probes targeting the centromeric regions of chromosomes 3, 7, 17 and the 9p21 locus. Signal patterns were recorded for 50 non-consecutive transitional cells. Specimens were considered positive if ≥5 cells were polysomic cells (gains in ≥2 probes), ≥10 cells were trisomy (three signals in one of the probes) or ≥20 cells showed homozygous 9p21 loss (zero copies of 9p21 probe). Correlation with the pathologic diagnosis and clinical history was performed.

Results: The 13 benign specimens were all FISH disomy (negative; 100% specific). In the 4 biopsies with cancer, the 2 high grade cancers were polysomic and homozygous for loss of 9p21; and the two low grade papillary cancers were FISH negative.

Conclusions: Our pilot study failed to detect FISH abnormalities in benign bladder biopsies from patients who had previously undergone radiation in which the radiation field included the bladder mucosa. In biopsy specimens from patients with flat urothelial atypia subsequent to radiation, FISH may help distinguish between radiation cystitis and urothelial carcinoma. We are currently evaluating FISH in urine specimens from patients with a history of radiation to assess the role of FISH when cystoscopy identifies worrisome areas of mucosal erythema.

931 ERG, TMPRSS2 and SLC45A3 Expression in Prostate Cancers with Rearrangements of these Genes.

NJ Rupp, S Perner, M Braun, H Moch, F Fend, MA Rubin, G Kristiansen. University Hospital Bonn, Germany; University Hospital Zürich, Switzerland; University Hospital Tübingen, Germany; Weill Cornell Medical College, New York, NY.

Background: The majority of prostate cancer harbours recurrent gene fusions involving *ERG,* a member of the ETS gene family, and the 5' untranslated region of the androgen regulated *TMPRSS2* gene and less commonly the prostate specific solute carrier SLC45A3 gene. The aim of our study was to quantify the protein expression of ERG, TMPRSS2 and SLC45A3 in a large prostatectomy cohort with known gene rearrangement status of these genes and to assess for diagnostic or prognostic capabilities.

Design: We analysed tumors from 640 cases with known *TMPRSS2-ERG* and *SLC45A3-ERG* gene rearrangement status for protein expression of these genes on tissue microarrays using commercially available antibodies and a four class scoring system (negative, weak, moderate and strong). Resultant data was correlated to the respective gene rearrangement status and clinico-pathological parameters including PSA follow up data.

Results: Protein expression analysis for ERG showed no expression in benign prostate glands as compared to an average low expression in the cancerous tissue. In cancer tissue, high ERG protein expression was strongly associated with a positive rearrangement status ($r = 0.647$; $p < 0.0001$) but showed no correlation with outcome data. In 23 of 218 cases (11%) ERG protein was expressed without evidence of gene rearrangement and 58 of 253 cases (23%) showed no ERG protein expression despite positive gene rearrangement status.

SLC45A3 exhibited a significantly weaker protein expression in the prostate cancer samples in relation to the benign tissue and revealed a significantly negative association with the rearrangement status in the cancerous tissue. Correlations with outcome data showed a significantly shorter survival time for patients with lower SLC45A3 protein expression.

No significant protein expression difference was found for TMPRSS2 between benign and malignant tissue. Furthermore, no correlation between protein expression and rearrangement status in the malignant glands could be detected.

Conclusions: This study confirms that ERG protein expression is highly restricted to prostate carcinomas that harbor the ERG rearrangement but does not occur in benign glands and might therefore be a relevant diagnostic marker for ERG-rearranged prostate cancer. The negative prognostic value of SLC45A3 protein expression clearly warrants further study.

932 Diagnostic Value of ERG Oncoprotein Detection in Biopsy Specimens.

D Russell, GL Lee, P Parker, B Furusato, DY Young, Y Chen, T Sreenath, A Dobi, DG Mcleod, S Srivastava, IA Sesterhenn, JT Moncur. Department of Surgery, Uniformed Services University of the Health Sciences, Rockville, MD; Armed Forces Institute of Pathology, Washington, DC; Walter Reed Army Medical Center, Washington, DC.

Background: In the last 10 to 15 years, the increasing need for diagnostic precision has led to the introduction of biochemical markers, such as α-Methylacyl coenzyme A racemase (AMACR), 34βE12, and p63 to support the diagnosis of prostate cancer. However, these markers are not without shortcomings. In recent years, TMPRSS2-ERG genomic fusion has been demonstrated in 40 to 80% of prostate cancers. We have developed a monoclonal anti-ERG antibody (ERG-MAb, clone 9F4) that demonstrated an unprecedented 99.9% specificity in detecting the protein product of the recurrent TMPRSS2-ERG fusions. Previously we have shown that when AMACR and ERG expression were examined together, 96.4% of patients with prostate cancer were positive for at least one of the two genes. The hypothesis of this study was that diagnostic accuracy can be improved by adding ERG to AMACR immunohistochemical (IHC) staining in prostate biopsy specimens.

Design: In a retrospective set of 88 patients undergoing prostate biopsies, prostate cancer was identified in 44 patients. 10 of these patients subsequently underwent radical prostatectomy. The 385 slides from the 88 biopsy sets were evaluated by IHC with 350 stained with ERG-MAb only and 35 stained for both ERG-MAb and AMACR.

Results: AMACR was detected in 28 of 31 and ERG in 37 of 70 of tumor positive biopsies. Of the three biopsies with benign tissue only, one was positive for AMACR. However, in six other biopsies, both tumor and benign tissue were positive for AMACR. ERG was detected only in 0.4% (1/280) of benign glands total. Of the three slides with AMACR negative tumors, two were positive for ERG.

Conclusions: Our findings highlight that the highly specific detection of ERG oncoprotein, a product of the TMPRSS2-ERG gene fusion, when combined with AMACR improves the diagnostic specificity in prostate biopsy specimens.

933 The Lymphoma-Associated EZH2 Codon 641 Mutation Is Not Detected in Localized Prostate Carcinoma.

RJ Ryan, S Wu, D Borger, J Iafrate, C-L Wu, L Le. Massachusetts General Hospital, Boston.

Background: *EZH2* encodes the enzymatic subunit of the polycomb repressive complex 2 (PRC2) that mediates gene repression through trimethylation of histone H3 at lysine 27. *EZH2* overexpression is associated with poor prognosis in several carcinomas, including prostate carcinoma (PCa). In many cases of advanced PCa, *EZH2* overexpression results from genomic deletion of microRNA-101. Recurrent, heterozygous point mutations affecting codon 641 of *EZH2* were recently described in a subset of diffuse large B cell lymphomas (DLBCL) and follicular lymphomas (FL). The occurrence of *EZH2* codon 641 mutations in PCa has not been previously investigated to our knowlege. While the function of codon 641 mutant Ezh2 protein is not known, the pattern of a heterozygous missense mutation at a stereotyped residue within the enzyme active site suggests a gain-of-function. We sought to determine whether *EZH2* codon 641 mutations occur in organ-localized prostate carcinoma, and to determine any association between mutation status and PSA failure in a series of PCa patients with clinical follow-up

Design: Paraffin blocks of tissue from radical prostatectomy performed for prostate cancer were identified from our archives, and foci of PCa were targeted for extraction by punch biopsy, with the highest grade foci targeted whenever possible. Total nucleic acid was extracted, and a 149 bp fragment of genomic DNA containing *EZH2* codon 641 was PCR amplified. We then performed SNaPshot single-nucleotide extension genotyping (Applied Biosystems) with 4 extension primers designed to interrogate the 1st 2 nucleotides of *EZH2* codon 641 on both the coding and noncoding strand. Extension products were analyzed by capillary electrophoresis. To date, this assay has been validated on 142 paraffin-embedded lymphoma samples, with 21 *EZH2* codon 641 mutant lymphoma samples detected, representing four different amino acid substitutions.

Results: Overall, 92 cases of PCa were successfully analyzed. Gleason scores (GS) for analyzed cases were as follows: GS ≤ 3+3 n=50, GS 3+4 n=17, GS 4+3 n=9, GS ≥ 4+4 n=16. Primary tumor stage was pT2 (n=55) or pT3 (n=37). 10-year clinical follow-up showed PSA failure in 29/92 cases. *EZH2* codon 641 mutations were not detected in any case (0/92). Clear wild-type genotype signals were seen from all samples.

Conclusions: *EZH2* codon 641 mutations are rare or absent in organ-localized prostate carcinoma. Oncogenic disregulation of EZH2 seems to occur by different genetic mechanisms in prostate carcinoma and B cell lymphomas.

934 Inflammation Confined to the Stromal Compartment in Benign Prostate Biopsy May Be Associated with Decreased Risk of Subsequent Prostate Cancer (PCa).

BA Rybicki, A Rundle, D Tang, NS Gupta, DA Chitale, ON Kryvenko. Henry Ford Hospital, Detroit, MI.

Background: Benign changes ranging from atrophy and inflammation to prostatic intraepithelial neoplasia (PIN) are common findings on prostate core needle biopsies. Only high grade PIN is recommended to be included in surgical report although atrophy and inflammation may be precursors of PCa. The disease risk associated with these potential disease risk factors has not been assessed in a controlled study.

Design: A matched case-control study of 316 PCa-control pairs nested within a historical cohort of healthy men with a benign prostate specimen from 1991-2002. Eligible cases were diagnosed with PCa at least one year after cohort entry. Controls were selected through incidence density sampling and matched to cases on date and age at cohort entry, race, and type of specimen. The initial benign specimens and controls were reviewed by one pathologist for presence of PIN, atrophy (simple, lobular, and partial) and inflammation (glandular and/or stromal). Conditional logistic regression was used to model the independent risk of each of these conditions.

Results: After adjusting for the effect of the other factors, only PIN was found to significantly increase the risk for PCa (Odds Ratio (OR) = 1.92). Presence of inflammation was associated with decreased risk for PCa (OR = 0.69), but this decreased risk was primarily for inflammation within the stromal compartment (OR = 0.63). Inflammation in the glandular or periglandular regions was not associated with increased risk. Irrespective of whether inflammation was present or absent, presence of atrophy failed to show an increased PCa risk. When stratified by PSA level (<4 or >4 ng/ml) at time of initial assessment, the strongest association of PIN (OR= 2.35) and stromal inflammation (OR = 0.51) with PCa was in cases with PSA >4 ng/ml. PIN primarily increased the risk for PCa diagnosed within three years of initial assessment

(OR=3.77), whereas the negative association between stromal inflammation and PCa was stronger three years or more after initial assessment (OR=0.57).
Conclusions: We find that the association of PIN with increased risk for subsequent PCa is seen mainly in patients with PSA >4 ng/ml and within three years of initial assessment. There is no increased risk for PCa associated with atrophy and/or glandular inflammation. Patients with stromal inflammation who fail to develop PCa within three years after initial assessment are up to half as likely to develop PCa upon further follow-up. These previously unreported findings may be used by clinicians in managing patients with high PSA but a negative biopsy.

935 Concomitant ERBB2-ERBB3 Expression in Prostatic Large Duct Carcinoma.

MA Salomao, L Araujo, M Mansukhani, MJ Szabolcs. Columbia University Medical Center, New York, NY.
Background: The ERBB2-ERBB3 receptor tyrosin kinase (RTK) heterodimer has been linked to aggressive prostate cancer due to androgen independent activation of multiple signaling pathways involved in oncogenesis and tumor progression. Prostatic large duct carcinoma of the periurethral ducts (PLDC), comprising up to 5% of all prostate cancers, behaves more aggressively than its acinar counterpart (PAC). This study was undertaken to determine whether PLDCs display higher levels of ERBB RTK expression compared to PACs, similar to what is seen in the non-neoplastic prostate.
Design: Prostate tissue from TURP specimens (n=10) was used to determine the distribution of ERBBs in the normal prostate. A total of 220 cases of prostate cancer with known patient age, stage and Gleason's score were selected from the files in the Surgical Pathology Division of CUMC. Tissue microarrays were built and immunostained for ERBB1 (EGFR), ERBB2 (NEU) and ERBB3 and scored as no, weak or strong staining (>15% cells). All PLDCs (n=34) and a control set of age and stage-matched PACs cases were stained for C-MYC to determine overall signaling pathway activation. The proliferation index was determined by Ki-67 labeling. Fisher exact test and student's T-test was used in the data analysis.
Results: ERBB1 and 3 were present in the basal cells of benign prostatic acini, with NEU absent. Both NEU and ERBB3 but not EGFR consistently displayed strong labeling of benign prostatic urethra and periurethral prostatic ducts. PLDCs (n=34) vs. PACs (n=186) showed strong staining for EGFR in 35.3% vs. 22.6% (p=0.13), for NEU in 41.2% vs. 10.8% ($p<10^{-5}$) and for ERBB3 in 94.1% vs. 62.4% ($p<10^{-4}$). To overcome its defective kinase activity, ERBB3 needs to dimerize with another ERBB family member. Co-expression of ERBB3 with either EGFR or NEU occurred in 58.8% (20/34) of PLDCs, but only 19.4% (36/186) of PACs ($p<10^{-6}$). ERBB3-positive PLDCs display high levels of NEU (70%), whereas ERBB3-positive PACs upregulate EGFR (69.4%). PLDCs have a 4x higher Ki-67 index ($p<10^{-4}$, T-test) and strong MYC signaling (58.8% vs. 20.6%, $p<0.0001$).
Conclusions: In this study, we show that prostatic PLDC recapitulates the phenotype of prostatic periurethral ducts with high prevalence of concomitant NEU and ERBB3 expression. The high levels of NEU and ERBB3 in PLDC could explain the higher proliferation indices and MYC levels when compared to PAC due to known potent androgen independent activation of tumor signaling pathways of the ERBB2/ERBB3 dimer. This distinct molecular phenotype may explain the more aggressive clinical behavior of ductal prostatic carcinoma.

936 Immunohistochemical Expression of Prostate-Specific Antigen (PSA), Prostatic Acid Phosphatase (PAP) and Antibody Cocktail (P63/HMWCK/AMACR) in Ductal Adenocarcinoma of the Prostate.

H Samaratunga, M Adamson, J Yaxley, B Delahunt. Aquesta Pathology, Brisbane, QLD, Australia; University of Queensland, Brisbane, Australia; Royal Brisbane Hospital, Brisbane, QLD, Australia; University of Otago, Wellington, New Zealand.
Background: Ductal adenocarcinoma of the prostate (DAP) is an aggressive variant of prostatic adenocarcinoma displaying several architectural patterns mimicking carcinoma from other organs. Prostate specific antigen (PSA) and prostatic acid phosphatase (PAP) immunostaining is frequently used to establish prostatic origin. The extent of immunostaining for these in DAP has not been studied, particularly the significance of negative staining in a small biopsy. The extent of immunostaining for AMACR and basal cell markers relating to different architectural patterns in DAP has also not been fully examined.
Design: Immunohistochemical staining for monoclonal PSA (Clone ER-PR8, Dako, Denmark), monoclonal PAP (Clone PASE/4LJ, Dako, Denmark) and antibody cocktail 34betaE12, p504s (AMACR), and p63 was performed on paraffin sections containing DAP from 50 radical prostatectomy specimens. Staining was categorized as negative (0%), 1+ (1-30%), 2+ (31-60%) or 3+ (61-100%). The percentage of tumor negative for PSA and PAP in the same area was noted.
Results: Thirty nine cases had cribriform, 11 papillary, 7 solid and 35 glandular architecture (34 had >1pattern). PSA was positive in 92%; 1+ in 24%, 2+ in 20% and 3+ in 48%. PAP was positive in 94%; 1+ in 6%, 2+ in 28% and 3+ in 60%.Both PSA and PAP were negative in the same area in ≥30% of tumour in 28%, including 1 entirely negative for both. These represented 30% of cribriform, 36% papillary, 15% solid and 22% glandular patterns. AMACR was positive in 84% but negative in ≥30% of tumour in 90%. Basal cells were undetected by 34betaE12 and p63 in 46% and patchy in 1-30% of tumour in 42%. These included 84% of cribriform, 100% of papillary and 85% of solid pattern. All glandular lesions were entirely devoid of basal cells.
Conclusions: Absence or minimal retention of basal cells in all patterns of DAP confirms that this is not intraductal carcinoma but a distinct variant of prostatic adenocarcinoma. Although only 2% were entirely negative for PSA and PAP, nearly one third had large areas negative for both irrespective of architectural pattern. AMACR was positive in the majority of DAP, however, large areas were negative. Negative staining for these markers in small volumes of tumor as seen in biopsies does not rule out a diagnosis of DAP.

937 Evaluation of Putative Renal Cell Carcinoma Markers PAX-2, PAX-8, and hKIM-1 in Germ Cell Tumors (GCT): A Tissue Microarray Study of 100 Cases.

A Sangoi, J Higgins, J Brooks, J Bonventre, J McKenney. Stanford University Medical Center, CA; Harvard Medical School, Boston, MA.
Background: Within the spectrum of genitourinary neoplasia, metastatic GCT and renal cell carcinoma may show morphologic overlap. Expression of putative renal cell carcinoma markers PAX-2, PAX-8, and hKIM-1 have been reported in a few GCT, which have included mostly seminoma (PAX-8) and yolk sac tumor (PAX-2, PAX-8, hKIM-1); however, a thorough characterization of staining by GCT subtype within a large series has not been previously reported.
Design: Immunohistochemical expression of PAX-2, PAX-8, and hKIM-1 was evaluated in 100 GCTs using tissue microarray technology (in triplicate) with standard avidin-biotin technique. Normal renal cortex and clear cell renal cell carcinoma were used as control tissues. Positive reactivity was scored as nuclear (PAX-2, PAX-8) or membranous/cytoplasmic (hKIM-1).
Results: Of the 100 GCT evaluated [including choriocarcinoma (1), embryonal carcinoma (21), intratubular germ cell neoplasia unclassified (2), seminoma (61), spermatocytic seminoma (1), teratoma (5), and yolk sac tumor (8)], expression for hKIM-1 was identified in 48% of embryonal carcinomas and 50% of yolk sac tumors (weak to strong in both tumors). PAX-2 and PAX-8 reactivity was identified in 50% and 25% of yolk sac tumors, respectively.
Conclusions: While this study confirms PAX-2/PAX-8/hKIM-1 reactivity in yolk sac tumor as previously noted from a smaller series by our group. This study also demonstrates hKIM-1 reactivity in embryonal carcinoma, supporting the notion that these putative renal cell carcinoma markers should be used cautiously.

938 NKX3.1, PTEN, ERG and AR Define Genetic Alteration Patterns Correlating with Tumor Progression in Prostate Cancer.

V Scheble, G Scharf, R Menon, P Nikolov, K Petersen, F Fend, M Reischl, S Perner. University Hospital Tuebingen, Germany; Karlsruhe Institute of Technology, Germany.
Background: Prostate Cancer (PCa) is a common and clinically heterogeneous disease. While some PCa cases remain indolent over decades, others progress rapidly. Yet, little is known about genetic alterations resulting in progression of this disease. So far, a large number of genetic aberrations have been identified in PCa, of which the ERG rearrangement, the loss of PTEN and NKX3.1, the gain of CMYC, GOLPH3 and AR are the most common. Unfortunately, none of these genes alone is a strong marker of disease progression. Aim of our study was to assess the alterations of these genes in cases of different stages in order to identify patterns of genetic alterations associated with PCa progression.
Design: We collected consecutive cases of patients who underwent either prostatectomy or metastasis resection. For localized cancer (N0), we identified 138 cases, for regional LN metastasis (N1), we identified 105 patients with primary PCa and corresponding LN metastasis, and for distant metastasis (M1), we identified 39 samples. To assess for alterations of the above mentioned genes, we applied fluorescence in-situ hybridization (FISH) assays.
Results: We found one case with a low level amplification (LLA) of GOLPH 3 in a LN. For CMYC assessment, we found one LLA in a primary focus and the corresponding LN, one LLA in a LN without available primary and two independent LLA and one HLA in M1 cases. PTEN deletions occurred in 3/186 N0 samples, 21/105 N1 cases and 8/39 M1 cases. We found the *ERG* rearrangement in ~50% of N0 and N1 samples but only in 10/39 M1 PCa samples. AR amplification could only be detected in M1 cases (14/39). Deletions of NKX3.1 occurred in 55/138 N0, 75/105 N1 and 32/39 M1 samples.
Conclusions: We could show that there are specific genetic alteration patterns that distinguish localized PCa from metastasized PCa. Of note, there are alterations that occur frequently in N1 PCa but at much lesser frequencies in M1. Deletions of PTEN and NKX3.1 in combination with AR amplification characterize the metastatic phenotype. We found the *ERG* rearrangement in ~50% of N0 and N1 PCa. Interestingly, we detected an ERG rearrangement frequency of only 25.6% our M1 samples. In concordance with previous reports, AR amplification could only be detected in M1 samples. In summary, the number of alterations increased from localized cancer to progressed PCa.

939 Histopathologic Correlation of Prostatic Adenocarcinoma on Radical Prostatectomy with Pre-Operative Anti-18F Fluorocyclobutyl-Carboxylic Acid Positron Emission Tomography/Computed Tomography.

D Schuster, B Fei, T Fox, AO Osunkoya. Emory University School of Medicine, Atlanta.
Background: In the present era of active surveillance/deferred treatment and focal therapy for prostatic adenocarcinoma, accurate quantification and staging of prostatic adenocarcinoma clinically or pathologically has even more profound therapeutic and prognostic implications. Currently, there are no definitive imaging techniques for the detection or staging of locally advanced prostatic adenocarcinoma. Anti-18F fluorocyclobutyl-carboxylic acid (FACBC) is a synthetic L-leucine analog Positron Emission Tomography/Computed Tomography (PET/CT) radiotracer that has demonstrated promising results in brain tumors.
Design: Prior to surgery, 8 patients were injected with FACBC and underwent PET/CT imaging. All slides obtained from the radical prostatectomy specimens were reviewed. Areas of Gleason patterns 3, 4 and 5 were outlined with different colored markers. Foci with inflammation were also similarly outlined. All slides were then digitally scanned, to reconstruct the location of the dominant nodule /multifocal tumor nodules. Pathologic findings were subsequently correlated with FACBC PET/CT imaging.

Results: Mean patient age was 61 years (range: 53-70 years). Gleason scores were as follows; 3+4=7 (3 patients), 4+3=7 (4 patients) and 4+5=9 with ductal differentiation (1 patient). All patients had bilateral disease, with a definitive dominant tumor nodule. Pathologic stage was as follows; pT2c (2 patients), pT3a (4 patients), pT3b (2 patients). Mean tumor volume was 20% (range: 10-60%). Strong FACBC PET/CT uptake was demonstrated in the dominant tumor nodule in all cases. In the six patients with pT3a or pT3b disease, there was correlation between FACBC PET/CT uptake and pathology, with regards to laterality of extraprostatic extension and seminal vesicle involvement. There was no significant FACBC PET/CT uptake in areas of inflammation.
Conclusions: The preliminary findings of our study suggest that (a) FACBC PET/CT may be a very useful tool for clinical staging of patients with localized organ confined, or locally advanced prostatic adenocarcinoma (b) FACBC PET/CT may also have a role in targeted needle core biopsies in patients with prior negative or atypical biopsies, but with unexplained elevated PSA levels (c) It is also highly conceivable that FACBC PET/CT may be utilized in the selection of patients for definitive treatment versus active surveillance/deferred treatment even if they have small tumor volume on needle core biopsies.

940 Localized/Segmental Testicular Infarction: A Potential Clinical and Radiologic Mimic of Testicular Cancer. Clinicopathologic Study of 10 Cases.

JD Schwartz, WR Porter, RK Malhotra, M Aquino, SZH Jafri, MB Amin. William Beaumont Hospital, Royal Oak, MI.
Background: Localized or segmental testicular infarction is a rare entity, with less than 50 reported cases. Most reports have been published in the urology and radiology literature. Literature search revealed only one published case report of this entity in the pathology literature. We present the first pathology case series consisting of 10 cases with their clinical, radiologic, and pathologic findings.
Design: 10 cases of segmental testicular infarction were retrieved from the pathology records of one institution. We excluded patients that had clinical or pathologic evidence of torsion. Also excluded were cases that showed diffuse testicular infarction. Clinical signs and symptoms, as well as pertinent radiologic and pathologic findings were noted. An extensive review of the published literature was performed.
Results: The patients ranged in age from 18 to 79 years. Presenting clinical features included pain (n=8) or evidence of a mass lesion (n=2). Ultrasound performed in all cases showed hypoechoic and hypovascular testicular lesions with inability to completely exclude malignancy. All these patients underwent orchiectomy. Gross pathology showed well demarcated lesions that were either hemorrhagic (n=3) or pale-fibrotic (n=7) depending on the age of the infarct. The size of these infarcts varied from 0.6 cm to 3 cm (mean 1.7 cm). Etiologic factors identified included cholesterol embolism (n=1), giant cell vasculitis (n=1), familial hypercoaguable state (n=1), and organizing thrombi (n=4); with these etiologies being clinically unknown at the time of diagnosis.
Conclusions: Segmental testicular infarcts are being increasingly recognized due to a ready availability of radiologic testing modalities such as ultrasound in out-patient clinical offices. This clinical mimic of cancer is, however, easliy diagnosed under the microscope. Both localized and systemic diseases can be causative factors in segmental testicular infarction. Careful pathologic examination of these specimens is warranted, as testicular infarction may be the first presenting sign of a systemic vasculopathy or constitutional coagulopathy. Literature review showed that although most cases are deemed idiopathic, many such patients were noted to have etiologic risk factors that include coronary and peripheral vascular disease, vasculitis, sickle cell disease, and surgical manipulation of the inguinal region.

941 Clinicopathological Correlation of ERG Protein Expression in Single Focus Prostate Cancer.

IA Sesterhenn, S-H Tan, A Dobi, S Srivastava, DG McLeod, SA Brassell, B Furusato. Armed Forces Institute of Pathology, Washington, DC; Uniformed Services University of the Health Sciences, Bethesda, MD; Walter Reed Army Medical Center, Washington, DC.
Background: A single cross section of a cohort of 132 whole mount radical prostatectomies were previously stained with an ERG antibody developed in the Center for Prostate Disease Research revealed either positive or negative tumors. The purpose of this study was to determine by immunohistochemistry if single large prostatic carcinomas are homogeneous with respect to their ERG oncoprotein expression status despite their heterogeneous appearance in the H&E stained sections.
Design: In 14 (10.6%) of the 132 specimens a single tumor was identified. Laterality, zone of origin, tumor volume, Gleason score, and pathologic stage were recorded. Eight of these were utilized for immunohistochemical evaluation of the entire tumors. Following deparaffinization and antigen retrieval the sections were incubated with the ERG MAb at a dilution of 1:1280 followed by biotinylated horse anti-mouse antibody at a dilution of 1:200 (Vector Laboratories, Burlingame, CA, USA) followed by treatment with the ABC Kit (Vector Laboratories) The color detection was achieved by treatment with VIP (Vector Laboratories).
Results: Patient's median age was 61 years and median PSA was 5.2 ng/mL. Single focus cancers were unilateral in five of eight cases and all five cases were located in the peripheral zone. The median tumor volume was 7.2 cc. (range: 2 cc. to 18.8 cc.) Gleason score (Gl) distribution was: Gl 7 (3+4) in four of eight, and Gl 8-10 in three of eight cases. One case consisted of a minute focus of carcinoma, too small to give Gleason score. Pathological stage was pT2 in three of eight, pT2 R1 in one of eight and pT3/4 in four of eight cases. ERG expression was detected in all tumors. Six of eight cases showed intratumoral heterogeneity. The other two cases showed homogeneous ERG expression.
Conclusions: Although the number of cases is small, the results suggest that the ERG expression correlates with either a single or multiple clonal origin of prostatic carcinoma in these high volume, and high-grade tumors.

942 Differential Expression of microRNA in Papillary Renal Cell Carcinoma.

G Sharma, AH Hughes, S Roy, MA Lyons, CM Sciulli, JM Krill-Burger, LA Kelly, S Bastacky, R Dhir, WA LaFramboise, AV Parwani. University of Pittsburgh Medical Center, PA.
Background: Micro Ribonucleic Acids (miR) are small non-protein-coding RNAs that bind messenger RNA to post-transcriptionally regulate gene expression impacting cell proliferation, apoptosis and differentiation. Papillary Renal Cell Carcinoma (PRCC) comprises 10 to 15 percent of all RCCs and is subdivided into two types: Type 1 (papillae lined by single layer of cells with low grade nuclear features and scant cytoplasm) and Type 2 (papillae lined by pseudostratified nuclei of higher nuclear grade and abundant eosinophilic cytoplasm). We identified a panel of statistically significant miRs that are differentially expressed in PRCC compared to normal renal tissue consistent with morphological differences between PRCC types.
Design: We selected tumor and adjacent normal renal tissue from 5 cases of Type 1 PRCC, 5 cases of Type 2 PRCC and performed high-throughput microarray (Exiqon, Woburn MA) and quantitative real-time PCR analysis of miR expression levels (TaqMan, AB, Carlsbad CA). The data were subjected to statistical analyses and hierarchical clustering (Partek, St. Louis MO) revealing a discrete set of miRs that exhibited robust statistically significant changes in each PRCC type compared to normal renal tissue and other PRCC type.
Results: Sixteen miRs were differentially expressed amongst the 3 specimen classes. In type 1 PRCC, 4 miRs (including miR-105, $p<1.11x10^{-6}$ and miR-301b, $p < 1.33 \times 10^{-5}$) were increased 2.3 to 10.5 folds while 3 miRs (including miR-10b, $p < 2.91 \times 10^{-4}$) were decreased. In Type 2 PRCC, 4 miRs (including miR-105, $p<3.4x10^{-5}$ and miR-21, $p<1.44 \times 10^{-5}$) were increased 3.7 to 6.5 folds while 6 miRs (including miR-136, $p< 2.37 \times 10^{-5}$ and miR-559,$p< 1.98 \times 10^{-4}$) were decreased. miR-105 was common to both types and was increased 10.5 folds in type 1 PRCC and 6.5 folds in type 2 PRCC. The mRNA transcripts representing targets of these sixteen miRs displayed significant correlated expression changes (15 transcripts in type 1 and 32 in type 2) including CASP2, GRB2 (both increased) and NR3C2 (decreased).
Conclusions: In summary, this study indicates the important role of miR expression in regulating mRNA transcription in RCC. Common miR changes may play a role in PRCC formation. However, exclusionary differences in the miR expression profile may provide a basis for discriminating between the two types of PRCC.

943 Prognostic Values of Histologic Subtype and Other Clinicopathologic Features: A Study of 961 Patients with Renal Cell Carcinomas Treated by Radical Nephrectomy.

SS Shen, JY Ro, LD Truong, AG Ayala. The Methodist Hospital and Weill Medical College of Cornell University, Houston, TX.
Background: Several clinicopathologic features have been previously shown to be important prognostic factors in renal cell carcinoma (RCC). However, there remains significant controversy on their difference in prognosis among the three most common subtypes of RCC, namely clear cell, papillary and chromophobe RCC and whether histologic subtype is an independent prognostic factor. We investigated the clinicopathologic features, in particular the histologic subtype and their prognostic significance.
Design: We retrospectively reviewed clinicopathologic features of 961 consecutive patients with RCC treated by radical nephrectomy (1990-2009). The features studied include patients' age and sex, TNM stage of tumor, tumor size, Fuhrman nuclear grade, vascular invasion, margin status, and sarcomatoid changes. Univariate and multivariate Cox regression analysis was performed to evaluate the independent significance of each variable.
Results: Of the 961 patients with RCC, 751 (78.2%), 126 (13.1%), 64 (6.7%), and 20 (2.0%) had clear cell, papillary, chromophobe, and other RCC, respectively. There were no significant differences in patients' age or tumor size among the three most common subtypes of RCC. There was a higher percentage of chromophobe RCC in female than clear cell and papillary RCC ($P<0.05$). There were higher percentages of local advanced stages (≥pT3) of clear cell RCC than papillary and chromphobe RCC ($P<0.05$). The 5-year survival rates were 62%, 52%, 86% for clear cell, papillary and chromophobe RCC, respectively. Type 1 papillary RCC has significant better survival than type 2 (63% vs. 33%). Features that were shown to be significant prognostic factors in multivariate analysis include: patients' age and sex, histologic type, TNM stage, Fuhrman nuclear grade, sarcomatoid changes, vascular invasion and positive margin.
Conclusions: In addition to patients' age, sex, TNM stage, Fuhrman nuclear grade, sarcomatoid change, vascular invasion, positive margin, *histologic subtype* is an independent prognostic factor in patients with RCC. As a group, papillary RCC has a worse prognosis than clear cell and chromphobe RCC, and type 2 papillary RCC has a worse prognosis than type 1 papillary RCC.

944 Common Diagnostic Problems in Interpretation of Early Invasive Bladder Cancer: A Consensus Study.

SS Shen, CC Guo, JY Ro, R Anton, L Cheng, O Hameed, LD Truong, J Huang, MA Weiss, F Lin, JR Srigley, JK McKenney, P Tamboli, DJ Grignon, RE Jimenez, M Zhou, GP Paner, P Troncoso, MB Amin, AG Ayala. The Methodist Hospital, Houston; UT M.D. Anderson Cancer Center, Houston; Univ. of Indiana, Indianapolis; Univ. of Alabama at Birmingham; Univ. of California Los Angeles; The Urology Group, Cincinnati; Geisinger Medical Center, Danville; Credit Valley Hospital, Mississauga, ON, Canada; Stanford Univ., Stanford; Mayo Clinic, Rochester; Cleveland Clinic; Univ. of Chicago; Cedars-Sinai Medical Center, Los Angeles.

Background: Diagnosis of early invasive bladder cancer in biopsy or transurethral resection of bladder tumor (TURBT) specimens is often problematic due to a variety of reasons.

Design: 26 cases of biopsy or TURBT specimens that were initially categorized as "suspicious for invasion" were selected for this study. Three photomicrographs of each case were reviewed by 19 genitourinary (GU) pathologists and 17 senior pathology residents/fellows (PGY3 or above). A uniform answer sheet was provided to participants and each case was recorded as either an invasive or non-invasive cancers. The results were summarized and comparison of diagnosis of each case by GU pathologists and senior pathology trainees was made by Fisher's exact test.

Results: Among the 26 cases of "suspicious for invasion", 9 and 8 cases were diagnosed as invasive or non-invasive carcinoma respectively by at least 15 of the 19 GU pathologists. The remaining 9 cases were diagnosed as invasive tumors by 42.1% to 73.4% (average 53.8%) GU pathologists. The most common shared features of the 9 invasive carcinomas were: high grade nuclear features, alteration of cytoplasm, subepithelial nests with angulated edges, peritumoral clefting, confluent growth, and dense desmoplasia. The most common shared features that had the least agreement were cases with severe cautery and crush artifact and marked inflammation. In 10 of 26 (38.5%) cases, there was statistically significant diagnostic discordance between GU pathologists and senior pathology residents/fellows ($p<0.05$), including both over diagnoses and under diagnoses of invasion.

Conclusions: Our study highlighted the significant problems in evaluating early invasive bladder cancer and identified features that are the most helpful to GU pathologists for a more definitive diagnosis of invasion. Furthermore, problems of over- and under-diagnosis are frequent among the senior pathology trainees, necessitating focused training and education.

945 Histopathologic Features of Preoperative Transurethral Prostatic Urethral Biopsy Specimens in Patients with Bladder Cancer.

SS Shen, JY Ro, AG Ayala. The Methodist Hospital and Weill Medical College of Cornell University, Houston.

Background: The finding of prostatic involvement by urothelial carcinoma (UCa) preoperatively is very important for surgical planning especially the decision to do a radical cystectomy. Although transurethral biopsy of the prostatic urethra is commonly performed for patients with bladder cancer, the histopathologic findings of prostatic urethra have not been well characterized. This study summarizes the results of histopathologic features of large series of consecutive prostatic urethra biopsies.

Design: Preoperative prostatic urethral biopsies were performed at 5:00-7:00 o'clock along the prostatic verumontanum. A total of 241 preoperative prostatic urethra biopsies (1988-2009) were reviewed. The histopathologic features were evaluated and summarized.

Results: Prostatic involvement of UCa was identified in 64 of 241 (26.6%) consecutive prostatic urethra biopsy specimens: 41 (64%) of these were urothelial carcinoma in-situ and 23 (36%) were invasive UCa. Prostatic adenocarcinoma was identified in 3 patients, 2 of which were ductal (endometroid) types and 1 were acinar adenocarcinoma. Other lesions identified were one each of urethral low grade non-invasive papillary urothelial carcinoma, nephrogenic adenoma, and prostatic urethral polyp.

Conclusions: Prostatic involvement by UCa is a common finding in patients with bladder cancer. Using the appropriate sampling strategy, the biopsy can detect the majority of the prostatic involvement by UCa. In addition, incidental prostate adenocarcinomas, low grade urothelial carcinoma and benign lesions such as nephrogenic adenoma and prostatic urethral polyp may also be identified.

946 Global Gleason Score on Prostate Needle Biopsies as Predictor of Prostatectomy Gleason Score: Comparison with Highest Gleason Score, Greatest-Percent and Largest-Length Gleason Scores.

MM Shevchuk, A Strivastava, A Tewari. Weill Cornell Medical College, New York, NY.

Background: According to the literature, the Gleason score on prostate needle biopsies predicts the exact prostatectomy Gleason score in 50-70% of cases, when assessed by genitourinary pathologists. The Gleason score is +/- 1 from the biopsy Gleason score in 85+% of cases. If different Gleason scores are reported on different needle biopsy cores, the urologists usually use the highest Gleason score (hi Gl) to predict the prostatectomy Gleason score and for use in nomograms. The literature also supports the use of the Gleason score of the core with the largest percent of tumor (hi % Gl), or of the core with the longest length of tumor (long Gl). The global Gleason score (gl Gl) reflects the primary and secondary patterns on all of the cores, taken together. We compared all these methods as to their ability to predict the prostatectomy Gleason score.

Design: Prostate biopsies with different Gleason scores and the subsequent prostatectomies from a single urologist's practice were reviewed by a single uropathologist. A gl Gl, hi Gl, hi % Gl, and long Gl was assigned to each of 44 Gleason-score-discordant cases, and these were compared to the prostatectomy Gleason score.

Results: The exact Gleason score and the exact component primary and secondary Gleason patterns were identified by gl Gl in 66% of cases, by hi Gl in 61% of cases, by hi % Gl in 50% of cases, and by long Gl in 48% of cases. If only the Gleason scores were compared (without consideration of primary and secondary patterns), the concordance with prostatectomy Gleason score was: 89% for gl Gl; 84% for hi Gl; 68% for hi % Gl; and 66% for long Gl. The difference in predictive value for gl Gl and for hi Gl was not statistically significant, because these two methods identified the identical primary and secondary patterns in 61% of cases, and the same Gleason score in 93% of cases in our series.

Conclusions: Global Gleason score is slightly better, but similar to the hi Gl in predicting prostatectomy Gleason score, and both methods outperform the hi % Gl and long Gl methods. Recording the gl Gl on the biopsy report may give the urologist additional information for therapy choices, in cases such as those with a hi Gl of 4+4 but gl Gl of 4+3, or a hi Gl of 4+5 but gl Gl of 4+3, with tertiary 5.

947 Enrichment of Cancer Stem Cells in Urothelial Carcinoma and Small Cell Carcinoma of the Urinary Bladder.

Q Si, L Xiao, Y Bondaruk, Y Wang, B Czerniak, CC Guo. University of Texas MD Anderson Cancer Center, Houston.

Background: Recent studies have shown that most human cancers originate from a few cancer-initiating cells or cancer stem cells (CSCs). To understand the role of CSCs in bladder cancer, we determined the expression of aldehyde dehydrogenase 1 (ALDH1), a CSC marker, in urothelial carcinoma (UC) and small cell carcinoma (SmCC) of the urinary bladder.

Design: Tissue microarray blocks were constructed using urinary bladder specimens, which included UC (n=143), SmCC (n=19), and normal urothelium (n=11) tissue. Three 1.0-mm tissue cores were obtained from each case. Four-mm tissue microarray slides were used for immunohistochemical staining with ALDH1 (BD Transduction Laboratories, San Jose, CA). Cases were considered positive if more than 5% of analyzed cells showed robust immunostaining signaling for ALDH1 in the cytoplasm.

Results: The mean UC patient age was 66 years (range, 27-85 years). UC tumors were noninvasive in 90 cases, invasive in 53, high grade in 109, and low grade in 34. The mean SmCC patient age was 68 years (range, 34-90 years). No normal urothelial cells (0 of 11) showed immunoreactivity for ALDH1 on immunostaining, but 17% of UC samples (24 of 143) were positive. ALDH1 immunoreactivity was significantly higher in invasive UC (38%) than in noninvasive UC (4.7%) ($p<0.05$), but there was no significant difference between high- and low-grade UC. In addition, 55% of SmCC samples (10 of 19) were positive for ALDH1, which was significantly higher than in invasive UC ($p<0.05$).

Conclusions: Our results suggest that CSCs are present in UC of the urinary bladder. CSCs are more commonly present in invasive UC than in noninvasive UC, suggesting that they play an important role in UC progression. The enrichment of CSCs in SmCC raises the possibility that SmCC may have a close association with CSCs.

948 Asparagine Synthetase Is a Target in Castration Resistant Prostate Cancer.

K Sircar, H Huang, D Cogdell, J Dhillon, V Tzelepi, N Navone, T Bismar, H Koumakpayi, F Saad, A Aprikian, P Troncoso, W Zhang. UT MD Anderson Cancer Center, Houston, TX; UT Arlington, TX; University of Calgary, AB, Canada; University of Montreal, QC, Canada; McGill University, Montreal, QC, Canada.

Background: Recent developments in the treatment of the lethal, castration resistant phenotype of prostate cancer (CRPC) have largely focused on abrogating the androgen signaling axis. Novel targets that work by a different mechanism are also needed for this therapy resistant phase of disease. Gene expression studies, with an inherent high false discovery rate, have been further hindered by the paucity of frozen CRPC samples. We sought to narrow the list of candidate genes to those that are biologically meaningful and potential drivers by integrating DNA copy number with mRNA expression and to validate our results at the proteomic level.

Design: Clinical samples and xenografts of locally advanced CRPC tissues from 27 patients were interrogated using high throughput molecular profiling platforms: DNA copy number was assessed by high resolution aCGH (Agilent 244K); the transcriptome was studied using whole genome gene expression microarray (Agilent 44K). We compared our expression data to existing GEO datasets of CRPC. Validation of the proteins of interest was performed using reverse phase protein lysate arrays (RPPA) on frozen samples from 25 patients and immunohistochemistry on tissue arrays from 120 unique CRPC patients.

Results: Our integrative analysis of overexpressed (n=711) and amplified (n=2171) genes in CRPC showed only 32 genes with both increased copy number and mRNA overexpression, including (predictably) the androgen receptor. The asparagine synthetase (ASNS) gene was prioritized for further study as it survived both our integrative genomic analysis and was overexpressed in other CRPC datasets. Validation at the protein level by both RPPA and IHC methods showed ASNS to be significantly overexpressed in CRPC ($p<0.05$) of both adenocarcinoma and small cell carcinoma histologies. Further, we identified parent/mouse xenograft models of CRPC that possess and lack ASNS overexpression, respectively.

Conclusions: We have identified and validated asparagine synthetase as a novel target in both glandular and small cell CRPC. Future functional studies using asparagine depletion strategies may be performed using our identified xenograft model system.

949 The Expression and Prognostic Significance of RalA and RalB Expression in Bladder Cancer.

SC Smith, MD Nitz, AS Baras, DT Theodorescu. University of Michigan Health System, Ann Arbor; University of Virginia Health System, Charlottesville; University of Colorado, Aurora.

Background: The Ral family of GTPases, including RalA and RalB, have been established as key mediators of cancer phenotypes in several tumors, while we have identified roles for both in models of metastatic progression of bladder cancer. Despite these findings, the expression of these GTPases has not been examined in human bladder tumor samples.

Design: A tissue microarray consisting of 145 quadruplicate cores of human bladder cancer cystectomy specimens (urothelial N=110, squamous N=22, adenocarcinoma N=7, other N=6), with paired staging and follow-up data, was stained for RalA and RalB using paralog-specific antibodies. Staining intensity was scored semiquantatively as low or high. Association between staining and clinicopathologic parameters was tested by the chi-squared test and Gehan-Wilcoxon-Breslow tests, as appropriate.

Results: RalA and RalB variably stained both cytoplasmic and membrane compartments of tumor cells, and were not strongly correlated (P=0.10). Neither RalA nor RalB were significantly associated with gender, pT, pN, LVSI, or concomitant CIS. RalB, but not RalA, was significantly associated with histologic type of bladder cancer (P=0.009), with strong staining in squamous carcinomas and adenocarcinomas. RalA, but not RalB, staining was significantly associated with decreased survival post cystectomy in urothelial carcinomas (P=0.04), but not in non-urothelial tumors (P=0.37).

Conclusions: While the Ral GTPase activity may be regulated by mechanisms other than expression, our findings associate overexpression of RalA with decreased patient survival, supportive of the relevance of prior experimental findings to human disease. Association of RalB with non-urothelial histology was unexpected and suggests investigation in this area.

950 Urine microRNAs Are Sensitive and Specific for Bladder Cancer: Results of a Pilot Study.

J Snowdon, X Zhang, J Izard, A Boag, R Siemens, H Feilotter. Queen's University, Kingston, ON, Canada.

Background: Bladder cancer is the second most common urologic tumour. Voided urine cytology along with direct visualization of the bladder with cystoscopy are the primary methods for diagnosis and surveillance. However, the invasiveness of cystoscopy along with the poor sensitivity of cytology make these tests suboptimal. The aims of this pilot study are to determine whether urine microRNAs can be used to distinguish between patients with known bladder cancer and normal controls.

Design: Firstly, voided urine samples were collected from 8 patients with urothelial carcinoma and 5 control patients. Total RNA was isolated and quantitative RT-PCR was performed using primers for 4 microRNAs shown previously to be dysregulated in solid urothelial carcinomas with RNU6B as the endogenous control. Subsequently, those microRNAs that showed the highest fold change were investigated in an independent set of samples (n=8).

Results: Two microRNAs were found to be dysregulated in the urine from cancer patients with miR-A showing an average 10.42-fold decrease ($p<0.05$) and miR-B showing an average 2.70-fold increase (p=0.30) in the cancer samples compared to the normal controls. Using these 2 microRNAs, a prediction model was generated yielding an accuracy of 100%. When tested with an independent set of samples (5 with urothelial carcinoma and 3 controls), the levels of miR-A and miR-B enabled the detection of bladder cancer from urine with a sensitivity of 80% and a specificity of 100%.

Conclusions: This pilot study demonstrates that microRNAs are dysregulated in voided urine from cancer patients. Based on our prediction model which exploits the dysregulation of two microRNAs, we are able to detect bladder cancer from urine with a high sensitivity and specificity.

951 Urinary Met Level as a Novel Biomarker for Urothelial Carcinoma of the Bladder.

M Sorbellini, B McNeal, G Athauda, B Cohen, A Giubellino, H Simpson, J Coleman, RH Getzenberg, GJ Netto, MW Linehan, PA Pinto, DP Bottaro. National Cancer Institute, Bethesda, MD; Memorial Sloan Kettering Cancer Center, New York, NY; Johns Hopkins University, Baltimore, MD.

Background: Urothelial carcinoma (UrCa) of the bladder continues to be a major cause of mortality and morbidity in the US. Non invasive molecular markers that can improve upon current approaches for detection and surveillance are crucially needed. This study aims to determine whether soluble urinary Met (sMet) can differentiate between benign urinary bladder conditions and urinary bladder cancer. Correlation of sMet levels with UrCa tumor grade and stage is also assessed.

Design: Urinary samples from patients with and without UrCa from three different institutions were prospectively collected prior to cystosopy, transurethral resection of bladder tumor (TURBT) or cystectomy. sMet levels were determined using electrochemiluminescence immunoassays. sMet levels were normalized to urinary creatinine values. Normalized Met values were compared to final pathologic stage and grade. AUC values were obtained comparing patients with and without UrCa.

Results: Urinary sMet levels accurately differentiated between patients with and without UrCa (AUC: 78%, sensitivity, specificity and negative predictive value were: 68%, 78% and 95%, respectively), patients with no UrCa and those with lamina propria invasion (AUC: 79%, sensitivity, specificity and negative predictive value were: 65%, 81% and 95%, respectively) and patients with no UrCa and those with muscle invasive disease (AUC: 85%, sensitivity, specificity and negative predictive value were: 75%, 83% and 97%, respectively).

Conclusions: Urinary sMet level may provide a new biomarker for UrCa of the bladder. sMet levels accurately distinguish patients with UrCa from those without, and between patients with different tumor stages. These results suggest that urinary sMet may have utility as a bladder cancer marker for screening, treatment follow-up and clinical trial design.

952 Does Gleason Grade Progress over Time?

MJ Stampfer, K Penney, J Sinnott, R Flavin, J Stark, S Finn, E Giovannucci, H Sesso, M Loda, L Mucci, M Fiorentino. Dana Farber/Harvard Cancer Center, Boston, MA.

Background: Pathologists have speculated on whether prostate cancers arise as well differentiated tumors, and then progress, or whether grade is an early and unchanging feature. This cannot readily be addressed through repeated biopsy, due to selection of subjects and heterogeneity of tumor within the prostate. However, the advent of PSA screening affords the opportunity to assess this issue on a population level. PSA screening provides a lead time of 10-12 years, and widespread screening has dramatically reduced the number and proportion of tumors diagnosed at advanced stage. If Gleason grade progresses, one would expect a similar reduction in high grade tumors.

Design: We studied 1,077 US participants in the Physician's Health Study and the Health Professionals Follow-up Study, diagnosed between 1982 and 2005, and treated with prostatectomy. Using the ISUP 2005 revised criteria, we re-reviewed H&E slides to assign major and minor Gleason grades, blinded to clinical outcome, to avoid the problem of the shift in Gleason scoring over the past several decades. We assessed clinical stage at diagnosis from medical records. We compared the distribution of grade and stage across four time categories, to span the pre- and PSA eras.

Results: As expected, the proportion of tumors diagnosed at advanced stage dropped dramatically. In the earliest period (1982-1992, pre-PSA) 19.6% were Stage T3 or higher. This proportion decreased steadily until the last period (2000-2005), with only 2.3% of tumors Stage T3, and none Stage T4 or M1. In contrast, the proportion of Gleason grade 8-10 decreased only modestly, from 21.1% in the first period to 14.3%.

Conclusions: The dramatic shift in stage at diagnosis after introduction of PSA screening was accompanied by only a modest shift to lower Gleason scores. On a population basis, these finding suggest that Gleason grade may be established early in the pathogenesis of prostate tumors. This finding has implications for our understanding of prognosis and of tumor progression.

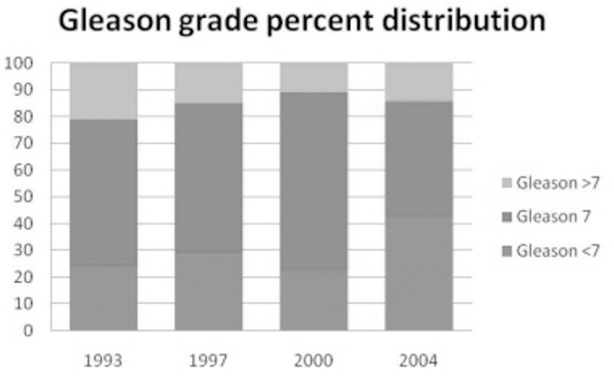

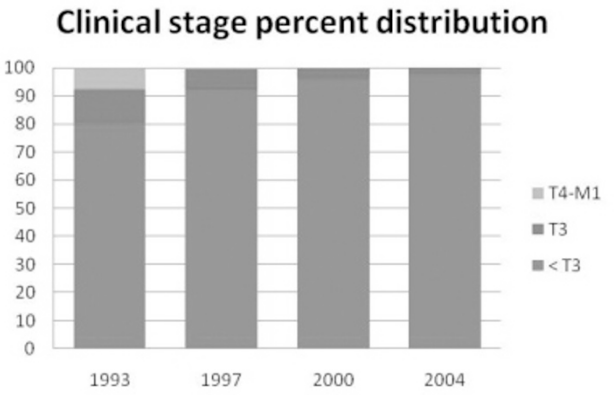

953 Alternative Pathways of Akt Pathway Activation in HPV Positive and Negative Penile Carcinomas.

E Stankiewicz, D Mesher, M Ng, J Cuzick, D Prowse, F Hiscock, Y-J Lu, W Lam, N Watkin, C Corbishley, DM Berney. Barts and The London School of Medicine, Queen Mary, University of London, United Kingdom; St George's Hospital, London, United Kingdom.

Background: The pathogenesis of penile cancer (PC) is not well understood, and although risk factors include human papillomavirus (HPV) the pathogenesis of HPV negative cancers is not understood. Disruption of the HER/PTEN/Akt pathway is present in many cancers, however, there is little information on its function in PC. Therefore,

we investigated the status of HER family receptors and phosphatase and tension homolog (PTEN) in HPV-positive and negative PC and its impact on Akt activation, using fluorescent in situ hybridisation (FISH) and immunohistochemistry to examine differences in HPV positive and negative carcinomas.
Design: 148 PCs from St George's Hospital were tissue microarrayed and immunostained for phosphorylated EGFR (pEGFR), HER2, HER3, HER4, phosphorylated Akt (pAkt) and Akt1 proteins. Immunostains were assesed semi-quantitatively. EGFR and PTEN gene status was also evaluated using the FISH probes LSI EGFR (7p12)/CEP 7 Dual Color Probe and the LSI PTEN (10q23) / CEP 10 Dual Color Probe. FISH slides were scanned and a minimum of 100 cells with clear hybridization signals were counted per tumour core. HPV presence was assessed by a broad-spectrum HPV PCR method using SPF10 primers.
Results: pEGFR protein expression was positive in 25% of patients and significantly correlated with activated Akt (p<0.0001). There was no EGFR gene amplification. HER2 was not detected. HER3 (p=0.0054) and HER4 (p=0.0002) receptors significantly correlated with cytoplasmic Akt1 expression. All three proteins positively correlated with tumour grade (HER3, p=0.0029; HER4, p=0.01118; Akt1, p=0.0001). PTEN protein expression was reduced or absent in 62% of tumours. PTEN gene copy loss was present at different levels in 46% of tumours and did not correlate with PTEN protein expression. HER3 expression positively (p=0.0128) and pEGFR (p=0.0143) negatively correlated with HPV. HER4, pAkt, Akt and PTEN expression were not related to HPV.
Conclusions: HER3 and HER4 are the main HER receptors involved in PC. Both receptors work through the Akt1 pathway and may lead to increased tumour grade. EGFR may play a role in early stages of the disease. HER2 is not involved in penile carcinogenesis. HPV-positive tumours mainly rely on the HER3 receptor to activate Akt pathway, while HPV-negative cancers seem to depend more on EGFR.

954 Adiponectin Receptor 2 Expression Predicts Lethal Prostate Cancer.

JR Stark, SP Finn, J Ma, JA Sinnott, F Schumacher, R Lis, KL Penney, JL Kasperzyk, HD Sesso, MJ Stampfer, EL Giovannucci, M Loda, LA Mucci. Brigham and Women's Hospital, Boston, MA; University of Dublin, Trinity College, Dublin, Ireland; Harvard School of Public Health, Boston, MA; UCLA Keck School of Medicine, Los Angeles, CA; Dana-Farber Cancer Institute, Boston, MA.
Background: We previously showed that adiponectin, an adipokine, is inversely associated with adiposity and prostate cancer (PCa) risk and progression. Polymorphisms in *ADIPOQ*, the gene encoding adiponectin, are associated with PCa risk and plasma adiponectin levels. Little is known about the role of adiponectin or its receptors locally in the prostate. We assessed adiponectin receptor 2 (ADIPOR2) tumor expression, as well as genetic variation in *ADIPOQ* and in adiponectin receptor genes *ADIPOR1* and ADIPOR2 with respect to PCa survival.
Design: Using TMAs from 753 archival prostatectomy specimens from men in the Physicians' Health Study (PHS) and Health Professionals Follow-up Study, we semi-quantitatively scored tumor expression of ADIPOR2 protein by immunohistochemistry. Among 1286 cases from PHS we evaluated 29 common SNPs in *ADIPOQ, ADIPOR1* and *ADIPOR2*. We related genotype and ADIPOR2 expression with development of lethal PCa during 25 years of follow-up using Cox proportional hazards models. Using ANOVA, we also evaluated each genotype in relation to tumor expression of ADIPOR2 for a subset of 180 cases.
Results: Men with greater waist circumference had increased tumor expression of ADIPOR2. ADIPOR2 expression was positively associated with Gleason score (p=0.05) and Ki67 expression (p=0.001). Controlling for age at diagnosis, Gleason, Ki67 expression and BMI, hazard ratios (HR) for lethal PCa comparing cases in the 3rd and 4th quartiles of ADIPOR2 expression to those in the lowest quartile were 5.5 (95% CI. 1.7 -18.9) and 3.8 (95% CI: 1.1-13.3), respectively. Two of 29 polymorphisms evaluated, one in *ADIPOR1* (rs16850799) and one in *ADIPOR2* (rs1044471), were significantly associated with time to lethal PCa. For ADIPOR2 rs1044471, HRs compared to wildtype homozygotes were 0.6 (95% CI: 0.4, 0.9) for heterozygotes and 0.8 (95% CI: 0.6, 1.2) for rare homozygotes (likelihood ratio p=0.03). Variant carriers of *ADIPOR2* rs1044471 had significantly lower ADIPOR2 expression (p-trend=0.02).
Conclusions: ADIPOR2 predicts lethal PCa independently of other prognostic markers. Variant allele status in *ADIPOR2* rs1044471 predicted ADIPOR2 expression levels and lethal PCa in the anticipated direction. Our work suggests a role of germ-line variation in adiponectin and its receptors, circulating adiponectin levels, and local prostatic expression of ADIPOR2 in aggressive PCa.

955 The Role of Periprostatic and Periseminal Vesicle Lymph Node Metastasis in the Staging and Prognosis of Prostate Cancer.

MK Subik, JL Yao, PA di Sant'Agnese, H Miyamoto. University of Rochester, NY.
Background: Pelvic lymph node (LN) metastases in prostate cancer (PC) are associated with a poor prognosis. Periprostatic (PP)/periseminal vesicle (PSV) LNs are occasionally found in radical prostatectomy (RP) specimens, but the significance of their involvement by PC metastases is poorly understood.
Design: We searched the Surgical Pathology database of our institution from August of 2002 to June of 2010 and identified 33 RP cases (age range: 51-70 years; mean: 62.8 years) where PP/PSV LNs had been assessed.
Results: Of the 33 patients, 20 (60.6%) had a single PP/PSV LN, whereas 13 (39.4%) had multiple (up to 8) LNs. Their size ranged from 0.1 to 1.8 cm (mean: 0.47 cm). The location was determined in 27 LNs: 11 (40.7%) on the right and 16 (59.3%) on the left; and 2 (7.4%) at apex, 6 (22.2%) at mid, 12 (44.4%) at base, and 7 (25.9%) at SV. Of the 20 PP LNs, 16 (80.0%) were located posteriorly, the remaining 4 (20.0%) were anteriorly, and none were laterally. Six of 33 (18.2%) patients had metastasis to the PP/PSV LNs. All of these were involved by metastasis, but not by contiguous extension of the tumors. Two of these 6 cases additionally had metastases to the pelvic LNs. Another patient had a metastasis in a pelvic LN, but not in PP/PSV LNs. The 6 LNs with metastasis included 4 PP (2 at posterior apex; 2 at posterior base) and 2 PSV. The maximal size of the metastatic tumor in each PP/PSV LN ranged from 0.05 to 1.0 cm (mean: 0.29 cm). All the patients with PP/PSV LN metastasis, except one [pT2c/ Gleason score (GS) 7], were of advanced pathologic stage with a grade of GS7 or higher (1 pT3a; 5 pT3b). Despite undergoing adjuvant radiotherapy, one of the 4 cases with limited PP/PSV LN metastasis was radiologically found to develop pelvic LN metastasis 11 months after RP. In contrast, 27 cases without PP/PSV LN involvement were of lower grades (12 GS6; 14 GS7; 1 GS8) (p=0.0648) and stages (19 pT2; 5 pT3a; 3 pT3b) (p=0.0248), and none of them developed biochemical/clinical recurrences with a mean follow-up of 12.8 months.
Conclusions: PP/PSV LNs were uncommon, but isolated PC metastasis to these LNs could occur. PP/PSV LN metastases correlated with advanced disease. Further studies including larger patient cohorts with longer follow-up are necessary to validate the current findings. However, PCs with metastases limited to PP/PSV LNs may need to be staged as "N1". In addition, the potential difficulty of grossly identifying the PP/PSV LNs, even in the presence of metastasis, suggests the importance of thorough histological examination of RP specimens.

956 Frozen Section Assessment in Testicular and Paratesticular Lesions Suspicious for Malignancy: Its Role in Preventing Unnecessary Orchiectomy.

MK Subik, J Gordetsky, JL Yao, PA di Sant'Agnese, H Miyamoto. University of Rochester, NY.
Background: Men with testicular and paratesticular lesions clinically suspicious for malignancy may benefit from a frozen section assessment (FSA) in order to spare unnecessary orchiectomy. The purpose of this study is to investigate the role of FSA in suspected testicular/paratesticular tumors.
Design: We performed a retrospective review of intraoperative testicular and paratesticular FSAs performed at our institution between the years 1993-2010.
Results: FSAs were performed on 41 testicular lesions [age: 5-60 (mean 32.5) yr; lesion size: 0.5-9.7 (mean 2.1) cm] and 19 paratesticular lesions [age: 26-76 (mean 43.3) yr; lesion size: 0.4-11.0 (mean 2.8) cm] prior to the decision to complete radical orchiectomy. Benign/malignant diagnoses on FSA were reported in 25/16 testicular cases and 16/3 paratesticular cases, respectively. Of the 25 benign testicular FSAs, 6 cases resulted in orchiectomy. Permanent diagnoses on the 6 orchiectomy specimens included epidermoid cyst (2 cases), large cell calcifying Sertoli cell tumor, fibrous pseudotumor, abscesses, and sarcoidosis. Of the 16 malignant testicular FSAs, orchiectomy was performed in 13 cases with germ cell tumor, but not in the remaining 3 cases with lymphoma. Of the 16 benign paratesticular FSAs, 2 cases, both fibrous pseudotumors, resulted in orchiectomy due to questionable viability of the testicles. In an additional paratesticular lesion, a malignant diagnosis of small round blue cell neoplasm made on FSA resulted in orchiectomy and then the final diagnosis was revised to reactive changes. There were statistically significant differences in the size of the testicular (p=0.001) or paratesticular (p<0.001) lesions between benign and malignant FSAs. Similarly, among the 16 cases with benign diagnosis on paratesticular FSA, the ages of the patients (p=0.031) or the sizes of the lesions (p=0.065) were different between 14 cases of excisional biopsy only vs. 2 cases of ultimate orchiectomy. Additionally, 34 FSAs were performed directly on orchiectomy specimens, including 26 malignant neoplasms, 6 benign neoplasms, and 2 other benign conditions.
Conclusions: An orchiectomy was performed in six testicular and two paratesticular cases despite a benign diagnosis on FSA. Thus, in 33 of 41 (80.5%) cases with benign FSAs in addition to all 3 cases of lymphoma, orchiectomy was successfully avoided. In a paratesticular case, a false-positive diagnosis resulted in unnecessary orchiectomy. Further analyses revealed that the size of the lesions was associated with the risk of malignancy.

957 ERG Rearrangement Status Is Associated with Castration Resistant Prostate Cancer.

MA Svensson, S Perner, J-M Mosquera, K Fall, LA Mucci, S-O Andersson, O Andren, J-E Johansson, MA Rubin, JR Stark. Orebro University Hospital, Orebro, Sweden; Bonn University Hospital, Germany; Weill Cornell Medical College, New York, NY; Karolinska Institutet, Stockholm, Sweden; Harvard School of Public Health, Boston, MA; Brigham & Women's Hospital, Boston, MA.
Background: Since the discovery of the *TMPRSS2-ERG* gene fusion in prostate cancer (PCa) studies have investigated associations between the fusion and clinical outcome of PCa with discrepant results. Most studies show that having the fusion is a sign of a more aggressive disease, but some report that the fusion is associated with more favorable prognostic markers. Few studies have examined the association between fusion-positive cancer and castration resistant disease, despite strong biologic rationale given that *TMPRSS2* is androgen regulated. We aimed to investigate if there is an association between fusion status and time to castration resistance.
Design: We utilized 154 patients who were hormonally treated and had data on fusion status available from the Swedish Watchful Waiting cohort that includes PCa cases diagnosed with T1a or T1b cancer with TURP between 1977-99. Castration resistant disease was classified as two consecutive rises in PSA >3ng/ml after hormonal therapy. Fusion status was assessed by FISH using an *ERG* break-apart assay.
Results: We found an overall *ERG* rearrangement frequency of 25% (59% rearranged through insertion and 41% through deletion). During a median of 5.5 years, 100 men on hormonal therapy became castration resistant. *ERG* rearrangement was more common among men who developed castration resistant disease (30.4% vs. 15.4%; p=0.04). Having the rearrangement led to a 75% increase in risk of becoming castration resistant (95% CI: 1.14-2.70). Adjusting for Gleason score, age at diagnosis, calendar year at diagnosis and T-stage, men with fusion-positive tumors were 52% more likely to become

castration resistant (95% CI: 0.97-2.38). The attenuation was mainly due to adjustment for Gleason score. Stratifiying according to the two rearrangement mechanisms, we found the increase in risk was limited to those with rearrangement through insertion.
Conclusions: Hormonally treated PCa patients having an *ERG* rearrangement have a significantly increased risk of becoming castration resistant compared to patients without the rearrangement. The results from our study indicate that the *ERG* rearrangement is a sign of a more aggressive disease and could potentially be used to identify patients less likely to respond to hormone treatment.

958 Necessity and Usefulness of Pathological T1 Subclassfication in the Management of Bladder Urothelial Carcinoma.

H Takahashi, T Yamamoto, S Mizukami, M Furusato, S Egawa, M Fujime, H Hano. The Jikei University School of Medicine, Tokyo, Japan; School of Medicine, Juntendo University, Tokyo, Japan.
Background: Superficial urothelial carcinoma of urinary bladder is treated by transurethral resection (TUR) in contemporary urological practice. In the current TNM classification, T1 tumor is defined as invading subepithelial tissue, although it seems to contain various degrees of tumors from early microinvasion through massive invasive cancer.
Design: Primary urothelial carcinoma of urinary bladder obtained by TUR from 2000 through 2008 (n=772) was evaluated and pT1 tumor was chosen. Clinicopathological data were analyzed. Subclassification of pT1 was defined as follows; pT1a: microinvasion with width<5mm, depth<1mm, less than 5 invasive foci; pT1c: massive invasive tumor with >50% of invasive area; pT1b: between a and c. Cases of pT1b and c containing no muscularis propria in the specimens were omitted from this study. Recurrence-free, progression-free, and cause-specific survivals (RFS, PFS, and CSS) were assessed.
Results: 122 cases of pT1 tumors were identified and follow-up data (range: 36-120 months; median 48 m) were available in 105 cases. Median patients' age was 68y. Second-look TUR was not performed in most of the cases. They were subclassified as 46 of pT1a, 34 of pT1b and 25 of pT1c. In pT1a tumors, invasive areas were from 0.1x0.1mm to 4x1mm and foci ranged from 1 to 4. In pT1c tumors, % of invasive tumors ranged from 70 to 100%. RFS was not statistically significant among 3 groups. PFS of pT1c was significantly lower than pT1a and b. CSS of pT1c was significantly lower than pT1a. In pT1a tumor, 5-year RFS rate was 44% but PFS and CSS rates were 92 and 98%, respectively.

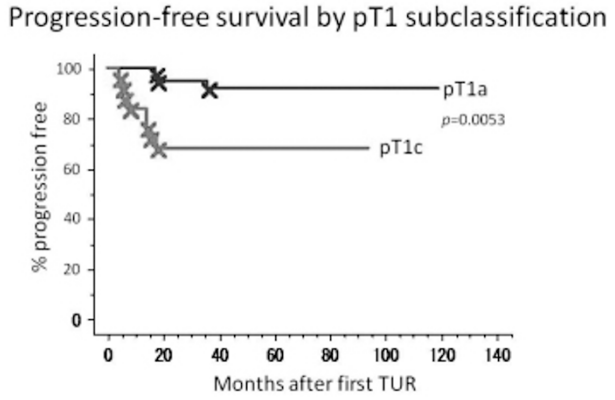

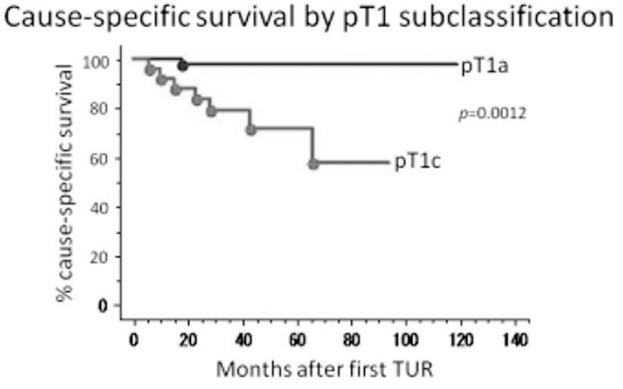

Conclusions: Subclassification of pT1 is necessary and useful in the management of bladder urothelial carcinoma. Second-look TUR without recurrent findings may not be necessary to pT1a tumor, whereas it should be done to pT1c tumor.

959 Antibody Based Detection of ERG Rearrangements in Prostate Core Biopsies, Including Diagnostically Challenging Cases.

SA Tomlins, N Palanisamy, K Suleman, AM Chinnaiyan, LP Kunju. University of Michigan Medical School, Ann Arbor.
Background: Fusions between the untranslated regions of androgen regulated genes and *ERG* occur in ~50% of prostate cancers (PCAs) and encode a truncated ERG product. By FISH, *ERG* rearrangements are 100% specific for PCA or HGPIN immediately adjacent to *ERG* rearranged carcinoma. Previous studies using monoclonal antibodies against ERG on prostatectomy specimens confirmed exquisite assocation between *ERG* gene rearrangement by FISH and ERG expression by immunohistochemistry (IHC). The current aim is to evaluate ERG expression by IHC on prostate core biopsies, including those with atypical foci.
Design: Unstained levels from 90 prostate needle biopsies containing PCA, HGPIN or atypical foci requiring IHC for diagnosis (using basal cell markers and AMACR) were stained with a monoclonal antibody against ERG (clone EPR 3864, Epitomics). Staining of vessels and lymphocytes was used as positive staining control.
Results: ERG expression was confined to PCA glands, HGPIN and atypical foci, with no expression in any unequivocal benign glands from all 90 evaluated biopsies, including 17 biopsies requiring IHC to confirm benign diagnoses. ERG was expressed in PCA glands in 18 of 42 (43%) biopsies, including 8 of 25 (32%) biopsies with small foci of PCA requiring IHC for diagnosis. ERG was expressed in HGPIN in 3 of 17 (18%) biopsies. Two of 15 (13%) biopsies with atypical foci, including 1 biopsy with HGPIN with adjacent small atypical glands (PINATYP) requiring IHC for diagnosis and 1 biopsy with foci diagnosed as atypical after IHC expressed ERG.
Conclusions: 1) By IHC, ERG shows increased cancer specificity compared to AMACR, with no background staining of benign glands. 2) ERG expression in an atypical focus supports a diagnosis of PCA. 3) Unlike AMACR, which is expressed in nearly all HGPIN foci, ERG is expressed in only a subset. 4) As *ERG* rearrangements and ERG expression in PIN in prostatectomy specimens is invariably associated with adjacent PCA, ERG expression in isolated HGPIN on biopsy may be associated with a higher risk of PCA on subsequent biopsy. 5) Prospective studies are ongoing to determine the value of ERG expression in combination with standard IHC for diagnostically challenging biopsies and for risk stratifying men with isolated HGPIN.

960 Raman Spectroscopy of Oncocytic Kidney Tumors.

M Tretiakova, S Stewart, J Maier. University of Chicago, IL; ChemImage Corporation, Pittsburgh.
Background: The differential diagnosis of malignant chromophobe renal cell carcinoma (ChRCC) and benign renal oncocytoma (ONC) can be challenging. Even though morphologically ChRCC and ONC significantly overlap, they are characterized by different genetic, ultrastructural and molecular composition. Raman Molecular Imaging (RMI) is a non-destructive optical technique based on the analysis of laser light scattered from a sample. This molecule-specific scattering allows elucidation of relative molecular proportions and biochemical bonds in a tissue, thus generating tissue-specific "fingerprints". We hypothesized that different molecular make-ups of ChRCC and ONC can be captured by RMI.
Design: Four micron unstained paraffin tissue microarray sections containing 25 cases of ChRCC and 7 ONC were subjected to RMI using Falcon II™ Wide-Field Raman Chemical Imaging System, and analyzed by ChemImage Xpert® software. For each case, represented by three 1 mm tissue cores, multiple RMI spectra were extracted, followed by principal component analysis (PCA). The true diagnoses were kept blinded during the data acquisition and processing steps. Additionally, we performed immunohistochemical staining with CK7 and CD117 antibodies.
Results: Evaluation of 615 spectra from 32 cases was expressed graphically in scatter plots after PCA, which, following several optimization steps, allowed classification of cases in either ChRCC or ONC group based on the values of principal component 3 (t-test, $p < 0.001$). There was 90% concordance between different spectra derived from each case. However significant overlap existed between two groups of tumors, and after unblinding of histology data 2 ChRCC and 2 ONC were found to be misclassified. Comparison of RMI and immunostaining with CK7 and CD117 is shown in a table.

Cross-validation of RMI vs cytoplasmic CK7 and membranous CD117 staining

Method	Sensitivity	Specificity	PPV	NPV	Accuracy
RMI	85.7%	76%	50%	95%	0.79
CK7	100%	60%	41%	100%	0.8
CD117	100%	64%	44%	100%	0.8

Conclusions: This is the first study attempting molecular "fingerprinting" of ChRCC and ONC. It appears that both tumors show very close, and often overlapping, spectral characteristics by RMI proving their biochemical similarity. However, correct molecular classification of these tumors was possible in 92% of ChRCC and 71% ONC cases. Comparison of RMI with well-established markers CK7 and CD117 demonstrated comparable accuracy, lower sensitivity, but higher specificity. The diagnostic utility of RMI needs to be further elucidated on a larger data set.

961 Sporadic Hybrid Oncocytic/Chromophobe Tumor (HOCT) of the Kidney – The Quest To Define It Continues!.

K Trpkov, M Brunelli, G Martignoni, A Yilmaz. University of Calgary, AB, Canada; Universitá di Verona, Verona, Italy.
Background: HOCT of the kidney have been typically described in patients with Birt-Hogg-Dubé syndrome and in renal oncocytosis. Although rare sporadic HOCT have also been described, it remains uncertain what is the spectrum of their features, their long-term behavior and if they are different or similar to the hybrid tumors in Birt-Hogg-Dubé and oncocytosis. To our knowledge, only one multiinstitutional study has attempted to better characterize sporadic HOCT (Virchows Arch 2010; 456:355-65).

Design: We studied 6 tumors from patients who had no clinical evidence of BHD or renal oncocytosis. The tumors showed oncocytoma-like appearances with focal chromophobe-like changes: perinuclear halos, nuclear irregularities (raisinoid nuclei) and/or prominent cell membranes. All tumors were diffusely positive for C-kit and, similar to oncocytoma, only rare cells were positive for CK7 (less than 5% of cells), which is different from the diffuse CK7 positivity in chromophobe renal cell carcinoma (RCC). We performed fluorescence in-situ hybridization (FISH) to evaluate the numerical chromosomal alterations in 5 of 6 cases.
Results: HOCT were identified in 3 males and 2 females (one male patient had bilateral solitary tumors). Mean patient age was 72 years (range, 57 to 83). All tumors were stage pT1 (4 were pT1a and 2 were pT1b). The tumors ranged from 3.2 to 6.5 cm (mean 4.5). On gross examination, 5 tumors were light-brown and 1 tumor was mahogany-brown. No central scar was seen grossly in any tumor. On light microscopy, 5 tumors showed combinations of solid and tubulo-alveolar growth patterns and 1 tumor was tubulocystic. All cases showed only luminal staining for colloidal iron (Müller-Mowry) of variable intensity, similar to oncocytoma. Parvalbumin was positive in 3/3 evaluated cases. In 3/5 tumors evaluated by FISH, there were multiple chromosomal monosomies (loss: 1, 6, 10; 2, 6, 10 and 1, 2, 6, 10), as typically seen in chromophobe RCC. In the remaining 2/5 cases evaluated by FISH, in addition to chromosomal losses (loss 1, 2 and 2, 6, 10, respectively), we also found chromosomal gains (gain: 6, 10, 17 and 1, 17, respectively). After a mean follow-up of 68 months (range, 36 to 109), no recurrence or metastatic disease were documented in any patient.
Conclusions: Sporadic HOCT of the kidney are indolent tumors which show features intermediate between oncocytoma and chromophobe RCC. Although some sporadic HOCT exhibit multiple chromosomal losses, similar to chromophobe RCC, some HOCT show chromosomal gains, similar to those seen in oncocytosis, but not in chromophobe RCC.

962 Under-Expression of Nuclear Matrix Protein Sp100: A Basis for Why Prostate Cancer Nuclei Look Different Than Benign Nuclei.

LD True, I Coleman, D Gifford, R Coleman, P Nelson. University of Washington, Seattle; Fred Hutchinson Cancer Research Center, Seattle.
Background: Nuclear histological features – nucleomegaly, nucleolomegaly, irregular nuclear membranes, and irregular coarse clumping of heterochromatin – distinguish cancer from non-cancer cells in such solid organs as the prostate. However, the molecular basis of these structural features is unknown. DNA aneuploidy is an insufficient explanation; only a minority of prostate cancers is characterized by changes in DNA ploidy. We hypothesized that changes in expression level of nuclear matrix proteins underlie the histologic features of carcinoma nuclei and, thus, might be used as molecular markers of cancer.
Design: Cancer and paired non-carcinoma luminal epithelial cells were laser-microdissected from 35 primary carcinomas of the prostate, Gleason grades 6 through 9. Amplified cDNA was hybridized to oligonucleotide microarrays. Samples from each adjacent tissue block were used to create tissue microarrays of formalin-fixed paraffin embedded tissue. Sections of this TMA and of 3 additional TMAs (50 prostate cancers altogether) were immunostained for nuclear matrix protein SP100 using a commercially available antibody (AbCAM. 1:800). SP100 expression levels were recorded on a 4-point scale (absent, faint/focal, intense in the minority or intense in the majority of cells). The median expression levels of cancer and non-cancer cells from all cases were compared.
Results: Nuclear matrix protein SP100 transcripts were differentially expressed to the greatest degree of all matrix genes, from 0.5 to 2-fold greater in normal luminal cells compared with paired cancer cells from 33 of the 35 same 10 prostates. Degree of expression did not correlate with the grade of the cancer. The median expression values of immunohistochemically defined protein in the TMAs was **faint** for cancer cells and **intense** in >75% of benign luminal cells.
Conclusions: We identified a nuclear matrix protein, SP100, which is expressed at lower levels in cancer cell nuclei compared with non-cancer luminal cell nuclei. Since SP100 inhibits expression of ets1, a transcription factor that enhances production of tissue matrix proteases, under-expression of SP100 by cancer cells may facilitate invasion by repressing SP100 mediated inhibition of protease expression. Our finding also begins to provide a molecular basis for the histologic features of cancer cells, which enable pathologists to microscopically distinguish cancer cells from non-cancer cells.

963 Growth Pattern: A New Prognostic Parameter of Clear Renal Cell Carcinoma.

T Tsuzuki, A Fukatsu, N Sassa, T Nishikimi, S Katsuno, T Fujita, Y Yoshino, R Hattori, M Gotoh. Nagoya Daini Red Cross Hospital, Japan; Komaki City Hospital, Japan; Nagoya University Hospital, Japan; Okazaki Municipal Hospital, Japan; Chukyo Hospital, Nagoya, Japan.
Background: Pathological tumor stage (pT), Fuhrman nuclear grade (FNG), lymph-vascular invasion (LVI) is thought to be useful prognostic parameter in clear cell renal cell carcinoma (CCRCC). Recently, we reported growth pattern could be a new prognostic parameter in pT1a CRCC. Herein, we assess the validity of growth pattern in CCRCC.
Design: In total, 501 patients with CCRCC without preoperative metastasis at five participating institutions were studied. Various clinicopathological parameters were analyzed in 293 patients with CCRCC without pre-operative metastasis to predict the disease-free survival rate (DFS) and the cancer-specific survival rate (CSS). Clinicopathological parameters included patient age, tumor size, pT, FNG, presence of capsule, presence of scarring, presence of hemorrhage, presence of necrosis, presence of LVI, and growth pattern (expansive or infiltrating). The expansive pattern was defined as when the tumor margin was well-circumscribed without the presence of normal renal tissue in the tumors. The infiltrative pattern was defined as when the tumor margin was ill circumscribed, and cancer cells were extensively infiltrating normal renal tissues. The infiltrative pattern was also defined as the presence of normal renal tissues in the tumors, regardless of tumor circumscription.
Results: Male to female ratio was 3.6. Patient's age ranged from 21 to 85 years (mean 60.1 years). Follow up duration ranged from one to 246 months (median 55.7 months). 59 patients showed distant metastasis. 35 patients were died with the disease. In the univariable analysis, Fuhrman grade (grade 1+2+3 vs. 4), LVI, growth pattern, and necrosis were parameters associated with a worse prognosis ($p<.0001$) in both the DFS and CSS. In the multivariate analysis, FNG (grade 1+2+3 vs. 4) ($p=0.0185$), necrosis ($p=0.0044$), and growth pattern ($p=0.0125$) were statistical significant in DFS. FNG (grade 1+2+3 vs. 4) ($p=0.0010$) and growth pattern ($p=0.0055$) were statistical significant in CSS.
Conclusions: In this study FNG and growth pattern were independent prognostic parameters in CCRCC. Growth pattern, a previously unrecognized parameter for prognosis, can be considered a new prognostic parameter in CCRCC.

964 Differential Expression of UBE2C and ASCL1 in Neuroendocrine Carcinoma and Adenocarcinoma of the Prostate in Xenograft Models and Human Samples.

V Tzelepi, S Maity, J Zhang, M Karlou, S Liang, A Hoang, J-F Lu, B Kleb, E Efstathiou, N Navone, A Aparicio, P Troncoso. UT MD Anderson Cancer Center, Houston, TX.
Background: Neuroendocrine carcinoma (NECa) of the prostate can emerge either de novo or as castrate-resistant progression of a typical acinar adenocarcinoma (AdCa) and has an aggressive clinical course. We used xenograft models obtained from castrate-resistant primary prostate carcinomas to gain an understanding of the pathways implicated in the emergence of NECa.
Design: Xenograft models with features of typical AdCa (n=3) and NECa (n=4) were subjected to gene-expression profiling using Affymetrix HGU133 Plus 2.0. One-way ANOVA was applied to identify differentially expressed probes (DEPs). The Web-based Gene Ontology (GO) Tree Machine was used to examine GO hierarchies. Selected genes were validated by quantitative real-time PCR (qRT-PCR) and immunohistochemistry in the xenografts, their respective donor tumors and a tissue microarray (TMA) containing cores from prostatectomy specimens with AdCa (n=42) and NECa (n=10).
Results: Unsupervised hierarchical clustering of the raw data classified the xenografts according to morphology. Using FDR 0.05, we identified 140 DEPs (0.3%) between the two groups. GO analysis on these DEPs revealed significant enrichment in the "M phase of mitotic cell cycle" biologic process subtree ($adjP=7.04e^{-08}$). Among them, UBE2C, a member of the anaphase-promoting complex (APC), was confirmed to be up-regulated, relative to AdCa, in NECa xenografts by both qRT-PCR ($p=0.036$) and immunohistochemistry ($p<0.001$). The APC is associated with increased expression of basic helix-loop-helix (bHLH) transcription factors; thus, we further examined the expression of ASCL1, a member of the bHLH family and a master regulator of neuronal differentiation. Expression of ASCL1 correlated with expression of UBE2C ($p=0.013$) and was higher in NECa than in AdCa xenografts ($p<0.001$). Up-regulated expression of both UBE2C and ASCL1 in NECa relative to that in AdCa was also found in the TMA of human samples ($p<0.001$), thus confirming preclinical findings.
Conclusions: Both UBE2C and ASCL1 are candidate biomarkers of prostatic NECa. Their up-regulated expression noted in xenograft models and, more importantly, in human samples of prostatic NECa, relative to that in AdCa, provides correlative evidence of a possible role in the emergence of the neuroendocrine phenotype of the disease in a subset of patients and implicates them as candidate therapeutic targets. Moreover, a mechanistic link between them is suggested by their correlation in NECa. Further elucidation of the role of ASCL1 and UBE2C in the pathogenesis of prostatic NECa is warranted.

965 miR-210 (Hypoxia-Responsive) a Marker of Poor Prognosis in Clear Cell Renal Cell Carcinoma.

VA Valera Romero, BA Walter Rodriguez, M Sobel, WM Linehan, MJ Merino. National Cancer Institute, NIH, Bethesda.
Background: Clear cell renal cell carcinomas are characterized by the inactivation or loss of the VHL protein. Such inactivation is usually followed by accumulation of hypoxia inducible factors (HIFs), mostly HIF1-A with a resulting pseudo-hypoxic state. Small non-coding RNAs (micro-RNAs) have been shown to be altered in response to hypoxia. Particularly, the hypoxia-responsive miR-210 has been described to be regulated in hypoxic tumors. In this study, we investigated the expression pattern of miR-210 in clear cell RCCs and other tumor types, and correlated its expression with HIFs and clinicopathologic characteristics.
Design: Forty-three tumor samples and corresponding normal kidney from 39 patients were evaluated. Samples included 21 sporadic clear cell RCCs, fifteen CCRCC arising in VHL syndrome, and 2 clear cell tumors in BHD patients. Three hybrid oncocytic tumors, one papillary type I and one tumor with sarcomatoid differentiation were also included for analysis. miR-210 and HIF-1A mRNA expression were evaluated by Real-Time PCR. A two-fold change compared to the adjacent normal kidney was considered significant. In some cases, IHC evaluation for HIF1-a was also included. Only HIF1-A nuclear accumulation was considered positive staining.
Results: Seventy-six per cent of tumors showed at least a 2-fold increase compared with normal kidney ($p<0.05$). On average, sporadic clear cell tumors showed an 8.1 fold increase compared to 12.1, 13.9 and 3.5 fold-change in clear cell VHL, sarcomatoid, and papillary tumors respectively. Clear cell tumors in BHD patients showed a 2-fold decrease, while no change was seen in hybrid oncocytic tumors. A higher increase on miR-210 levels was seen in patients with advanced disease ($p<0.05$) and with larger tumors. Low transcript levels (>2 fold-downregulation) for HIF1-a were seen in 13 sporadic cases and only two showed an increase in HIF1-a mRNA. Similarly, 11 out

of 15 of VHL cases (73%) showed at least a 2-fold decrease in transcript levels. In the cases where HIF1-a mRNA was elevated, a good correlation with IHC findings was obtained.
Conclusions: The hallmark of clear cell kidney tumors is the activation of the hypoxia pathway. Our results demonstrate that miR-210 is part of the hypoxic phenotype of these tumors. While miR-210 overexpression correlates with poor prognostic factors, the data also suggest that miR-210 could be used as a biomarker for the noninvasive evaluation of tumor hypoxia in renal cell carcinomas.

966 Radial Distance of Extraprostatic Extension Correlates with Biochemical Recurrence after Radical Prostatectomy.

BAMH van Veggel, IM van Oort, AJ Witjes, LALM Kiemeney, CA Hulsbergen-van de Kaa. Radboud University Nijmegen Medical Centre, Netherlands.
Background: No consensus exists on which method should be used to substage extraprostatic extension (EPE) in prostate cancer. We compared radial distance to other methods, and correlated these to biochemical recurrence (BCR) after radical prostatectomy.
Design: 157 consecutive prostate specimens with EPE were sectioned at 4 mm intervals and completely embedded. The radial distance of EPE was measured by an ocular micrometer. Focal and established EPE were also determined according to the criteria of Epstein and to the criteria of Wheeler. 23 patients with adjuvant therapy or detectable postoperative PSA levels were excluded, leaving 134 patients for BCR analysis. Data were analyzed using Kaplan-Meier survival and Cox regression analyses.
Results: Radial distance ranged from 0.1 to 11.0 mm (median 1.0 mm). Larger radial distance correlated with higher Gleason score (P=0.02) and positive surgical margins (P=0.008). In univariable analysis, maximal radial distance was associated with risk of BCR, as a continuous (P=0.006) and dichotomous (P=0.002) parameter, as were other methods to quantify EPE, such as Epstein's criterion (P = 0.001), Wheeler's criterion (P = 0.004) and total radial distance (P < 0.001). Larger circumferential length of EPE, bilateral versus unilateral EPE and multifocal versus unifocal EPE were not associated with risk of BCR. In multivariable analysis, radial distance dichotomized at one high-power field (0.6 mm) remained strongly correlated with BCR (HR 3.4; 95%CI 1.48 – 7.85; P=0.004). The 5-year risk of BCR was 20% (95%CI: 0.65 – 0.94) in patients with radial distance ≤ 0.6 mm and 47% (95%CI: 0.41 – 0.65) with radial distance > 0.6 mm. Independent predictors of BCR were also Gleason score (P=0.001), positive surgical margins (P=0.005), preoperative PSA (P=0.006), total radial distance (P=0.009) and EPE quantification according to Epstein (P=0.002), and to Wheeler (P=0.004). According to Wheeler's criteria the 5-year risk of BCR was 21% for focal and 43% for established EPE. The additional criterion regarding the limit of focal EPE in no more than 2 slides, gave no better results.
Conclusions: Maximal radial distance dichotomized at one high-power field is a simple and objective method to subdivide EPE and a strong independent predictor for BCR after radical prostatectomy. We recommend to substage pT3a in future TNM classifications according to this parameter.

967 Expression of MUC4 Is Downregulated in Urothelial Carcinoma.

D Wagner, A Horn, S Kaur, N Momi, M Lele, SK Batra, SM Lele. University of Nebraska Medical Center, Omaha.
Background: MUC4, a high-molecular weight glycoprotein, has many unique domains involved in signaling pathways, tumor growth and metastasis. We have previously shown that the expression of MUC4 is significantly decreased in prostatic adenocarcinoma as compared to benign/hyperplastic foci. In this study, we examined the expression of MUC4 in non-invasive and invasive urothelial carcinoma (UC) which has not been previously published.
Design: Archival formalin-fixed paraffin-embedded tissues diagnosed as UC in-situ, non-invasive papillary UC and invasive UC from resection specimens were used for the present study to assess the expression of MUC4. Expression of MUC4 was also assessed in UC metastatic to regional lymph nodes. Cases with benign/non-neoplastic urothelium were used as controls. Representative tissue was selected by two of the authors followed by immunostaining with anti-MUC4 (monoclonal, prepared in our laboratory). The immunostained slides were scored using the H-score which is a summation of the product of staining intensity and proportion of cells staining.
Results: Expression of MUC4 was significantly higher in benign urothelium as compared to UC: non-invasive low grade papillary UC ($p<0.0001$), urothelial carcinoma in-situ/non-invasive high grade papillary UC ($p<0.0084$) and invasive high grade UC ($p<0.0001$). Expression of MUC4 did not correlate with presence or absence of invasion ($p<0.1231$), tumor grade ($p<0.1124$) or depth of invasion ($p<0.3175$). Expression of MUC4 was higher in benign urothelium as compared to metastatic UC within regional lymph nodes ($p<0.0222$), however, there was no significant difference in expression of MUC4 between that noted in the primary UC and the matched metastatic focus.
Conclusions: MUC4 is consistently downregulated in urothelial carcinoma and may have diagnostic value in difficult cases. As a tumor modulator, it may confer a protective effect that might have therapeutic significance.

968 microRNA Expression Profiling in Prostate Cancer: Possible Role as a Biomarkers and/or Molecular Therapy.

BA Walter Rodriguez, MP Vargas, VA Valera Romero, M Sobel, P Pinto, MJ Merino. National Cancer Institute, Bethesda; NCI/NIH, Bethesda.
Background: miRNAs are small non-coding RNA molecules that have been shown to regulate the expression of genes linked to cancer. The relevance of miRNAs in the development, progression and prognosis of prostate cancer is not fully understood. It is also possible that these specific molecules may assist in the recognition of aggressive tumors and the development of new molecular targets. Our study investigated the importance of several miRNAs in cases of prostate cancer and correlated them with clinicopathological parameters.
Design: A total of 114 samples from 37 prostate cancer patients were manually microdissected to obtain pure populations of tumor cells, normal epithelium and adjacent stroma. miRNA was extracted for PCR array profiling. Differentially expressed miRNAs for each case comparing tumor vs. normal epithelium and tumor-adjacent stroma samples were defined as those with a two-fold change and a p value <0.001. All the cases were histologically reviewed and the grade, presence of extracapsular, perineural, seminal vesicle and lymphatic invasion was recorded to further evaluate them as prognostic factors.
Results: Patients' mean age was 57 years. Five patients were histologically Gleason score 6, 20 had Gleason score 7 (3+4) and 12 Gleason score 8 or higher. Two patients had clinical stage T2a, 1 T2b, 25 T2c, 7 T3a and 1 case T3b. Three cases had positive lymph nodes. Loss of 18 miRNAs (e.g.miR34c, miR29b, miR212 and miR10b) and upregulation of miR143 and miR146b were significantly found in all the tumors in comparison with normal epithelium and/or stroma ($p\leq 0.001$). A different signature was found in the high grade tumors (Gleason score ≥ 8) when compared with tumors Gleason score 6. Upregulation of miR122, miR335, miR184, miR193, miR34, miR138, miR373, miR9, miR198, miR144 and miR215 and downregulation of miR96, miR222, miR148, miR92, miR27, miR125, miR126, miR27 was found in the high grade tumors. miR193b and 181b, miR20a and 10b, and miR125a and 155 were differentially expressed in patients having perineural (PI), extracapsular (ECI) and lymphatic invasion, respectively.
Conclusions: miRNA profiling in prostate cancer appears to have unique and different expression patterns, in low and high grade Gleason tumors. A miRNA signature was also found correlated to poor prognostic factors such as ECI, PI and lymphatic involvement. These differential expressed miRNAs may provide novel diagnostic and prognostic tools that will assist in the recognition of prostate cancers with aggressive behavior.

969 Non-Xp11 Translocation Associated Renal Cell Carcinoma in Patients Less Than 20 Years Old: A Clinicopathologic Study with Follow-Up.

J Wang, BM Shehata, SM Langness, A Davis, L Cheng, AO Osunkoya. Emory University School of Medicine, Atlanta; Indiana University School of Medicine, Indianapolis.
Background: Renal cell carcinoma (RCC) is a rare neoplasm in patients younger than 20 years old, accounting for less than 2% of all RCC cases and 5% of pediatric renal tumors. Non-translocation associated RCC are even more uncommon, in view of the fact that Xp11 translocation-associated carcinomas comprise a significant proportion of pediatric RCC. Very few large clinicopathologic studies of this subset of tumors in the pediatric population have been published to date.
Design: A search was made through the surgical pathology and consultation files of two academic institutions for non-Xp11 translocation associated RCC in patients less than 20 years old from 1995-2009. Patients with renal medullary carcinoma were excluded from the study. Clinicopathologic data including follow up was obtained.
Results: Clinical data: 12 cases of non-Xp11 translocation associated RCC were identified from 350 pediatric patients with renal tumors (prevalence = 3.4%). The patient population consists of 6/12 males (50%) and 6/12 females (50%). The mean age at diagnosis was 10 years (range 1-18 years). Pathologic data: 10/12 (83%) patients had radical nephrectomy, and 2/12 (17%) patients had partial nephrectomy. The mean tumor size was 6.8 cm (range 1.6-12 cm). 5 cases were papillary RCC (42%), 4 cases were clear cell RCC (33%), and 3 cases were chromophobe RCC (25%). A TFE-3 stain was performed and was negative in all cases. 9/12 cases (75%) were Fuhrman nuclear grade 2, and 3/12 cases (25%) were Fuhrman nuclear grade 3. Pathologic staging was as follows: pT1, 6/12 cases (50%); pT2, 3/12 cases (25%); pT3, 2/12 cases (17%); unknown, 1/12 case (8%). 3/12 cases (25%) had regional lymph node metastasis. Angiolymphatic invasion (ALI) was identified in 4 cases (33%). 1/12 case (8%) each had perinephric adipose tissue and renal sinus fat invasion. Tumor necrosis was present in 5/12 cases (42%). Follow-up data: Mean duration of follow-up was 33 months (range 11-55 months). All patients were alive at last follow-up, including 1 patient with lung metastasis, and another with local recurrence.
Conclusions: Pathologic parameters typically associated with poor outcome in adults, including metastasis/high tumor stage, high Fuhrman nuclear grade, ALI, and tumor necrosis did not lead to death in any of the patients in our series. Non-Xp11 translocation associated RCC though relatively rare, should be considered in the differential diagnosis of pediatric renal tumors, and may have a better outcome than in adults.

970 Correlation of Recently Proposed Chromophobe Tumor Grade (CTG) with Initial Stage in 82 Chromophobe Renal Cell Carcinomas (RCC) from a Single Institution.

E Weinzierl, B Chung, J McKenney. Stanford, Stanford, CA.
Background: It is well-recognized that the Fuhrman grading system is not appropriate for chromophobe RCC, because the majority of cases would receive a Fuhrman grade ≥ 3 despite the expected indolent behavior. A novel grading system specific to chromophobe RCC was recently proposed (Paner et al. *Am J Surg Pathol* 2010;34(9):1233-40), but has not yet been evaluated by other investigators.
Design: All available chromophobe RCCs were identified from the surgical pathology archives of a single hospital from 1987-2010. No consultation cases were included. Patient age and sex were recorded. Each case was re-reviewed by two pathologists to confirm diagnoses and each case was graded following the novel chromophobe tumor grade system criteria described by Paner et al. The percentage of tumor comprised of each grade was also recorded. Grade was correlated with AJCC 7th ed. stage at initial surgery.

Results: 82 chromophobe RCCs were identified. 53 patients were male and 29 female. The patients' ages ranged from 17 to 87 years (mean=60; median=61). 53 (65%) were CTG1, 27 (33%) CTG2, and 2 (2%) CTG3. Both CTG3 cases had sarcomatoid differentiation. All cases with CTG2 also had foci of CTG1; the percentage of tumor comprised of CTG2 ranged from less than 5% to 60%. Cases presenting at AJCC 7th ed. stage ≥ 3 were as follows: 9/53 CTG1 (17%), 4/27 CTG2 (15%), and 2/2 CTG3 (100%). The anatomic stage matched the pT stage for all cases. Only one case (1.2%), which was CTG2 in 15% of the tumor, presented with lymph node metastasis. The one case presenting with pT4 disease had sarcomatoid differentiation (i.e. CTG3). No distant metastases were present at the time of initial diagnosis in any of the cases.

Conclusions: The newly proposed chromophobe tumor grade did not correlate with AJCC stage in this study; however, the number of cases with CTG3 and/or extrarenal extension or metastatic disease was extremely limited. In contrast to the Fuhrman grading system, the chromophobe tumor grade system assigned a low grade designation (CTG1) to the majority of cases in this series. Further study of the chromophobe tumor grade system is warranted, and correlation with long-term clinical follow-up data is ongoing to determine the utility of this novel chromophobe grading system for the prediction of subsequent recurrence and/or metastasis.

971 microRNA Profiling in Clear Cell Renal Cell Carcinoma: Biomarker Discover and Identification of Potential Controls and Consequences of miRNA Dysregulation.

NMA White, TT Bao, J Grigull, YM Youssef, A Girgis, M Diamandis, E Fatoohi, M Metias, RJ Honey, R Stewart, KT Pace, GA Bjarnason, GM Yousef. Li Ka Shing Knowledge Institute of St. Michael's Hospital, Toronto, ON, Canada; University of Toronto, ON, Canada; York University, Toronto, ON, Canada; St. Michael's Hospital, Toronto, ON, Canada; Sunnybrook Odette Cancer Center, Toronto, ON, Canada.

Background: Renal cell carcinoma (RCC) is the most common neoplasm of the adult kidney. Currently, there are no biomarkers for the diagnostic, prognostic, or predictive applications in RCC. MicroRNAs (miRNAs) are short non protein-coding RNAs that negatively regulate gene expression and have been shown to be potential biomarkers for cancer.

Design: We analyzed a total of 70 matched pairs of clear cell RCC (ccRCC) and normal kidney tissues from the same patients by microarray analysis and validated our results by quantitative real time PCR. We also did extensive bioinformatic analyses to explore the role and regulation of miRNAs in ccRCC.

Results: We identified 166 miRNAs significantly dysregulated in ccRCC. MiR-122, miR-155 and miR-210 had the highest fold changes of overexpression while miR-200c, miR-335, and miR-218 were the most downregulated. Combinatorial analysis of previously reported miRNAs dysregulated in RCC showed an overlap of many miRNAs. Extensive target prediction analysis showed many miRNAs were predicted to target a number of genes involved in RCC pathogenesis. MiRNA dysregulation in RCC can be attributed in part, to chromosomal aberrations, the co-regulation of miRNA clusters, and co-expression with host genes. We also correlated miRNA expression with clinical characteristics and found miR-155 expression was correlated with ccRCC tumor size.

Conclusions: Our analysis showed that a number of miRNAs are dysregulated in ccRCC and may contribute to kidney cancer pathogenesis by targeting key molecules. We identified mechanisms that may contribute to miRNA dysregulation in ccRCC. Dysregulated miRNAs represent potential biomarkers and therapeutic targets for kidney cancer.

972 Reevaluation of Expression of SALL4 and PAX8 in Carcinomas from Various Organs.

M Wilkerson, J Shi, H Liu, JW Prichard, F Lin. Geisinger Medical Center, Danville, PA.

Background: SALL4 and PAX8 are two recently described useful immunohistochemical markers. SALL4 is a sensitive and specific maker for germ cell tumors, including seminoma, embryonal carcinoma, and yolk sac tumor. PAX8 is a sensitive marker for thyroid carcinomas, ovarian serous carcinoma and renal cell carcinomas. However, the published data were limited and inconsistent. In this study, we attempted to re-evaluate the expression of SALL4 and PAX8 in a large series of carcinomas from various organs using a single immunostaining system (Ventana XT).

Design: Immunohistochemical evaluation of the expression of SALL4 (Cat. No CM384C; Biocare Medical) and PAX8 (Cat. No. CP379AK; Biocare Medical) on 872 cases of carcinomas from various organs using tissue mircroarray sections was performed. The staining intensity and the distribution were recorded.

Results: The positive staining results (%) and the total number of cases for each entity (N) are summarized in Table 1. Twenty-two cases of intratubular germ cell neoplasia (ITGCN) were also positive for SALL4. One case of carcinoma from each of the colon, esophagus, endocervix and ovary was positive for SALL4. Both SALL4 and PAX8 are negative for lung ADC (N=50), lung SCC (N=49), medullary thyroid CA (N=10), gastric ADC (N=21), Pancreatic ADC (N=50), urothelial CA (N=40), prostatic ADC (N=100), cholangiocarcinoma (N=11), breast ductal CA (N=110) and lobular CA (N=31), hepatocellular CA (N=18) and adrenal cortical neoplasm (N=24).

Table 1. Summary of immunostaining results

Tumor	SALL4 (%)	PAX8 (%)
Seminoma (N=30)	100	0
Embryonal CA (N=24)	100	0
Yolk sac tumor (N=12)	100	0
Papillary thyroid CA (PTC, N=45)	0	93
Follicular thyroid CA (FTC, N=36)	0	100
Anaplastic thyroid (ATC, N=5)	0	40
Clear cell RCC (N=36)	0	97
Papillary RCC (N=25)	0	100
Colonic ADC (N=38)	3	3
Esophageal ADC (N=30)	3	0
Endocervical ADC (N=17)	6	53
Ovarian serous CA (N=15)	6	100
Pancreatic endocrine neoplasm (PEN, N=15)	0	33

ADC-adenocarcinoma; CA-carcinoma; RCC-renal cell carinoma

Conclusions: Our data confirm that 1) SALL4 is a sensitive and specific marker for the diagnosis of germ cell tumors and ITGCN, with an exception that the positivity can be seen in rare cases of carcinoma of the colon, esophagus, endocervix and ovary; 2) PAX8 is a useful marker in the diagnosis of papillary and clear cell RCCs, PTC, FTC, and ovarian serous CA. Caution should be taken, as a high percentage of endocervical ADC, PEN, and rare colonic ADC can be positive for PAX8.

973 Lymphoepithelioma-Like Carcinoma of the Urinary Bladder: Clinicopathologic, Immunohistochemical, and Molecular Features.

SR Williamson, S Zhang, A Lopez-Beltran, RB Shah, R Montironi, P-H Tan, M Wang, LA Baldridge, GT MacLennan, L Cheng. Indiana University, Indianapolis; Cordoba University, Spain; Caris Diagnostics, Irving, TX; Polytechnic University of the Marche Region, Ancona, Italy; Singapore General Hospital, Singapore; Case Western Reserve University, Cleveland.

Background: Lymphoepithelioma-like carcinoma (LELC) in the urinary tract is a rare malignancy, named for its resemblance to nasopharyngeal undifferentiated carcinoma or lymphoepithelioma. Investigation of immunohistochemical and molecular characteristics of bladder LELC is limited. The pathogenesis and biological behavior of these tumors are controversial.

Design: We examined clinicopathologic features of urinary tract LELC, including light microscopy; immunohistochemistry (IHC) for CK7, CK20, 34BE12, p53, AMACR, TTF-1, EBV LMP-1 and CD30; in situ hybridization for HPV; and UroVysion fluorescence in situ hybridization (FISH).

Results: We identified tumors from 34 patients (M:F 2.8:1), ranging from 54 to 84 years of age (mean 70.2). Urothelial carcinoma in situ (CIS) was identified in 50% of patients. 34BE12 (75%) and CK7 (57%) were frequently positive in tumor cells, while TTF-1 and CD30 were consistently negative. Expression of p53 was noted in a subset of tumors (61%), while CK20 staining was negative with weak positivity in a single case. UroVysion FISH demonstrated frequent chromosomal abnormalities similar to those of urothelial carcinoma. In studied tumors with concurrent urothelial, squamous, sarcomatoid, and glandular components, identical FISH abnormalities were noted in both areas. In situ hybridization for HPV and immunostaining for EBV were negative in all studied lesions. All patients with pure or predominant LELC tumors treated with transurethral resection followed by chemotherapy were alive without evidence of disease at 2-5 years, while two patients treated in this manner with less than 50% LELC morphology had death from disease or distant metastasis.

Conclusions: Urinary tract LELC is a rare and interesting histologic variant of urothelial carcinoma. The frequent presence of UroVysion FISH abnormalities, urothelial CIS and p53 positivity by IHC in cases of urinary tract LELC suggest a similar pathogenesis to high-grade invasive urothelial carcinoma. In contrast to typical urothelial carcinoma, CK20 is frequently negative in LELC. Our findings support the hypothesis that pure or predominant LELC may be treated with transurethral resection and chemotherapy; however, a large-scale study with long-term followup is needed to better understand the biologic behavior of urinary bladder LELC.

974 The Spectrum of Morphologic Findings in Clear Cell Papillary Renal Cell Carcinoma.

SR Williamson, JN Eble, L Cheng, DJ Grignon. Indiana University, Indianapolis.

Background: Clear cell papillary renal cell carcinoma (CCPRCC) is an interesting renal neoplasm recently recognized in kidneys with and without end-stage renal disease (ESRD). Immunohistochemical (IHC) and molecular properties are distinct from clear cell and papillary RCC. The spectrum of morphologic features and prominence of the papillary component have not been well elucidated.

Design: We retrieved cases of CCPRCC from the authors' archives. Light microscopic features were evaluated and IHC was performed for CK7, CA-IX, CD10, AMACR, SMA, desmin, ER, and PR.

Results: We identified 23 tumors from 13 patients, 3 with ESRD (23%). Age ranged from 46 to 71 years (mean 58), with M:F ratio of 11:2. Tumor size ranged from 0.3 to 7.5 (mean 2.6) cm. The majority of cases were Fuhrman grade 2 (69%), while fewer were grade 1 (23%) or 3 (8%). Stage was predominantly pT1 (92%). In 77% of cases papillary architecture was limited to a minority of the tumor, some with only minute abortive papillae. Only 23% showed a majority of papillary architecture or large fields composed of branched papillae. All tumors showed gross or microscopic cystic spaces, some with prominent peripheral cysts. All were encapsulated. The majority showed secretory cells (85%) with nuclei aligned at the apical end of the cells, and all showed at least focal branched/stellate ductular structures. Calcification or ossification was present for 3 cases, and no case showed psammoma bodies or foamy macrophages within papillae. IHC demonstrated the typical profile for CCPRCC (CK7+, AMACR -, CD10 -, CA-IX+), with the following exceptions: 4 cases with weak CD10 membrane positivity in only the flattened cyst lining cells, and 1 case with weak AMACR staining.

The stromal component demonstrated SMA positivity in all cases, with capsular desmin staining in only 3 cases. ER and PR were uniformly negative.
Conclusions: CCPRCC is a unique neoplasm that typically presents at low grade and stage. Although papillary architecture is characteristic, abundant extensively branched papillae are infrequent. Key features that suggest the diagnosis include a prominent, often peripheral cystic component, alignment of cell nuclei away from the basement membrane (secretory cells), and stellate ductular structures (similar in shape to benign prostatic acini). Some tumors may be nearly entirely cystic with only minute papillary structures. Tumor ossification or calcification can be seen. We have expanded the IHC profile of CCPRCC to include focal SMA positivity in the stromal component, lack of ER/PR expression in the stroma, and occasional positivity of the flattened cyst lining for CD10.

975 ERG-TMPRSS2 Rearrangement Is Shared by Concurrent Prostatic Adenocarcinoma and Prostatic Small Cell Carcinoma and Absent in Small Cell Carcinoma of the Urinary Bladder.

SR Williamson, S Zhang, JL Yao, J Huang, A Lopez-Beltran, S Shen, AO Osunkoya, GT MacLennan, R Montironi, L Cheng. Indiana University, Indianapolis; University of Rochester; University of California at Los Angeles; Cordoba University, Spain; The Methodist Hospital, Houston; Emory University, Atlanta; Case Western Reserve University, Cleveland; Polytechnic University of the Marche Region, Ancona, Italy.
Background: Prostatic carcinoma is a heterogeneous disease with frequent multifocality and variability in morphology. Particularly, prostatic small cell carcinoma (SmCC) is a rare variant with aggressive behavior. Distinction between SmCC of the prostate and urinary bladder may be challenging, especially in small biopsy specimens without associated prostatic adenocarcinoma or urothelial carcinoma. Recently, gene fusions between ETS genes, particularly ERG, and TMPRSS2 have been identified as a frequent event in prostate cancer. Thus, molecular methods may be helpful in determining the primary site of SmCC.
Design: Twenty-nine cases of prostatic SmCC from the authors' archives were studied, among which 13 had coexisting prostatic adenocarcinoma. Tricolor fluorescence in situ hybridization (FISH) was performed on formalin-fixed paraffin-embedded tissue sections with a probe cocktail for 3'/5' ERG and TMPRSS2. 25 cases of bladder SmCC were also tested.
Results: ERG gene alterations were found only in prostate malignancy and not in benign prostate tissue or bladder SmCC. TMPRSS2-ERG gene fusion was found in 48% (14/29) of prostatic SmCC. Of cases with concurrent prostatic adenocarcinoma, 85% (11/13) had identical findings in both components. In 10% of cases, rearrangement was associated with 5' ERG deletion. In 17% (5/29), gain of chromosome 21q was present. Two cases (7%) showed discordant aberrations in the SmCC and adenocarcinoma, 1 with deletion of 5' ERG and 1 with gain of chromosome 21q, both in only the adenocarcinoma component.
Conclusions: SmCC of the prostate demonstrates TMPRSS2-ERG rearrangement with comparable frequency to prostatic adenocarcinoma. In cases with concurrent adenocarcinoma and SmCC, 85% showed identical abnormalities in both components, indicating a likely common clonal origin. Discordant alterations were present in 2 cases, suggesting that acquisition of additional genetic changes in multifocal tumors may be responsible for phenotypic variation. TMPRSS2-ERG fusion is absent in bladder SmCC, supporting the utility of FISH in distinguishing prostate from bladder primary tumors and identifying metastatic SmCC of unknown origin.

976 4-miRNA Signature To Predict Clear Cell Renal Cell Carcinoma Metastasis and Prognosis.

H Wu, X Wu, L Weng, X Li, C Guo, SK Pal, JM Jin, RA Nelson, B Mu, SH Onami, JJ Wu, NH Ruel, H Gao, M Covarrubias, RA Figlin, LM Weiss. City of Hope National Medical Center and Beckman Research Institute, Duarte, CA.
Background: Clear cell renal cell carcinoma (ccRCC) represents the most common renal cancer histology. In the setting of metastatic disease, few patients achieve a durable remission with available therapies. The early detection of ccRCC metastatic potential may be beneficial for a more precise prediction of clinical outcomes and may ultimately be used to identify subsets of patients that stand to benefit from specific targeted therapies. RCC metastasis cannot be reliably predicted based on patients' clinical magnifications, pathologic findings or other currently available molecular tests. For this purpose, we analyzed microRNA (miRNA) expression in ccRCC and aimed to develop a miRNA expression signature to determine the risk of ccRCC metastasis and predict the prognosis of disease.
Design: We used the microarray technology to profile 10 benign kidney specimens and 68 ccRCC samples. Using a 28-sample training cohort of localized and metastatic ccRCCs and the univariate Logistic regression method, we developed a miRNA signature model to calculate a risk score for predicting the risk of metastasis. We validated the signature model in an independent 40-sample testing cohort of different stages of primary ccRCCs and further tested the signature model using a quantitative PCR (qPCR) platform.
Results: Utilizing the training cohort, we constructed a 4-miRNA expression signature model in which the expression levels of the 4 miRNAs were used to stratify ccRCC patients into high and low risk groups for metastasis. The signature was then validated in the testing cohort. With a 5-year follow-up if no metastasis developed, the signature showed a high sensitivity (75%) and specificity (100%). The risk status was proven to be associated with the cancer-specific survival. This molecular signature has further been developed into a qPCR-based assay, which showed to have the same high sensitivity and specificity.
Conclusions: The 4-miRNA signature can reliably predict ccRCC metastasis and prognosis. It is ready for further large clinical cohort validation and potential routine clinical application.

977 Urothelial Carcinoma with Lymphoepithelioma like Carcinoma Features: A Clinicopathologic Study of Ten Patients.

A Wu, J Montie, D Smith, LP Kunju. University of Michigan Medical Center, Ann Arbor.
Background: Lymphoepithelioma like carcinoma (LEC) is an extremely rare type of mixed/divergent differentiation in urothelial carcinoma and there is limited literature regarding the biologic behavior of this entity.
Design: The clinical, morphologic, and immunohistochemical features of patients in our database from 2000 to 2010 diagnosed with urothelial carcinoma with lymphoepithelioma like carcinoma features were analyzed.
Results: Ten patients were diagnosed with urothelial carcinoma with LEC features. All were older adults (55-84, median age 74) with no gender predilection (M:F=1). Carcinomas were located in the urinary bladder (8), renal pelvis (1), and bladder and ureter (1). All cases had extensive LEC features (>=50%), with three showing exclusive LEC. All had high grade cells arranged in syncytia embedded within a dense lymphoid background. Two patients had a concomitant low grade B cell lymphoma involving adjacent soft tissue/lymph nodes. Immunohistochemistry did not have a significant role in establishing the diagnosis. Most (80%) presented at a high clinical stage (>=cT3). Treatment included radical cystectomy (7), ureterectomy (1), nephroureterectomy (1), neoadjuvant chemotherapy (4) and/or adjuvant chemotherapy (3). Of 5 patients who underwent resection without neoadjuvant chemotherapy, the pathologic stages were pT3 (3), pT2b(1), and pT0(1). Of 4 patients who received neoadjuvant chemotherapy, three had significant downstaging of their tumor at resection (pT1 or pT0) while one had pT3. Follow-up was available for 9 patients; the median duration was 2.6 years (range 0.7-9.5 years). Seven patients have no evidence of disease; two patients developed distant metastases despite neoadjuvant chemotherapy.
Conclusions: LEC differentiation is usually extensive when present and most often presents at a high clinical stage. In our experience, this subtype of carcinoma has a somewhat mixed response to chemotherapy, but it does not always confer resistance to chemotherapy. Interestingly, two of ten patients had a concomitant low grade B cell lymphoma, which may imply an increased risk of low grade lymphoma associated with this subtype.

978 The Utility of Novel ERG/P63 Cocktail in the Diagnosis of Limited Cancer in Prostate Needle Biopsies.

O Yaskiv, K Simmerman, S Zhang, T Daly, H He, S Falzarano, L Chen, C Magi-Galluzzi, M Zhou. Cleveland Clinic, OH.
Background: Diagnosis of limited cancer can be challenging in prostate needle biopsies and immunohistochemistry is commonly used in such settings. Recently, *TMPRSS2:ERG* gene rearrangement was found to be highly specific for and was present in approximately 50% of prostate cancer. Immunohistochemical results using a novel anti-ERG antibody highly correlated with *TMPRSS2:ERG* gene rearrangement status. We developed an immunohistochemical cocktail containing both ERG and basal cell marker P63 antibodies and evaluated its utility in the diagnosis of limited cancer in prostate needle biopsies.
Design: Sixty prostate biopsies (PBx) containing cancer occupying ≤ 10% of the length of only one core out of the entire biopsy tissue were selected and stained with a cocktail containing ERG and P63 antibodies. ERG positivity and its staining intensity in cancer and benign lesions were recorded.
Results: ERG expression was detected in 38% (23/60) of cases, with strong, moderate and weak staining intensity in 78%, 13% and 9% cases, respectively. The staining was uniform in 87% cases and heterogeneous in 13% cases with different staining intensities in ≥ 25% of cancer cells. High grade prostatic intraepithelial neoplasia (HGPIN) was present in 15 out of 60 PBx and 4 (26%) HGPIN lesions were positive for ERG. They were all adjacent to cancer glands. Benign lesions, present within the PBx cores, including simple and partial atrophy, and basal cell hyperplasia, were negative for ERG. P63 was negative in all cancer glands and positive in benign lesions and HGPIN.
Conclusions: ERG protein expression was detected in 38% of limited cancer in prostate biopsies. It was also detected in 26% of HGPIN lesions, all of which were immediately adjacent to cancer. ERG immunoreactivity was not found in benign lesions. ERG protein expression is highly specific for prostate cancer. The cocktail containing P63 and ERG provides high sensitivity with P63 and high specificity with ERG and is potentially useful in the work-up of difficult prostate biopsies.

979 Do the Extent or Location of Vascular Invasion Stratify the Risk of Relapse in Clinical Stage I Patients with Nonseminomatous Germ Cell Tumors (NSGCT)?

A Yilmaz, T Cheng, K Trpkov. University of Calgary and Calgary Laboratory Services, AB, Canada; University of Calgary, AB, Canada.
Background: Current focus of testicular cancer management is to reduce the treatment related morbidity without jeopardizing the excellent survival rate. Predictors of relapse are critical in tailoring clinical management of individual patients. Previous studies showed that vascular invasion (VI) in the primary tumor is associated with high risk of relapse in patients with clinical stage I NSGCT. Our objective was to investigate whether the extent and/or the location of VI will improve the risk stratification in patients with stage I NSGCT, who are managed by surveillance.
Design: We identified 94 (62%) patients with clinical stage I of a total of 152 NSGCT patients. All patients had radical orchiectomy in our center between 10/1999 and 06/2009. VI was detected in 27 (29%) of cases. All clinical stage I patients were initially managed by surveillance. Pathology slides and reports were reviewed and follow-up was obtained. Extent of VI was defined on H&E slides as focal (1-3 foci) vs. extensive (≥4 foci). We also documented the location of VI as hilar and/or extratesticular vs. parenchymal vessels. We recorded the following clinical and morphologic features: age,

tumor size, histologic type, percentage of tumor components and pathologic stage.
Results: Patient mean age was 34 years (range, 18 to 74) and mean tumor size was 3.5 cm (range, 0.8 to 10.5). Mixed tumor histology was identified in 20 (74%) cases and pure embryonal carcinoma was identified in 7 (26%) cases. Embryonal carcinoma was the most common type of tumor identified in lymphovascular spaces, followed by yolk sac tumor. We found extensive VI in 20 (74%) cases and focal in 7 (26%). Hilar and/or extratesticular VI was identified in 15 (56%) cases and parenchymal in 12 (44%). After a mean follow-up of 48 months (range, 7 to 84), 18 (67%) patients relapsed and 2 (7%) patients died with metastatic disease. Median time to relapse was 10 months and the most common site of relapse was retroperitoneal nodes. Relapse rates did not differ significantly when stratified by the extent of VI (focal 86% vs. extensive 60%) or location (hilar 67% vs. parenchymal 67%).
Conclusions: Evaluation of VI by extent or location did not improve the risk stratification for relapse in the studied patient cohort. We confirm that the presence of VI in the primary tumor is an adverse prognostic parameter associated with high disease progression rate in patients with clinical stage I NSGCT.

980 Nodal Yield, Size and Distribution of Pelvic Lymph Node Metastases in Prostatic Adenocarcinoma: A Study of 72 Cases.

J Yoon, O Kryvenko, S Kaul, N Patil, N Gupta. Henry Ford Hospital, Detroit, MI.
Background: Pelvic lymph node dissection (PLND) in prostate cancer generally involves removal of external iliac and obturator group (EO) of lymph nodes (LN). Several studies have shown that prostate cancer nodal metastases (MET) do not follow a pre-defined pathway of metastatic spread. The aim of our study was to determine the nodal yield, size and distribution of MET in different anatomic LN sites and study the benefit of inclusion of internal iliac (INT) LN in our PLND for intermediate to high risk group patients.
Design: Pathology files of our hospital were searched for cases of PLND with MET from a period of Jan 2008 to May 2010. All positive cases were evaluated for anatomic sites of MET, number of LNs, size of largest LN, size of largest metastatic LN, and size of largest and smallest metastatic focus.
Results: A total of 72 cases of MET were identified. All of these patients had PLND with EO and INT group. A total of 827 LN were submitted, 131 LN were positive for MET. Data on LN sites were available in 43 cases. Out of these, 22 cases had MET in EO group (51.1%) and 31 cases had MET in INT group (72%). MET in both groups were seen in 10 cases (23%). 21 cases had isolated MET to INT group (48.8%) where as 12 cases had isolated MET to EO group (27.9%). The mean LN yield was 11.49±5.83; the mean number of positive LN was 1.82±1.5; the size of largest LN was 3.51±1.54 cm; the mean size of positive LN was 0.9±0.8 cm. 43 patients had largest positive LN measuring less than 1.0 cm (59%, 43/72). The mean size of metastatic focus in these LN was 0.49 (range 0.05 – 0.6 cm).
Remainder of the adipose tissue (FAT) was submitted entirely in 31 cases. 87 LN were identified in FAT. Mean additional number of LN found in FAT was 2.8±2.3. 7 cases had positive LN (22.6%); the mean size of positive LN was 0.15 cm. Submission of FAT increased LN yield up to 11.8% and positive LN detection rate up to 5.6%. Lymph node staging itself was changed in 3 cases (3/7) from N0 to N1.
Conclusions: 1) Metastasis from prostate carcinoma is frequently (59%) seen in small LNs (less than 1 cm). 2) Entire adipose tissue submission substantially increases the yield of LN and provides more accurate N staging. 3) Metastasis to INT group, either in combination with EO metastases or isolated INT metastasis is frequent and warrants inclusion of this LN group in all PLND done for intermediate to high risk prostate cancer patients.

981 microRNA Profiling in Kidney Cancer: Accurate Molecular Classification of Subtypes and Correlation with Cytogenetic and mRNA Data.

YM Youssef, NMA White, J Grigull, A Krizova, C Samy, S Mejia-Guerrera, A Evans, GM Yousef. University of Toronto, ON, Canada; Li Ka Shing Knowledge Institute, Toronto, ON, Canada; York University, Toronto, ON, Canada; Toronto General Hospital, ON, Canada.
Background: Renal cell carcinoma (RCC) encompasses different histological subtypes. Distinguishing between the subtypes is usually made on morphological basis but this is not always feasible or accurate. The aim of this study was to identify microRNA (miRNA) signatures that can distinguish between the different RCC tumor types and to explore their unique and shared biological pathways.
Design: miRNA microarray analysis was performed on fresh frozen tissues of three common RCC subtypes [clear cell RCC (ccRCC), chromophobe RCC (chRCC) and papillary (pRCC)], and the benign oncocytoma tumor. Results were validated on an independent set of tumors using quantitative real time PCR analysis with miRNA-specific primers. Extensive target prediction analysis was performed for differentially expressed miRNAs. We also did a comprehensive bioinformatics analysis to examine the correlation of gene expression and cytogenetic profiling data with the predicted miRNA targets.
Results: Unique miRNA signatures can distinguish between the different RCC subtypes and oncocytoma. We developed a hierarchical multi-step decision tree that can accurately identify each tumor type with very high sensitivity and specificity using specific miRNA pairs. Also a miRNA signature can also be used to distinguish between pairs of subtypes with almost 100% sensitivity (e.g. ccRCC vs. chRCC and chRCC vs. oncocytoma). Bioinformatics analysis showed that the pathogenesis of ccRCC is more closely related to pRCC, whereas chRCC showed a comparable expression profile to oncocytoma.
Conclusions: miRNA expression patterns can distinguish between RCC tumor types. Our hierarchical decision tree can accurately distinguish between RCC tumor types when diagnosis based on morphology alone is difficult. miRNA expression profiles point out to the presence of shared and unique dysregulated pathways among different RCC subtypes and oncocytoma.

982 Atypical Adenomatous Hyperplasia (AAH) That Is Associated with Prostatic Adenocarcinoma Has Higher Expression of -Methylacyl Coenzyme A Racemase (AMACR) Than AAH Not Associated with Cancer.

C Zhang, GT MacLennan, R Montironi, A Lopez-Beltran, Y Li, P-H Tan, KA Iczkowski, L Cheng. Indiana University, Indianapolis; Case Western Reserve University, Cleveland, OH; Polytechnic University of the Marche Region, Ancona, Italy; Cordoba University, Spain; Amylin Pharmaceuticals Inc, San Diego, CA; Singapore General Hospital, Singapore; University of Colorado, Aurora.
Background: Alpha-methylacyl coenzyme A racemase (AMACR) is highly expressed in prostatic adenocarcinoma. Atypical adenomatous hyperplasia (AAH) is a histologic mimicker of prostatic adenocarcinoma. A detailed analysis of AMACR expression in AAH and its association with prostatic adenocarcinoma (PCA) is lacking.
Design: One hundred twenty one AAH foci from 101 patients who underwent transurethral prostatic resection or prostatectomy were immunohistochemically analyzed for AMACR, keratin 34βE12, and p63 expression by a triple antibody (PIN-4) cocktail stain.
Results: Sixty-eight foci (56%) of AAH showed no AMACR immunostaining. Fourteen cases (12%) showed weak AMACR immunoreactivity in 1-9% of lesional cells. Sixteen cases (13%) showed strong immunopositivity for AMACR in >50% of lesional cells. AMACR expression in AAH was significantly higher in cases in which co-existing PCA was present, when compared with its expression in AAH foci without co-existing PCA (p=0.029). Strong diffuse P504S positivity in over 50% of lesional cells was seen almost exclusively in AAH foci with co-existing PCA (p=0.003). P504S expression in AAH showed no correlation with patient age (p=0.053), specimen type (p=0.053), prostate weight (p=0.32), zonal location (p=0.50), distance to cancer (p=0.16), Gleason score (p=0.38), or pathologic stage (p=0.23). Increased AMACR expression showed a negative correlation with the size of AAH foci (p=0.03). All AAH lesions showed fragmented basal cell layers, highlighted by p63 and high-molecular weight cytokeratin stainings.
Conclusions: A significant percentage of AAH cases show stronger and more extensive AMACR expression when associated with prostatic adenocarcinoma, as compared to AAH foci found without coexisting prostate cancer, providing additional evidence linking AAH to prostatic adenocarcinoma.

983 Differential Expression of IMP3 between Male and Female Mature Teratomas.

L Zhang, L Cheng, Z Jiang. Umass Memorial Medical Center, Worcester, MA; Indiana University School of Medicine, Indianapolis.
Background: Ovarian mature teratoma is benign, whereas mature teratoma components in adult testicular germ cells tumors are considered malignant since they have a metastatic potential and often resistant to chemotherapy. Although different theories have been postulated, no biological marker is found so far related to such gender and clinical difference. IMP3, an oncofetal protein plays an important role in embryogenesis and carcinogenesis of certain malignant neoplasms. Several studies have shown that IMP3 is a cancer specific biomarker. In this study, we analyzed IMP3 expression in germ cell tumors, especially compared its expression between male and female teratomas.
Design: Total of 195 germ cell tumors (77 male patients with testicular germ cell tumors without teratoma components including 22 seminomas; 55 non seminomatous germ cell tumors ; 37 male patients with testicular non seminomatous germ cell tumors with teratoma components; 54 female patients with ovarian mature teratomas; 27 male patients with metastatic germ cell tumors with teratoma components) obtained from archives of two large Academic Medical Center were examined by immunohistochemistry for IMP3 expression.
Results: IMP3 are stained in germ cell tumors by immunohistochemical method, as illustrated in Figure 1. IMP3 expression is present in 99% (76/77) male testicular germ cell tumors without teratoma components. The expression is present in 100% (37/37) tumors with teratoma components. Similarly, IMP3 expression is present in 100% (27/27) male metastatic teratomas. In contrast, IMP3 expression is present in only 7% (4/54) of female mature teratomas. IMP3 expression however is also seen in normal spermatogonia and intratubular germ cell neoplasia.

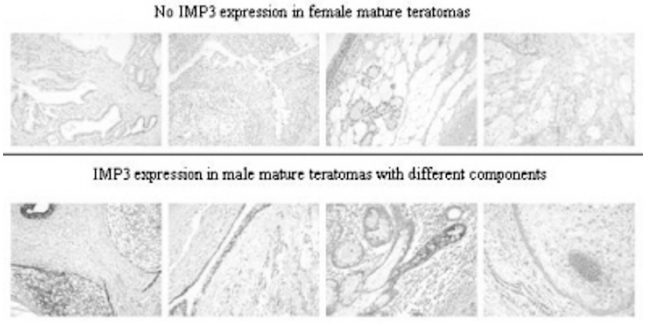

Conclusions: Differential expression of IMP3 between male and female mature teratomas demonstrates that IMP3 may play an important role for the metastasis of testicular germ cell tumors. As IMP3 is highly expressed in male germ cell tumors

including all mature teratoma components, IMP3 may serve as a potential tissue biomarker to distinguish metastatic teratoma from its benign mimickers, especially in the setting of status post chemotherapy for germ cell tumors.

984 Clear Cell Papillary Renal Cell Carcinoma and XP11.2 Translocation-Associated Renal Cell Carcinoma Are Derived from Distal Nephron Tubules and Proximal-Tubules Respectively.

PL Zhang, MB Amin. William Beaumont Hospital, Royal Oak, MI.

Background: Clear cell papillary renal cell carcinoma (CCP-RCC) and XP11.2 translocation-associated renal cell carcinoma (XP-TC) are two recently described variants of RCC, but their origin as to which portion of renal tubules they arise from remains unclear. Kidney injury molecule-1 (KIM-1) is a type I transmembranous protein and specific injury marker of proximal tubules. Previous studies have demonstrated that KIM-1 is upregulated in proximal tubule derived RCC (clear cell RCC and papillary RCC) but negative in distal nephron tubule derived tumors (chromophobe RCC and oncocytoma). We attempted to determine the origin of CCP-RCC and XP-TC using KIM-1 expression. Since KIM-1 has a phagocytotic function in injured proximal tubules, we also investigated for correlation with CD68 expression, which is a phagocytic transmembrane glycoprotein, mainly present in macrophages.

Design: The study included three group of RCC. Group 1 had 16 cases which included both clear cell RCC and papillary RCC (KIM-1 positive control group), Group 2 consisted of 11 cases of CCP-RCC (CK7 positive/P504S negative) and Group 3 had 11 cases of XP-TC (TFE-3 positive). Tumors were immunohistochemically stained for KIM-1 (AKG7 monoclonal antibody, JB Bonventre's lab, Brigham and Women's Hospital, Boston) and CD68 (KP1 clone, Dako Cytomation) and staining intensity was graded from 0 to 3+.

Results: KIM-1 showed membranous and/or cytoplasmic staining in all group 1 cases (16/16; 5 with 1+, 7 with 2+ and 4 with 3+ staining). None of group 2, CCP-RCC cases (0/11) expressed KIM-1. In contrast, all group 3, XP-TC cases (11/11) revealed positive KIM-1 expression (1 with 1+, 7 with 2+ and 3 with 3+ staining), suggesting origin from proximal tubules. The cytoplasmic expression of CD68 was present all group 1 cases (16/16, 5 with 1+, 7 with 2+ and 4 with 3+ staining), absent in all group 2 cases (0/11); and present in 9/10 group 3 cases (2 with 1+, 7 with 2+ and 1 with 3+ staining, 1 case was not available).

Conclusions: Using KIM-1 as a differentiation marker, the negative staining in CCP-RCC suggests derivation from distal nephron tubules and positive staining in XP-TC suggests derivation from proximal tubules. CD68 expression closely mirrored KIM-1 expression both in extent and intensity. The expression of CD68 in RCC subtypes is a novel finding and in our opinion this CD68 expression most likely represents a functional relationship with KIM-1, and may not necessarily have a real diagnostic utility; although this finding needs further evaluation.

985 Venous Invasion in Renal Cell Carcinoma: Preoperative Imaging-Gross Correlation.

CX Zhao, KO Ojemakinde, A Bhalodia, M Heldmann, D Elmajian, SM Bonsib. Louisiana State University Health Sciences Center-Shreveport, Shreveport.

Background: Renal sinus vein (SV) invasion is the principal invasive pathway for most renal cell carcinomas(RCC). Emphasis on nephron sparing surgery requires accurate preoperative imaging to optimize surgical strategies. Computed tomography (CT) and magnetic resonance imaging (MRI) are the most sensitive studies for preoperative imaging of RCC. Their accuracy in imaging sinus involvement in RCC has not been investigated.

Design: Fifteen cases of RCC were retrospectively selected and staged by 2010 TNM (3-pT1/2, 10-pT3a and 2-pT3b). The original radiology reports were obtained (11 LSUHSC/4 outside hospitals). A radiologist with expertise in urologic imaging received a brief tutorial on sinus invasive properties of RCC and re-examined the CT/MRI images for sinus invovlement. These interpretations were correlated with RCC gross photos.

Results: The mean tumor sizes were 8.7, 8.9, and 8.2cm by original radiologist, expert radiologist and patholgosist gross examination, respectively. SV invasion was not mentioned in any original CT/MRI reports (0/15) but was present in 12/15 cases by pathology review. Upon re-review of CT/MRI by radiology expert following tutorial, SV involvement was identified in 9/15.

RCC Tumor Stage Frequencies

Interpretation	pT1/2	pT3	
		SV	MRV
Original Radiologist	14	0	1
Expert Radiologist	6	3	6
Pathologist	3	3	9

Main renal vein (MRV) involvement was noted in 6/15 cases by expert radiologist but in 9/15 by patholgists. The 3 discrepant cases involved the left kidney.

When compared with radiology images the 3 involved veins were large primary tributaries of the MRV.

Conclusions: 1) Sinus involvement is not routinely mentioned by radiologists 2) Sinus involvement is usually detectable by CT/MRI (9/12) when present 3) Unrecognized sinus invasion by radiologists may lead to overestimate of tumor size and understaging that can be corrected by education on pathologic features of RCC 4) Discrepant MRV involvement by radiologists versus pathologists affecting the left kidney is due to differing definitions of what constitutes the MRV.

Gynecologic & Obstetrics

986 Secretory Cell Expansion of the Fallopian Tube Epithelium May Represent an Initial Cellular Change in Pelvic Serous Carcinogenesis.

N AbuShahin, L Xiang, O Fadare, B Kong, W Zheng. University of Arizona Collage of Medicine, Tucson; Vanderbilt University School of Medicine, Nashville, TN; Qilu Hospital, Shandong University, Jinan, Shandong, China.

Background: The distal fallopian tube is a common site of origin for tubal intraepithelial carcinoma and pelvic serous carcinoma in high-risk women (i.e BRCA mutation carriers and/or those with a breast cancer history). It has recently been further defined at the cellular level, that the secretory cell as opposed to cililated cell of the fallopian tube is the cell-of-origin of these cancers. However, under normal conditions, secretory and ciliated cells are intimately admixed within the tubal epithelial lining. We hypothesized that a change in ratio between tubal secretory and ciliated cells may represent one of the early steps in the process of female pelvic serous carcinogenesis

Design: Cellular compositions (secretory versus ciliated) in fallopian tubal segments (fimbriated end versus ampulla), *secretory cell expansion* (> 10 but < 30 cells in a row) and *secretory cell outgrowth* (≥ 30 cells in a row) were studied in 3 groups of patients: patients with benign gynecologic diseases ("no-risk"), "high-risk" patients as previously defined, and patients with "ovarian" high-grade serous carcinomas. The numbers of secretory and ciliated cells were counted by 2 methods: light microscopy and immunostainings with PAX8 for secretory cells and tubulin for ciliated cells. The ratio of cellular compositions was statistically compared among the 3 groups

Results: As compared with the "no risk" group, the numbers of tubal secretory cells in the high-risk and cancer groups were increased by a factor of at least 2 and 4 respectively. The frequency of secretory cell expansion was 3 to 4-fold higher in the high-risk and cancer groups, while the frequency of secretory cell outgrowth was 4-fold higher in the high-risk and 6-fold higher in the cancer group, respectively. Overall, immunohistochemistry with PAX8 and tubulin was more sensitive than morphologic evaluation for distinguishing the cell types. There was no significant difference between the tubal fimbriated end and ampulla regarding the number of secretory cells

Conclusions: An increase in the number of secretory cells in fallopian tube epithelium may represent an early, morphologically identifiable event in the process of pelvic serous carcinogenesis, although the underlying molecular mechanism of secretory cell expansion or outgrowth and how they eventuate in cancers, remain unclear.